PERMAFROST IN A WARMER WORLD:

NET ECOSYSTEM CARBON IMBALANCE

By

Benjamin W. Abbott

RECOMMENDED:

M. Syndonia Bret-Harte Ph.D.
Advisory Committee Member

F.S. Chapin III Ph.D.
Advisory Committee Member

Edward A.G. Schuur Ph.D.
Advisory Committee Member

Jeremy B. Jones Jr. Ph.D.
Advisory Committee Chair

Diane Wagner Ph.D.
Chair, Department of Biology and Wildlife

APPROVED:

Paul W. Layer Ph.D.
Dean, College of Natural Science and Mathematics

John C. Eichelberger Ph.D.
Dean of the Graduate School

12/8/14

Date

PERMAFROST IN A WARMER WORLD:

NET ECOSYSTEM CARBON IMBALANCE

A

DISSERTATION

Presented to the Faculty
of the University of Alaska Fairbanks

in Partial Fulfillment of the Requirements
for the Degree of

DOCTOR OF PHILOSOPHY

By

Benjamin W. Abbott, B.S.

Fairbanks, AK

December 2014

Abstract

Arctic tundra and boreal forest have accumulated a vast pool of organic carbon, twice as large as the atmospheric carbon pool and three times as large as the carbon contained by all living things. As the permafrost region warms, more of this carbon will be exposed to decomposition, combustion, and hydrologic export. This permafrost carbon feedback has been described as the largest terrestrial feedback to climate change as well as one of the most likely to occur; however, estimates of its strength vary by a factor of thirty. Models predict that some portion of this release will be offset by increased arctic and boreal biomass, but the lack of robust estimates of net carbon balance increases the risk of further overshooting international emissions targets with serious societal and environmental consequences.

In this dissertation I investigate the potential and actual response of arctic and boreal carbon balance to climate change. First, I present estimates from 98 permafrost-region experts of the response of circumarctic biomass, wildfire, and hydrologic carbon flux to warming over the next several centuries. Because precise estimates of the factors driving arctic and boreal carbon balance are unlikely in the near future, these qualitative estimates provide a holistic summary of current scientific understanding and provide a framework for assessing uncertainty and risk. Assessments indicate that little agreement exists on the magnitude and even sign of change in high-latitude biomass, and that end-of-the-century organic carbon release from arctic rivers and collapsing coastlines could increase three-fold while carbon loss via burning could increase seven-fold. Second, I test the impact of permafrost collapse (thermokarst) on carbon and nutrient release from upland tundra on the North Slope of Alaska. The biogeochemical consequences of thermokarst are not adequately conceptualized or characterized to incorporate into numerical models, though thermokarst may impact a third of the permafrost region by the end of the century. I employ a coupled aquatic and terrestrial experimental design to address this knowledge gap, measuring the displacement of soil organic carbon, surface flux of CO_2, CH_4, and N_2O, and hydrologic export of dissolved carbon and nutrients. Results show that thermokarst can stimulate or suppress ecosystem respiration depending on feature morphology; remove a large portion of ecosystem carbon; mobilize highly biodegradable dissolved organic carbon; disrupt the nitrogen cycle resulting in N_2O production and hydrologic nitrogen losses; and influence offsite organic matter decomposition by the release of labile dissolved organic carbon,

nitrogen, and other nutrients. Spatial patterns of carbon and nutrient export from thermokarst suggest that upland thermokarst may be a dominant linkage between terrestrial and aquatic ecosystems as the permafrost region warms.

I conclude that the strength of the permafrost climate feedback depends largely on coupled carbon and nutrient dynamics, which will interact with disturbance such as wildfire and thermokarst. My results indicate that three-quarters of permafrost carbon release could be avoided if human emissions are actively reduced, though the window of opportunity to keep that carbon in the ground is rapidly closing.

Table of Contents

Page

Page

Page

Page

Page

List of Figures

Page

Page

List of Tables

Page

List of Appendices

Page

Page

Page

Acknowledgements

I thank my advisor Jeremy B. Jones. When Jay took me on as a Ph.D. student I had just finished my B.S. and had read a total of six scientific papers. On my first day in the field I dropped our most important instrument into a small lake. Jay stayed up most of the night resuscitating the drowned analyzer and had it ready for sampling the following day. He has covered many missteps and corrected many mistakes since then and has done so patiently and conscientiously. Jay taught me about balance and priorities—that a fruitful career in science is compatible with family life and personal pursuits. I am grateful for his example and friendship.

Second, I thank my graduate committee M. Syndonia Bret-Harte (Donie), F.S. Chapin III (Terry), and E.A.G. Schuur (Ted). Not only did they teach me that you do not have to go by the name you were born with, they have displayed a contagious love of science and passion for human society. They taught me there was no such thing as a side project, that hard questions are the best kind, and that your first impressions are often opposite your eventual conclusions. They have generously shared their time, ideas, and opportunities.

Third, I thank my labmates, fellow students, and the Thermokarst Team. They turned long days of fieldwork and long nights of labwork into activities that were enjoyed rather than endured. Their shared analyzer time, lunches, dry socks, and scientific contributions are an important part of this dissertation. Together we explored and sampled some of the wildest and quietest landscapes anywhere in the world.

Fourth, I thank my mom and dad. They gave me fire-bellied toads, tapes to record *Nature* and *National Geographic*, and books that taught accessible, real science. I am eternally grateful for their love. I also thank my grandpa for hundreds of days and nights outside. He may never believe in climate change but he has always believed in me.

Finally, I would like to thank my wife Rachel. This never could have happened without Rachel's emotional and practical support. She shouldered most of the work raising our three children while also finishing her Ph.D. and has operated as a single parent for weeks on end when I was away for fieldwork. She sent me off to conferences with clean socks and despite my sour moods she only made me sleep at the office a few nights over the past five years. Her grit has made this come to pass.

This work was supported by the National Science Foundation ARCSS program (OPP-0806465 and OPP-0806394).

Dedication

For my children Ingrid, Henry, and Caspian,
and for my friend Archana Bali (1978-2014).

Chapter 1. Introduction

1.1 The permafrost carbon feedback

Net ecosystem carbon balance (NECB) is a complete accounting of inputs and outputs to and from an ecosystem (Chapin et al. 2006). NECB includes vertical carbon fluxes across the surface-atmosphere boundary such as primary production, ecosystem respiration, emissions from wildfire, and trace gas flux, as well as lateral carbon fluxes such as hydrologic flow moving into and out of the system. It is not the magnitude of these fluxes that determines whether an ecosystem is a carbon sink or source, but the difference between the deposits and the withdrawals. Despite low rates of primary production in the boreal forest and arctic tundra, these ecosystems have accumulated a vast pool of soil carbon over the last 2.5 million years due to cold and waterlogged conditions limiting decomposition (Ping et al. 1997, Tarnocai et al. 2009, Jahn et al. 2010, Schirrmeister et al. 2011). Because soil temperature and moisture are largely determined by climate, permafrost carbon has been described as climate protected (Trumbore 2009). As climate change strips away this protection, the response of biomass, decomposition, hydrologic carbon release, and wildfire will determine the NECB of the permafrost zone (Mack et al. 2004, Davidson and Janssens 2006, Field et al. 2007, Shur and Jorgenson 2007, Balshi et al. 2009, McGuire et al. 2009, Chapin et al. 2010, Kokelj and Jorgenson 2013).

The projected release of carbon dioxide (CO_2) and methane (CH_4) from thawing permafrost has been termed the permafrost carbon feedback (Schaefer et al. 2014) and has been described as the largest terrestrial feedback to climate change as well as one of the most likely to occur (Schuur et al. 2008, Schuur et al. 2009). There is substantial complexity associated with this feedback beyond uncertainty surrounding the rate of permafrost degradation. While simulations of the extent of permafrost thaw by 2100 vary by a factor of two (from 40-80% permafrost loss), estimates of permafrost carbon release vary by a factor of thirty (from 17-500 Pg C) (MacDougall et al. 2012, Zhuang et al. 2006, Slater and Lawrence 2013, Schaefer et al. 2014). Several key sources of uncertainty in anticipating the rate, magnitude, and type of permafrost carbon release have been identified: 1. Surface collapse during the degradation of ice-rich permafrost, termed thermokarst, which can alter rate of thaw and conditions after thaw (Schuur et al. 2008, Grosse et al. 2011, Kokelj and Jorgenson 2013), 2. Uptake of carbon by boreal and tundra biomass associated with longer growing season and CO_2 fertilization, (Waelbroeck et al. 1997, Koven et al. 2011, Schuur et al. 2013), 3. Hydrologic mobilization of

carbon from terrestrial to aquatic ecosystems (Kling et al. 1991, Frey and Smith 2005, Kicklighter et al. 2013), and 4. Changes in extent and severity of wildfire (Flannigan et al. 2009a, Kelly et al. 2013).

In this dissertation I investigate all four of these dynamics, though at different scales and with contrasting methods. First, I use expert surveys to summarize scientific understanding of the response of boreal and tundra biomass, wildfire, and hydrologic carbon flux to climate change. The hypotheses generated from this work have a circumarctic spatial scale and a multi-century temporal scale. Second, I investigate how upland thermokarst affects both vertical and horizontal carbon export on the North Slope of Alaska. This work has a plot to regional spatial scale and tests hypotheses on annual to decadal temporal scales. Because carbon does not cycle in isolation (Sterner and Elser 2002), I expand the concepts of NECB and the permafrost carbon feedback to include changes in other coupled elemental cycles, particularly nitrogen.

1.2 Background

1.2.1 Characteristics of permafrost

Permafrost, perennially frozen ground, underlies 16% of global soil area but contains more than 50% of the world's soil organic matter (SOM), amounting to 1400-1800 petagrams of carbon (Pg = billion tonnes; Tarnocai et al. 2009) and 70-90 Pg of nitrogen, based on typical high-latitude C:N ratios (Jonasson et al. 1999, Weintraub and Schimel 2003, Harden et al. 2012). The permafrost zone occupies 24% of exposed land surface in the Northern Hemisphere (22.79 x 10^6 km^2) and is classified into four categories based on extent of frozen ground: continuous (>90% of the land surface is underlain by frozen ground), discontinuous (50-90%), sporadic (10-50%), and isolated (<10%). These categories occupy 47, 19, 17, and 17% of the permafrost zone, respectively (Brown et al. 1998, Zhang et al. 1999) (See Appendices A and B for a detailed treatment of permafrost carbon dynamics).

Unlike most terrestrial ecosystems where SOM occurs primarily in the top meter of soil where plant inputs are highest (Chapin et al. 2011), more than half of permafrost SOM is stored below 1 m (Tarnocai et al. 2009). Three mechanisms account for this deeper distribution of SOM. First, seasonal freezing and thawing of the active-layer above the permafrost table can cause cryogenic mixing, incorporating chunks of SOM into the permafrost (Bockheim 2007). Second, arctic rivers transport globally relevant loads of dissolved and particulate organic carbon (Aufdenkampe et al. 2011, Holmes et al. 2012), some of which they lose into fluvial sediment

deposits, which can have considerable extent and depth (Schirrmeister et al. 2011). Third, the deposition of windblown silt during periods of glaciation can raise the soil surface and underlying permafrost table, incorporating plant matter into syngenetic permafrost (Zimov et al. 2006, Kanevskiy et al. 2011).

The question of how arctic carbon balance will respond to climate change has fueled over two decades of debate (Oechel et al. 1993, Waelbroeck et al. 1997) and remains an important uncertainty with ecological and societal implications (Schaefer et al. 2011, Schuur et al. 2013). The permafrost SOM pool is so large that the release of even a small portion could entrain serious consequences for regional ecosystem processes and global carbon and nutrient cycles.

There is growing evidence that permafrost carbon has been a key player regulating global climate in the past. Permafrost greenhouse gas release is implicated in the abrupt warming that occurred 56 million years ago during the Paleocene-Eocene Thermal Maximum (DeConto et al. 2012). Changes in earth's orbit in combination with high atmospheric CO_2 may have triggered widespread permafrost degradation and massive SOM decomposition, leading to a 5°C increase in global mean temperature over several thousand years (DeConto et al. 2012). This warm period lasted ca. 170,000 years and was potentially terminated by the re-accumulation of permafrost SOM drawing down atmospheric CO_2 (Bowen and Zachos 2010). In contrast, climate change during the early Holocene from 9,000-5,000 years ago increased Arctic temperature by 2-4°C but resulted in limited permafrost degradation and carbon release (French 1999, Schirrmeister et al. 2002). Current human disturbance of the earth-climate system is occurring on much more rapid timescales than either of these events and it is unknown how arctic and boreal NECB will respond to this unprecedented change.

1.2.2 Boreal forest, arctic tundra, and the circumarctic watershed

The tundra biome covers 5.0 x 10^6 km^2 (Raynolds et al. 2012) and the boreal forest biome covers 13.7 x 10^6 km^2 (Chapin et al. 2011), though the extent of the boreal forest depends on the definition of the southern transition to temperate forest and varies in the literature from 11.4 - 18.5 x 10^6 km^2 (McGuire et al. 1995, Potter and Klooster 1997, Chapin et al. 2011, Pan et al. 2011). Because most tundra falls in the continuous permafrost zone (with over 90% permafrost cover) and most boreal forest in the discontinuous, sporadic, or isolated zones (with 0-90% cover), almost all arctic tundra is underlain by permafrost, whereas most of the boreal forest is not (Zhang et al. 1999, Zhang et al. 2000).

The boreal and arctic biomes contain 111 Pg carbon in non-soil biomass including above and belowground living biomass, standing dead wood, and litter (see Table 2.2). The size and behavior of these pools depend on the balance between primary productivity, ecosystem respiration, and disturbance such as wildfire, drought, permafrost collapse or thermokarst, and insect outbreaks. The effect of climate change on arctic and boreal biomass depends on its direct and indirect impact on these carbon inputs and outputs.

The pan-arctic watershed, defined as the drainages of the Arctic Ocean and surrounding seas, covers 20.5 x 10^6 km^2 and yields 3700 km^3 of discharge annually (McGuire et al. 2009, Holmes et al. 2012). Worldwide, freshwater ecosystems are active conduits, transporting and transforming globally relevant loads of dissolved and particulate organic carbon (DOC and POC, respectively; (Cole et al. 2007, Battin et al. 2009). Freshwater ecosystems play a particularly influential role in regulating carbon cycling at high latitudes, where they cover more than 50% of the landscape in some regions (McGuire et al. 2009) and account for 11% of global runoff, 36% of global lake area, and over 50% of global wetland area (Loveland et al. 2000, Lammers et al. 2001, Aufdenkampe et al. 2011, Avis et al. 2011). As permafrost volume shrinks due to climate change, more of the large SOM pool will thaw and some portion will become available for transport to aquatic ecosystems, depending on changes in local and regional hydrology (Frey and McClelland 2009, O'Donnell et al. 2012, Tank et al. 2012). The response of hydrologic carbon flux to climate change is a highly uncertain and relatively understudied component of the arctic carbon cycle (McClelland et al. 2008).

1.2.3 Arctic and boreal climate change

High latitude air temperature is increasing twice as fast as global mean temperature due largely to feedbacks associated with sea-ice loss and decreasing snow cover (Holland and Bitz 2003, ACIA 2005, AMAP 2011, Parmentier et al. 2013). Warming has been most prevalent during the autumn and early winter in coastal areas when sea ice is at its minimum and in the spring at latitudes from 50° – 60° N as snow cover decreases (AMAP 2011). Precipitation has increased 5% over land north of 55° since 1950, though due to high interannual variability this trend is not significant (Peterson et al. 2006, AMAP 2011). Circumpolar precipitation minus evapotranspiration is projected to increase by 13 – 25% by 2100, however much of this increase is due to changes in winter precipitation (Kattsov et al. 2007), and growing season precipitation in some areas is not expected to keep up with enhanced evapotranspiration (Chapin et al. 2010).

An intensification of the freshwater cycle is projected across the arctic, including increases in precipitation, evapotranspiration, storage, and discharge (Rawlins et al. 2010); however, the relative magnitude of these parameters is poorly constrained (Holmes et al. 2012).

As a result of changes in temperature and precipitation, both permafrost and non-permafrost soil temperatures have warmed over the past century, causing increased active layer thickness, freeze-thaw cycling, longer duration of thaw, and widespread ground collapse or thermokarst (Osterkamp and Romanovsky 1999, Hinkel and Nelson 2003, Osterkamp and Jorgenson 2006, Osterkamp 2007, Osterkamp et al. 2009, Grosse et al. 2011, Kokelj and Jorgenson 2013). Models predict widespread near-surface (in the top 3 m) permafrost degradation with projections varying between 40 – 80 % loss by 2100 (Saito et al. 2007, Schaefer et al. 2011, Lawrence et al. 2012, Slater and Lawrence 2013).

Growing season length, historically 100 days for tundra and 150 days for boreal forest, has increased 2 – 4 days per decade from 1960 – 2000, due mostly to earlier spring thaw (Euskirchen et al. 2006, Chapin et al. 2011), and is projected to lengthen a total of 37 – 60 days over pre-industrial conditions by the end of the century (Euskirchen et al. 2006, Koven et al. 2011). Increased primary productivity due to CO_2 fertilization accounts for over 60% of carbon sequestered in the pan-boreal region over the past two decades (Balshi et al. 2007) and CO_2 fertilization is expected to strongly influence vegetation response to climate change (Schaefer et al. 2011). Wildfire extent and severity have increased throughout the permafrost region (Kasischke and Turetsky 2006, Balshi et al. 2009, Flannigan et al. 2009b) including in arctic tundra (Rocha et al. 2012).

The widespread degradation of permafrost is correlated with increasing winter base flow and the seasonal contribution of ground water relative to surface water (Smith et al. 2007, Walvoord and Striegl 2007, Frey and McClelland 2009). Coupled to changes in hydrology, aquatic chemistry has experienced substantial shifts, including an increase in DOC flux in areas with peat and thick organic soil (Frey and McClelland 2009), a decrease in DOC where organic soils are shallow (Striegl et al. 2005, Petrone et al. 2006, McClelland et al. 2007), increases in major ion concentrations (Frey and McClelland 2009, Giesler et al. 2014), accelerated chemical weathering (Tank et al. 2012), and increased inorganic nutrient concentrations (Jones et al. 2005, Petrone et al. 2006, McClelland et al. 2007).

Climate change is accelerating thaw and erosion of arctic coastlines due to warming air and water in combination with increased exposure to wave action and storms due to reductions in sea ice cover (IPCC 2007, Stroeve et al. 2007). Thermal collapse and erosion of arctic coastlines delivers DOC and POC to coastal shelf waters, with collapse most pronounced in northeastern Alaska and East-Siberia (Rachold et al. 2000, Jones et al. 2009, Lantuit et al. 2012a). Along the Beaufort Sea coast, coastal retreat rates have increased during the last decades from 6.8 m yr^{-1} during 1955-1979 to 13.6 m yr^{-1} during 2002-2007 (Jones et al. 2009).

1.2.4 Pathways of permafrost degradation

Permafrost degradation follows two basic trajectories. In permafrost with little ground ice, the soil profile can thaw from the top down without disturbing the surface. Alternatively, permafrost thaw causes surface subsidence or collapse, termed thermokarst, when ground ice volume exceeds soil pore space (Kokelj and Jorgenson 2013). If thermokarst occurs on hillslopes it can abruptly expose SOM from meters below the surface and alter soil conditions at depth, influencing thawed SOM mineralization and export (Schuur et al. 2008, Vonk et al. 2012).

The term thermokarst includes a suite of thermo-erosional features with different morphologies determined primarily by ice content, substrate type, landscape position, and slope (Jorgenson and Osterkamp 2005, Jorgenson et al. 2008, Osterkamp et al. 2009). In upland landscapes, the three most common thermokarst morphologies are retrogressive thaw slumps, active-layer detachment slides, and thermo-erosion gullies (Jorgenson and Osterkamp 2005, Krieger 2012, Kokelj and Jorgenson 2013). In addition to surface subsidence due to ground ice loss, mechanical erosion and mass wasting play a role in the formation of these features, however, I refer to them collectively as thermokarst following literature convention (Kokelj and Jorgenson 2013). Active-layer detachment slides form when the seasonally thawed surface layer of vegetation and soil slips downhill over an ice-rich transition zone. They can be triggered by fire and acute weather events such as late summer storms or heat spells, and can form on steep or shallow hillslopes, including those of less than 2° (Lewkowicz 1990, Lewkowicz and Harris 2005). Slides typically form suddenly, over a period of weeks, days, or even hours (Lewkowicz 2007). The removal of the organic layer can trigger secondary degradation extending the period of disturbance (Lewkowicz 1990), but otherwise slides often stabilize the same season they appear (Lafreniere and Lamoureux 2013). Thermo-erosion gullies form when ice wedges melt, often due to thermal loading and erosion from flowing water or after surface disturbance (Shur et

al. 2004, Jorgenson and Osterkamp 2005, Fortier et al. 2007, Bowden et al. 2008, Godin and Fortier 2012). Gully size depends primarily on the depth and lateral extent of the ice-wedge network, with features taking on polygonal, linear, or dendritic morphologies depending on the ice-wedge configuration (Fortier et al. 2007, Godin and Fortier 2012). Though there very few estimates exist of gully longevity, based on average headwall retreat rates they remain active for five to ten years (Jorgenson and Osterkamp 2005), with large features lasting over a decade (Godin and Fortier 2012). Retrogressive thaw slumps are characterized by a retreating headwall and are fueled by a variety of massive ground ice types, including buried glacial ice, coalesced ice wedges, and lacustrine deposits (Jorgenson and Osterkamp 2005, Kokelj et al. 2009a, Lantuit et al. 2012b). Slumps can be initiated due to extreme weather events, such as early spring warming (Balser et al. 2014), by mechanical erosion or thermal perturbation from water bodies (Kokelj et al. 2009a), or when surface disturbances such as fire or slides expose ice-rich permafrost (Lewkowicz 1990, Burn 2000). Feature longevity depends on the dimensions and volume of ground ice and the transport of thawed sediments, which can stabilize features by covering and insulating exposed ice if these sediments are not removed by colluvial or fluvial processes (Lewkowicz 1987, Jorgenson and Osterkamp 2005). Small slumps can stabilize in less than ten years (Kokelj et al. 2009a) but more commonly larger features can remain active for 12–50 years (Lewkowicz 1987, Burn 2000).

These three morphologies currently impact approximately 1.5% of the landscape in the western foothills of the Brooks Range (Krieger 2012) and could affect 20–50% of uplands in the continuous permafrost region by the end of the century based on projections of permafrost degradation and the distribution of ground ice (Zhang et al. 2000, Slater and Lawrence 2013). Upland thermokarst in the discontinuous permafrost zone already impacts 12% of the overall landscape in some areas and up to 35% of some vegetation classes (Belshe et al. 2013b). Observations over the past half-century indicate accelerated upland thermokarst formation, but circumarctic prevalence and change of thermokarst extent are poorly constrained (Yoshikawa and Hinzman 2003, Jorgenson et al. 2006, Lantz and Kokelj 2008).

1.2.5 Biogeochemical consequences of upland thermokarst

Thermokarst influences elemental cycles in two distinct ways: 1. By removing overlying soil, bringing previously frozen material in permafrost soil and ice nearer the surface, and 2. By altering physical conditions at the surface such as soil structure, temperature, moisture, and redox

potential, affecting the processing of both permafrost and active layer carbon and nutrients. Numerous studies have demonstrated the potential of upland thermokarst to alter terrestrial and aquatic biogeochemical cycles, including increased amplitude in the terrestrial carbon cycle (Schuur et al. 2009, Belshe et al. 2013a) and changes in hydrologic export of carbon and nutrients (Bowden et al. 2008, Kokelj et al. 2009b, Thompson et al. 2012, Lamoureux and Lafrenière 2014). However, it is unknown how these alterations vary between feature morphologies and through space and time (Belshe et al. 2013b, Kokelj and Jorgenson 2013, Lafreniere and Lamoureux 2013).

The warm and nutrient-rich soil conditions following permafrost collapse can stimulate both photosynthesis and respiration, tipping the system toward carbon release or carbon uptake depending on the relative response of these two processes (Schuur et al. 2009, Lee et al. 2010). Thermokarst can displace all or a substantial portion of the organic layer (Lantuit et al. 2012b, Pizano et al. 2014), increasing radiative and conductive heat transfer to soils (Burn 2000), and decreasing growing season respiration from residual mineral soils, which can be compacted and relatively low in organic carbon (Jensen et al. 2014). The export of this SOM could lead to substantial off-site mineralization of carbon and nutrients in downslope or downstream ecosystems such as valley bottoms, rivers, and lakes. In addition to changes in magnitude of surface carbon flux, thermokarst can affect the age of carbon released by enhancing mineralization of old carbon from thawing permafrost at depth (Schuur et al. 2009). Coupled to changes in carbon cycling, thermokarst can modify nutrient uptake, export, and mineralization. The removal or disruption of surface vegetation during ground collapse can eliminate or reduce plant nutrient uptake (Osterkamp et al. 2009). Thermokarst formation can bring nutrient-rich mineral soils to the surface (Harms et al. 2013, see also Appendix C), and plants growing in thermokarst scars show elevated nitrogen content (Schuur et al. 2007). Microenvironments in thermokarst can favor deciduous shrub establishment, including nitrogen-fixing species (Tsuyuzaki et al. 1999, Lantz et al. 2009, Pizano et al. 2014), which can contribute labile SOM and inorganic nitrogen (Sturm et al. 2001, DeMarco et al. 2011). Increased nutrient availability and high quality carbon inputs can in turn accelerate decomposition of SOM (Mack et al. 2004, Hartley et al. 2012). Therefore, overall surface carbon balance from an upland thermokarst feature depends on the amount of SOM exported offsite during formation and on physical conditions within the feature controlling photosynthesis and processing of residual SOM.

The impact of thermokarst on hydrologic export of carbon and nutrients depends on the magnitude and duration of initial disturbance, the recovery trajectory, and location of disturbance in relation to hydrologic networks. If thermokarst disturbance is hydrologically connected to aquatic ecosystems, it can cause substantial loading of sediment, carbon, and nutrients (Kokelj et al. 2005, Bowden et al. 2008, Shirokova et al. 2013, Thienpont et al. 2013, Vonk et al. 2013). Because tundra mineral soils are richer in solutes, including inorganic nutrients, than overlying organic soils (Nadelhoffer et al. 1991, Hobbie and Gough 2002, Kokelj and Burn 2003, Keuper et al. 2012), thermokarst disruption or removal of the organic layer can increase solutes available for hydrological transport (Kokelj and Burn 2003, Harms et al. 2013). Thermokarst can alter the age and degradability of particulate and dissolved organic carbon (POC and DOC), releasing older POC (Lafreniere and Lamoureux 2013) and more labile DOC during formation (Cory et al. 2013, Vonk et al. 2013, Abbott et al. 2014). Sediment delivery, changes in light penetration, and nutrients can cause shifts in aquatic food webs (Mesquita et al. 2010, Thompson et al. 2012, Thienpont et al. 2013). If thermokarst is hydrologically isolated from surface waters, such as when it occurs on high on hillslopes, even dramatic disturbance can have little or no impact on aquatic chemistry and elemental budgets (Lewis et al. 2012, Lafreniere and Lamoureux 2013). However, even when features are connected to surface waters thermokarst does not necessarily result in enhanced carbon and nutrient export (Thompson et al. 2012). Mineral soils exposed by thermokarst can adsorb DOC, reducing concentrations in feature outflows and receiving waters, resulting in greater water clarity after sediment loading and settling (Kokelj et al. 2005, Thompson et al. 2012). The duration of carbon and nutrient release and the persistence of biogeochemical disturbance after feature stabilization are largely unknown. Some studies have observed altered surface water chemistry decades after stabilization due to legacy effects of nutrient loading or surface disturbance (Kokelj et al. 2005, Thienpont et al. 2013), while others have observed fading of effects after less than a year (Lafreniere and Lamoureux 2013).

1.3 Questions and hypotheses

One fundamental question has motivated my research: how will climate change affect net ecosystem carbon balance in the permafrost zone? To broach this broad topic I generated several specific questions and hypotheses, which are outlined below by chapter.

Chapter 2. Can increased biomass offset carbon release from soils, streams, and wildfire across the permafrost region? An expert elicitation.

Q1. How will the hydrologic load and lability of organic carbon change in a warmer world?

Q2. How will boreal forest and arctic tundra non-soil biomass respond to climate change?

Q3. How will wildfire extent and emissions release change in the boreal forest and arctic tundra?

Q4. How do these fluxes compare to projected carbon release from permafrost SOM?

To address these questions I used an expert elicitation survey to collect quantitative estimates of boreal and arctic response to climate change from 98 permafrost carbon balance experts. My goal was not to arrive at definitive answers to these questions, but to characterize the range of scientific opinion and identify sources of uncertainty to inform future research and provide context to current projections of artic and boreal NECB.

Chapter 3. Elevated dissolved organic carbon biodegradability from thawing and collapsing permafrost

Q1. How biodegradable is permafrost DOC compared to active-layer DOC?

Q2. What determines the biodegradability of permafrost DOC?

Q2. What are the controls on DOC processing in arctic systems?

In this study I measured the biodegradability of DOC released by 19 thermokarst features across the North Slope of Alaska. I hypothesized two mechanisms explaining permafrost DOC biodegradability. First, permafrost DOC may consist of biodegradable chemical compounds due to limited prior microbial processing or different DOC sources. Second, high nutrient concentrations in permafrost melt water may accelerate DOC breakdown by relieving nutrient limitation of heterotrophic microorganisms.

I tested these hypotheses and predictions by 1) characterizing DOC composition released by thermokarst, 2) incubating DOC with and without added nutrients, 3) comparing BDOC between feature and vegetation types, and 4) developing relationships between DOC composition, nutrient content, and BDOC.

Chapter 4. Patterns and persistence of hydrologic carbon and nutrient export from collapsing upland permafrost

Q1. How does upland thermokarst formation alter hydrologic flux of carbon and nutrients?

Q2. How long do these effects persist?

Q3. Can the biogeochemical effects of thermokarst be predicted based on feature morphology or landscape characteristics?

I hypothesized that upland thermokarst would initially stimulate nutrient release due to disturbance but this pulse of nutrients would be followed by a period of elemental retention due to enhanced nutrient uptake by recovering vegetation. I hypothesized that DOC export would depend on the balance between enhanced DOC production from disruption of organic and mineral soils and DOC decreases from adsorption by exposed mineral soils and the rapid processing of DOC within features due to abundant nutrients and biodegradable DOC from permafrost.

To test these hypotheses, I collected outflow water from 83 upland thermokarst features on the North Slope of Alaska. I classified features by activity as a proxy for age, and compared outflow concentrations and loads across this chronosequence.

Chapter 5. Upland permafrost collapse stimulates N_2O production but effect on growing-season respiration depends on thermokarst morphology

Q1. How does upland thermokarst affect respiration, CH_4, and N_2O flux to the atmosphere?

Q2. How do these effects differ between various thermokarst forms?

Q3. How does the initial pulse of carbon displaced by thermokarst formation compare to altered surface gas fluxes after stabilization?

I hypothesized that the impact of thermokarst on respiration and trace gas flux would depend on changes in soil carbon content, temperature, and moisture. I further hypothesized that soil moisture and associated O_2 limitation would increase with feature depth, resulting in a gradient from aerobic to anaerobic metabolism.

To test these hypotheses I measured changes in physical conditions, SOM displacement, and gas flux at 26 upland thermokarst features. I used the type and severity of disturbance to define several ground-surface patches and scaled to the feature level by the proportional coverage of each patch.

1.4 Authorship

None of the work presented in this dissertation was accomplished alone. I was the lead investigator and author of Chapters 1-6 and the following individuals contributed in the capacity listed below by chapter:

Chapter 2

Benjamin W. Abbott[1], Jeremy B. Jones[1], Edward A.G. Schuur[2], and F.S. Chapin III[1] contributed to the original idea of creating an expert survey, assisted in crafting and refining the questionnaires and materials, and gave input on the manuscript written by Abbott. William B. Bowden[3], M. Syndonia Bret-Harte[1], Howard E. Epstein[4], Michael D. Flannigan[5], Tamara K. Harms[1], Teresa N. Hollingsworth[6], Michelle Mack[2], A. David McGuire[1], Susan M. Natali[7], Adrian V. Rocha[8], Suzanne E. Tank[9], Merrit R. Turetsky[10], Jorien E. Vonk[11], and Kimberly P. Wickland[12] tested the surveys, provided comments on the manuscript, and assisted writing the background information distributed with the surveys as indicated in Appendix 2.0. The Permafrost Carbon Network includes all 98 permafrost region experts who filled out the survey and gave input on the subsequent manuscript. Individual names and affiliations are listed in Appendix 2.0.2.1.

Chapter 3

Abbott and Julia R. Larouche[3] designed the experiment, collected and analyzed samples, and collaborated closely on the manuscript written by Abbott. Jones and Bowden provided input and were closely involved throughout the process. Andrew W. Balser[1] assisted with the refinement of the manuscript and landscape analysis of sites.

Chapter 4

[1]Institute of Arctic Biology and Department of Biology & Wildlife, University of Alaska Fairbanks, [2] Department of

Abbott and Jones designed the experiment and worked closely on the manuscript written by Abbott. Larouche and Sarah E. Godsey[23] helped refine the experimental design, assisted with sample collection and analysis, and provided input on the manuscript.

Chapter 5

Abbott and Jones designed and implemented the experiment and worked together closely on the manuscript written by Abbott.

[23]Department of Geosciences, Idaho State University

Chapter 2. Can increased biomass offset carbon release from permafrost region soils, streams, and wildfire across the permafrost region? An expert elicitation.[3]

2.1 Summary

As the permafrost region warms, its large organic carbon pool will be increasingly vulnerable to decomposition, combustion, and hydrologic export. Models predict that some portion of this release will be offset by increased arctic and boreal biomass; however, the lack of robust estimates of net carbon balance increases the risk of further overshooting international emissions targets. Precise empirical or model-based measurements of the critical factors driving carbon balance are unlikely in the near future, so to address this gap, we present estimates from 98 permafrost-region experts of the response of biomass, wildfire, and hydrologic carbon flux to climate change. Results suggest that contrary to model projections total permafrost-region biomass could decrease due to water stress and disturbance. Assessments indicate that end-of-the-century organic carbon release from arctic rivers and collapsing coastlines could increase three-fold while carbon loss via burning could increase seven-fold. Experts identified water balance, shifts in vegetation community, and permafrost degradation as the key sources of uncertainty in predicting future system response. In combination with previous findings, results suggest the permafrost region will become a substantial carbon source to the atmosphere by 2040 given current emission trends, or by 2100 if human emissions are actively reduced.

2.2 Permafrost zone carbon balance

The United Nations has set a target of limiting warming to 2°C above pre-industrial temperatures to mitigate risk of the most damaging consequences of climate change[1]. Maintaining global climate within this target depends on understanding ecosystem feedbacks to climate change so that adequate limits on human emissions can be set. As high latitudes warm, more of the large permafrost carbon (C) pool will be exposed to decomposition, combustion, and hydrologic export[2]. Up to 220 Petagrams (Pg) C could be released from permafrost-region soil by 2100, and 500 Pg by 2300[3,4], representing 10-30% of greenhouse gas emissions required to push the global climate system beyond the 2°C target[5]. Models project some permafrost C release will be offset by increases in arctic and boreal primary productivity due to extended

[3]Submitted to Nature Climate Change. BW Abbott, JB Jones, EAG Schuur, F Stuart Chapin III, WB Bowden, H Epstein, M Flannigan, TK Harms, TN Hollingsworth, MC Mack, SM Natali, AV Rocha, SE Tank, MR Turetsky, JE Vonk, KP Wickland, and the Permafrost Carbon Network.

growing season, CO_2 fertilization, and nutrient release from decomposing soil organic matter. However, many processes and dynamics known to influence biomass accumulation, such as ecosystem disturbance and nutrient limitation, are incompletely represented or absent in current models[6-8]. Likewise, only a few models projecting future permafrost C release consider wildfire emissions, and none include hydrologic C flux[4-6], though past hydrologic flux has been simulated[9-11]. Despite clear policy implications of this climate feedback, considerable uncertainty of both C inputs and outputs limits our ability to model C balance of the permafrost region. To bring to bear the best available quantitative and qualitative scientific information[12] on this climate feedback, we present results from a survey of experts indicating that there is little consensus on the magnitude and even sign of change in high-latitude biomass, whereas most researchers expect fire emissions and hydrologic organic C (OC) release to more than double by the end of the century.

We collected estimates of the components of net ecosystem C balance from 98 permafrost-region experts (Table 2.1; see Methods). Our goal was to assess current consensus on the timing and magnitude of non-soil biomass accumulation, hydrologic OC flux, and wildfire C emissions, and to identify sources of uncertainty in future C balance. Expert elicitation complements modeling and empirical approaches because it allows researchers to consider a range of factors known to affect C balance but insufficiently quantified for inclusion in models. These factors include nutrient dynamics, non-linear shifts in vegetation community, human disturbance, land-water interactions, and the relationship of permafrost degradation with water balance.

Participants were selected based on contribution to peer-reviewed literature or referrals from other experts and represented all major boreal and arctic regions (Table 2.1). Questionnaires were distributed via email and participants responded independently. Experts provided quantitative estimates of change in biomass, hydrologic flux, or wildfire for three time points (2040, 2100, and 2300) and four regional warming scenarios based on representative concentration pathway (RCP) scenarios from the IPCC Fifth Assessment Report[13]. Warming scenarios ranged from cessation of human emissions before 2100 (RCP2.6) to sustained human emissions (RCP8.5) and correspond to permafrost-region mean annual warming of 2 to 7.5°C by 2100 (see Methods). Experts were encouraged to consider all available information when

generating their estimates including published and unpublished modeled and empirical data as well as professional judgment. Participants self-rated their confidence and expertise for each question, described rationale for their estimates, and provided background information (A1.1; Table 1).

2.3 Pools and fluxes

Expert estimates revealed a broad diversity of opinion on the response of boreal biomass to warming, with over a third of responses predicting a decrease or no change in boreal biomass across scenarios and time periods (Fig. 2.1). Mean change in biomass was lower for the higher warming scenarios with confidence intervals ranging from -6 to 11% change by 2100 and -5 to 25% by 2300. Experts projecting a decrease in boreal biomass attributed their estimates primarily to water-stress and disturbance such as fire and permafrost degradation. In contrast, there was general agreement that tundra biomass would respond positively to warming, with end-of-century increases of 17-45% projected for RCP2.6 and 33-90% for RCP8.5. Because of these contrasting responses to increased warming, tundra accounted for half of total biomass gain by 2100 for RCP8.5, though it currently constitutes less than 10% of total permafrost region biomass (Table 2.2). Consequently, estimates of total biomass accumulation were relatively constant across scenarios for each time period, with -1 to 10 Pg C taken up by 2040, -3 to 19 by 2100, and 1 to 38 by 2300 (Fig. 2.2a). Estimates of boreal biomass were generally symmetrically distributed while tundra biomass estimates were right-skewed (A1.1; Fig. 1).

Experts projected major shifts in both fire and hydrologic OC regimes, with up to a three-fold increase in hydrologic OC release and a seven-fold increase in fire emissions by 2100 for RCP8.5 (Fig. 2.1). Fire and hydrologic OC release estimates peaked at 2100, followed by a 10-40% decrease through 2300. In contrast to biomass, the response of both fire-driven and hydrologic OC flux varied strongly by warming scenario, with RCP8.5 resulting in 2-7 times more C release than RCP2.6. While the boreal forest dominated total wildfire emissions, the relative change in tundra fire emissions was much greater, with 4 to 11-fold increases projected by 2100 for RCP8.5 (A1.1; Fig. 4). Changes in fire emissions were predicted to result from changes to fire extent rather than severity, which varied less than 5% among scenarios and time periods. Though dissolved organic C (DOC) represented the majority of total hydrologic OC release, experts projected higher relative increases for riverine and coastal particulate organic C

(POC), with end-of-the-century increases of 9-38% for RCP2.6 and 28-170% for RCP8.5. There was a lack of consensus on the response of DOC delivery to the ocean, with 21% of estimates predicting a decrease or no change. Experts predicting a decrease attributed their estimates to increased mineralization, changes in hydrologic flowpath, and changes in photo- and bio-lability[14]. Responses indicated no change in the proportion of OC delivered to freshwater systems that is mineralized or trapped in sediment before reaching the ocean, with 63-69% of DOC and 68-74% of POC lost in transport. Fire and hydrologic C flux estimates were strongly right-skewed with a few experts projecting more extreme change (A1.1; Figs. 2 and 3).

2.4 Sources of uncertainty

Along with quantitative estimates of C balance, experts identified sources of uncertainty currently limiting the prediction of system response to climate change (Table 2.3). Water balance, including precipitation, soil moisture, runoff, infiltration, and discharge, was the most frequently mentioned source of uncertainty for both biomass and hydrologic OC flux and the second most mentioned for fire. Many experts noted that water balance is as or more important than temperature in controlling future C balance, yet projections of water balance are less well constrained[15]. Almost three-quarters of wildfire experts identified the future distribution of vegetation as the primary source of uncertainty in projecting wildfire, noting strong differences in flammability between different boreal and tundra species. Permafrost degradation was identified as an important source of uncertainty for biomass, hydrologic flux, and wildfire, due to both disturbance from ground collapse (thermokarst) and interactions with water-table dynamics and surface soil moisture as deeper thaw affects soil drainage.

2.5 Carbon balance

The permafrost region has been a sink of C for the past several decades, removing an average of 500 Tg C yr^{-1} from the atmosphere[16,17]. Combining our estimates of biomass uptake with a recent projection of permafrost soil C release[3] suggests that the permafrost region will become a C source to the atmosphere by 2040 for RCP8.5 and by 2100 for RCP2.6 (Fig. 2.3). Experts predicted that boreal and arctic biomass would respond more quickly to warming than soil C release, offsetting 5-121% of mid-century emissions from permafrost-region soil for lower-warming scenarios (Fig. 2.2b). However, permafrost soil C release is expected to strongly exceed projected C gains for all scenarios by 2100. Because estimates of change in biomass are

similar across warming scenarios but permafrost C release is strongly temperature-sensitive, the emissions gap widens for warmer scenarios. For RCP2.6, biomass increase offsets 8-52% of permafrost C release by the end of the century and 6-28% by 2300, whereas for RCP8.5 it offsets -1 to 17% by 2100 and 0 to 14% by 2300 (Fig. 2.2b).

2.6 Comparison with quantitative models

Model projections of future boreal and arctic biomass agree in sign but vary widely in magnitude, with increases of 9 to 61 Pg C projected by 2100[6-8,18]. While some of these models fall within the range estimated here of -3 to 19 Pg C by 2100, none include zero or negative change in biomass as predicted by over a third of participants in our expert elicitation. Two potential reasons for this disagreement are an overestimation of the effect of CO_2 fertilization or an underestimation of the role of disturbance in some models. Firstly, CO_2 fertilization exerts a larger effect on C balance than all other climate effects in many models[19], with up to 88 Pg C difference between model runs with and without CO_2 fertilization effects for some models[7]. However, there is little field evidence that CO_2 fertilization results in long-term biomass accumulation in tundra and boreal ecosystems[20-22]. Additionally, many models with large CO_2 effects do not include other limiting factors, such as nutrients and water, known to interact with CO_2 fertilization[23-25]. Secondly, models that do not account for disturbance such as wildfire, permafrost collapse, insect damage, and human resource extraction likely overestimate the positive response of biomass to climate change[26].

Considering the scenario of a complete biome shift is useful in evaluating both model projections of change and estimates from our survey. If all boreal forest became temperate forest, living biomass would increase by 27%, resulting in the uptake of 16 Pg C based on average C densities from both ecosystems[17]. However, 22 Pg C would be lost due to decreases in dead wood and litter, resulting in a net circumboreal loss of 6 Pg C. If all tundra became boreal forest, non-soil biomass would increase by 205%[27-29], taking up 17 Pg C. This scenario may not represent the upper limit of possible C uptake if other unforeseen shifts in C allocation take place; however, it highlights the relatively modest C gains probable on century timescales.

While current model projections of regional boreal wildfire vary in sign and magnitude, there is general agreement that circumboreal fire emissions will increase several-fold, with increases of 200-560% projected by the end of the century[30,31]. Confidence intervals from this

study are even wider (140-650%, mean 240%), suggesting considerable uncertainty in the future response of boreal fire. The projected 4 to 11-fold increase in tundra fire would represent an even larger ecological shift than experienced by the boreal forest, with implications for regional biomass, habitat, and C balance, though there are few models that project changes in tundra fire[32] and none at a circumarctic scale[33].

The production of arctic DOC and POC depends on abundance of C sources in terrestrial ecosystems (influenced by biomass, wildfire, temperature, and permafrost degradation) and the ability of hydrologic flow to transport that C (determined by factors such as precipitation, runoff, depth of flow through soil, and coastal erosion)[10,34]. Due to these complexities and others, there are currently no quantitative projections of future DOC and POC flux from the circumarctic. However, estimates from our study suggest a substantial departure from historical rates of change. For RCP8.5, hydrologic OC loading would increase 4-20 times faster in the 21st century than it did in the 20th [10], representing a non-linear response to high-latitude warming. The lack of consensus on the response of DOC, the largest component of hydrologic OC flux, highlights the importance of developing and testing conceptual frameworks to be incorporated into models[11].

An alternative explanation for differences between expert estimates and modeled projections is the possibility of bias in the group of experts. Participants in this elicitation tended to have more field than modeling experience (Table 2.1) and may have therefore been skeptical of simulated ecosystem responses that have not been observed in the field such as CO_2 fertilization and rapid migration of treeline[16]. Because future dynamics cannot always reliably be predicted on the basis of past system behavior, this bias may or may not result in overly conservative estimates. Furthermore, because experts are likely to base projections on the study areas with which they are most familiar, regional differences could be a source of bias. Asia, which represents more than half of the total permafrost region, was under-represented in all three surveys, particularly wildfire (Table 2.1). However, the regional bias in this study may not be greater than that of model projections, which depend on observational and experimental data that are not evenly distributed throughout the permafrost region.

2.7 Utility of expert elicitation

Expert elicitation allows the synthesis of multiple types of system information from multiple individuals with the goal of evaluating uncertainty, identifying future research priorities,

and informing public policy. The approach is similar to the concept of ensemble models where multiple estimates built on different assumptions and data provide a more robust estimate and measure of variance[35]. Expert elicitation has been used in risk assessment and forecasting when data are sparse but management decisions are pressing, such as gauging the risk of volcanic eruption[36], quantifying human impacts on marine ecosystems[37], and identifying tipping points in the climate system[38]. Because the experimental unit is an individual researcher, each data point represents an integration of quantitative knowledge from modeling, field, and laboratory studies as well as qualitative information based on professional opinion and personal experience with the system. While expert elicitation cannot definitively answer questions of future system response, in a data-limited environment such as the permafrost region, the best available qualitative and quantitative scientific information[12] should be brought to bear to inform decisions in the face of uncertainty.

2.8 Conclusions

Expert estimates suggest that arctic and boreal biomass may offset much or all of mid-century permafrost C release if human emissions are actively reduced (RCP2.6). However, results indicate that the permafrost region will become a net C source to the atmosphere within the next several decades given current emission trends (RCP8.5). Experts projected major changes in the role of wildfire and hydrologic OC flux, with peak C release occurring around 2100. Models projecting a strong boreal C sink and models which do not consider hydrologic and fire emissions may substantially underestimate net C release from the permafrost region. If such projections are used as the basis for emissions negotiations, climate targets are likely to be overshot.

2.9 Methods

2.9.1 Survey development and design

In the fall of 2013 we developed a series of expert elicitation surveys to quantify uncertainty in the scientific community surrounding the response of biomass, wildfire, and hydrologic C flux to warming. To assure comparability with previous work, we followed methods developed during an elicitation administered at the Vulnerability of Permafrost Carbon Research Coordination Network meeting in Seattle 2011 that estimated permafrost degradation and soil C release[3]. Three to five lead experts for each system refined survey questions and

developed a system summary document providing relevant literature and background information (A1.2.3 – A1.2.8). System summaries included regional and pan-arctic estimates of C pools and fluxes, a brief treatment of historical trends, and a summary of model projections where available. We identified potential participants by querying Thomas Reuters Web of Science with applicable search terms (e.g. arctic, boreal, biomass, dissolved organic carbon, fire, permafrost). To reach researchers with applicable expertise who were underrepresented in the literature, we supplemented the list with personal referrals from lead experts and all participants. In total 256 experts were invited to participate. We distributed the surveys and system summaries via email with a two-week deadline. After sending out three reminders and accepting responses for three months after initial invitation, we received 115 responses from 98 experts (38% response rate), with 15 experts participating in more than one survey (Supplementary information; list of experts). Experts who provided estimates and input to this paper are coauthors listed as the Permafrost Carbon Network (see Supplementary information for complete list of group members and affiliations).

All surveys were driven by the same scenarios of regional warming generated from RCP2.6, 4.5, 6.0, and 8.5 with the National Center for Atmospheric Research's Community Climate System Model 4 [39]. For the purposes of this survey, warming was assumed to stabilize at 2100 levels for all scenarios so that responses through 2300 accounted for lags in ecosystem responses to climate drivers. While we only provided temperature scenarios with the surveys, we asked experts to consider all accompanying direct climate effects (e.g. temperature, precipitation, and atmospheric CO_2) and indirect effects (e.g. vegetation shifts, permafrost degradation, invasive species, and disturbance). The biomass survey consisted of a single question asking for cumulative change in tundra and boreal non-soil biomass including above and belowground living biomass, standing deadwood, and litter. The wildfire survey asked for estimates of change in wildfire extent and CO_2 emissions for the boreal and tundra regions to assess changes in both fire extent and severity. The hydrologic flux survey asked for estimates of DOC and POC delivery to freshwater ecosystems in the pan-arctic watershed and delivery to the Arctic Ocean and surrounding seas via riverine flux and coastal erosion, allowing the calculation of losses during transport due to burial or mineralization. Dissolved inorganic C fluxes were not included in this survey.

2.9.2 Analysis and calculations

Prior to analysis, responses with self-rated expertise of 1 (little or no expertise) were removed. All data were non-normally distributed at $p < 0.05$. Distributions were right skewed, except for estimates of boreal biomass, which were symmetrical but over-dispersed. Most datasets had 1-4 outliers beyond 1.5 times the inter-quartile range. In an effort to include outliers but not allow them to dominate estimates of center and spread, we Winsorized the upper and lower 20% of each dataset before calculating summary statistics[40]. Complete un-trimmed distributions are presented in A1.1 figures 1-3. We used non-parametric resampling (bootstrapping) with 1000 iterations to calculate mean and 95% confidence intervals for each time period and warming scenario. To calculate the portion of permafrost C release offset by biomass accumulation, we reanalyzed data from Schuur et al.[3] with the same Winsorization and bootstrapping protocol. The low confidence interval (CI) for offset was calculated by dividing the low CI of uptake by the high CI interval of C release and conversely for the high CI. All analyses were performed in R 3.0.2. The complete dataset of quantitative estimates and comments from survey participants stripped of personal identifiers is available at www.aoncadis.org/dataset/Permafrost_carbon_balance_survey.html.

Any use of trade, firm, or product names is for descriptive purposes only and does not imply endorsement by the U.S. Government.

2.10 Acknowledgements

Martin D. Robards and Peter J. Fix provided valuable input on the methods and manuscript. This work was supported by the National Science Foundation ARCSS program and Vulnerability of Permafrost Carbon Research Coordination Network (grants OPP-0806465, OPP-0806394, and 955713).

2.11 References

1 UNEP. The Emissions Gap Report 2013. United Nations Environment Programme (UNEP). (Nairobi, 2013).

2 Harden, J. W. *et al.* Field information links permafrost carbon to physical vulnerabilities of thawing. *Geophysical Research Letters* **39**, L15704, doi:10.1029/2012GL051958 (2012).

3 Schuur, E. A. G. *et al.* Expert assessment of vulnerability of permafrost carbon to climate change. *Climatic Change*, 1-16, doi:10.1007/s10584-013-0730-7 (2013).

4 MacDougall, A. H., Avis, C. A. & Weaver, A. J. Significant contribution to climate warming from the permafrost carbon feedback. *Nature Geosci* **5**, 719-721, doi:http://www.nature.com/ngeo/journal/v5/n10/abs/ngeo1573.html - supplementary-information (2012).

5 Schaefer, K., Lantuit, H., Romanovsky, V. E., Schuur, E. A. G. & Witt, R. The impact of the permafrost carbon feedback on global climate. *Environmental Research Letters* **9**, 085003 (2014).

6 Qian, H., Joseph, R. & Zeng, N. Enhanced terrestrial carbon uptake in the Northern High Latitudes in the 21st century from the Coupled Carbon Cycle Climate Model Intercomparison Project model projections. *Glob. Change Biol.* **16**, 641-656, doi:10.1111/j.1365-2486.2009.01989.x (2010).

7 Koven, C. D. *et al.* Permafrost carbon-climate feedbacks accelerate global warming. *P Natl Acad Sci USA* **108**, 14769-14774, doi:10.1073/pnas.1103910108 (2011).

8 Schaefer, K., Zhang, T., Bruhwiler, L. & Barrett, A. P. Amount and timing of permafrost carbon release in response to climate warming. *Tellus B*, no-no, doi:10.1111/j.1600-0889.2011.00527.x (2011).

9 McGuire, A. D. *et al.* An analysis of the carbon balance of the Arctic Basin from 1997 to 2006. *Tellus B* **62**, 455-474, doi:10.1111/j.1600-0889.2010.00497.x (2010).

10 Kicklighter, D. W. *et al.* Insights and issues with simulating terrestrial DOC loading of Arctic river networks. *Ecological Applications* **23**, 1817-1836, doi:10.1890/11-1050.1 (2013).

11 Laudon, H. *et al.* Cross-regional prediction of long-term trajectory of stream water DOC response to climate change. *Geophysical Research Letters* **39**, L18404, doi:10.1029/2012GL053033 (2012).

12 Joly, J. L., Reynolds, J. & Robards, M. Recognizing When the "Best Scientific Data Available" Isn't. *Stanford Environmental Law Journal* **29**, 247-282 (2010).

13 Moss, R. H. *et al.* The next generation of scenarios for climate change research and assessment. *Nature* **463**, 747-756, doi:http://www.nature.com/nature/journal/v463/n7282/suppinfo/nature08823_S1.html (2010).

14 Cory, R. M., Ward, C. P., Crump, B. C. & Kling, G. W. Sunlight controls water column processing of carbon in arctic fresh waters. *Science* **345**, 925-928, doi:10.1126/science.1253119 (2014).

15 Zhang, X. *et al.* Enhanced poleward moisture transport and amplified northern high-latitude wetting trend. *Nature Clim. Change* **3**, 47-51, doi:http://www.nature.com/nclimate/journal/v3/n1/abs/nclimate1631.html - supplementary-information (2013).

16 McGuire, A. D. *et al.* Sensitivity of the carbon cycle in the Arctic to climate change. *Ecological Monographs* **79**, 523-555, doi:doi:10.1890/08-2025.1 (2009).

17 Pan, Y. *et al.* A Large and Persistent Carbon Sink in the World's Forests. *Science* (2011).

18 Falloon, P. D. *et al.* Role of vegetation change in future climate under the A1B scenario and a climate stabilisation scenario, using the HadCM3C Earth system model. *Biogeosciences* **9**, 4739-4756, doi:10.5194/bg-9-4739-2012 (2012).

19 Balshi, M. S. *et al.* Vulnerability of carbon storage in North American boreal forests to wildfires during the 21st century. *Glob. Change Biol.* **15**, 1491-1510, doi:10.1111/j.1365-2486.2009.01877.x (2009).

20 Hickler, T. *et al.* CO(2) fertilization in temperate FACE experiments not representative of boreal and tropical forests. *Glob. Change Biol.* **14**, 1531-1542, doi:10.1111/j.1365-2486.2008.01598.x (2008).

21 Peñuelas, J., Canadell, J. G. & Ogaya, R. Increased water-use efficiency during the 20th century did not translate into enhanced tree growth. *Global Ecology and Biogeography* **20**, 597-608, doi:10.1111/j.1466-8238.2010.00608.x (2011).

22 Gedalof, Z. e. & Berg, A. A. Tree ring evidence for limited direct CO2 fertilization of forests over the 20th century. *Global Biogeochemical Cycles* **24**, GB3027, doi:10.1029/2009GB003699 (2010).

23 Hyvonen, R. *et al.* The likely impact of elevated CO2 , nitrogen deposition, increased temperature and management on carbon sequestration in temperate and boreal forest ecosystems: a literature review. *New Phytol* **173**, 463-480, doi:10.1111/j.1469-8137.2007.01967.x (2007).

24 Yarie, J. & Van Cleve, K. Long-term monitoring of climatic and nutritional affects on tree growth in interior Alaska. *Canadian Journal of Forest Research-Revue Canadienne De Recherche Forestiere* **40**, 1325-1335, doi:Doi 10.1139/X10-114 (2010).

25 Thornton, P. E., Lamarque, J.-F., Rosenbloom, N. A. & Mahowald, N. M. Influence of carbon-nitrogen cycle coupling on land model response to CO2 fertilization and climate variability. *Global Biogeochemical Cycles* **21**, GB4018, doi:10.1029/2006GB002868 (2007).

26 Kurz, W. A., Stinson, G. & Rampley, G. Could increased boreal forest ecosystem productivity offset carbon losses from increased disturbances? *Philosophical Transactions of the Royal Society B: Biological Sciences* **363**, 2259-2268, doi:10.1098/rstb.2007.2198 (2008).

27 Epstein, H. E. *et al.* Dynamics of aboveground phytomass of the circumpolar Arctic tundra during the past three decades. *Environmental Research Letters* **7**, doi:10.1088/1748-9326/7/1/015506 (2012).

28 Raynolds, M. K., Walker, D. A., Epstein, H. E., Pinzon, J. E. & Tucker, C. J. A new estimate of tundra-biome phytomass from trans-Arctic field data and AVHRR NDVI. *Remote Sensing Letters* **3**, 403-411, doi:10.1080/01431161.2011.609188 (2012).

29 Saugier, B., Roy, J. & Mooney, H. A. in *Terrestrial Global Productivity* (eds J. Roy, B. Saugier, & H.A. Mooney) 543-557 (Academic Press, 2001).

30 Kloster, S., Mahowald, N. M., Randerson, J. T. & Lawrence, P. J. The impacts of climate, land use, and demography on fires during the 21st century simulated by CLM-CN. *Biogeosciences* **9**, 509-525, doi:10.5194/bg-9-509-2012 (2012).

31 Flannigan, M., Stocks, B., Turetsky, M. & Wotton, M. Impacts of climate change on fire activity and fire management in the circumboreal forest. *Glob. Change Biol.* **15**, 549-560, doi:10.1111/j.1365-2486.2008.01660.x (2009).

32 Rupp, T. S., Starfield, A. M. & Chapin Iii, F. S. A frame-based spatially explicit model of subarctic vegetation response to climatic change: comparison with a point model. *Landscape Ecol* **15**, 383-400 (2000).

33 Mack, M. C. *et al.* Carbon loss from an unprecedented Arctic tundra wildfire. *Nature* **475**, 489-492, doi:http://www.nature.com/nature/journal/v475/n7357/abs/nature10283.html - supplementary-information (2011).

34 Guo, L. D., Ping, C. L. & Macdonald, R. W. Mobilization pathways of organic carbon from permafrost to arctic rivers in a changing climate. *Geophysical Research Letters* **34**, doi:L13603 10.1029/2007gl030689 (2007).

35 Sharkey, A. J. C. *Combining artificial neural nets : ensemble and modular multi-net systems*. (Springer, 1999).

36 Aspinall, W. A route to more tractable expert advice. *Nature* **463**, 294-295, doi:10.1038/463294a (2010).

37 Halpern, B. S. *et al.* A global map of human impact on marine ecosystems. *Science* **319**, 948-952, doi:10.1126/science.1149345 (2008).

38 Lenton, T. M. *et al.* Tipping elements in the Earth's climate system. *P Natl Acad Sci USA* **105**, 1786-1793, doi:10.1073/pnas.0705414105 (2008).

39 Lawrence, D. M., Slater, A. G. & Swenson, S. C. Simulation of Present-Day and Future Permafrost and Seasonally Frozen Ground Conditions in CCSM4. *Journal of Climate* **25**, 2207-2225, doi:10.1175/jcli-d-11-00334.1 (2012).

40 Algina, J., Keselman, H. J. & Penfield, R. D. An alternative to Cohen's standardized mean difference effect size: A robust parameter and confidence interval in the two independent groups case. *Psychol. Methods* **10**, 317-328, doi:10.1037/1082.989x.10.3.317 (2005).

41 Potter, C. S. & Klooster, S. A. Global model estimates of carbon and nitrogen storage in litter and soil pools: Response to changes in vegetation quality and biomass allocation. *Tellus B* **49**, 1-17, doi:10.1034/j.1600-0889.49.issue1.1.x (1997).

42 Balshi, M. S. *et al.* The role of historical fire disturbance in the carbon dynamics of the pan-boreal region: A process-based analysis. *J Geophys Res-Biogeo* **112**, -, doi:Artn G02029 Doi 10.1029/2006jg000380 (2007).

43 Giglio, L. *et al.* Assessing variability and long-term trends in burned area by merging multiple satellite fire products. *Biogeosciences* **7**, 1171-1186, doi:10.5194/bg-7-1171-2010 (2010).

44 Hayes, D. J. *et al.* Is the northern high-latitude land-based CO2 sink weakening? *Global Biogeochem. Cycles* **25**, GB3018, doi:10.1029/2010gb003813 (2011).

45 van der Werf, G. R. *et al.* Global fire emissions and the contribution of deforestation, savanna, forest, agricultural, and peat fires (1997–2009). *Atmos. Chem. Phys.* **10**, 11707-11735, doi:10.5194/acp-10-11707-2010 (2010).

46 Rocha, A. V. *et al.* The footprint of Alaskan tundra fires during the past half-century: implications for surface properties and radiative forcing. *Environmental Research Letters* **7**, doi:10.1088/1748-9326/7/4/044039 (2012).

47 Aufdenkampe, A. K. *et al.* Riverine coupling of biogeochemical cycles between land, oceans, and atmosphere. *Frontiers in Ecology and the Environment* **9**, 53-60, doi:10.1890/100014 (2011).

48 Battin, T. J. *et al.* The boundless carbon cycle. *Nature Geosci* **2**, 598-600 (2009).

49 Holmes, R. M. *et al.* Seasonal and Annual Fluxes of Nutrients and Organic Matter from Large Rivers to the Arctic Ocean and Surrounding Seas. *Estuaries and Coasts* **35**, 369-382, doi:10.1007/s12237-011-9386-6 (2012).

50 Vonk, J. E. *et al.* Activation of old carbon by erosion of coastal and subsea permafrost in Arctic Siberia. *Nature* **489**, 137-140, doi:10.1038/nature11392 (2012).

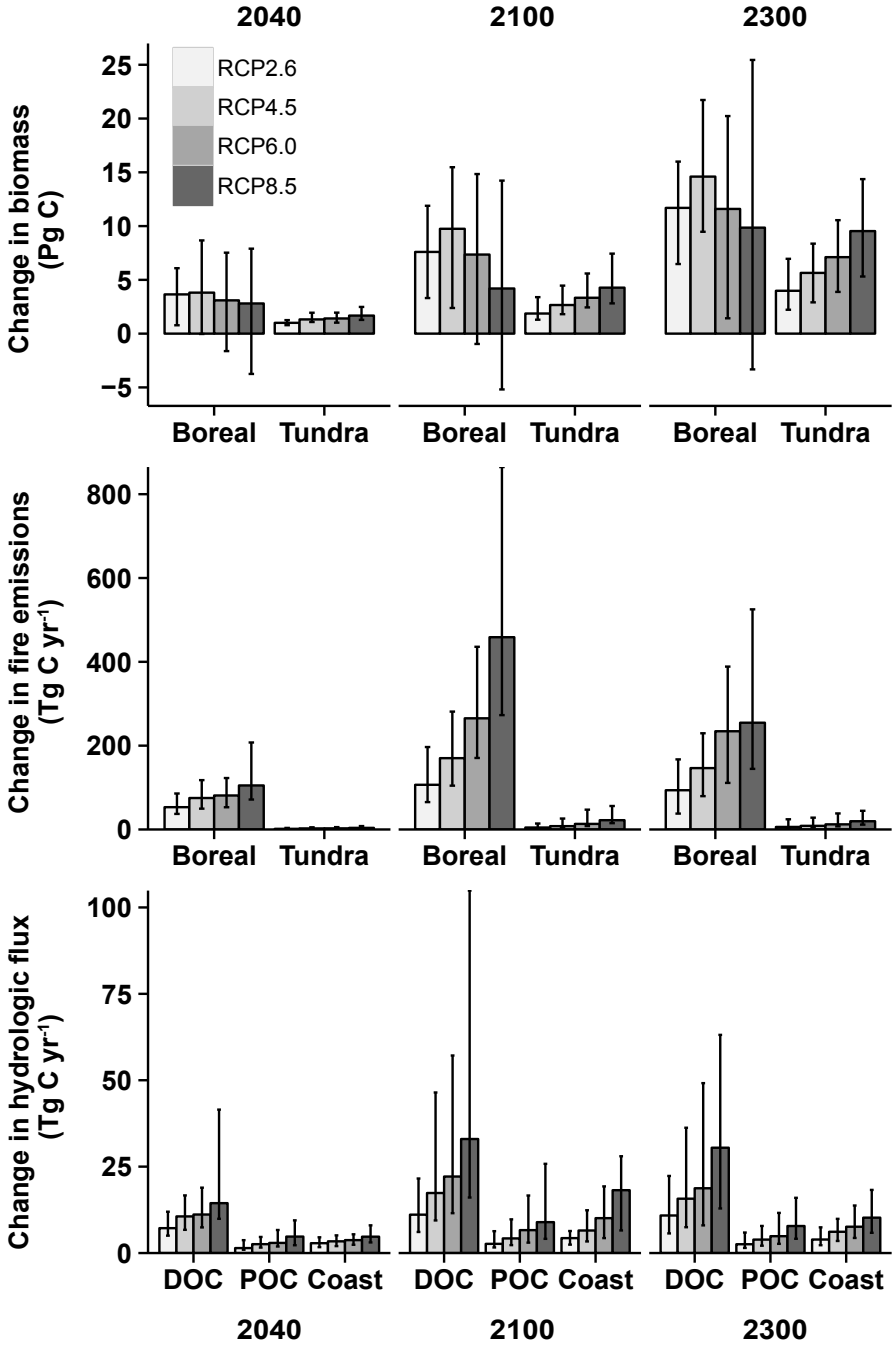

Figure 2.1 Estimates of change in non-soil biomass, wildfire emissions, and hydrologic C flux from the permafrost region for four warming scenarios at three time points. All values represent change from current pools or fluxes reported in Table 2.1. Biomass includes above and belowground living biomass, standing deadwood, and litter. Dissolved and particulate organic C (DOC and POC respectively) fluxes represent transfer of C from terrestrial to aquatic ecosystems. "Coast" represents POC released by coastal erosion. Columns represent bootstrapped means and error bars represent bootstrapped 95% confidence intervals. All data were Winsorized at 20% before calculating means and intervals. For relative change see A1.1; Fig. 4. Representative concentration pathway (RCP) scenarios range from aggressive emissions reductions (RCP2.6) to sustained human emissions (RCP8.5).

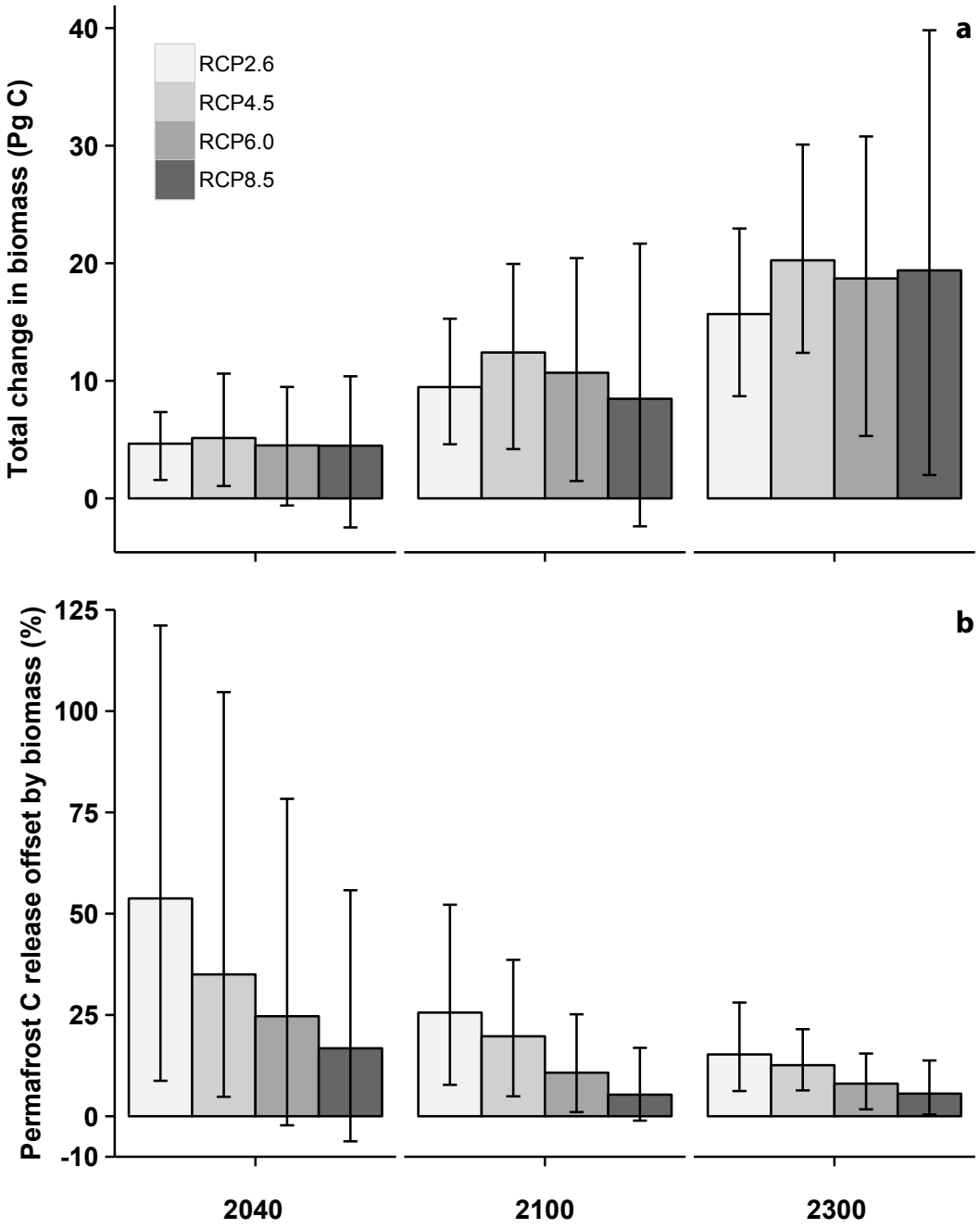

Figure 2.2 Total change in non-soil biomass (a) and percentage of permafrost region C release offset by change in non-soil biomass (b). Estimates of permafrost C release used in estimating percentage offset are recalculated from data presented in Schuur et al. [3]. See Fig. 2.1 for definition of RCP scenarios and symbology.

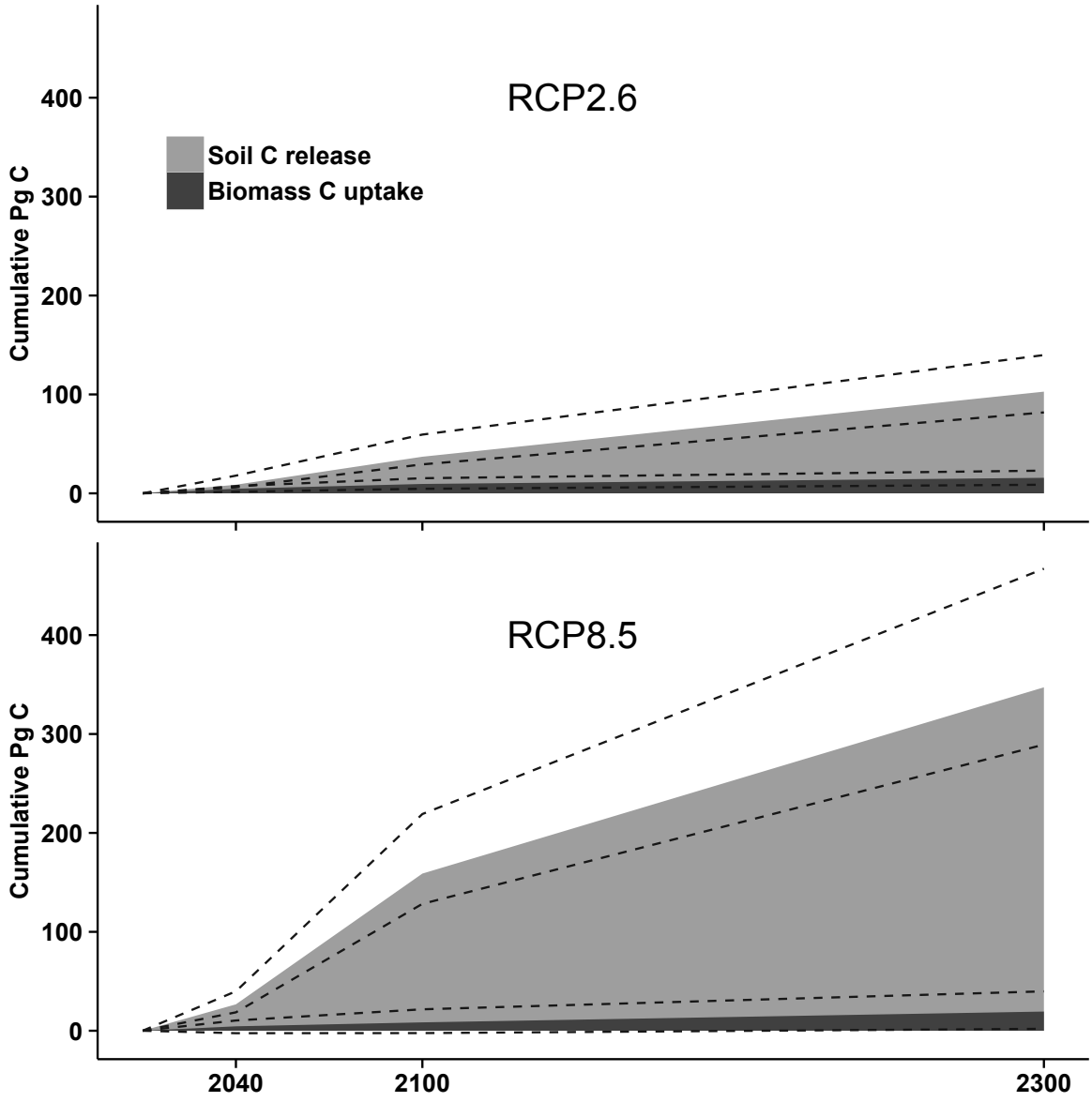

Figure 2.3 A comparison of soil C release (recalculated from Schuur et al.[3]) and non-soil biomass uptake in the permafrost region for two warming scenarios. Polygons represent mean cumulative change and dotted lines represent bootstrapped 95% confidence intervals. Biomass C uptake is overlayed on soil C release to show the proportion of C release potentially offset by biomass. Linear rates of change were assumed between the three dates where estimates were provided. See Fig. 2.1 for definition of RCP scenarios.

Table 2.1 Composition and characteristics of participant group

	Biomass	Wildfire	Hydrologic flux
Number of respondents	46	34	35
Average responses per question*	37	29	31
Primary region of study			
Asia	10	3	8
Europe	12	5	9
North America	27	27	18
Circumpolar	12	6	9
Primary biome of study			
Arctic	31	13	27
Boreal	27	29	18
Both	14	9	12
Average modeling/field self rating**	3.6	3.7	4.1
Combined years of experience	762	533	521
Ratio male:female	2.6	2.8	4.9

Background information on survey participants. Experts could indicate multiple regions and biomes of study. *Responses with self-rated expertise of 1 were excluded and not all experts provided estimates for all questions. **Experts rated themselves on a 1-5 scale where 1=exclusive modeler and 5=exclusive field researcher.

Table 2.2 Estimates of current permafrost region organic carbon pools and fluxes

Biomass

	Aboveground biomass	Belowground biomass [29]	Dead wood [17]	Litter	Total non-soil biomass
Boreal forest (Pg C)	43.6 [16]	16.1	16	27 [17]	102.7
Tundra (Pg C)	2.4 [27]	4.0		2 [41]	8.4

Wildfire

	Boreal forest (Eurasia)	Boreal forest (N. America)	Total Boreal forest [42-45]	Total Tundra
Area burned (km^2 yr^{-2})	62,100	22,500	84,600	4,200 [46]
CO_2 emissions from fire (Tg C yr^{-1})	194	56	250	8 [33]

Hydrologic OC flux

	DOC	POC (Riverine)	POC (coastal)	Total OC
Delivery to freshwater ecosystems (Tg yr^{-1})	100 [16]	20 [47,48]	na	120
Delivery to Arctic Ocean and surrounding seas (Tg yr^{-1})	36 [49]	6 [16]	18 [16,50]	60

Literature-based estimates of belowground biomass were calculated from aboveground or total biomass with ratios from Saugier et al.[29]. POC delivery to freshwater ecosystems was calculated from ocean POC delivery with downscaled global ratio of 0.75 for sedimentation. POC from coastal erosion is the sum of Vonk et al.[50] and McGuire et al.[16]. Considerable uncertainty remains around many of these estimates

Table 2.3 Sources of uncertainty in system response to climate change

Biomass		**Wildfire**		**Hydrologic C flux**	
Source of uncertainty	%	Source of uncertainty	%	Source of uncertainty	%
Water balance	56	Vegetation shift	73	Water balance	41
Wildfire	47	Water balance	58	Hydrologic flowpath	39
Permafrost degradation	40	Human disturbance	27	Permafrost degradation	24
Human disturbance	29	Permafrost degradation	18	Photo and bio-lability	24
Insect damage	27	Seasonality	15	Vegetation shift	20
Vegetation shift	24	Regional differences	12	Fluvial erosion	11
Treeline dynamics	16				
Nutrient availability	13				
Non-insect herbivores	11				

Major factors contributing uncertainty to projections of future system response based on expert comments. Rank is based on percent of experts who listed each factor in their responses. All sources listed by 10% or more of each group are included here. Water balance includes comments mentioning precipitation, soil moisture, runoff, infiltration, or discharge. Permafrost degradation includes comments referring to permafrost collapse (thermokarst) and active layer deepening.

Appendix 2.0 Extended data and supplementary information to Chapter 2

A2.0.1 Extended Data

Table A2.1 Average self-rated expertise and confidence by survey and question

	Expertise	Confidence
Biomass		
Boreal Forest	3.1	2.2
Arctic Tundra	3.5	2.8
Wildfire		
Q1 Boreal Forest	3.5	2.6
Q1 Arctic Tundra	2.8	2.0
Q2 Boreal Forest	3.4	2.3
Q2 Arctic Tundra	2.6	1.7
Hydrologic C flux		
Q1 DOC	3.4	2.4
Q1 POC	2.8	2.1
Q2 DOC	3.4	2.4
Q2 POC	2.8	2.2

Experts rated themselves on a 1-5 scale for expertise and confidence for each question and biome (or parameter for the hydrologic C flux survey). Full definitions below. Responses where experts rated themselves a 1 on the expertise scale (little familiarity or direct experience) were excluded before quantitative analyses but are included in the averages here. The “Confidence level” scale was defined as follows: 1. My answer is my best guess but I am not confident in it; it could easily be far off the mark. 2. My answer is an educated guess; it could be far off the mark, but I have some confidence in it. 3. I am moderately confident in my answer; it surely isn’t precise, but it likely is in the ballpark. 4. I am confident in my answer; the true value is likely to be somewhat different from my answer, but it is unlikely to be dramatically different. 5. Given current understanding, I would be surprised if my answer were far off from the true value. The “Expertise level” scale was defined as follows: 1. I have little familiarity with the literature and I do not actively work on these particular questions. 2. I have some familiarity with the literature and I’ve worked on related questions but haven't contributed to the literature on this issue; it is

not an area of central expertise for me. 3. I have worked on related issues and have contributed to the relevant literature but do not consider myself one of the foremost experts on this particular issue. 4. I am very familiar with relevant literature and have worked on related questions. This is an area of central expertise for me. 5. I contribute actively to the literature directly concerned with this issue, and I consider myself one of the foremost experts on it.

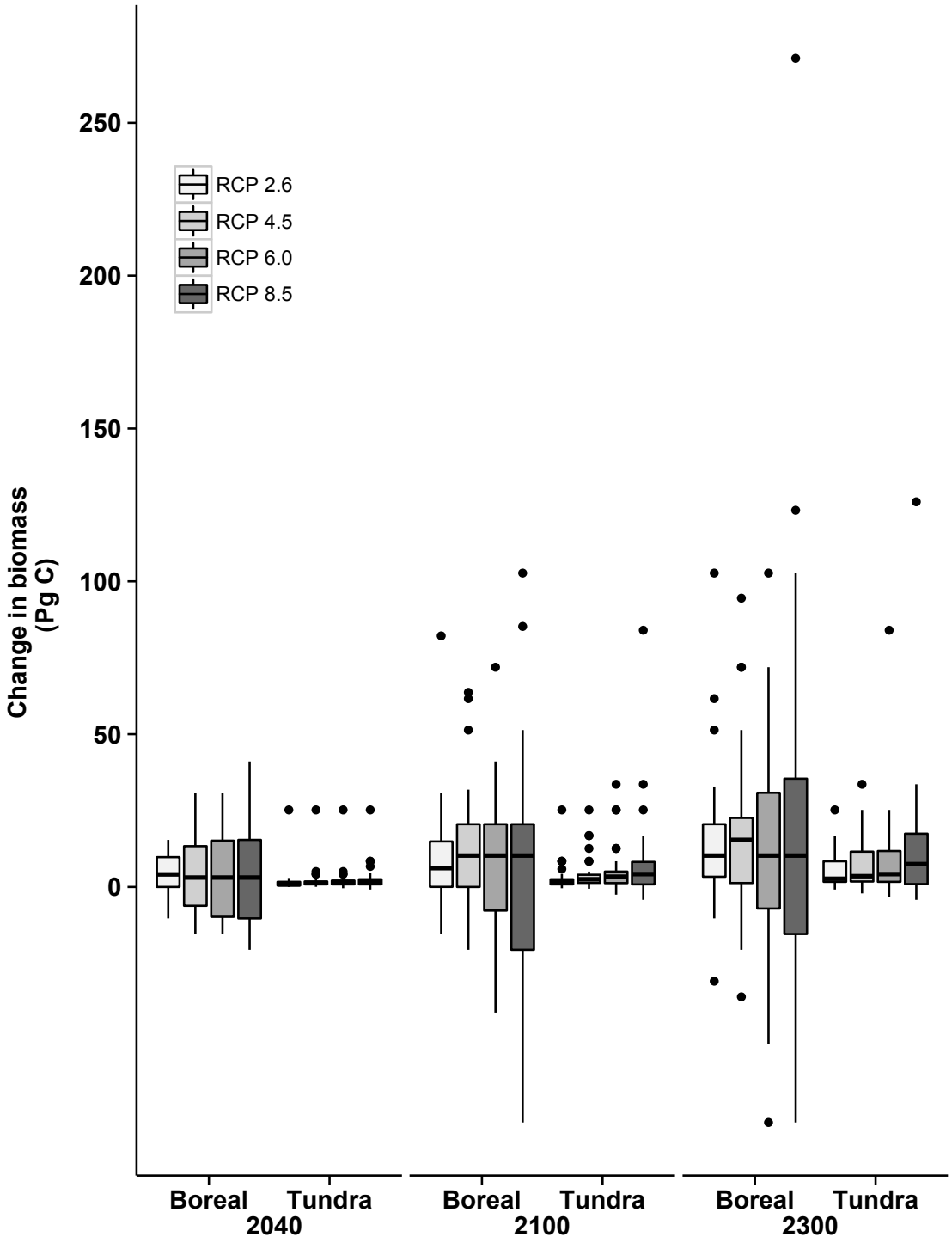

Figure A2.1 Distribution of biomass estimates for boreal forest and tundra at three time points and four warming scenarios. Box plots represent median, quartiles, minimum and maximum within 1.5 times the interquartile range, and outliers beyond 1.5 IQR. Representative concentration pathway (RCP) scenarios range from aggressive emissions reductions (RCP2.6) to sustained human emissions (RCP8.5).

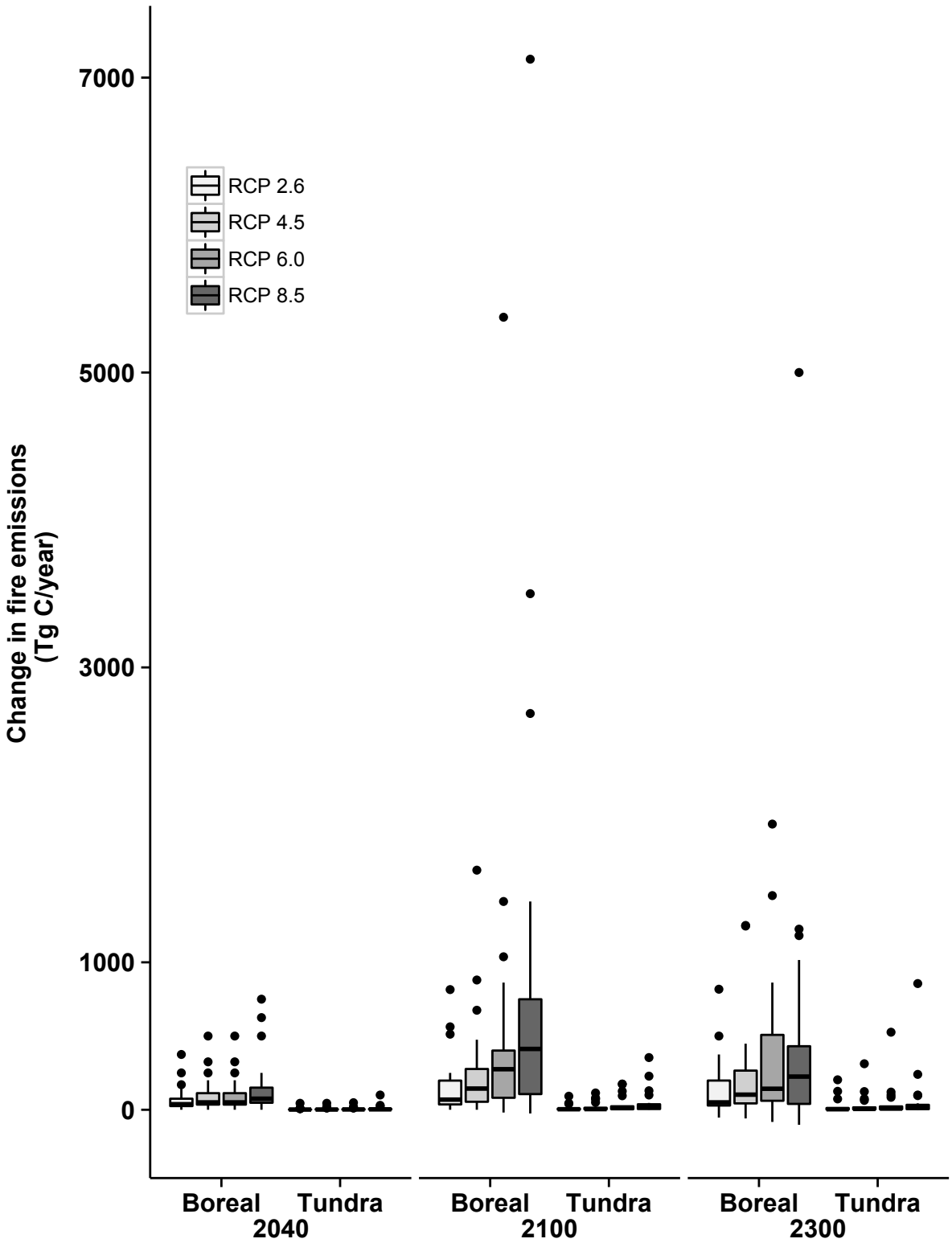

Figure A2.2 Distribution of wildfire estimates for boreal forest and tundra at three time points and four warming scenarios. See Fig. 2.1 for definition of RCP scenarios and symbology.

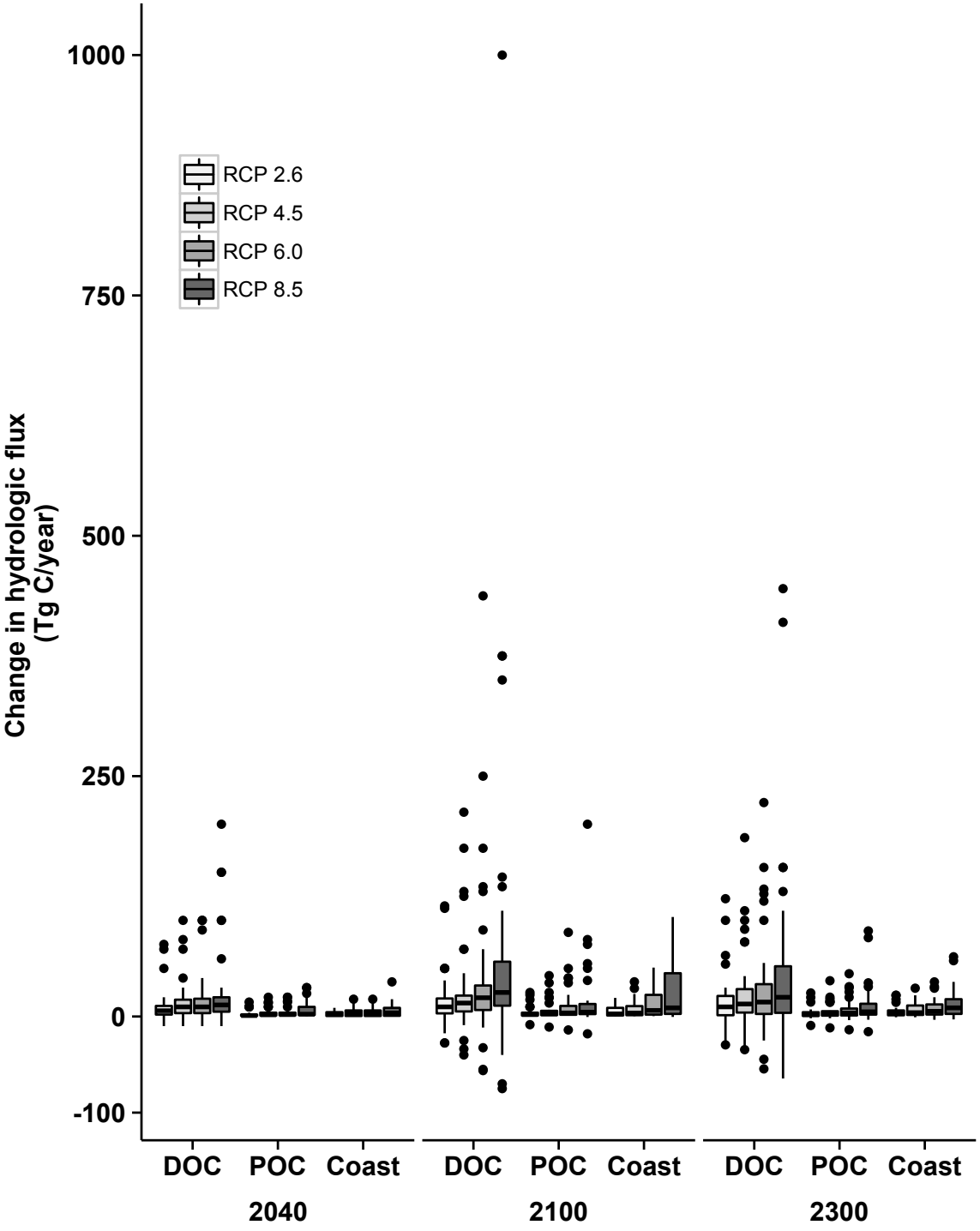

Figure A2.3 Distribution of hydrologic carbon flux estimates for boreal forest and tundra at three time point and four warming scenarios. See Fig. 1 for definition of RCP scenarios and symbology.

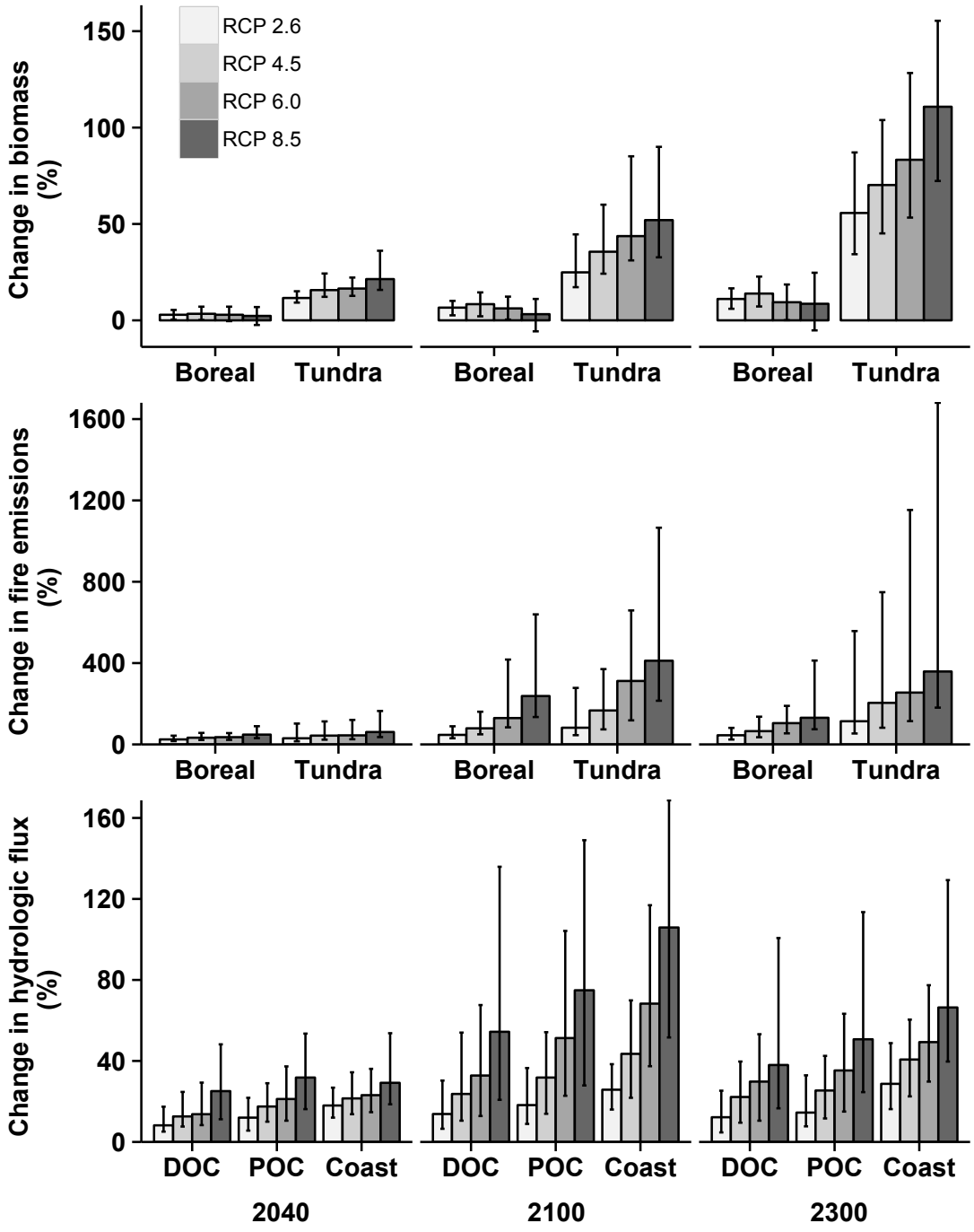

Figure A2.4 Change in biomass, wildfire emissions, and hydrologic carbon flux relative to current levels. Columns represent mean values, and error bars represent 95% confidence intervals of the 20% Winsorized data. Statistics were bootstrapped since distributions did not meet assumptions of normality.

A2.0.2 Supplementary information

A2.0.2.1 Names and affiliations of contributing authors from the Permafrost Carbon Network

Benjamin W. Abbott
University of Alaska Fairbanks, AK, USA
George R. Aiken
US Geological Survey, Boulder, CO, USA
Heather D. Alexander
University of Texas-Brownsville, TX, USA
Rainer M.W. Amon
Texas A&M University at Galveston, TX, USA
Brian W Benscoter
Florida Atlantic University, Davie, FL, USA
Yves Bergeron
Forest Research Institute, Université du Québec en Abitibi-Témiscamingue, QC, Canada
Kevin Bishop
Uppsala University, Department of Earth Sciences, Department of Aquatic Sciences and Assessment, Swedish University of Agricultural Sciences, Uppsala, Sweden
Olivier Blarquez
Université du Québec à Montréal, QC, Canada
Benjamin Bond-Lamberty
Pacific Northwest National Lab, College Park, MD, USA
William B. Bowden
University of Vermont, Burlington, VT, USA
Amy L. Breen
Scenarios Network for Alaska & Arctic Planning, International Arctic Research Center, University of Alaska Fairbanks, AK, USA
M. Syndonia Bret-Harte
University of Alaska Fairbanks, AK, USA
Ishi Buffam
University of Cincinnati, OH, USA
Yihua Cai
State Key Laboratory of Marine Environmental Science, Xiamen University, China
Christopher Carcaillet
Ecole Pratique des Hautes Etudes, Paris, France
Sean K. Carey
McMaster University, Hamilton, ON, Canada
F. Stuart Chapin, III
University of Alaska Fairbanks, AK, USA
Jing M. Chen
University of Toronto, ON, Canada

Han Chen
Lakehead University, Thunder Bay, ON, Canada
Torben R. Christensen
Lund University, Sweden, Arctic Research Centre, Aarhus University, Denmark
Lee W. Cooper
University of Maryland Center for Environmental Science, Cambridge, MD, USA
J. Hans C. Cornelissen
Systems Ecology, VU University, Amsterdam, Netherlands
William de Groot
Canadian Forest Service, Natural Resources, Sault Ste. Marie, ON, Canada
Thomas H. DeLuca
School of Environmental and Forest Sciences, University of Washington, Seattle, WA, USA
Ellen Dorrepaal
Climate Impacts Research Centre, Umeå University, Sweden
Howard E. Epstein
University of Virginia, Charlottesville, VA, USA
Ned Fetcher
Wilkes University, Wilkes-Barre, PA, USA
Jacques C. Finlay
Department of Ecology, Evolution and Behavior, University of Minnesota, St. Paul, MN
Michael D. Flannigan
University of Alberta, AB, Canada
Bruce C. Forbes
Arctic Centre, University of Lapland, Rovaniemi, Finland
Nancy H.F. French
Michigan Tech Research Institute, Michigan Technological University, Ann Arbor, Michigan, USA
Sylvie Gauthier
Natural Resources Canada, Canadian Forest Service, Laurentian Forestry Center, Stn. Sainte-Foy, QC, Canada
Martin P. Girardin
Natural Resources Canada, Canadian Forest Service, QC, Canada
Scott J. Goetz
Woods Hole Research Center, Falmouth, MA, USA
Johann G. Goldammer
Global Fire Monitoring Center, Freiburg, Germany
Laura Gough
University of Texas Arlington, Arlington, TX, USA
Paul Grogan
Department of Biology, Queen's University, Kingston, ON, Canada
Laodong Guo
University of Wisconsin-Milwaukee, School of Freshwater Sciences, Milwaukee, WI, USA

Tamara K. Harms
University of Alaska Fairbanks, Fairbanks, AK, USA
Philip E. Higuera
Department of Forest, Rangeland, and Fire Sciences, University of Idaho, Moscow, ID, USA
Larry Hinzman
University of Alaska Fairbanks, AK, USA
Teresa N. Hollingsworth
USDA Forest Service, PNW Research Station, Fairbanks, AK, USA
Feng Sheng Hu
Department of Plant Biology, University of Illinois, Champaign, IL, USA
Gustaf Hugelius
Department of Physical Geography and Quaternary Geology, Stockholm University, Sweden
Elchin E. Jafarov
National Snow and Ice Data Center, Cooperative Institute for Research in Environmental Sciences, University of Colorado at Boulder, CO, USA
Randi Jandt
University of Alaska Fairbanks, AK, USA
Jill F. Johnstone
Biology Department, University of Saskatchewan, Saskatoon, SK, Canada
Jeremy B. Jones
University of Alaska Fairbanks, Fairbanks, AK, USA
Jan Karlsson
Climate Impacts Research Centre Abisko, Department of Ecology and Environmental Science, Umeå University, Sweden
Eric S. Kasischke
Department of Geographical Sciences, University of Maryland, College Park, MD, USA
Gerhard Kattner
Alfred Wegener Institute Helmholtz Center for Polar and Marine Research, Bremerhaven, Germany
Ryan Kelly
Department of Plant Biology, University of Illinois, Champaign, IL, USA
Frida Keuper
Climate Impacts Research Centre Abisko, Umeå University, Sweden, Climate Impacts Research Centre Abisko, Umeå University, Sweden; INRA, AgroImpact UPR1158, Barenton Bugny, France
George W. Kling
University of Michigan, Ann Arbor, MI, USA
Pirkko Kortelainen
Finnish Environment Institute, Helsinki, Finland
Jari Kouki
School of Forest Sciences, University of Eastern Finland, Finland

Peter Kuhry
Department of Physical Geography and Quaternary Geology, Stockholm University, Sweden
Hjalmar Laudon
Swedish University of Agricultural Sciences, Umeå, Sweden
Isabelle Laurion
Centre Eau Terre Environnement, Institut national de la recherche scientifique, Québec, QC, Canada
Robie W. Macdonald
Institute of Ocean Science, Sidney, BC, Canada
Michelle C. Mack
University of Florida, Department of Biology, Gainesville, FL, USA
Paul J. Mann
Northumbria University, Newcastle Upon Tyne, UK
Pertti J. Martikainen
University of Eastern Finland, Joensuu, Finland
James W. McClelland
University of Texas at Austin, Marine Science Institute, Port Aransas, TX, USA
A. David McGuire
U.S. Geological Survey, Alaska Cooperative Fish and Wildlife Research Unit, University of Alaska Fairbanks, AK, USA
Ulf Molau
University of Gothenburg, Department of Biological and Environmental Sciences, Sweden
Susan M. Natali
Woods Hole Research Center, Falmouth, MA, USA
Steven F. Oberbauer
Florida International University, Miami, FL, USA
David Olefeldt
University of Alberta, Edmonton, AB, Canada
David Paré
Natural Resources Canada, Canadian Forest Service, QC, Canada
Marc-André Parisien
Natural Resources Canada, Canadian Forest Service, Northern Forestry Centre, Edmonton, AB, Canada
Serge Payette
Université Laval, Québec City, QC, Canada
Changhui Peng
Center of CEF/ESCER, University of Quebec at Montreal, Canada and State Key Laboratory of Soil Erosion and Dryland Farming on the Loess Plateau, College of Forestry, Northwest A&F University, Yangling, China
Oleg S. Pokrovsky
Georesources and Environment, CNRS, Toulouse, France and BIO-GEO-CLIM Laboratory, Tomsk State University, Tomsk, Russia
Edward B. Rastetter
The Ecosystems Center, Marine Biological Laboratory, Woods Hole, MA, USA

Peter A. Raymond
Yale School of Forestry and Environmental Studies, New Haven, CT, USA
Martha K. Raynolds
Institute of Arctic Biology, University of Alaska Fairbanks, AK, USA
Guillermo Rein
Department of Mechanical Engineering, Imperial College London, UK
James F. Reynolds
Nicholas School of the Environment, Duke University, Durham, NC, USA, and Institute of Arid AgroEcology, School of Life Sciences, Lanzhou University, Lanzhou, China
Adrian V. Rocha
University of Notre Dame, Department of Biological Sciences, IN, USA
Brendan M. Rogers
Woods Hole Research Center, Falmouth, MA, USA
Christina Schädel
University of Florida, Department of Biology, Gainesville, FL, USA
Kevin Schaefer
National Snow and Ice Data Center, Cooperative Institute for Research in Environmental Sciences, University of Colorado at Boulder, Colorado, USA
Inger K. Schmidt
Department of Geosciences and Natural Resource Management, University of Copenhagen, Denmark
Anatoly Shvidenko,
International Institute for Applied Systems Analysis, Laxenburg, Austria and Institute of Forest, Krasnoyarsk, Russia
Jasper Sky
Affiliate, Cambridge Centre for Climate Change Research, UK
Robert G.M. Spencer
Woods Hole Research Center, Falmouth, MA, USA
Gregory Starr
University of Alabama, Department of Biological Sciences, Tuscaloosa AL, USA.
Robert G. Striegl
US Geological Survey, Boulder, CO, USA
Suzanne E. Tank
Department of Geography, York University, Toronto, ON, Canada, Department of Biological Sciences, University of Alberta, Edmonton, AB, Canada
Roman Teisserenc
Université de Toulouse: INPT, UPS, CNRS. Laboratoire Écologie Fonctionnelle et Environnement (EcoLab), Castanet-Tolosan, France
Lars J. Tranvik
Limnology, Department of Ecology and Genetics, Uppsala University, Sweden
Merritt Turetsky
Department of Integrative Biology, University of Guelph, ON, Canada
Tarmo Virtanen
Department of Environmental Sciences, University of Helsinki, Finland

Jorien E. Vonk
Utrecht University, Department of Earth Sciences, Netherlands
Jeffrey M. Welker
University of Alaska Anchorage, AK, USA
Kimberly P. Wickland
US Geological Survey, Boulder, CO, USA
Sergei Zimov
Northeast Science Station of the Russian Academy of Sciences, Cherskii, Russia

A2.0.2.2 Survey respondents

Biomass survey respondents (* signifies lead expert)

Heather Alexander
Benjamin Bond-Lamberty
Amy L. Breen
M. Syndonia Bret-Harte
F. Stuart Chapin, III*
Han Chen
Jing M. Chen
Torben R. Christensen
J. Hans C. Cornelissen
William de Groot
Ellen Dorrepaal
Howard E. Epstein*
Ned Fetcher
Michael D. Flannigan
Bruce C. Forbes
Scott J. Goetz
Laura Gough
Paul Grogan
Philip E. Higuera
Teresa N. Hollingsworth*
Gustaf Hugelius
Elchin E. Jafarov
Frida Keuper
Peter Kuhry
Michelle C. Mack*
Pertti J. Martikainen
A. David McGuire
Ulf Molau
Susan M. Natali
Steven F. Oberbauer
David Paré
Changhui Peng
Edward B. Rastetter
Martha K. Raynolds
James F. Reynolds
Adrian V. Rocha
Christina Schädel
Kevin Schaefer
Inger K. Schmidt
Gaius R. Shaver
Anatoly Shvidenko
Gregory Starr

Merritt Turetsky*
Tarmo Virtanen
Jeffrey M. Welker
Sergei Zimov

Wildfire survey respondents (* signifies lead expert)

Brian W Benscoter
Yves Bergeron
Olivier Blarquez
Benjamin Bond-Lamberty
Amy L. Breen
M. Syndonia Bret-Harte
Christopher Carcaillet
F. Stuart Chapin, III
Han Chen
William de Groot
Thomas H. DeLuca
Michael D. Flannigan*
Nancy H.F. French
Sylvie Gauthier
Martin P. Girardin
Johann G. Goldammer
Philip E. Higuera
Teresa N. Hollingsworth
Feng Sheng Hu
Randi Jandt
Jill F. Johnstone
Eric S. Kasischke
Ryan Kelly
Jari Kouki
Michelle C. Mack
A. David McGuire*
Marc A. Parisien
Serge Payette
Guillermo Rein
Adrian V. Rocha*
Brendan Rogers
Gaius R. Shaver
Anatoly Shvidenko
Merritt Turetsky

Hydrologic carbon flux survey respondents (* signifies lead expert)

Benjamin W. Abbott*
George R. Aiken
Rainer M.W. Amon
Kevin Bishop
William B. Bowden*
Ishi Buffam
Yihua Cai
Sean K. Carey
Lee W. Cooper
Jacques C. Finlay
Laodong Guo
Tamara K. Harms*
Larry Hinzman
Jeremy B. Jones*
Jan Karlsson
Gerhard Kattner
George W. Kling
Pirkko Kortelainen
Hjalmar Laudon
Isabelle Laurion
Robie W. Macdonald
Paul J. Mann
James W. McClelland
A. David McGuire
David Olefeldt
Oleg S. Pokrovsky
Peter A. Raymond
Robert G.M. Spencer
Robert G. Striegl
Suzanne E. Tank*
Roman Teisserenc
Lars J. Tranvik
Jorien E. Vonk*
Kimberly P. Wickland*
Sergei Zimov

A2.0.2.3 Biomass questionnaire

Net Ecosystem Carbon Balance of the Permafrost Region: Arctic and Boreal Biomass Survey

Introduction

The goal of this survey is to document expert opinion on the possible net ecosystem carbon balance of the permafrost region under arctic and boreal warming scenarios. Possible thresholds and tipping points in the relationship between temperature increase and high-latitude biomass are of particular interest, since such non-linearity is difficult to predict on the basis of models.

We recognize that climate-change-driven feedbacks in complex Earth systems are not, and cannot be, precisely and definitively modeled. As such, we are only asking for your informed opinion, realizing that some of the included parameters may not be well understood. By administering this survey to scientists with the most applicable expertise, we want to identify and evaluate the possible and probable magnitude of biomass response in the arctic and subarctic.

Instructions

You will be asked to provide estimates of boreal forest and arctic tundra non-soil biomass over short-term (2010-2040), medium-term (2010-2100), and long-term (2010-2300) time frames for four warming scenarios. These scenarios of regional arctic warming were generated with NCAR's Community Climate System Model (CCSM4) with inputs from the most recent IPCC radiative forcing scenarios (**Figure 1**). To minimize the possibility of misinterpretation, we have also provided a table showing the amount of warming predicted in Figure 1 by the end of each of the three time scales (**Table 1**). Climate projections, and estimates of system response, become increasingly uncertain for distant time frames. However, because carbon balance in the permafrost region can take many decades or centuries to fully respond to disturbance, we have included the 2300 time step to account for lags in this response.

In addition to answering each question, you will have a chance to indicate your level of confidence and expertise concerning your answer; and provide additional comments on how you selected your estimates. These supporting questions allow us to compare responses from multiple experts and are just as valuable as your quantitative estimates. We also ask that you identify key sources of uncertainty concerning the future response of the system (what processes missing from current models will likely play an important role, what data gaps exist, etc.), and provide any comments on how you generated your estimates. If there is not yet clear supporting evidence in the literature, but you have some basis for an estimate based on professional judgment, please make a note of that.

The five-point "**Confidence level**" scale is defined as follows:

- **1=** My answer is my best guess but I am not confident in it; it could easily be far off the mark.
- **2=** My answer is an educated guess; it could be far off the mark, but I have some confidence in it.
- **3=** I am moderately confident in my answer; it surely isn't precise, but it likely is in the ballpark.
- **4=** I am confident in my answer; the true value is likely to be somewhat different from my answer, but it is unlikely to be dramatically different.
- **5=** Given current understanding, I would be surprised if my answer were far off from the true value.

The five-point "**Expertise level**" scale is defined as follows:

- **1=** I have little familiarity with the literature and I do not actively work on these particular questions.
- **2=** I have some familiarity with the literature and I've worked on related questions but haven't contributed to the literature on this issue; it is not an area of central expertise for me.

3= I have worked on related issues and have contributed to the relevant literature but do not consider myself one of the foremost experts on this particular issue.

4= I am very familiar with relevant literature and have worked on related questions. This is an area of central expertise for me.

5= I contribute actively to the literature directly concerned with this issue, and I consider myself one of the foremost experts on it.

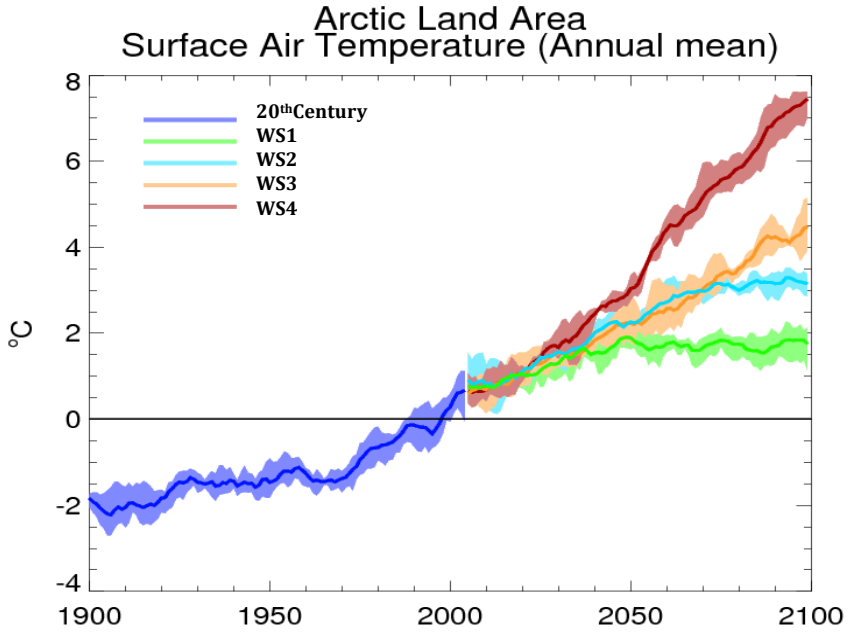

Figure 1. CCSM4: Anomaly from 1985-2004 (7-yr running average; Greenland excluded). Though not shown in this figure, temperature increase is assumed to stabilize and level off after 2100 for the purposes of this survey.

	Warming at 2040 (°C)	Warming at 2100 (°C)	Warming at 2300 (°C)
WS 1	1.5	2.0	2.0
WS 2	2.0	3.0	3.0
WS 3	2.0	4.5	4.5
WS 4	2.5	7.5	7.5

Table 1. Temperature increases for the four warming scenarios (designated here as WS 1-4). Values given represent the regional Arctic temperature increase achieved by the year indicated. Values for WS1-4 correspond to the IPCC representative concentration pathways (RCP): 2.6, 4.5, 6.0, and 8.5 respectively.

Questions

1. How much change in boreal forest and arctic tundra non-soil biomass would result from the following increases in pan-arctic mean annual surface air temperature? (Positive numbers represent % increase, negative represent % decrease).

Note: This question addresses changes in non-soil biomass for the circumpolar tundra and boreal forest due to direct climate forcing (temperature, precipitation, atmospheric CO_2, seasonality etc.) as well as indirect effects (changes in primary productivity, vegetation shifts, nutrient availability, insects, pathogens, wildfire, etc.). The table below provides estimates of current biome area and biomass. While the tundra and boreal biomes may shift over time, we are asking you to estimate biomass change for the current distribution of these biomes. For example, if biomass increased for a patch of land which currently is tundra but which becomes boreal forest, that increment would be included in your % change in biomass of arctic tundra.

	Area (10^6 km^2)[1]	**NEP (Tg C year^{-1})**[2]	**Aboveground biomass (Pg C)**[3]	**Belowground biomass (Pg C)**[4]	**Dead wood (Pg C)**[5]	**Litter (Pg C)**[6]	**Total non-soil biomass (Pg C)**
Boreal forest	13.7	500	43.6	16.1	16	27	102.7
Tundra	5.0	3.5	2.4	4.0		2	8.4

[1]Chapin et al. 2011 and Raynolds et al. 2012, [2]Pan et al. 2011 and McGuire et al. 2009, [3]McGuire et al. 2009 and Epstein et al. 2012, [4]estimated from aboveground or total biomass with ratios from Saugier et al. 2001, [5]Pan et al. 2011, [6]Pan et al. 2011 and Potter and Klooster 1997.

Warming Scenario **(use Table 1 for temperature increase)**	**Short-term** (2010-2040) **change in biomass** (% change)		**Medium-term** (2010-2100) **change in biomass** (% change)		**Long-term** (2010-2300) **change in biomass** (% change)	
	Boreal Forest	**Arctic Tundra**	**Boreal Forest**	**Arctic Tundra**	**Boreal Forest**	**Arctic Tundra**
WS1						
WS2						
WS3						
WS4						

Comments:		**Tundra expertise level (1-5)**	
		Tundra confidence level (1-5)	
		Boreal expertise level (1-5)	
		Boreal confidence level (1-5)	

What are the largest sources of uncertainty in this system's response to warming in the future?	

2. What additional comments or insights do you have concerning the content, format and implementation of this survey?

References:

Chapin, F. S., P. A. Matson, and P. M. Vitousek. 2011. Principles of terrestrial ecosystem ecology. 2nd edition. Springer, New York.

Epstein, H. E., M. K. Raynolds, D. A. Walker, U. S. Bhatt, C. J. Tucker, and J. E. Pinzon. 2012. Dynamics of aboveground phytomass of the circumpolar Arctic tundra during the past three decades. Environmental Research Letters **7**.

McGuire, A. D., L. G. Anderson, T. R. Christensen, S. Dallimore, L. Guo, D. J. Hayes, M. Heimann, T. D. Lorenson, R. W. Macdonald, and N. Roulet. 2009. Sensitivity of the carbon cycle in the Arctic to climate change. Ecological Monographs **79**:523-555.

Pan, Y., R. A. Birdsey, J. Fang, R. Houghton, P. E. Kauppi, W. A. Kurz, O. L. Phillips, A. Shvidenko, S. L. Lewis, J. G. Canadell, P. Ciais, R. B. Jackson, S. Pacala, A. D. McGuire, S. Piao, A. Rautiainen, S. Sitch, and D. Hayes. 2011. A Large and Persistent Carbon Sink in the World's Forests. Science.

Potter, C. S. and S. A. Klooster. 1997. Global model estimates of carbon and nitrogen storage in litter and soil pools: Response to changes in vegetation quality and biomass allocation. Tellus Series B-Chemical and Physical Meteorology **49**:1-17.

Raynolds, M. K., D. A. Walker, H. E. Epstein, J. E. Pinzon, and C. J. Tucker. 2012. A new estimate of tundra-biome phytomass from trans-Arctic field data and AVHRR NDVI. Remote Sensing Letters **3**:403-411.

Saugier, B., J. Roy, and H. A. Mooney. 2001. Estimations of global terrestrial productivity: Converging toward a single number? Pages 543-557 *in* J. Roy, B. Saugier, and H. A. Mooney, editors. Terrestrial Global Productivity. Academic Press, San Diego.

A2.0.2.4 Wildfire questionnaire

Net Ecosystem Carbon Balance of the Permafrost Region: Tundra and Boreal Forest Wildfire Survey

Introduction

The goal of this survey is to document expert opinion on the possible net ecosystem carbon balance of the permafrost region under arctic and boreal warming scenarios. Possible thresholds and tipping points in the relationship between temperature increase and high-latitude wildfire are of particular interest, since such non-linearity is difficult to predict on the basis of models.

We recognize that climate-change-driven feedbacks in complex Earth systems are not, and cannot be, precisely and definitively modeled. As such, we are only asking for your informed opinion, realizing that some of the included parameters may not be well understood. By administering this survey to scientists with the most applicable expertise, we want to identify and evaluate the possible and probable magnitude of wildfire response in the arctic and subarctic.

Instructions

You will be asked to provide estimates of boreal and arctic wildfire over short-term (2010-2040), medium-term (2010-2100), and long-term (2010-2300) time frames for four warming scenarios. These scenarios of regional Arctic warming were generated with NCAR's Community Climate System Model (CCSM4) with inputs from the most recent IPCC radiative forcing scenarios (**Figure 1**). To minimize the possibility of misinterpretation, we have also provided a table showing the amount of warming predicted in Figure 1 by the end of each of the three time scales (**Table 1**). Climate projections, and estimates of system response, become increasingly uncertain for distant time frames. However, because carbon balance in the arctic and boreal biomes can take many decades or centuries to fully respond to disturbance, we have included the 2300 time step to account for lags in this response.

In addition to answering each question, you will have a chance to indicate your level of confidence and expertise concerning your answer; and provide additional comments on how you selected your estimates. These supporting questions allow us to compare responses from multiple experts and are just as valuable as your quantitative estimates. We also ask that you identify key sources of uncertainty concerning the future response of the system (what processes missing from current models will likely play an important role, what data gaps exist, etc.), and provide any comments on how you generated your estimates. If there is not yet clear supporting evidence in the literature, but you have some basis for an estimate based on professional judgment, please make a note of that.

The five-point "**Confidence level**" scale is defined as follows:

- **1=** My answer is my best guess but I am not confident in it; it could easily be far off the mark.
- **2=** My answer is an educated guess; it could be far off the mark, but I have some confidence in it.
- **3=** I am moderately confident in my answer; it surely isn't precise, but it is likely in the ballpark.
- **4=** I am confident in my answer; the true value is likely to be somewhat different from my answer, but it is unlikely to be dramatically different.
- **5=** Given current understanding, I would be surprised if my answer were far off from the true value.

The five-point "**Expertise level**" scale is defined as follows:

- **1=** I have little familiarity with the literature and I do not actively work on these particular questions.
- **2=** I have some familiarity with the literature and I've worked on related questions but haven't contributed to the literature on this issue; it is not an area of central expertise for me.
- **3=** I have worked on related issues and have contributed to the relevant literature but do not consider myself one of the foremost experts on this particular issue.

4= I am very familiar with relevant literature and have worked on related questions. This is an area of central expertise for me.

5= I contribute actively to the literature directly concerned with this issue, and I consider myself one of the foremost experts on it.

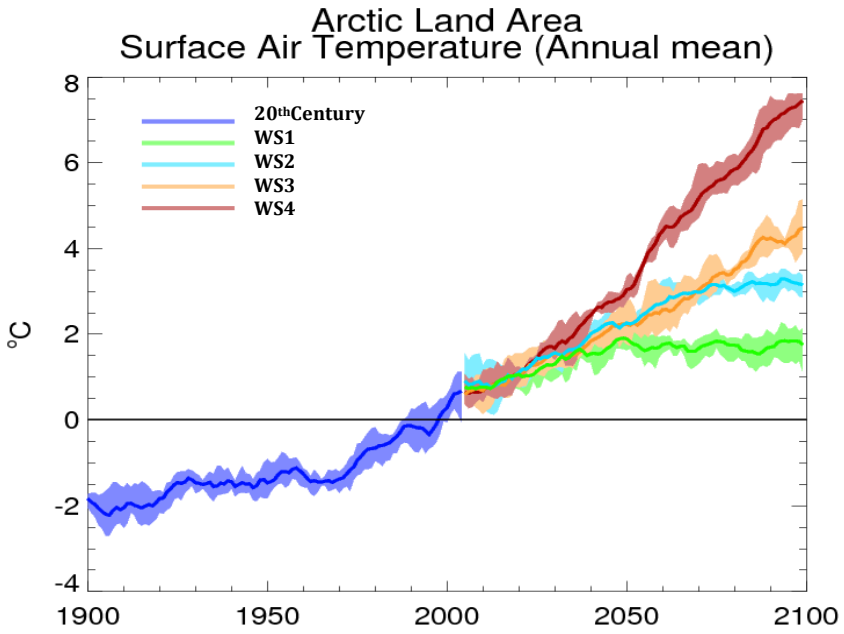

Figure 2. CCSM4: Anomaly from 1985-2004 (7-yr running average; Greenland excluded). Though not shown in this figure, temperature increase is assumed to stabilize and level off after 2100 for the purposes of this survey.

	Warming at 2040 (°C)	Warming at 2100 (°C)	Warming at 2300 (°C)
WS 1	1.5	2.0	2.0
WS 2	2.0	3.0	3.0
WS 3	2.0	4.5	4.5
WS 4	2.5	7.5	7.5

Table 1. Temperature increases for the four warming scenarios (designated here as WS 1-4). Values given represent the regional Arctic temperature increase achieved by the year indicated. Values for WS1-4 correspond to the IPCC representative concentration pathways (RCP): 2.6, 4.5, 6.0, and 8.5 respectively.

Questions

1. How much change in the annual extent of boreal and arctic wildland fire would result from the following increases in the mean annual surface air temperature in the pan-arctic? (Positive numbers represent % increase, negative represent % decrease).

Note: This question addresses changes in wildfire extent in the circumpolar boreal forest and tundra due to direct climate effects (temperature, precipitation, atmospheric CO_2, seasonality etc.) as well as indirect effects (vegetation shifts, insects, pathogens etc.).

	Boreal forest (Eurasia)	**Boreal forest (N. America)**	**Boreal forest (pan-arctic)**	**Tundra (pan-arctic)**
Area burned (km^2 yr^{-2})	64,400	22,500	84,600	4,200
CO_2 emissions from fire (Tg C yr^{-2})	194	56	250	8

Boreal forest burn and emission estimates based on observed and modeled data for the period 1997-2009 (Balshi et al. 2007, Giglio et al. 2010, Hayes et al. 2011, van der Werf et al. 2010). Tundra burn and emission estimates are upscaled from Rocha et al. 2012 and Mack et al. 2011, respectively.

Warming Scenario (use Table 1 for temperature increase)	**Short-term** (2010-2040) **change in wildfire extent** (% change)		**Medium-term** (2010-2100) **change in wildfire extent** (% change)		**Long-term** (2010-2300) **change in wildfire extent** (% change)	
	Boreal Forest	**Tundra**	**Boreal Forest**	**Tundra**	**Boreal Forest**	**Tundra**
WS1						
WS2						
WS3						
WS4						

Comments:		**Tundra expertise level (1-5)**	
		Tundra confidence level (1-5)	
		Boreal expertise level (1-5)	
		Boreal confidence level (1-5)	

What are the largest sources of uncertainty in this system's response to warming in the future?	

2. How much change in CO_2 release due to boreal and arctic wildland fire would result from the following increases in the mean annual surface air temperature in the pan-arctic?

Note: This question addresses changes in carbon emissions due directly to boreal and arctic wildfire. It excludes indirect carbon release due to changes in permafrost extent, net ecosystem production, biome shift, etc. Refer to Question 1 table for estimates of current emissions from wildfire.

Warming Scenario **(use Table 1 for temperature increase)**	**Short-term** (2010-2040) **CO_2 release** (% change)		**Medium-term** (2010-2100) **CO_2 release** (% change)		**Long-term** (2010-2300) **CO_2 release** (% change)	
	Boreal Forest	**Tundra**	**Boreal Forest**	**Tundra**	**Boreal Forest**	**Tundra**
WS1						
WS2						
WS3						
WS4						

Comments:		**Tundra expertise level (1-5)**	
		Tundra confidence level (1-5)	
		Boreal expertise level (1-5)	
		Boreal confidence level (1-5)	

What are the largest sources of uncertainty in this system's response to warming in the future?	

3. What additional comments or insights do you have concerning the content, format and implementation of this survey?

References:

Balshi, M. S., A. D. McGuire, Q. Zhuang, J. Melillo, D. W. Kicklighter, E. Kasischke, C. Wirth, M. Flannigan, J. Harden, J. S. Clein, T. J. Burnside, J. McAllister, W. A. Kurz, M. Apps, and A. Shvidenko. 2007. The role of historical fire disturbance in the carbon dynamics of the pan-boreal region: A process-based analysis. Journal of Geophysical Research-Biogeosciences **112**.

Hayes, D. J., A. D. McGuire, D. W. Kicklighter, K. R. Gurney, T. J. Burnside, and J. M. Melillo. 2011. Is the northern high-latitude land-based CO2 sink weakening? Global Biogeochem. Cycles **25**:GB3018.

Giglio, L., J. T. Randerson, G. R. van der Werf, P. S. Kasibhatla, G. J. Collatz, D. C. Morton, and R. S. DeFries. 2010. Assessing variability and long-term trends in burned area by merging multiple satellite fire products. Biogeosciences **7**:1171-1186.

Mack, M. C., M. S. Bret-Harte, T. N. Hollingsworth, R. R. Jandt, E. A. G. Schuur, G. R. Shaver, and D. L. Verbyla. 2011. Carbon loss from an unprecedented Arctic tundra wildfire. Nature **475**:489-492.

Rocha, A. V., M. M. Loranty, P. E. Higuera, M. C. Mack, F. S. Hu, B. M. Jones, A. L. Breen, E. B. Rastetter, S. J. Goetz, and G. R. Shaver. 2012. The footprint of Alaskan tundra fires during the past half-century: implications for surface properties and radiative forcing. Environmental Research Letters **7**.

van der Werf, G. R., J. T. Randerson, L. Giglio, G. J. Collatz, M. Mu, P. S. Kasibhatla, D. C. Morton, R. S. DeFries, Y. Jin, and T. T. van Leeuwen. 2010. Global fire emissions and the contribution of deforestation, savanna, forest, agricultural, and peat fires (1997–2009). Atmos. Chem. Phys. **10**:11707-11735.

A2.0.2.5 Hydrologic carbon flux questionnaire

Net Ecosystem Carbon Balance of the Permafrost Region: Hydrologic Carbon Flux Survey

Introduction

The goal of this survey is to document expert opinion on the possible net ecosystem carbon balance of the permafrost region under arctic and boreal warming scenarios. Possible thresholds and tipping points in the relationship between temperature increase and hydrologic carbon flux are of particular interest, since such non-linearity is difficult to predict on the basis of models.

We recognize that climate-change-driven feedbacks in complex Earth systems are not, and cannot be, precisely and definitively modeled. As such, we are only asking for your informed opinion, realizing that some of the included parameters may not be well understood. By administering this survey to scientists with the most applicable expertise, we want to identify and evaluate the possible and probable magnitude of hydrologic carbon flux in the arctic and subarctic.

Instructions

You will be asked to provide estimates of pan-arctic particulate and dissolved organic carbon flux over short-term (2010-2040), medium-term (2010-2100), and long-term (2010-2300) time frames for four warming scenarios. These scenarios of regional Arctic warming were generated with NCAR's Community Climate System Model (CCSM4) with inputs from the most recent IPCC radiative forcing scenarios (**Figure 1**). To minimize the possibility of misinterpretation, we have also provided a table showing the amount of warming predicted in Figure 1 by the end of each of the three time scales (**Table 1**). Climate projections, and estimates of system response, become increasingly uncertain for distant time frames. However, because carbon balance in the permafrost region can take many decades or centuries to fully respond to disturbance, we have included the 2300 time step to account for lags in this response.

In addition to answering each question, you will have a chance to indicate your level of confidence and expertise concerning your answer; and provide additional comments on how you selected your estimates. These supporting questions allow us to compare responses from multiple experts and are just as valuable as your quantitative estimates. We also ask that you identify key sources of uncertainty concerning the future response of the system (what processes missing from current models will likely play an important role, what data gaps exist, etc.), and provide any comments on how you generated your estimates. If there is not yet clear supporting evidence in the literature, but you have some basis for an estimate based on professional judgment, please make a note of that.

The five-point "**Confidence level**" scale is defined as follows:

- **1=** My answer is my best guess but I am not confident in it; it could easily be far off the mark.
- **2=** My answer is an educated guess; it could be far off the mark, but I have some confidence in it.
- **3=** I am moderately confident in my answer; it surely isn't precise, but it is likely in the ballpark.
- **4=** I am confident in my answer; the true value is likely to be somewhat different from my answer, but it is unlikely to be dramatically different.
- **5=** Given current understanding, I would be surprised if my answer were far off from the true value.

The five-point "**Expertise level**" scale is defined as follows:

- **1=** I have little familiarity with the literature and I do not actively work on these particular questions.
- **2=** I have some familiarity with the literature and I've worked on related questions but haven't contributed to the literature on this issue; it is not an area of central expertise for me.
- **3=** I have worked on related issues and have contributed to the relevant literature but do not consider myself one of the foremost experts on this particular issue.

4= I am very familiar with relevant literature and have worked on related questions. This is an area of central expertise for me.

5= I contribute actively to the literature directly concerned with this issue, and I consider myself one of the foremost experts on it.

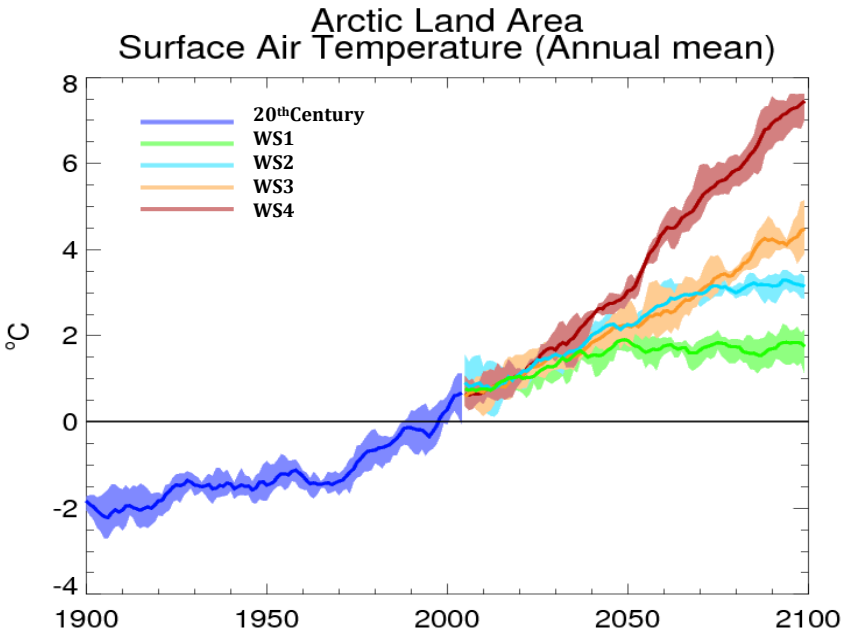

Figure 3. CCSM4: Anomaly from 1985-2004 (7-yr running average; Greenland excluded). Though not shown in this figure, temperature increase is assumed to stabilize and level off after 2100 for the purposes of this survey.

	Warming at 2040 (˚C)	Warming at 2100 (˚C)	Warming at 2300 (˚C)
WS 1	1.5	2.0	2.0
WS 2	2.0	3.0	3.0
WS 3	2.0	4.5	4.5
WS 4	2.5	7.5	7.5

Table 1. Temperature increases for the four warming scenarios (designated here as WS 1-4). Values given represent the regional Arctic temperature increase achieved by the year indicated. Values for WS1-4 correspond to the IPCC representative concentration pathways (RCP): 2.6, 4.5, 6.0, and 8.5 respectively.

Questions

1. How much change in the amount of organic carbon delivered to freshwater ecosystems in the pan-Arctic watershed would result from the following increases in the mean annual surface air temperature in the pan-arctic? (Positive numbers represent % increase, negative represent % decrease).

Note: Questions 1 and 2 address changes in dissolved and particulate organic carbon (DOC and POC) flux in the pan-Arctic watershed (20.5 x 10^6 km^2 (Holmes et al. 2012)) due to direct climate perturbation (temperature, precipitation, etc.) as well as indirect disturbance (permafrost degradation, vegetation shift, etc.). The table below provides estimates of current DOC and POC delivery to freshwater ecosystems (lakes, rivers, and streams) and the Arctic Ocean and surrounding seas.

	DOC (Tg/yr)	Riverine POC (Tg/yr)	Coastal erosion POC (Tg/yr)
Delivery to freshwater ecosystems	100**	20	
Delivery to ocean	36*	6**	18***

*(Holmes et al. 2012), **(McGuire et al. 2009), ***sum of coastal erosion POC delivered to ocean from Vonk et al. 2012 and McGuire et al. 2009. Terrestrial to freshwater delivery of POC was calculated by dividing ocean delivery (6 Tg/yr) with the downscaled global ratio of 0.75 sedimentation of POC (Aufdenkampe et al. 2011, Battin et al. 2009, McGuire et al. 2009).

Warming Scenario (use Table 1 for temperature increase)	**Short-term** (2010-2040) **carbon load** (% change)		**Medium-term** (2010-2100) **carbon load** (% change)		**Long-term** (2010-2300) **carbon load** (% change)	
	DOC	**POC**	**DOC**	**POC**	**DOC**	**POC**
WS1						
WS2						
WS3						
WS4						
Comments:			**DOC Expertise level (1-5)**			
			DOC Confidence level (1-5)			
			POC Expertise level (1-5)			
			POC Confidence level (1-5)			
What are the largest sources of uncertainty in this system's response to warming in the future?						

2. How much change in the amount of organic carbon delivered to the Arctic Ocean and surrounding seas would result from the following increases in the mean annual surface air temperature in the pan-arctic? (Positive numbers represent % increase, negative represent % decrease).

Note: This question addresses changes in riverine DOC and POC flux to the ocean as well as changes in POC release from coastal erosion. The difference between the riverine to marine fluxes reported in this question and the terrestrial to freshwater fluxes reported in Question 1 represent the amount of carbon lost in transit due to mineralization and storage in sediment. Refer to the Question 1 table for estimates of current DOC and POC delivery to the Arctic Ocean and surrounding seas.

Warming Scenario (use Table 1 for temperature increase)	**Short-term** (2010-2040) **carbon load** (% change)			**Medium-term** (2010-2100) **carbon load** (% change)			**Long-term** (2010-2300) **carbon load** (% change)		
	DOC	**POC (riverine)**	**POC (coastal)**	**DOC**	**POC (riverine)**	**POC (coastal)**	**DOC**	**POC (riverine)**	**POC (coastal)**
WS1									
WS2									
WS3									
WS4									

Comments:		**DOC Expertise level (1-5)**	
		DOC Confidence level (1-5)	
		POC Expertise level (1-5)	
		POC Confidence level (1-5)	

What are the largest sources of uncertainty in this system's response to warming in the future?	

3. What additional comments or insights do you have concerning the content, format and implementation of this survey?

A2.0.2.6 Biomass background information sent to participants

Net ecosystem carbon balance of the permafrost region: arctic and boreal biomass background information[1]

Benjamin W. Abbott, University of Alaska Fairbanks
Michelle C. Mack, University of Florida
F. Stuart Chapin III, University of Alaska Fairbanks

Question: How will boreal forest and arctic tundra biomass change in a warmer world?

System characteristics: The boreal and arctic biomes contain 111 petagrams (Pg) carbon (C) in non-soil biomass including above and belowground living biomass, standing dead wood, and litter (see Table A2.2). The size and behavior of these pools depend on the balance between net primary productivity (NPP), ecosystem respiration, and disturbance such as wildfire, drought, permafrost collapse and insect outbreaks. The effect of climate change on arctic and boreal biomass depends on its direct and indirect impact on these C inputs and outputs.

The tundra biome covers 5.0 million km^2 (Raynolds et al. 2012) and the boreal forest biome covers 13.7 million km^2 (Chapin et al. 2011), though the extent of the boreal forest depends on the definition of the southern transition to temperate forest and varies in the literature from 11.4 - 18.5 million km^2 (McGuire et al. 1995, Potter and Klooster 1997, Chapin et al. 2011, Pan et al. 2011). Because most tundra falls in the continuous permafrost zone (with over 90% permafrost cover) and most boreal forest in the discontinuous, sporadic, or isolated zones (with 0-90% cover), almost all arctic tundra is underlain by permafrost, whereas most of the boreal forest is not (Zhang et al. 1999, Zhang et al. 2000).

[1] This document is not intended as a comprehensive or endorsed list of citations or information. It is a partial summary of the current understanding of biomass pools and potential changes to be used as a reference if desired while filling out the arctic and boreal biomass survey.

Arctic and boreal environmental change: High latitude air temperature is increasing twice as fast as global mean temperature, due largely to feedbacks associated with sea-ice loss and decreasing snow cover (Holland and Bitz 2003, ACIA 2005, AMAP 2011, Parmentier et al. 2013). Warming has been most prevalent during the autumn and early winter in coastal areas, when sea ice is at its minimum, and in the spring at latitudes from 50° – 60° N as snow cover decreases (AMAP 2011). Precipitation has increased 5% over land north of 55° since 1950, though due to high interannual variability this trend is not significant (Peterson et al. 2006, AMAP 2011). While circumpolar precipitation minus evapotranspiration is projected to increase by 13 – 25% by 2100, much of this increase is due to changes in winter precipitation (Kattsov et al. 2007), and growing season precipitation in some areas is not expected to keep up with enhanced evapotranspiration (Chapin et al. 2010). As a result of changes in temperature and precipitation, both permafrost and non-permafrost soil temperatures have warmed over the past century, causing increased active layer thickness, freeze-thaw cycling, longer duration of thaw, and widespread ground collapse or thermokarst (Osterkamp and Romanovsky 1999, Hinkel and Nelson 2003, Osterkamp and Jorgenson 2006, Osterkamp 2007, Osterkamp et al. 2009). Models predict widespread near-surface (in the top 3 m) permafrost degradation with projections varying between 40 – 72 % loss by 2100 (Saito et al. 2007, Schaefer et al. 2011, Lawrence et al. 2012). Growing season length, historically 100 days for tundra and 150 days for boreal forest, has increased 2 – 4 days per decade from 1960 – 2000, due mostly to earlier spring thaw (Euskirchen et al. 2006, Chapin et al. 2011), and is projected to lengthen a total of 37 – 60 days over pre-industrial conditions by the end of the century (Euskirchen et al. 2006, Koven et al. 2011). Increased primary productivity due to CO_2 fertilization accounts for over 60% of C sequestered in the pan-boreal region over the past two decades (Balshi et al. 2007) and CO_2 fertilization is expected to strongly influence vegetation response to climate change (Schaefer et al. 2011). Wildfire extent and severity have increased throughout the permafrost region (Kasischke and Turetsky 2006, Balshi et al. 2009, Flannigan et al. 2009), including in arctic tundra (Rocha et al. 2012). The question of how arctic C balance will respond to these changes has fueled over two decades of debate (Oechel et al. 1993, Waelbroeck et al. 1997) and remains an important uncertainty with ecological and societal implications (Schaefer et al. 2011, Schuur et al. 2013).

Carbon pools: The boreal forest is estimated to contain 43.6 Pg C aboveground and 16.1 Pg C belowground in living biomass (Saugier et al. 2001, McGuire et al. 2009) and arctic tundra

contains 2.4 Pg C aboveground and 4.0 Pg C belowground (Saugier et al. 2001, Epstein et al. 2012, Raynolds et al. 2012). However circumpolar estimates of living biomass, particularly belowground biomass, are coarse and uncertain (Epstein et al. 2012).

Table A2.2 System characteristics and non-soil biomass pools in the boreal forest and arctic tundra.

	Area (10^6 km^2)[1]	NPP (Tg C year^{-1})[2]	Aboveground biomass (Pg C)[3]	Belowground biomass (Pg C)[4]	Dead wood (Pg C)[5]	Litter (Pg C)[6]	Total non-soil biomass (Pg C)
Boreal forest	13.7	500	43.6	16.1	16	27	102.7
Tundra	5.0	3.5	2.4	4.0		2	8.4

[1]Chapin et al. 2011 and Raynolds et al. 2012, [2]Pan et al. 2011 and McGuire et al. 2009, [3]McGuire et al. 2009 and Epstein et al. 2012, [4]estimated from aboveground or total biomass with ratios from Saugier et al. 2001, [5]Pan et al. 2011, [6]Pan et al. 2011 and Potter and Klooster 1997.

In the boreal forest, living biomass density varies strongly by plant community (Hollingsworth et al. 2008), which in turn interacts with permafrost, successional stage, near-surface hydrology, topography, and micro-climate (Van Cleve et al. 1983, Camill 1999, Bakalin and Vetrova 2008, Tchebakova et al. 2009). Non-soil biomass in the boreal forest varies over two orders of magnitude from 0.3 kg m^{-2} in boreal grassland, 4.1 kg m^{-2} in spruce-lichen woodland, 10 kg m^{-2} in coniferous stands underlain by permafrost, and 25 kg m^{-2} in permafrost free mixed conifer-deciduous stands and larch forests (for detailed tables of boreal biomass see Van Cleve et al. 1983, Balshi et al. 2007, and de Groot et al. 2013). Non-soil biomass is generally lower in tundra than in boreal forest and decreases going north, with an average density of 2.5 kg m^{-2} near the boreal forest transition, down to 0.39 kg m^{-2} in the high arctic (Potter and Klooster 1997, Roy et al. 2001, Saugier et al. 2001, Epstein et al. 2012, Raynolds et al. 2012). Total non-soil biomass also decreases farther north due to diminishing landmass resulting in 80% of total tundra biomass occurring in the warmest, most southerly bioclimate zones (Raynolds et al. 2012). Some tundra types, including tussock and shrub tundra, can have 3-5 kg m^{-2} of non-soil biomass, within the range of biomass in the boreal forest (Potter and Klooster 1997, Saugier et al. 2001, Hobbie et al. 2005, Bret-Harte et al. 2013).

Standing deadwood is a relatively small (16 Pg) and potentially transient C pool due to its vulnerability to wildfire, but it can accumulate rapidly—deadwood buildup accounts for 27% of the total C sink in the boreal forest over the past two decades (Pan et al. 2011, de Groot et al. 2013). Litter is also a transient C pool but is important to C and nutrient cycles because of its fast turnover and its role as a major intermediary between biomass and soil organic matter, dissolved organic C (via leaching), and the atmosphere (via decomposition). Litter accounts for 27 Pg C in the boreal forest (Pan et al. 2011) and 2 Pg C in the tundra (Potter and Klooster 1997). Litter cycling rates depend on chemical makeup of the litter, with fast-growing species typically producing more nutrient rich and biodegradable litter (Metcalfe et al. 2011), and environmental conditions such as soil temperature and moisture (Schmidt et al. 2011, Bonan et al. 2013). Shifts in vegetation community and climate can affect the amount and rate of cycling of boreal and arctic litter and consequently nutrient and C availability in both terrestrial and aquatic ecosystems (Aerts et al. 2012, Bonan et al. 2013).

Contemporary carbon fluxes: The tundra and boreal biomes account for 10% of global gross primary production, 10 Pg yr^{-1} (McGuire et al. 2009, Tarnocai et al. 2009). Estimates of the net ecosystem C balance (based on atmospheric inversions and inventory based studies) are in good agreement that the tundra and boreal biomes sequestered 400 – 500 Tg of C and emitted 15 – 50 Tg of CH_4 annually over the last half-century (McGuire et al. 2009, Pan et al. 2011). There is high interannual variability, however, in the strength of this C sink, due largely to disturbance such as wildfire (Baker et al. 2006). The strength of the arctic C sink has also decreased by 73% when comparing the last decade with the historical record, due to increases in soil organic matter decomposition and fire (Hayes et al. 2011). Arctic tundra is a small net C sink on average over the last 25 years, taking up between 3 – 4 Tg C $year^{-1}$, though this is within the uncertainty range of field based estimates (McGuire et al. 2009). In cold, wet years tundra tends to be a net C sink while in warm, dry years it acts as a source of C to the atmosphere (McGuire et al. 2009).

Boreal and arctic biomass response to change: Boreal and arctic primary productivity and biomass may respond to climate change in two temporally distinct but causally linked ways: 1. The performance (C fixation or growth) of current vegetation communities can rapidly respond to changes in air and soil temperature, precipitation, CO_2, and nutrient availability, and 2. On a multi-decadal scale, the distribution of vegetation communities may shift in response to

sustained environmental change. The short-term response of arctic biomass to climate forcing may depend primarily on the response of plant communities as they are currently distributed, while the long-term response may depend more on the ultimate redistribution of plant communities throughout the permafrost region.

Observational and experimental studies in the tundra have shown significant shifts in vegetation community, particularly in the southern extent of tundra, with trends towards increased shrub abundance (Tape et al. 2006, Myers-Smith et al. 2011, Elmendorf et al. 2012, Lantz et al. 2013). Over the past 30 years tundra biomass near the tundra-boreal transition has increased 20-26% resulting in 0.4 Pg C accumulation (Epstein et al. 2012). Movement of the tundra-taiga transition (tree line) has been complex, shifting northward in some areas at a very slow rate (McGuire et al. 2009) and staying the same or shifting southward due to anthropogenic impacts, life-history traits, fire, and changes in hydrology (Callaghan et al. 2004, Gamache and Payette 2005). Rapid transitions between steppe, tundra, and various boreal communities have happened in the past (Lloyd et al. 2006, Kienast et al. 2008) and may be accelerated by fire, permafrost collapse, and other community-replacing disturbance (Racine et al. 2004, Higuera et al. 2008, Kelly et al. 2013).

While primary productivity in the arctic is largely limited by nitrogen availability, during much of the growing season water limitation may be the ultimate control on growth (Vitousek and Howarth 1991, Chapin et al. 1995, Nasholm et al. 1998, Zhang et al. 2007, Yarie and Van Cleve 2010). Climate warming, therefore, may relieve temperature constraints on nutrient cycling, but the overall response of primary productivity and biomass may depend on how temperature and water availability interact to influence both growth and disturbance (Wookey et al. 1993, Allison and Treseder 2008, Chapin et al. 2010). Increased winter precipitation will interact with permafrost degradation-induced changes in hydrology and soil temperature to determine overall water availability in northern ecosystems. In areas where nutrient limitation is alleviated, vegetation response can be variable (Hobbie et al. 2005), and increased aboveground biomass may be partially or completely offset by belowground losses (Neff et al. 2002, Mack et al. 2004, Hartley et al. 2012).

Coupled carbon climate models vary widely in their projections of boreal and arctic vegetation response to climate change, with increases of 9 – 61 Pg C projected by 2100 (Qian et al. 2010,

Koven et al. 2011, Schaefer et al. 2011, Falloon et al. 2012). Substantial increases in shrub cover and the expansion of deciduous and coniferous forest is projected in Siberia with less dramatic changes over northeastern Russia and Alaska (Falloon et al. 2012). Although projections generally agree concerning the sign of C balance, variability in the magnitude of flux is large (Ahlstrom et al. 2012) due to incomplete characterization of permafrost degradation, nutrient limitation, CO_2 fertilization, site-level hydrology, and soil moisture in model projections (Qian et al. 2010, Koven et al. 2011).

References:

ACIA. 2005. Arctic Climate Impacts Assessment. Cambridge University Press, Cambridge, United Kingdom.

Aerts, R., T. V. Callaghan, E. Dorrepaal, R. S. P. van Logtestijn, and J. H. C. Cornelissen. 2012. Seasonal climate manipulations have only minor effects on litter decomposition rates and N dynamics but strong effects on litter P dynamics of sub-arctic bog species. Oecologia **170**:809-819.

Ahlstrom, A., G. Schurgers, A. Arneth, and B. Smith. 2012. Robustness and uncertainty in terrestrial ecosystem carbon response to CMIP5 climate change projections. Environmental Research Letters **7**.

Allison, S. D. and K. K. Treseder. 2008. Warming and drying suppress microbial activity and carbon cycling in boreal forest soils. Global Change Biology **14**:2898-2909.

AMAP. 2011. Snow, Water, Ice and Permafrost in the Arctic (SWIPA): Climate Change and the Cryosphere. Arctic Monitoring and Assessment Programme (AMAP). Oslo, Norway.

Bakalin, V. A. and V. P. Vetrova. 2008. Vegetation-permafrost relationships in the zone of sporadic permafrost distribution in the Kamchatka Peninsula. Russian Journal of Ecology **39**:318-326.

Baker, D. F., R. M. Law, K. R. Gurney, P. Rayner, P. Peylin, A. S. Denning, P. Bousquet, L. Bruhwiler, Y. H. Chen, P. Ciais, I. Y. Fung, M. Heimann, J. John, T. Maki, S. Maksyutov, K. Masarie, M. Prather, B. Pak, S. Taguchi, and Z. Zhu. 2006. TransCom 3 inversion intercomparison: Impact of transport model errors on the interannual variability of regional CO2 fluxes, 1988-2003. Global Biogeochemical Cycles **20**.

Balshi, M. S., A. D. McGuire, P. Duffy, M. Flannigan, D. W. Kicklighter, and J. Melillo. 2009. Vulnerability of carbon storage in North American boreal forests to wildfires during the 21st century. Global Change Biology **15**:1491-1510.

Balshi, M. S., A. D. McGuire, Q. Zhuang, J. Melillo, D. W. Kicklighter, E. Kasischke, C. Wirth, M. Flannigan, J. Harden, J. S. Clein, T. J. Burnside, J. McAllister, W. A. Kurz, M. Apps, and A. Shvidenko. 2007. The role of historical fire disturbance in the carbon dynamics of the pan-boreal region: A process-based analysis. Journal of Geophysical Research-Biogeosciences **112**:-.

Bonan, G. B., M. D. Hartman, W. J. Parton, and W. R. Wieder. 2013. Evaluating litter decomposition in earth system models with long-term litterbag experiments: an example using the Community Land Model version 4 (CLM4). Global Change Biology **19**:957-974.

Bret-Harte, M. S., M. C. Mack, G. R. Shaver, D. C. Huebner, M. Johnston, C. A. Mojica, C. Pizano, and J. A. Reiskind. 2013. The response of Arctic vegetation and soils following an unusually severe tundra fire. Philosophical Transactions of the Royal Society B-Biological Sciences **368**.

Callaghan, T. V., L. O. Bjorn, Y. Chernov, T. Chapin, T. R. Christensen, B. Huntley, R. A. Ims, M. Johansson, D. Jolly, S. Jonasson, N. Matveyeva, N. Panikov, W. Oechel, G. Shaver, S. Schaphoff, and S. Sitch. 2004. Effects of changes in climate on landscape and regional processes, and feedbacks to the climate system. Ambio **33**:459-468.

Camill, P. 1999. Patterns of boreal permafrost peatland vegetation across environmental gradients sensitive to climate warming. Canadian Journal of Botany-Revue Canadienne De Botanique **77**:721-733.

Chapin, F. S., P. A. Matson, and P. M. Vitousek. 2011. Principles of terrestrial ecosystem ecology. 2nd edition. Springer, New York.

Chapin, F. S., A. D. McGuire, R. W. Ruess, T. N. Hollingsworth, M. C. Mack, J. F. Johnstone, E. S. Kasischke, E. S. Euskirchen, J. B. Jones, M. T. Jorgenson, K. Kielland, G. P. Kofinas, M. R. Turetsky, J. Yarie, A. H. Lloyd, and D. L. Taylor. 2010. Resilience of Alaska's boreal forest to climatic change. Canadian Journal of Forest Research-Revue Canadienne De Recherche Forestiere **40**:1360-1370.

Chapin, F. S., G. R. Shaver, A. E. Giblin, K. J. Nadelhoffer, and J. A. Laundre. 1995. Responses of Arctic Tundra to Experimental and Observed Changes in Climate. Ecology **76**:694-711.

de Groot, W. J., A. S. Cantin, M. D. Flannigan, A. J. Soja, L. M. Gowman, and A. Newbery. 2013. A comparison of Canadian and Russian boreal forest fire regimes. Forest Ecology and Management **294**:23-34.

Elmendorf, S. C., G. H. R. Henry, R. D. Hollister, R. G. Bjork, A. D. Bjorkman, T. V. Callaghan, L. S. Collier, E. J. Cooper, J. H. C. Cornelissen, T. A. Day, A. M. Fosaa, W. A. Gould, J. Gretarsdottir, J. Harte, L. Hermanutz, D. S. Hik, A. Hofgaard, F. Jarrad, I. S. Jonsdottir, F. Keuper, K. Klanderud, J. A. Klein, S. Koh, G. Kudo, S. I. Lang, V. Loewen, J. L. May, J. Mercado, A. Michelsen, U. Molau, I. H. Myers-Smith, S. F. Oberbauer, S. Pieper, E. Post, C. Rixen, C. H. Robinson, N. M. Schmidt, G. R. Shaver, A. Stenstrom, A. Tolvanen, O. Totland, T. Troxler, C. H. Wahren, P. J. Webber, J. M. Welker, and P. A. Wookey. 2012. Global assessment of experimental climate warming on tundra vegetation: heterogeneity over space and time. Ecology Letters **15**:164-175.

Epstein, H. E., M. K. Raynolds, D. A. Walker, U. S. Bhatt, C. J. Tucker, and J. E. Pinzon. 2012. Dynamics of aboveground phytomass of the circumpolar Arctic tundra during the past three decades. Environmental Research Letters **7**.

Falloon, P. D., R. Dankers, R. A. Betts, C. D. Jones, B. B. B. Booth, and F. H. Lambert. 2012. Role of vegetation change in future climate under the A1B scenario and a climate stabilisation scenario, using the HadCM3C Earth system model. Biogeosciences **9**:4739-4756.

Flannigan, M. D., M. A. Krawchuk, W. J. de Groot, B. M. Wotton, and L. M. Gowman. 2009. Implications of changing climate for global wildland fire. International Journal of Wildland Fire **18**:483-507.

Gamache, I. and S. Payette. 2005. Latitudinal response of subarctic tree lines to recent climate change in eastern Canada. Journal of Biogeography **32**:849-862.

Hartley, I. P., M. H. Garnett, M. Sommerkorn, D. W. Hopkins, B. J. Fletcher, V. L. Sloan, G. K. Phoenix, and P. A. Wookey. 2012. A potential loss of carbon associated with greater plant growth in the European Arctic. Nature Climate Change **2**:875-879.

Hayes, D. J., A. D. McGuire, D. W. Kicklighter, K. R. Gurney, T. J. Burnside, and J. M. Melillo. 2011. Is the northern high-latitude land-based CO2 sink weakening? Global Biogeochem. Cycles **25**:GB3018.

Higuera, P. E., L. B. Brubaker, P. M. Anderson, T. A. Brown, A. T. Kennedy, and F. S. Hu. 2008. Frequent Fires in Ancient Shrub Tundra: Implications of Paleorecords for Arctic Environmental Change. Plos One **3**.

Hinkel, K. M. and F. E. Nelson. 2003. Spatial and temporal patterns of active layer thickness at Circumpolar Active Layer Monitoring (CALM) sites in northern Alaska, 1995-2000. Journal of Geophysical Research-Atmospheres **108**.

Hobbie, S. E., L. Gough, and G. R. Shaver. 2005. Species compositional differences on different-aged glacial landscapes drive contrasting responses of tundra to nutrient addition. Journal of Ecology **93**:770-782.

Holland, M. M. and C. M. Bitz. 2003. Polar amplification of climate change in coupled models. Climate Dynamics **21**:221-232.

Hollingsworth, T. N., E. A. G. Schuur, F. S. Chapin, and M. D. Walker. 2008. Plant community composition as a predictor of regional soil carbon storage in Alaskan boreal black spruce ecosystems. Ecosystems **11**:629-642.

Kasischke, E. S. and M. R. Turetsky. 2006. Recent changes in the fire regime across the North American boreal region-Spatial and temporal patterns of burning across Canada and Alaska (vol 33, art no L09703, 2006). Geophysical Research Letters **33**.

Kattsov, V. M., J. E. Walsh, W. L. Chapman, V. A. Govorkova, T. V. Pavlova, and X. Zhang. 2007. Simulation and projection of arctic freshwater budget components by the IPCC AR4 global climate models. Journal of Hydrometeorology **8**:571-589.

Kelly, R., M. L. Chipman, P. E. Higuera, I. Stefanova, L. B. Brubaker, and F. S. Hu. 2013. Recent burning of boreal forests exceeds fire regime limits of the past 10,000 years. Proceedings of the National Academy of Sciences of the United States of America **110**:13055-13060.

Kienast, F., P. Tarasov, L. Schirrmeister, G. Grosse, and A. A. Andreev. 2008. Continental climate in the East Siberian Arctic during the last interglacial: Implications from palaeobotanical records. Global and Planetary Change **60**:535-562.

Koven, C. D., B. Ringeval, P. Friedlingstein, P. Ciais, P. Cadule, D. Khvorostyanov, G. Krinner, and C. Tarnocai. 2011. Permafrost carbon-climate feedbacks accelerate global warming. Proceedings of the National Academy of Sciences of the United States of America **108**:14769-14774.

Lantz, T. C., P. Marsh, and S. V. Kokelj. 2013. Recent Shrub Proliferation in the Mackenzie Delta Uplands and Microclimatic Implications. Ecosystems **16**:47-59.

Lawrence, D. M., A. G. Slater, and S. C. Swenson. 2012. Simulation of Present-Day and Future Permafrost and Seasonally Frozen Ground Conditions in CCSM4. Journal of Climate **25**:2207-2225.

Lloyd, A. H., M. E. Edwards, B. Finney, J. Lynch, V. A. Barber, and N. H. Bigelow. 2006. Holocene development of the Alaskan boreal forest. Pages 62-78 *in* F. S. Chapin, M. W. Oswood, K. Van Cleve, L. Viereck, and D. Verbyla, editors. Alaska's changing boreal forest. Oxford University Press, New York.

Mack, M. C., E. A. G. Schuur, M. S. Bret-Harte, G. R. Shaver, and F. S. Chapin. 2004. Ecosystem carbon storage in arctic tundra reduced by long-term nutrient fertilization. Nature **431**:440-443.

McGuire, A. D., L. G. Anderson, T. R. Christensen, S. Dallimore, L. Guo, D. J. Hayes, M. Heimann, T. D. Lorenson, R. W. Macdonald, and N. Roulet. 2009. Sensitivity of the carbon cycle in the Arctic to climate change. Ecological Monographs **79**:523-555.

McGuire, A. D., J. M. Melillo, D. W. Kicklighter, and L. A. Joyce. 1995. Equilibrium Responses of Soil Carbon to Climate Change: Empirical and Process-Based Estimates. Journal of Biogeography **22**:785-796.

Metcalfe, D. B., R. A. Fisher, and D. A. Wardle. 2011. Plant communities as drivers of soil respiration: pathways, mechanisms, and significance for global change. Biogeosciences **8**:2047-2061.

Myers-Smith, I. H., B. C. Forbes, M. Wilmking, M. Hallinger, T. Lantz, D. Blok, K. D. Tape, M. Macias-Fauria, U. Sass-Klaassen, E. Levesque, S. Boudreau, P. Ropars, L. Hermanutz, A. Trant, L. S. Collier, S. Weijers, J. Rozema, S. A. Rayback, N. M. Schmidt, G. Schaepman-Strub, S. Wipf, C. Rixen, C. B. Menard, S. Venn, S. Goetz, L. Andreu-Hayles, S. Elmendorf, V. Ravolainen, J. Welker, P. Grogan, H. E. Epstein, and D. S. Hik.

2011. Shrub expansion in tundra ecosystems: dynamics, impacts and research priorities. Environmental Research Letters **6**.

Nasholm, T., A. Ekblad, A. Nordin, R. Giesler, M. Hogberg, and P. Hogberg. 1998. Boreal forest plants take up organic nitrogen. Nature **392**:914-916.

Neff, J. C., A. R. Townsend, G. Gleixner, S. J. Lehman, J. Turnbull, and W. D. Bowman. 2002. Variable effects of nitrogen additions on the stability and turnover of soil carbon. Nature **419**:915-917.

Oechel, W. C., S. J. Hastings, G. Vourlitis, M. Jenkins, G. Riechers, and N. Grulke. 1993. Recent Change of Arctic Tundra Ecosystems from a Net Carbon-Dioxide Sink to a Source. Nature **361**:520-523.

Osterkamp, T. E. 2007. Characteristics of the recent warming of permafrost in Alaska. Journal of Geophysical Research-Earth Surface **112**.

Osterkamp, T. E. and J. C. Jorgenson. 2006. Warming of permafrost in the Arctic National Wildlife Refuge, Alaska. Permafrost and Periglacial Processes **17**:65-69.

Osterkamp, T. E., M. T. Jorgenson, E. A. G. Schuur, Y. L. Shur, M. Z. Kanevskiy, J. G. Vogel, and V. E. Tumskoy. 2009. Physical and Ecological Changes Associated with Warming Permafrost and Thermokarst in Interior Alaska. Permafrost and Periglacial Processes **20**:235-256.

Osterkamp, T. E. and V. E. Romanovsky. 1999. Evidence for warming and thawing of discontinuous permafrost in Alaska. Permafrost and Periglacial Processes **10**:17-37.

Pan, Y., R. A. Birdsey, J. Fang, R. Houghton, P. E. Kauppi, W. A. Kurz, O. L. Phillips, A. Shvidenko, S. L. Lewis, J. G. Canadell, P. Ciais, R. B. Jackson, S. Pacala, A. D. McGuire, S. Piao, A. Rautiainen, S. Sitch, and D. Hayes. 2011. A Large and Persistent Carbon Sink in the World's Forests. Science.

Parmentier, F. J. W., T. R. Christensen, L. L. Sorensen, S. Rysgaard, A. D. McGuire, P. A. Miller, and D. A. Walker. 2013. The impact of lower sea-ice extent on Arctic greenhouse-gas exchange. Nature Climate Change **3**:195-202.

Peterson, B. J., J. McClelland, R. Curry, R. M. Holmes, J. E. Walsh, and K. Aagaard. 2006. Trajectory shifts in the Arctic and subarctic freshwater cycle. Science **313**:1061-1066.

Potter, C. S. and S. A. Klooster. 1997. Global model estimates of carbon and nitrogen storage in litter and soil pools: Response to changes in vegetation quality and biomass allocation. Tellus Series B-Chemical and Physical Meteorology **49**:1-17.

Qian, H., R. Joseph, and N. Zeng. 2010. Enhanced terrestrial carbon uptake in the Northern High Latitudes in the 21st century from the Coupled Carbon Cycle Climate Model Intercomparison Project model projections. Global Change Biology **16**:641-656.

Racine, C., R. Jandt, C. Meyers, and J. Dennis. 2004. Tundra fire and vegetation change along a hillslope on the Seward Peninsula, Alaska, USA. Arctic Antarctic and Alpine Research **36**:1-10.

Raynolds, M. K., D. A. Walker, H. E. Epstein, J. E. Pinzon, and C. J. Tucker. 2012. A new estimate of tundra-biome phytomass from trans-Arctic field data and AVHRR NDVI. Remote Sensing Letters **3**:403-411.

Rocha, A. V., M. M. Loranty, P. E. Higuera, M. C. Mack, F. S. Hu, B. M. Jones, A. L. Breen, E. B. Rastetter, S. J. Goetz, and G. R. Shaver. 2012. The footprint of Alaskan tundra fires during the past half-century: implications for surface properties and radiative forcing. Environmental Research Letters **7**.

Roy, J., B. Saugier, and H. A. Mooney. 2001. Terrestrial global productivity. Academic Press.

Saito, K., M. Kimoto, T. Zhang, K. Takata, and S. Emori. 2007. Evaluating a high-resolution climate model: Simulated hydrothermal regimes in frozen ground regions and their change under the global warming scenario. Journal of Geophysical Research-Earth Surface **112**:-.

Saugier, B., J. Roy, and H. A. Mooney. 2001. Estimations of global terrestrial productivity: Converging toward a single number? Pages 543-557 *in* J. Roy, B. Saugier, and H. A. Mooney, editors. Terrestrial Global Productivity. Academic Press, San Diego.

Schaefer, K., T. Zhang, L. Bruhwiler, and A. P. Barrett. 2011. Amount and timing of permafrost carbon release in response to climate warming. Tellus Series B-Chemical and Physical Meteorology:no-no.

Schmidt, M. W. I., M. S. Torn, S. Abiven, T. Dittmar, G. Guggenberger, I. A. Janssens, M. Kleber, I. Kogel-Knabner, J. Lehmann, D. A. C. Manning, P. Nannipieri, D. P. Rasse, S. Weiner, and S. E. Trumbore. 2011. Persistence of soil organic matter as an ecosystem property. Nature **478**:49-56.

Schuur, E. A. G., B. W. Abbott, W. B. Bowden, V. Brovkin, P. Camill, J. G. Canadell, J. P. Chanton, F. S. Chapin, III, T. R. Christensen, P. Ciais, B. T. Crosby, C. I. Czimczik, G. Grosse, J. Harden, D. J. Hayes, G. Hugelius, J. D. Jastrow, J. B. Jones, T. Kleinen, C. D. Koven, G. Krinner, P. Kuhry, D. M. Lawrence, A. D. McGuire, S. M. Natali, J. A. O'Donnell, C. L. Ping, W. J. Riley, A. Rinke, V. E. Romanovsky, A. B. K. Sannel, C. Schädel, K. Schaefer, J. Sky, Z. M. Subin, C. Tarnocai, M. R. Turetsky, M. P. Waldrop, K. M. Walter Anthony, K. P. Wickland, C. J. Wilson, and S. A. Zimov. 2013. Expert assessment of vulnerability of permafrost carbon to climate change. Climatic Change:1-16.

Tape, K., M. Sturm, and C. Racine. 2006. The evidence for shrub expansion in Northern Alaska and the Pan-Arctic. Global Change Biology **12**:686-702.

Tarnocai, C., J. G. Canadell, E. A. G. Schuur, P. Kuhry, G. Mazhitova, and S. Zimov. 2009. Soil organic carbon pools in the northern circumpolar permafrost region. Global Biogeochemical Cycles **23**:-.

Tchebakova, N. M., E. Parfenova, and A. J. Soja. 2009. The effects of climate, permafrost and fire on vegetation change in Siberia in a changing climate. Environmental Research Letters **4**.

Van Cleve, K., L. Oliver, R. Schlentner, L. A. Viereck, and C. T. Dyrness. 1983. Productivity and Nutrient Cycling in Taiga Forest Ecosystems. Canadian Journal of Forest Research-Revue Canadienne De Recherche Forestiere **13**:747-766.

Vitousek, P. M. and R. W. Howarth. 1991. Nitrogen Limitation on Land and in the Sea - How Can It Occur. Biogeochemistry **13**:87-115.

Waelbroeck, C., P. Monfray, W. C. Oechel, S. Hastings, and G. Vourlitis. 1997. The impact of permafrost thawing on the carbon dynamics of tundra. Geophysical Research Letters **24**:229-232.

Wookey, P. A., A. N. Parsons, J. M. Welker, J. A. Potter, T. V. Callaghan, J. A. Lee, and M. C. Press. 1993. Comparitive responses of phenology and reproductive development to simulated environmental change in sub-arctic and high arctic plants. Oikos **67**:490-502.

Yarie, J. and K. Van Cleve. 2010. Long-term monitoring of climatic and nutritional affects on tree growth in interior Alaska. Canadian Journal of Forest Research-Revue Canadienne De Recherche Forestiere **40**:1325-1335.

Zhang, K., J. S. Kimball, M. S. Zhao, W. C. Oechel, J. Cassano, and S. W. Running. 2007. Sensitivity of pan-Arctic terrestrial net primary productivity simulations to daily surface meteorology from NCEP-NCAR and ERA-40 reanalyses. Journal of Geophysical Research-Biogeosciences **112**.

Zhang, T., J. A. Heginbottom, R. G. Barry, and J. Brown. 2000. Further statistics on the distribution of permafrost and ground ice in the Northern Hemisphere. Polar Geography **24**:126-131.

Zhang, T., R.G. Barry, K. Knowles, J.A. Heginbottom, and J. Brown. 1999. Statistics and characteristics of permafrost and ground ice distribution in the Northern Hemisphere. Polar Geography **23**:147-169.

A2.0.2.7 Wildfire background information sent to participants

Net ecosystem carbon balance of the permafrost region: arctic and boreal wildfire background information[1]

Benjamin W. Abbott, University of Alaska Fairbanks
Adrian V. Rocha, University of Notre Dame
Mike Flannigan, University of Alberta
Teresa N. Hollingsworth, USDA Forest Service
Merritt R. Turetsky, University of Guelph

Question: How will wildfire extent and carbon release change in the boreal forest and arctic tundra in a warmer world?

System characteristics: Wildfires burn on average 84,600 km^2 yr^{-2} in the boreal forest and 4,200 km^2 yr^{-2} in arctic tundra (Balshi et al. 2007, Giglio et al. 2010, Hayes et al. 2011, Rocha et al. 2012). This accounts for 10 % of global carbon emissions from fire (Table A2.3; van der Werf et al. 2010, Mack et al. 2011). Rapid environmental change at high latitudes is affecting both physical and ecosystem controls on wildfire including temperature, precipitation, evapotranspiration, lightning ignition, human ignition, permafrost thaw depth, vegetation distribution, insect outbreaks, and drought stress (ACIA 2004, AMAP 2011). High-latitude wildfire extent and emissions are projected to increase with climate change across most of the boreal and arctic regions (Flannigan et al. 2009, Joly et al. 2012). Increased wildfire has implications for local ecosystems and the global carbon cycle, however important uncertainties persist concerning the magnitude and timing of the response of boreal and arctic wildfire to climate change (Barrett et al. 2012, Kelly et al. 2013).

[1] This document is not intended as a comprehensive or endorsed list of citations or information. It is a partial summary of the current understanding of high-latitude wildfire and potential changes to be used as a reference if desired while filling out the arctic and boreal wildfire survey.

Wildfire affects ecosystem functioning and structure in both arctic tundra and boreal forest across the circumpolar north (Kasischke and Turetsky 2006), though the role of fire varies by biome and continent (Chambers et al. 2005, de Groot et al. 2013). The tundra biome covers 5.0 million km^2 (Raynolds et al. 2012) and the boreal forest biome covers 13.7 million km^2 (Chapin et al. 2011), though the extent of the boreal forest depends on the definition of the southern transition to temperate forest and varies in the literature from 11.4 – 18.5 million km^2 (McGuire et al. 1995, Potter and Klooster 1997, Chapin et al. 2011, Pan et al. 2011). Because most tundra falls in the continuous permafrost zone (with over 90% permafrost cover) and most boreal forest in the discontinuous, sporadic, or isolated zones (with 0-90% cover), almost all arctic tundra is underlain by permafrost, whereas most of the boreal forest is not (Zhang et al. 1999, Zhang et al. 2000).

Arctic and boreal environmental change: High latitude air temperature is increasing twice as fast as global mean temperature, due largely to feedbacks associated with sea-ice loss and decrease in snow cover (Holland and Bitz 2003, ACIA 2005, AMAP 2011). Warming has been most prevalent during the autumn and early winter in coastal areas, when sea ice is at its minimum, and in the spring at latitudes from 50° – 60° N as snow cover decreases (AMAP 2011). Growing season length, historically 100 days for tundra and 150 days for boreal forest, has increased 2 – 4 days per decade from 1960 – 2000, due mostly to earlier spring thaw (Euskirchen et al. 2006, Chapin et al. 2011), and is projected to lengthen a total of 37 – 60 days over pre-industrial conditions by the end of the century (Euskirchen et al. 2006, Koven et al. 2011). Changes in temperature and precipitation have warmed both permafrost and non-permafrost soils over the past century, causing a thicker active layer, more intense freeze-thaw cycles, longer duration of thaw, and widespread ground collapse or thermokarst (Osterkamp and Romanovsky 1999, Hinkel and Nelson 2003, Osterkamp and Jorgenson 2006, Osterkamp 2007, Osterkamp et al. 2009). Models predict a 40 – 72 % loss of near-surface permafrost (in the top 3 m) by 2100 (Saito et al. 2007, Schaefer et al. 2011, Lawrence et al. 2012). Annual precipitation minus evapotranspiration is expected to increase by 13 – 25 % by 2100, driven primarily by increased winter precipitation (Holland et al. 2007, Kattsov et al. 2007). However, soil and vegetation moisture are expected to decrease, due to an intensification of the hydrologic cycle, including warmer summer temperature, increased evapotranspiration, and changes in infiltration due to permafrost degradation (Hinzman et al. 2005, Rawlins et al. 2010), with some areas, such as

Alaska experiencing regional drying (Chapin et al. 2010). Wildfire severity, defined as the proportion of aboveground biomass consumed during combustion (Keeley 2009), and extent have increased throughout the permafrost region (Kasischke and Turetsky 2006, Balshi et al. 2009a, Flannigan et al. 2009), including in arctic tundra (Rocha et al. 2012).

Arctic and boreal vegetation has already been influenced by recent changes in climate, including precipitation, temperature, growing season length, CO_2 fertilization, and increased disturbance such as fire and insect outbreaks (Sturm et al. 2001, Goetz et al. 2005, McGuire et al. 2009, Kelly et al. 2013). Increased primary productivity due to CO_2 fertilization accounts for over 60 % of carbon (C) sequestered in the pan-boreal region over the past two decades (Balshi et al. 2007) and is expected to strongly influence vegetation response to climate change (Schaefer et al. 2011). Observational and experimental studies in tundra have shown significant vegetation community shifts, particularly along the southern transition to boreal forest, with trends towards increased shrub abundance (Tape et al. 2006, Myers-Smith et al. 2011, Elmendorf et al. 2012, Lantz et al. 2013). Over the past 30 years, tundra biomass near the tundra-boreal transition has increased 20 – 26 % resulting in 400 Tg C accumulation (Epstein et al. 2012). Movement of the tundra-taiga transition (tree line) is complex, shifting northward in some areas at a very slow rate (McGuire et al. 2009) and staying the same or shifting southward due to fire, anthropogenic impacts, life-history traits, and changes in hydrology in others (Callaghan et al. 2004, Gamache and Payette 2005, Payette et al. 2008). Rapid transitions between steppe, tundra, and various boreal communities have happened in the past (Lloyd et al. 2006, Higuera et al. 2008, Kienast et al. 2008) and may be accelerated by fire, permafrost collapse, and other community-replacing disturbance (Racine et al. 2004, Girardin et al. 2013, Kelly et al. 2013).

Boreal and arctic wildfire extent and carbon emissions: Fire is the dominant type of ecosystem disturbance in the boreal forest, affecting forest and peatland ecosystems (Soja et al. 2004, Kasischke and Turetsky 2006), and it appears to be increasing in arctic tundra (Higuera et al. 2011). The fire regime in the boreal forest is characterized by high interannual variability, with fire extent varying over 400 % interannually, and areal C emissions varying over an order of magnitude (Soja 2004, Giglio 2010, Hayes 2011). In both boreal and tundra systems, fire regime is determined primarily by weather, ignition, and vegetation (Flannigan et al. 2005, Higuera et al. 2011, Parisien et al. 2011, Rocha et al. 2012), with weather explaining most of the short-term

variance in area burned (Gillett et al. 2004, Cary et al. 2006, Balshi et al. 2009b, Hu et al. 2010). Fire in the boreal forest can be influenced by permafrost and associated soil drainage (Harden et al. 2000, Turetsky et al. 2011), climate (Chapin et al. 2000), and vegetation (Girardin et al. 2013, Kelly et al. 2013). Tundra fire can be limited by burnable aboveground biomass, particularly in barrens and the high arctic (Higuera et al. 2008, Rocha et al. 2012), and temperature and precipitation during the growing season where adequate fuel is present (Hu et al. 2010).

	Boreal forest (Eurasia)	Boreal forest (N. America)	Boreal forest (total)	Tundra (total)
Area burned (km^2 yr^{-2})	62,100	22,500	84,600	4,200
CO_2 emissions from fire (Tg C yr^{-1})	194	56	250	8

Table A2.3 Boreal forest burn and emission estimates based on observed and modeled data for the period 1997-2009 (Balshi et al. 2007, Giglio et al. 2010, Hayes et al. 2011, van der Werf et al. 2010). Tundra burn and emission estimates are upscaled from Rocha et al. 2012 and Mack et al. 2011, respectively. Considerable uncertainty remains around these estimates.

Carbon emissions from fire depend on pre-fire biomass, soil organic matter, bulk density and depth of burn. In both boreal forest and tundra, fires typically consume 5 – 30 % of ecosystem C (Kasischke et al. 2000, van der Werf et al. 2010, Mack et al. 2011). Biomass available for combustion varies by stand type (see de Groot et. al 2010 for detailed Canadian and Russian tree and forest floor fuel loads), with average combustion of 2662 and 1979 g C m^{-2} in boreal North America and boreal Eurasia, respectively (van der Werf et al. 2010). Emissions vary from 256 g C m^{-2} in the East Boreal Shield of Canada to 5110 g C m^{-2} in larch forests of Siberia (Balshi et al. 2007). Despite this large range, landscape-level carbon emissions depend more on fire extent than vegetation type or burn severity for most ecotypes (Amiro et al. 2009). CO_2 is the predominant C gas released from fire, however, CO and CH_4 can account for 8 and 4 % of total carbon emissions during flaming combustion, and 20 and 11 %, respectively, during smoldering combustion (French et al. 2002). Across the boreal forest, CO makes up 14 % and CH_4 makes up 1 % of total carbon emissions (Kasischke and Bruhwiler 2002), with another ~1 % of emissions coming from non-methane volatile organic compounds (Simpson et al. 2011).

There is strong continental divergence in tree species and associated fire regime between the boreal forest in North America and Eurasia (de Groot et al. 2013), with North American forests experiencing less frequent but higher severity fires associated with higher carbon emissions per square meter (van der Werf et al. 2010). Based on the 1997-2009 time period, boreal Eurasia accounts for 71 – 76 % of the total 84,600 km^2 yr^{-1} burned, and 70 – 83 % of the 250 Tg C yr^{-1} released from boreal fire (Balshi et al. 2007, Giglio et al. 2010, van der Werf et al. 2010, Hayes et al. 2011). Average boreal fire return interval is 550 years in North America and 236 years in Eurasia (van der Werf et al. 2010), though many areas experience an average interval of 50 – 180 years (de Groot et al. 2013). The longer period between fires in North America allows higher forest floor fuel loading, resulting in 25 – 53 % higher C emissions per square meter (van der Werf et al. 2010, de Groot et al. 2013). The majority of fires in Eurasian boreal forests are surface fires, limited to burning understory biomass and soil organic material, while the majority in North American boreal forests tend to be crown fires, resulting in greater combustion of tree biomass (Korovin 1996, Stocks et al. 2004). Consequently, combustion of soil organic matter accounts for 58 % of total C emitted from boreal forest fires in North America versus 64 % in Eurasia (Hayes et al. 2011). There are also differences in fire seasonality between the continents, with North American boreal fires occurring primarily in summer and Eurasian boreal forest fires occurring earlier in spring (de Groot et al. 2013).

Patterns of fire in tundra are less well characterized than in boreal systems, due to historically low frequency of fire and remoteness of tundra landscapes (Barrett et al. 2012). Tundra fire return intervals span over two orders of magnitude, from 30 – 5000 years, and are driven by local-scale vegetation and environmental conditions (Higuera et al. 2011). Most tundra ecosystems are susceptible to burn (Rocha et al. 2012), and fire-prone areas experience fire as frequently as the boreal forest, with return intervals of 100 – 300 years (Higuera et al. 2011). Emissions on an areal basis from tundra fire are comparable to those from the boreal forest, reaching 2016 g C m^{-2}, with 60 % of total emissions coming from soil organic matter (Mack et al. 2011). In areas with frequent fire or where fire severity is high, fire can affect long-term ecosystem carbon storage by 10 – 30 %, releasing several decades' worth of accumulated carbon in a single event (Harden 2000, Mack 2011).

Fire's net impact on C balance depends on the amount of C released from combustion, secondary C release due to changes in soil temperature or permafrost, and post-fire successional trajectory (Harden et al. 2000, Mack et al. 2008). Though some vegetation communities are self-replacing after disturbance (Perera et al. 2011), in many boreal systems, vegetation recovery follows predictable stages of succession, typically with fast-growing deciduous species recruiting immediately after burn, followed by a gradual transition, over decades or centuries, to slower growing conifers (Niklasson and Granstrom 2000, Korotkov et al. 2001, Bond-Lamberty et al. 2004, Uotila and Kouki 2005). In the boreal forest, net primary productivity is typically low immediately after fire (1-5 years), highest 10-20 years after disturbance, and moderate after that (Hicke et al. 2003, Bond-Lamberty et al. 2004, Jones et al. 2013). Remotely sensed metrics of primary productivity, such as normalized difference vegetation index (NDVI) and vegetation optical depth (VOD), typically show recovery to pre-fire levels within 3-10 years, though there is substantial variability between fires (Hicke et al. 2003, Goetz et al. 2005, Jones et al. 2013). Field studies show a much slower recovery, with net ecosystem productivity peaking between 6-80 years after fire and biomass still increasing after 150 years (Bond-Lamberty et al. 2004, Harden et al. 2006, Goulden et al. 2011). Pre-fire vegetation, size of burn, and seasonal timing affect the rate and trajectory of succession after fire (Kasischke and French 1997). In tundra ecosystems, primary productivity and biomass typically recover within 5 – 20 years after fire, following transient changes in plant functional groups and community makeup (Wein and Bliss 1973, Fetcher et al. 1984, Racine et al. 1987, Vavrek et al. 1999, Jandt et al. 2008, Bret-Harte et al. 2013). However, large or high-severity tundra fires can result in a shift towards deciduous shrubs and graminoid species, which can persist for decades after the burn, affecting susceptibility to future fire, forage or habitat quality, and ecosystem functioning (Landhausser and Wein 1993, Racine et al. 2004, Jandt et al. 2008, Barrett et al. 2012, Joly et al. 2012, Bret-Harte et al. 2013, Lantz et al. 2013).

Though not the subject of this survey, wildfire also affects net energy balance by changing surface albedo and releasing aerosols in both the arctic tundra and boreal forest (Chambers et al. 2005, Rocha and Shaver 2011, Rocha et al. 2012, Rogers et al. 2012). Depending on the region and time scale, these phenomena can affect overall energy balance as much or more than C-related climate forcing (Rogers et al. 2012).

Response of boreal and arctic wildfire to future change: Boreal and arctic fire may respond to climate change in two temporally distinct but causally linked ways: 1. Changes in weather may affect the flammability of current ecosystems, determining short-term fire extent and emissions, and, 2. On a multi-decadal scale, the distribution of vegetation communities may shift in response to sustained environmental change such as fire, modifying the structural linkage between climate and fire. The short-term response of arctic and boreal fire to climate forcing may depend primarily on changes in regional weather, while the long-term response may depend more on the ultimate redistribution of plant communities throughout the permafrost region.

In both the tundra and boreal forest, vegetation distribution strongly affects flammability. Conversely, fire extent and severity set the stage for succession and vegetation distribution. Two known vegetation-fire feedbacks exist which could potentially increase fire frequency in tundra and reduce fire frequency in the boreal forest. The shift towards shrubs and grass species observed after severe tundra fire could increase tundra biomass and result in more frequent fire (Bret-Harte et al. 2013, Lantz et al. 2013). Paleoclimate data suggest that this has happened in the past (e.g. 13,000-11,000 B.P.), creating large areas of shrub tundra with fire frequency and severity similar to modern boreal systems (Higuera et al. 2008, Higuera et al. 2011). In boreal systems, climate-driven increases in fire can lead to dominance of less-flammable, early successional species, exerting a stabilizing feedback on fire-climate interactions (Beck et al. 2011, Johnstone et al. 2011, Kelly et al. 2013). In past periods of elevated temperature and modified precipitation such as the Medieval Climate Anomaly (1,000-500 B.P.), increases in the area covered by deciduous stands limited fire frequency despite climatic conditions favorable to fire (de Groot et al. 2003, Flannigan et al. 2009, Kelly et al. 2013). However, burning in the past few decades has surpassed fire frequency in parts of the boreal forest for at least the last 10,000 years, suggesting a shift into a new regime of highly active fire (Kelly et al. 2013).

Simulations of future fire regime in the boreal forest and arctic tundra nearly all project an increase in fire extent, severity, and emissions (summarized in Flannigan et al. 2009), however, many uncertainties surrounding vegetation-induced feedbacks on fire still remain, including the effect on vegetation of CO_2 fertilization, nitrogen availability, permafrost degradation, and precipitation (Balshi et al. 2009a, McGuire et al. 2009). Ultimately, future fire behavior in boreal

and tundra systems will depend on the interaction between changes in climate as expressed in short-term weather conditions and shifts in vegetation.

References:

ACIA. 2004. Impacts of a Warming Arctic: Arctic Climate Impact Assessment. Cambridge University Press, Cambridge, United Kingdom.

ACIA. 2005. Arctic Climate Impacts Assessment. Cambridge University Press, Cambridge, United Kingdom.

AMAP. 2011. Snow, Water, Ice and Permafrost in the Arctic (SWIPA): Climate Change and the Cryosphere. Arctic Monitoring and Assessment Programme (AMAP). Oslo, Norway.

Amiro, B. D., A. Cantin, M. D. Flannigan, and W. J. de Groot. 2009. Future emissions from Canadian boreal forest fires. Canadian Journal of Forest Research-Revue Canadienne De Recherche Forestiere **39**:383-395.

Balshi, M. S., A. D. McGuire, P. Duffy, M. Flannigan, D. W. Kicklighter, and J. Melillo. 2009a. Vulnerability of carbon storage in North American boreal forests to wildfires during the 21st century. Global Change Biology **15**:1491-1510.

Balshi, M. S., A. D. McGuire, Q. Zhuang, J. Melillo, D. W. Kicklighter, E. Kasischke, C. Wirth, M. Flannigan, J. Harden, J. S. Clein, T. J. Burnside, J. McAllister, W. A. Kurz, M. Apps, and A. Shvidenko. 2007. The role of historical fire disturbance in the carbon dynamics of the pan-boreal region: A process-based analysis. Journal of Geophysical Research-Biogeosciences **112**:-.

Balshi, M. S., A. D. McGuirez, P. Duffy, M. Flannigan, J. Walsh, and J. Melillo. 2009b. Assessing the response of area burned to changing climate in western boreal North America using a Multivariate Adaptive Regression Splines (MARS) approach. Global Change Biology **15**:578-600.

Barrett, K., A. Rocha, M. J. van de Weg, and G. Shaver. 2012. Vegetation shifts observed in arctic tundra 17 years after fire. Remote Sensing Letters **3**:729-736.

Beck, P. S. A., S. J. Goetz, M. C. Mack, H. D. Alexander, Y. F. Jin, J. T. Randerson, and M. M. Loranty. 2011. The impacts and implications of an intensifying fire regime on Alaskan boreal forest composition and albedo. Global Change Biology **17**:2853-2866.

Bond-Lamberty, B., C. K. Wang, and S. T. Gower. 2004. Net primary production and net ecosystem production of a boreal black spruce wildfire chronosequence. Global Change Biology **10**:473-487.

Bret-Harte, M. S., M. C. Mack, G. R. Shaver, D. C. Huebner, M. Johnston, C. A. Mojica, C. Pizano, and J. A. Reiskind. 2013. The response of Arctic vegetation and soils following an unusually severe tundra fire. Philosophical Transactions of the Royal Society B-Biological Sciences **368**.

Callaghan, T. V., L. O. Bjorn, Y. Chernov, T. Chapin, T. R. Christensen, B. Huntley, R. A. Ims, M. Johansson, D. Jolly, S. Jonasson, N. Matveyeva, N. Panikov, W. Oechel, G. Shaver, S. Schaphoff, and S. Sitch. 2004. Effects of changes in climate on landscape and regional processes, and feedbacks to the climate system. Ambio **33**:459-468.

Cary, G. J., R. E. Keane, R. H. Gardner, S. Lavorel, M. D. Flannigan, I. D. Davies, C. Li, J. M. Lenihan, T. S. Rupp, and F. Mouillot. 2006. Comparison of the sensitivity of landscape-fire-succession models to variation in terrain, fuel pattern, climate and weather. Landscape Ecology **21**:121-137.

Chambers, S. D., J. Beringer, J. T. Randerson, and F. S. Chapin. 2005. Fire effects on net radiation and energy partitioning: Contrasting responses of tundra and boreal forest ecosystems. Journal of Geophysical Research-Atmospheres **110**.

Chapin, F. S., P. A. Matson, and P. M. Vitousek. 2011. Principles of terrestrial ecosystem ecology. 2nd edition. Springer, New York.

Chapin, F. S., A. D. McGuire, J. Randerson, R. Pielke, D. Baldocchi, S. E. Hobbie, N. Roulet, W. Eugster, E. Kasischke, E. B. Rastetter, S. A. Zimov, and S. W. Running. 2000. Arctic and boreal ecosystems of western North America as components of the climate system. Global Change Biology **6**:211-223.

Chapin, F. S., A. D. McGuire, R. W. Ruess, T. N. Hollingsworth, M. C. Mack, J. F. Johnstone, E. S. Kasischke, E. S. Euskirchen, J. B. Jones, M. T. Jorgenson, K. Kielland, G. P. Kofinas, M. R. Turetsky, J. Yarie, A. H. Lloyd, and D. L. Taylor. 2010. Resilience of Alaska's boreal forest to climatic change. Canadian Journal of Forest Research-Revue Canadienne De Recherche Forestiere **40**:1360-1370.

de Groot, W. J., P. M. Bothwell, D. H. Carlsson, and K. A. Logan. 2003. Simulating the effects of future fire regimes on western Canadian boreal forests. Journal of Vegetation Science **14**:355-364.

de Groot, W. J., A. S. Cantin, M. D. Flannigan, A. J. Soja, L. M. Gowman, and A. Newbery. 2013. A comparison of Canadian and Russian boreal forest fire regimes. Forest Ecology and Management **294**:23-34.

Elmendorf, S. C., G. H. R. Henry, R. D. Hollister, R. G. Bjork, A. D. Bjorkman, T. V. Callaghan, L. S. Collier, E. J. Cooper, J. H. C. Cornelissen, T. A. Day, A. M. Fosaa, W. A. Gould, J. Gretarsdottir, J. Harte, L. Hermanutz, D. S. Hik, A. Hofgaard, F. Jarrad, I. S. Jonsdottir, F. Keuper, K. Klanderud, J. A. Klein, S. Koh, G. Kudo, S. I. Lang, V. Loewen, J. L. May, J. Mercado, A. Michelsen, U. Molau, I. H. Myers-Smith, S. F. Oberbauer, S. Pieper, E. Post, C. Rixen, C. H. Robinson, N. M. Schmidt, G. R. Shaver, A. Stenstrom, A. Tolvanen, O. Totland, T. Troxler, C. H. Wahren, P. J. Webber, J. M. Welker, and P. A. Wookey. 2012. Global assessment of experimental climate warming on tundra vegetation: heterogeneity over space and time. Ecology Letters **15**:164-175.

Epstein, H. E., M. K. Raynolds, D. A. Walker, U. S. Bhatt, C. J. Tucker, and J. E. Pinzon. 2012. Dynamics of aboveground phytomass of the circumpolar Arctic tundra during the past three decades. Environmental Research Letters **7**.

Euskirchen, E. S., A. D. McGuire, D. W. Kicklighter, Q. Zhuang, J. S. Clein, R. J. Dargaville, D. G. Dye, J. S. Kimball, K. C. McDonald, J. M. Melillo, V. E. Romanovsky, and N. V. Smith. 2006. Importance of recent shifts in soil thermal dynamics on growing season length, productivity, and carbon sequestration in terrestrial high-latitude ecosystems. Global Change Biology **12**:731-750.

Fetcher, N., T. F. Beatty, B. Mullinax, and D. S. Winkler. 1984. Changes in Arctic Tussock Tundra 13 Years after Fire. Ecology **65**:1332-1333.

Flannigan, M. D., M. A. Krawchuk, W. J. de Groot, B. M. Wotton, and L. M. Gowman. 2009. Implications of changing climate for global wildland fire. International Journal of Wildland Fire **18**:483-507.

Flannigan, M. D., K. A. Logan, B. D. Amiro, W. R. Skinner, and B. J. Stocks. 2005. Future area burned in Canada. Climatic Change **72**:1-16.

French, N. H. F., E. S. Kasischke, and D. G. Williams. 2002. Variability in the emission of carbon-based trace gases from wildfire in the Alaskan boreal forest. Journal of Geophysical Research-Atmospheres **108**.

Gamache, I. and S. Payette. 2005. Latitudinal response of subarctic tree lines to recent climate change in eastern Canada. Journal of Biogeography **32**:849-862.

Giglio, L., J. T. Randerson, G. R. van der Werf, P. S. Kasibhatla, G. J. Collatz, D. C. Morton, and R. S. DeFries. 2010. Assessing variability and long-term trends in burned area by merging multiple satellite fire products. Biogeosciences **7**:1171-1186.

Gillett, N. P., A. J. Weaver, F. W. Zwiers, and M. D. Flannigan. 2004. Detecting the effect of climate change on Canadian forest fires. Geophysical Research Letters **31**.

Girardin, M. P., A. A. Ali, C. Carcaillet, O. Blarquez, C. Hely, A. Terrier, A. Genries, and Y. Bergeron. 2013. Vegetation limits the impact of a warm climate on boreal wildfires. New Phytologist **199**:1001-1011.

Goetz, S. J., A. G. Bunn, G. J. Fiske, and R. A. Houghton. 2005. Satellite-observed photosynthetic trends across boreal North America associated with climate and fire disturbance. Proceedings of the National Academy of Sciences of the United States of America **102**:13521-13525.

Goulden, M. L., A. M. S. McMillan, G. C. Winston, A. V. Rocha, K. L. Manies, J. W. Harden, and B. P. Bond-Lamberty. 2011. Patterns of NPP, GPP, respiration, and NEP during boreal forest succession. Global Change Biology **17**:855-871.

Harden, J. W., K. L. Manies, M. R. Turetsky, and J. C. Neff. 2006. Effects of wildfire and permafrost on soil organic matter and soil climate in interior Alaska. Global Change Biology **12**:2391-2403.

Harden, J. W., S. E. Trumbore, B. J. Stocks, A. Hirsch, S. T. Gower, K. P. O'Neill, and E. S. Kasischke. 2000. The role of fire in the boreal carbon budget. Global Change Biology **6**:174-184.

Hayes, D. J., A. D. McGuire, D. W. Kicklighter, K. R. Gurney, T. J. Burnside, and J. M. Melillo. 2011. Is the northern high-latitude land-based CO2 sink weakening? Global Biogeochem. Cycles **25**:GB3018.

Hicke, J. A., G. P. Asner, E. S. Kasischke, N. H. F. French, J. T. Randerson, G. J. Collatz, B. J. Stocks, C. J. Tucker, S. O. Los, and C. B. Field. 2003. Postfire response of North

American boreal forest net primary productivity analyzed with satellite observations. Global Change Biology **9**:1145-1157.

Higuera, P. E., L. B. Brubaker, P. M. Anderson, T. A. Brown, A. T. Kennedy, and F. S. Hu. 2008. Frequent Fires in Ancient Shrub Tundra: Implications of Paleorecords for Arctic Environmental Change. Plos One **3**.

Higuera, P. E., M. L. Chipman, J. L. Barnes, M. A. Urban, and F. S. Hu. 2011. Variability of tundra fire regimes in Arctic Alaska: millennial-scale patterns and ecological implications. Ecological Applications **21**:3211-3226.

Hinkel, K. M. and F. E. Nelson. 2003. Spatial and temporal patterns of active layer thickness at Circumpolar Active Layer Monitoring (CALM) sites in northern Alaska, 1995-2000. Journal of Geophysical Research-Atmospheres **108**.

Hinzman, L. D., N. D. Bettez, W. R. Bolton, F. S. Chapin, M. B. Dyurgerov, C. L. Fastie, B. Griffith, R. D. Hollister, A. Hope, H. P. Huntington, A. M. Jensen, G. J. Jia, T. Jorgenson, D. L. Kane, D. R. Klein, G. Kofinas, A. H. Lynch, A. H. Lloyd, A. D. McGuire, F. E. Nelson, W. C. Oechel, T. E. Osterkamp, C. H. Racine, V. E. Romanovsky, R. S. Stone, D. A. Stow, M. Sturm, C. E. Tweedie, G. L. Vourlitis, M. D. Walker, D. A. Walker, P. J. Webber, J. M. Welker, K. Winker, and K. Yoshikawa. 2005. Evidence and implications of recent climate change in northern Alaska and other arctic regions. Climatic Change **72**:251-298.

Holland, M. M. and C. M. Bitz. 2003. Polar amplification of climate change in coupled models. Climate Dynamics **21**:221-232.

Holland, M. M., J. Finnis, A. P. Barrett, and M. C. Serreze. 2007. Projected changes in arctic ocean freshwater budgets. Journal of Geophysical Research-Biogeosciences **112**.

Hu, F. S., P. E. Higuera, J. E. Walsh, W. L. Chapman, P. A. Duffy, L. B. Brubaker, and M. L. Chipman. 2010. Tundra burning in Alaska: Linkages to climatic change and sea ice retreat. Journal of Geophysical Research-Biogeosciences **115**.

Jandt, R., K. Joly, C. R. Meyers, and C. Racine. 2008. Slow recovery of lichen on burned caribou winter range in Alaska tundra: Potential influences of climate warming and other disturbance factors. Arctic Antarctic and Alpine Research **40**:89-95.

Johnstone, J., T. S. Rupp, M. Olson, and D. Verbyla. 2011. Modeling impacts of fire severity on successional trajectories and future fire behavior in Alaskan boreal forests. Landscape Ecology **26**:487-500.

Joly, K., P. A. Duffy, and T. S. Rupp. 2012. Simulating the effects of climate change on fire regimes in Arctic biomes: implications for caribou and moose habitat. Ecosphere **3**:art36.

Jones, M. O., J. S. Kimball, and L. A. Jones. 2013. Satellite microwave detection of boreal forest recovery from the extreme 2004 wildfires in Alaska and Canada. Global Change Biology **19**:3111-3122.

Kasischke, E., K. O'Neill, N. F. French, and L. Bourgeau-Chavez. 2000. Controls on Patterns of Biomass Burning in Alaskan Boreal Forests. Pages 173-196 *in* E. Kasischke and B. Stocks, editors. Fire, Climate Change, and Carbon Cycling in the Boreal Forest. Springer New York.

Kasischke, E. S. and L. P. Bruhwiler. 2002. Emissions of carbon dioxide, carbon monoxide, and methane from boreal forest fires in 1998. Journal of Geophysical Research-Atmospheres **108**.

Kasischke, E. S. and N. H. F. French. 1997. Constraints on using AVHRR composite index imagery to study patterns of vegetation cover in boreal forests. International Journal of Remote Sensing **18**:2403-2426.

Kasischke, E. S. and M. R. Turetsky. 2006. Recent changes in the fire regime across the North American boreal region-Spatial and temporal patterns of burning across Canada and Alaska (vol 33, art no L09703, 2006). Geophysical Research Letters **33**.

Kattsov, V. M., J. E. Walsh, W. L. Chapman, V. A. Govorkova, T. V. Pavlova, and X. Zhang. 2007. Simulation and projection of arctic freshwater budget components by the IPCC AR4 global climate models. Journal of Hydrometeorology **8**:571-589.

Keeley, J. E. 2009. Fire intensity, fire severity and burn severity: a brief review and suggested usage. International Journal of Wildland Fire **18**:116-126.

Kelly, R., M. L. Chipman, P. E. Higuera, I. Stefanova, L. B. Brubaker, and F. S. Hu. 2013. Recent burning of boreal forests exceeds fire regime limits of the past 10,000 years. Proceedings of the National Academy of Sciences of the United States of America **110**:13055-13060.

Kienast, F., P. Tarasov, L. Schirrmeister, G. Grosse, and A. A. Andreev. 2008. Continental climate in the East Siberian Arctic during the last interglacial: Implications from palaeobotanical records. Global and Planetary Change **60**:535-562.

Korotkov, V. N., D. O. Logofet, and M. Loreau. 2001. Succession in mixed boreal forest of Russia: Markov models and non-Markov effects. Ecological Modelling **142**:25-38.

Korovin, G. N. 1996. Analysis of the Distribution of Forest Fires in Russia. Pages 112-128 *in* J. Goldammer and V. Furyaev, editors. Fire in Ecosystems of Boreal Eurasia. Springer Netherlands.

Koven, C. D., B. Ringeval, P. Friedlingstein, P. Ciais, P. Cadule, D. Khvorostyanov, G. Krinner, and C. Tarnocai. 2011. Permafrost carbon-climate feedbacks accelerate global warming. Proceedings of the National Academy of Sciences of the United States of America **108**:14769-14774.

Landhausser, S. M. and R. W. Wein. 1993. Postfire vegetation recovery and tree establishment at the Arctic treeline-climate-change-vegetation-response hypotheses. Journal of Ecology **81**:665-672.

Lantz, T. C., P. Marsh, and S. V. Kokelj. 2013. Recent Shrub Proliferation in the Mackenzie Delta Uplands and Microclimatic Implications. Ecosystems **16**:47-59.

Lawrence, D. M., A. G. Slater, and S. C. Swenson. 2012. Simulation of Present-Day and Future Permafrost and Seasonally Frozen Ground Conditions in CCSM4. Journal of Climate **25**:2207-2225.

Lloyd, A. H., M. E. Edwards, B. Finney, J. Lynch, V. A. Barber, and N. H. Bigelow. 2006. Holocene development of the Alaskan boreal forest. Pages 62-78 *in* F. S. Chapin, M. W. Oswood, K. Van Cleve, L. Viereck, and D. Verbyla, editors. Alaska's changing boreal forest. Oxford University Press, New York.

Mack, M. C., M. S. Bret-Harte, T. N. Hollingsworth, R. R. Jandt, E. A. G. Schuur, G. R. Shaver, and D. L. Verbyla. 2011. Carbon loss from an unprecedented Arctic tundra wildfire. Nature **475**:489-492.

Mack, M. C., K. K. Treseder, K. L. Manies, J. W. Harden, E. A. G. Schuur, J. G. Vogel, J. T. Randerson, and F. S. Chapin. 2008. Recovery of aboveground plant biomass and productivity after fire in mesic and dry black spruce forests of interior alaska. Ecosystems **11**:209-225.

McGuire, A. D., L. G. Anderson, T. R. Christensen, S. Dallimore, L. Guo, D. J. Hayes, M. Heimann, T. D. Lorenson, R. W. Macdonald, and N. Roulet. 2009. Sensitivity of the carbon cycle in the Arctic to climate change. Ecological Monographs **79**:523-555.

McGuire, A. D., J. M. Melillo, D. W. Kicklighter, and L. A. Joyce. 1995. Equilibrium Responses of Soil Carbon to Climate Change: Empirical and Process-Based Estimates. Journal of Biogeography **22**:785-796.

Myers-Smith, I. H., B. C. Forbes, M. Wilmking, M. Hallinger, T. Lantz, D. Blok, K. D. Tape, M. Macias-Fauria, U. Sass-Klaassen, E. Levesque, S. Boudreau, P. Ropars, L. Hermanutz, A. Trant, L. S. Collier, S. Weijers, J. Rozema, S. A. Rayback, N. M. Schmidt, G. Schaepman-Strub, S. Wipf, C. Rixen, C. B. Menard, S. Venn, S. Goetz, L. Andreu-Hayles, S. Elmendorf, V. Ravolainen, J. Welker, P. Grogan, H. E. Epstein, and D. S. Hik. 2011. Shrub expansion in tundra ecosystems: dynamics, impacts and research priorities. Environmental Research Letters **6**.

Niklasson, M. and A. Granstrom. 2000. Numbers and sizes of fires: Long-term spatially explicit fire history in a Swedish boreal landscape. Ecology **81**:1484-1499.

Osterkamp, T. E. 2007. Characteristics of the recent warming of permafrost in Alaska. Journal of Geophysical Research-Earth Surface **112**.

Osterkamp, T. E. and J. C. Jorgenson. 2006. Warming of permafrost in the Arctic National Wildlife Refuge, Alaska. Permafrost and Periglacial Processes **17**:65-69.

Osterkamp, T. E., M. T. Jorgenson, E. A. G. Schuur, Y. L. Shur, M. Z. Kanevskiy, J. G. Vogel, and V. E. Tumskoy. 2009. Physical and Ecological Changes Associated with Warming Permafrost and Thermokarst in Interior Alaska. Permafrost and Periglacial Processes **20**:235-256.

Osterkamp, T. E. and V. E. Romanovsky. 1999. Evidence for warming and thawing of discontinuous permafrost in Alaska. Permafrost and Periglacial Processes **10**:17-37.

Pan, Y., R. A. Birdsey, J. Fang, R. Houghton, P. E. Kauppi, W. A. Kurz, O. L. Phillips, A. Shvidenko, S. L. Lewis, J. G. Canadell, P. Ciais, R. B. Jackson, S. Pacala, A. D. McGuire, S. Piao, A. Rautiainen, S. Sitch, and D. Hayes. 2011. A Large and Persistent Carbon Sink in the World's Forests. Science.

Parisien, M. A., S. A. Parks, M. A. Krawchuk, M. D. Flannigan, L. M. Bowman, and M. A. Moritz. 2011. Scale-dependent controls on the area burned in the boreal forest of Canada, 1980-2005. Ecological Applications **21**:789-805.

Payette, S., L. Filion, and A. Delwaide. 2008. Spatially explicit fire-climate history of the boreal forest-tundra (Eastern Canada) over the last 2000 years. Philosophical Transactions of the Royal Society B-Biological Sciences **363**:2301-2316.

Perera, A. H., D. L. E. I. D. T. Edited by Ajith H. Perera, D. L. Euler, and I. D. Thompson. 2011. Ecology of a Managed Terrestrial Landscape: Patterns and Processes of Forest Landscapes in Ontario. UBC Press.

Potter, C. S. and S. A. Klooster. 1997. Global model estimates of carbon and nitrogen storage in litter and soil pools: Response to changes in vegetation quality and biomass allocation. Tellus Series B-Chemical and Physical Meteorology **49**:1-17.

Racine, C., R. Jandt, C. Meyers, and J. Dennis. 2004. Tundra fire and vegetation change along a hillslope on the Seward Peninsula, Alaska, USA. Arctic Antarctic and Alpine Research **36**:1-10.

Racine, C. H., L. A. Johnson, and L. A. Viereck. 1987. Patterns of Vegetation Recovery after Tundra Fires in Northwestern Alaska, USA. Arctic and Alpine Research **19**:461-469.

Rawlins, M. A., M. Steele, M. M. Holland, J. C. Adam, J. E. Cherry, J. A. Francis, P. Y. Groisman, L. D. Hinzman, T. G. Huntington, D. L. Kane, J. S. Kimball, R. Kwok, R. B. Lammers, C. M. Lee, D. P. Lettenmaier, K. C. McDonald, E. Podest, J. W. Pundsack, B. Rudels, M. C. Serreze, A. Shiklomanov, Ø. Skagseth, T. J. Troy, C. J. Vörösmarty, M. Wensnahan, E. F. Wood, R. Woodgate, D. Yang, K. Zhang, and T. Zhang. 2010. Analysis of the Arctic System for Freshwater Cycle Intensification: Observations and Expectations. Journal of Climate **23**:5715-5737.

Raynolds, M. K., D. A. Walker, H. E. Epstein, J. E. Pinzon, and C. J. Tucker. 2012. A new estimate of tundra-biome phytomass from trans-Arctic field data and AVHRR NDVI. Remote Sensing Letters **3**:403-411.

Rocha, A. V., M. M. Loranty, P. E. Higuera, M. C. Mack, F. S. Hu, B. M. Jones, A. L. Breen, E. B. Rastetter, S. J. Goetz, and G. R. Shaver. 2012. The footprint of Alaskan tundra fires during the past half-century: implications for surface properties and radiative forcing. Environmental Research Letters **7**.

Rocha, A. V. and G. R. Shaver. 2011. Postfire energy exchange in arctic tundra: the importance and climatic implications of burn severity. Global Change Biology **17**:2831-2841.

Rogers, B. M., J. T. Randerson, and G. B. Bonan. 2012. High latitude cooling associated with landscape changes from North American boreal forest fires. Biogeosciences Discuss. **9**:12087-12136.

Saito, K., M. Kimoto, T. Zhang, K. Takata, and S. Emori. 2007. Evaluating a high-resolution climate model: Simulated hydrothermal regimes in frozen ground regions and their change under the global warming scenario. Journal of Geophysical Research-Earth Surface **112**:-.

Schaefer, K., T. Zhang, L. Bruhwiler, and A. P. Barrett. 2011. Amount and timing of permafrost carbon release in response to climate warming. Tellus Series B-Chemical and Physical Meteorology:no-no.

Simpson, I. J., S. K. Akagi, B. Barletta, N. J. Blake, Y. Choi, G. S. Diskin, A. Fried, H. E. Fuelberg, S. Meinardi, F. S. Rowland, S. A. Vay, A. J. Weinheimer, P. O. Wennberg, P. Wiebring, A. Wisthaler, M. Yang, R. J. Yokelson, and D. R. Blake. 2011. Boreal forest fire emissions in fresh Canadian smoke plumes: C-1-C-10 volatile organic compounds (VOCs), CO_2, CO, NO_2, NO, HCN and CH_3CN. Atmospheric Chemistry and Physics **11**:6445-6463.

Soja, A. J., W. R. Cofer, H. H. Shugart, A. I. Sukhinin, P. W. Stackhouse, D. J. McRae, and S. G. Conard. 2004. Estimating fire emissions and disparities in boreal Siberia (1998-2002). Journal of Geophysical Research-Atmospheres **109**.

Stocks, B. J., M. E. Alexander, and R. A. Lanoville. 2004. Overview of the International Crown Fire Modelling Experiment (ICFME). Canadian Journal of Forest Research-Revue Canadienne De Recherche Forestiere **34**:1543-1547.

Sturm, M., J. P. McFadden, G. E. Liston, F. S. Chapin, C. H. Racine, and J. Holmgren. 2001. Snow-shrub interactions in Arctic tundra: A hypothesis with climatic implications. Journal of Climate **14**:336-344.

Tape, K., M. Sturm, and C. Racine. 2006. The evidence for shrub expansion in Northern Alaska and the Pan-Arctic. Global Change Biology **12**:686-702.

Turetsky, M. R., E. S. Kane, J. W. Harden, R. D. Ottmar, K. L. Manies, E. Hoy, and E. S. Kasischke. 2011. Recent acceleration of biomass burning and carbon losses in Alaskan forests and peatlands. Nature Geoscience **4**:27-31.

Uotila, A. and J. Kouki. 2005. Understorey vegetation in spruce-dominated forests in eastern Finland and Russian Karelia: Successional patterns after anthropogenic and natural disturbances. Forest Ecology and Management **215**:113-137.

van der Werf, G. R., J. T. Randerson, L. Giglio, G. J. Collatz, M. Mu, P. S. Kasibhatla, D. C. Morton, R. S. DeFries, Y. Jin, and T. T. van Leeuwen. 2010. Global fire emissions and the contribution of deforestation, savanna, forest, agricultural, and peat fires (1997–2009). Atmos. Chem. Phys. **10**:11707-11735.

Vavrek, M. C., N. Fetcher, J. B. McGraw, G. R. Shaver, F. S. C. Iii, and B. Bovard. 1999. Recovery of Productivity and Species Diversity in Tussock Tundra Following Disturbance. Arctic, Antarctic, and Alpine Research **31**:254-258.

Wein, R. W. and L. C. Bliss. 1973. Changes in Arctic Eriophorum Tussock Communities Following Fire. Ecology **54**:845-852.

Zhang, T., J. A. Heginbottom, R. G. Barry, and J. Brown. 2000. Further statistics on the distribution of permafrost and ground ice in the Northern Hemisphere. Polar Geography **24**:126-131.

Zhang, T., R.G. Barry, K. Knowles, J.A. Heginbottom, and J. Brown. 1999. Statistics and characteristics of permafrost and ground ice distribution in the Northern Hemisphere. Polar Geography **23**:147-169.

A2.0.2.8 Hydrologic carbon flux background information sent to participants

Net ecosystem carbon balance of the permafrost region: hydrologic flux background information[1]

Benjamin W. Abbott, Jeremy B. Jones, University of Alaska Fairbanks
Jorien E. Vonk, Utrecht University

Question: How will organic carbon load and lability change in a warmer world?

System characteristics: The pan-arctic watershed, defined as the drainages of the Arctic Ocean and surrounding seas, covers 20.5 x 10^6 km^2 (Holmes et al. 2012b) and yields 3700 km^3 of discharge annually (McGuire et al. 2009, Holmes et al. 2012a). Worldwide, freshwater ecosystems are active conduits, transporting and transforming globally relevant loads of dissolved and particulate organic carbon (DOC and POC, respectively; Cole et al. 2007, Battin et al. 2009). Freshwater ecosystems play a particularly influential role in regulating carbon cycling at high latitudes, where they cover more than 50% of the landscape in some regions (McGuire et al. 2009) and account for 11% of global runoff, 36% of global lake area, over 50% of global wetland area (Loveland et al. 2000, Lammers et al. 2001, Aufdenkampe et al. 2011, Avis et al. 2011). As permafrost volume shrinks due to climate change, more of the 1670 Pg of organic carbon (C) stored in permafrost region soils (Tarnocai 2009) will thaw and some portion will become available for transport to aquatic ecosystems, depending on changes in local and regional hydrology (Frey and McClelland 2009, O'Donnell et al. 2012, Tank et al. 2012). The response of hydrologic C flux to climate change is a highly uncertain and relatively understudied component of the arctic C cycle (McClelland et al. 2008).

Arctic and boreal environmental change: High latitude air temperature is increasing twice as fast as global mean temperature, due largely to feedbacks associated with sea-ice loss and

[1] This document is not intended as a comprehensive or endorsed list of citations or information. It is a partial summary of the current understanding of biomass pools and potential changes to be used as a reference if desired while filling out the arctic and boreal biomass survey.

decrease in snow cover (Holland and Bitz 2003, ACIA 2005, AMAP 2011, Parmentier et al. 2013). Warming has been most prevalent during the autumn and early winter in coastal areas, when sea ice is at its minimum, and in the spring at latitudes from 50° - 60° N as snow cover decreases (AMAP 2011). Growing season length, historically 100 days for tundra and 150 days for boreal forest, has increased 2 – 4 days per decade from 1960 – 2000, due mostly to earlier spring thaw (Euskirchen et al. 2006, Chapin et al. 2011), and is projected to lengthen a total of 37 – 60 days over pre-industrial conditions by the end of the century (Euskirchen et al. 2006, Koven et al. 2011). An intensification of the freshwater cycle is projected across the arctic including increases in precipitation, evapotranspiration (ET), storage, and discharge (Rawlins et al. 2010), however the relative magnitude of these parameters is poorly constrained (Holmes et al. 2012a). Precipitation has increased 5 % over land north of 55° since 1950, though this trend is not significant due to high interannual variability (Peterson et al. 2006, AMAP 2011). Precipitation minus ET is expected to increase 13-25 % by 2100, mostly driven by increases in winter precipitation (Holland et al. 2007, Kattsov et al. 2007), but some areas are expected to experience regional drying (Chapin et al. 2010). While annual discharge is highly variable, average pan-arctic discharge has increased 6-10 % since the 1960s and 70s in many regions (Peterson et al. 2002, McClelland et al. 2006, Dery et al. 2009, Overeem and Syvitski 2010).

Changes in air temperature and precipitation have warmed both permafrost and non-permafrost soils over the past century, causing increased active layer thickness, extended freeze-thaw cycling, longer duration of thaw, and widespread ground collapse or thermokarst (Osterkamp and Romanovsky 1999, Hinkel and Nelson 2003, Osterkamp and Jorgenson 2006, Osterkamp 2007, Osterkamp et al. 2009). Models predict widespread near-surface permafrost degradation (in the top 3 m) with projections varying between 40 - 72 % loss by 2100 (Saito et al. 2007, Schaefer et al. 2011, Lawrence et al. 2012). This widespread degradation of permafrost is correlated with increasing winter base flow and the seasonal contribution of ground water relative to surface water (Smith et al. 2007, Walvoord and Striegl 2007, Frey and McClelland 2009). Coupled to changes in hydrology, aquatic chemistry has experienced substantial shifts, including an increase in DOC flux in areas with peat and thick organic soils (Frey and McClelland 2009), a decrease in discharge-normalized DOC where organic soils are shallow (Striegl et al. 2005), increases in major ion concentrations (Frey and McClelland 2009), accelerated chemical weathering (Tank et al. 2012), and increased inorganic nutrient concentrations (McClelland et al. 2007).

Climate change is accelerating thaw and erosion of arctic coastlines due to warming air and water in combination with increased exposure to wave action and storms due to reductions in sea ice cover (IPCC 2007, Stroeve et al. 2007). Thermal collapse and erosion of arctic coastlines delivers DOC and POC to coastal shelf waters, with collapse most pronounced in northeastern Alaska and East-Siberia (Rachold et al. 2000, Jones et al. 2009, Lantuit et al. 2012). Along the Beaufort Sea coast, coastal retreat rates have increased during the last decades (6.8 m yr^{-1} from 1955-1979 to 13.6 m yr^{-1} from 2002-2007; Jones et al. 2009).

Loads and lability: Arctic rivers deliver 36 Tg yr^{-1} of DOC to the ocean, which is 10% of the global terrigenous DOC load (Opsahl et al. 1999), and 6 Tg yr^{-1} of POC (McGuire et al. 2009). It is estimated that another 37-84 Tg yr^{-1} of DOC and 20 Tg yr^{-1} POC are delivered to inland waters but respired to the atmosphere or buried in lakes and streams before reaching the ocean (McGuire et al. 2009, Aufdenkampe et al. 2011), though direct measurements of delivery to inland waters are very scarce. In addition to C carried by inland waters, 18 Tg yr^{-1} or more of POC is released to the Arctic Ocean and surrounding seas from coastal erosion (McGuire et al. 2009, Vonk et al. 2012). In some areas, such as the Eastern Siberian and Laptev Seas, C release from coastal erosion makes up more than half the total C delivery to the ocean (Rachold et al. 2000, Vonk et al. 2012).

Table A2.4 Organic carbon fluxes in the permafrost region

	DOC (Tg $year^{-1}$)	Riverine POC (Tg $year^{-1}$)	Coastal erosion POC (Tg $year^{-1}$)
Delivery to freshwater ecosystems	100**	20	na
Delivery to Arctic Ocean and surrounding seas	36*	6**	18***

*(Holmes et al. 2012b), **(McGuire et al. 2009), ***sum of coastal erosion POC delivered to ocean from Vonk et al. 2012 and McGuire et al. 2009. Terrestrial to freshwater delivery of POC was calculated by dividing ocean delivery (6 Tg yr^{-1}) with the downscaled global ratio of 0.75 sedimentation of POC (Aufdenkampe et al. 2011, Battin et al. 2009, McGuire et al. 2009).

Arctic riverine C load is not distributed evenly through the year, with 49% of DOC flux occurring in the two months surrounding peak flow, typically mid-May to mid-July (Finlay et al. 2006, Holmes et al. 2012b). The character, age, and biodegradability of DOC and POC also vary seasonally with more aromatic, labile, and modern C transported in spring and less aromatic, recalcitrant, older C released late in the season, potentially due to differences in thaw depth and transport time (Neff et al. 2006, Holmes et al. 2008). Wintertime DOC can be highly biodegradable (Wickland et al. 2012), though concentrations are typically low (Striegl et al. 2005). Less is known about seasonal patterns of POC, which is typically much older than DOC and potentially more closely linked to permafrost thaw (Guo and Macdonald 2006, Guo et al. 2007).

DOC from surface water in the arctic was once considered inert but recent observations have quantified substantial pools of biodegradable DOC (BDOC). Some rivers transport labile DOC during winter, and BDOC constitutes 20 – 40% of the DOC pool during snowmelt, but less than 10% later in the season (Holmes et al. 2008, Mann et al. 2012, Wickland et al. 2012). These seasonal variations in BDOC are related to DOC composition and nutrient availability (Holmes et al., 2008; Balcarczyk et al., 2009; Mann et al., 2012; Wickland et al., 2012). High biodegradability of snowmelt DOC may be due to fast transport of terrestrially derived DOC to streams early in the season when thaw depth is shallow (Holmes et al. 2008, Wickland et al. 2012), the flush of DOC derived from microbial cells lysed the previous fall during soil freeze-up (Michaelson et al. 1998), and leachate from the previous growing season's leaf litter (Neff et al. 2006, Spencer et al. 2008, Mann et al. 2012). The effect of permafrost regime (areal extent and active layer depth) on DOC yield and biodegradability varies by region, with permafrost extent both positively and negatively correlated with DOC concentrations and lability (Kawahigashi et al. 2004, Striegl et al. 2005, Balcarczyk et al. 2009, Frey and McClelland 2009, Vonk et al. 2013). Biodegradability of permafrost-derived DOC varies from less than 10% DOC loss over 40 days (Balcarczyk et al. 2009) to 34% over 14 days (Vonk et al. 2013), but few estimates are available.

Hydrologic carbon flux response to change: Changes in the hydrologic cycle will affect C transport and processing, however the relationship between hydrology and C load and lability may change non-linearly as the volume of thawed C increases and flowpaths change. The rate of

C transport and processing in aquatic systems depends on two related factors: 1. exposure of C to hydrologic export, and 2. biodegradability of thawed C.

As the Arctic warms, C from thawing permafrost will play an increasingly important role governing freshwater and estuarine C and nutrient dynamics through the season. Before permafrost C can enter the modern aquatic C cycle, regardless of its biodegradability, it has to come in contact with surface or ground waters. Because hydraulic conductivity in arctic mineral soils is often very low, much permafrost C may be inaccessible to hydrologic transport even after thaw. However, when soil ice-content is high, permafrost thaw results in ground subsidence, or thermokarst, which can rapidly mobilize sediment, nutrients, and C (Bowden et al. 2008). Thermokarst can release permafrost C from meters below the active layer when exposed on coastal slopes, river banks, lake shores, or hillslopes (Vonk et al. 2012, Cory et al. 2013, Vonk et al. 2013), and may impact watershed-level C biodegradability and nutrient concentrations (Bowden et al. 2008, Woods et al. 2011). Approximately a third of the permafrost region has high ice content (Zhang et al. 1999) and is susceptible to this pathway of catastrophic permafrost collapse upon thaw (Jorgenson et al. 2006).

Little is known concerning mechanistic controls on persistence or processing of modern DOC in arctic and boreal rivers (Mann et al. 2012, Wickland et al. 2012), and even less is known about the behavior of permafrost-derived organic carbon in arctic freshwater and marine ecosystems (Cory et al. 2013, Vonk and Gustafsson 2013). A large portion of bulk soil C in permafrost can be mineralized upon thaw, and much of this mineralized C is from DOC in the soil solution (Dutta et al. 2006, Zimov et al. 2006, Waldrop et al. 2010). DOC from collapsing ice-rich Pleistocene permafrost is very biodegradable (Vonk et al. 2013). However, some DOC released from degrading permafrost is recalcitrant (Balcarczyk et al. 2009), potentially due to differences in permafrost or ground-ice type, previous thaw events, or preferential mineral sorption of hydrophobic C species, which tend to be recalcitrant, during permafrost formation (Kawahigashi et al. 2004). Ultimately, permafrost degradation and ecosystem response to climate change will influence DOC and POC sources as well as hydrologic transportation pathways and storage. These factors together will determine the magnitude and rate of hydrologic C flux from the pan-arctic watershed.

References:

ACIA. 2005. Arctic Climate Impacts Assessment. Cambridge University Press, Cambridge, United Kingdom.

AMAP. 2011. Snow, Water, Ice and Permafrost in the Arctic (SWIPA): Climate Change and the Cryosphere. Arctic Monitoring and Assessment Programme (AMAP). Oslo, Norway.

Aufdenkampe, A. K., E. Mayorga, P. A. Raymond, J. M. Melack, S. C. Doney, S. R. Alin, R. E. Aalto, and K. Yoo. 2011. Riverine coupling of biogeochemical cycles between land, oceans, and atmosphere. Frontiers in Ecology and the Environment **9**:53-60.

Avis, C. A., A. J. Weaver, and K. J. Meissner. 2011. Reduction in areal extent of high-latitude wetlands in response to permafrost thaw. Nature Geosci **4**:444-448.

Balcarczyk, K. L., J. B. Jones, R. Jaffe, and N. Maie. 2009. Stream dissolved organic matter bioavailability and composition in watersheds underlain with discontinuous permafrost. Biogeochemistry **94**:255-270.

Battin, T. J., S. Luyssaert, L. A. Kaplan, A. K. Aufdenkampe, A. Richter, and L. J. Tranvik. 2009. The boundless carbon cycle. Nature Geosci **2**:598-600.

Bowden, W. B., M. N. Gooseff, A. Balser, A. Green, B. J. Peterson, and J. Bradford. 2008. Sediment and nutrient delivery from thermokarst features in the foothills of the North Slope, Alaska: Potential impacts on headwater stream ecosystems. Journal of Geophysical Research-Biogeosciences **113**.

Chapin, F. S., P. A. Matson, and P. M. Vitousek. 2011. Principles of terrestrial ecosystem ecology. 2nd edition. Springer, New York.

Chapin, F. S., A. D. McGuire, R. W. Ruess, T. N. Hollingsworth, M. C. Mack, J. F. Johnstone, E. S. Kasischke, E. S. Euskirchen, J. B. Jones, M. T. Jorgenson, K. Kielland, G. P. Kofinas, M. R. Turetsky, J. Yarie, A. H. Lloyd, and D. L. Taylor. 2010. Resilience of Alaska's boreal forest to climatic change. Canadian Journal of Forest Research-Revue Canadienne De Recherche Forestiere **40**:1360-1370.

Cole, J. J., Y. T. Prairie, N. F. Caraco, W. H. McDowell, L. J. Tranvik, R. G. Striegl, C. M. Duarte, P. Kortelainen, J. A. Downing, J. J. Middelburg, and J. Melack. 2007. Plumbing the global carbon cycle: Integrating inland waters into the terrestrial carbon budget. Ecosystems **10**:171-184.

Cory, R. M., B. C. Crump, J. A. Dobkowski, and G. W. Kling. 2013. Surface exposure to sunlight stimulates CO2 release from permafrost soil carbon in the Arctic. Proceedings of the National Academy of Sciences of the United States of America **110**:3429-3434.

Dery, S. J., M. A. Hernandez-Henriquez, J. E. Burford, and E. F. Wood. 2009. Observational evidence of an intensifying hydrological cycle in northern Canada. Geophysical Research Letters **36**.

Dutta, K., E. A. G. Schuur, J. C. Neff, and S. A. Zimov. 2006. Potential carbon release from permafrost soils of Northeastern Siberia. Global Change Biology **12**:2336-2351.

Euskirchen, E. S., A. D. McGuire, D. W. Kicklighter, Q. Zhuang, J. S. Clein, R. J. Dargaville, D. G. Dye, J. S. Kimball, K. C. McDonald, J. M. Melillo, V. E. Romanovsky, and N. V. Smith. 2006. Importance of recent shifts in soil thermal dynamics on growing season length, productivity, and carbon sequestration in terrestrial high-latitude ecosystems. Global Change Biology **12**:731-750.

Finlay, J., J. Neff, S. Zimov, A. Davydova, and S. Davydov. 2006. Snowmelt dominance of dissolved organic carbon in high-latitude watersheds: Implications for characterization and flux of river DOC. Geophysical Research Letters **33**.

Frey, K. E. and J. W. McClelland. 2009. Impacts of permafrost degradation on arctic river biogeochemistry. Hydrological Processes **23**:169-182.

Guo, L. D. and R. W. Macdonald. 2006. Source and transport of terrigenous organic matter in the upper Yukon River: Evidence from isotope (delta(13)C, Delta(14)C, and delta(15)N) composition of dissolved, colloidal, and particulate phases. Global Biogeochemical Cycles **20**.

Guo, L. D., C. L. Ping, and R. W. Macdonald. 2007. Mobilization pathways of organic carbon from permafrost to arctic rivers in a changing climate. Geophysical Research Letters **34**.

Hinkel, K. M. and F. E. Nelson. 2003. Spatial and temporal patterns of active layer thickness at Circumpolar Active Layer Monitoring (CALM) sites in northern Alaska, 1995-2000. Journal of Geophysical Research-Atmospheres **108**.

Holland, M. M. and C. M. Bitz. 2003. Polar amplification of climate change in coupled models. Climate Dynamics **21**:221-232.

Holland, M. M., J. Finnis, A. P. Barrett, and M. C. Serreze. 2007. Projected changes in arctic ocean freshwater budgets. Journal of Geophysical Research-Biogeosciences **112**.

Holmes, R. M., M. T. Coe, G. J. Fiske, T. Gurtovaya, J. W. McClelland, A. I. Shiklomanov, R. G. M. Spencer, S. E. Tank, and A. V. Zhulidov. 2012a. Climate Change Impacts on the Hydrology and Biogeochemistry of Arctic Rivers. Pages 1-26 Climatic Change and Global Warming of Inland Waters. John Wiley & Sons, Ltd.

Holmes, R. M., J. W. McClelland, B. J. Peterson, S. E. Tank, E. Bulygina, T. I. Eglinton, V. V. Gordeev, T. Y. Gurtovaya, P. A. Raymond, D. J. Repeta, R. Staples, R. G. Striegl, A. V. Zhulidov, and S. A. Zimov. 2012b. Seasonal and Annual Fluxes of Nutrients and Organic Matter from Large Rivers to the Arctic Ocean and Surrounding Seas. Estuaries and Coasts **35**:369-382.

Holmes, R. M., J. W. McClelland, P. A. Raymond, B. B. Frazer, B. J. Peterson, and M. Stieglitz. 2008. Lability of DOC transported by Alaskan rivers to the arctic ocean. Geophysical Research Letters **35**.

IPCC. 2007. Intergovernmental Panel on Climate Change Fourth Assessment Report (AR 4). Fourth Assessment Report (AR4):212.

Jones, B. M., C. D. Arp, M. T. Jorgenson, K. M. Hinkel, J. A. Schmutz, and P. L. Flint. 2009. Increase in the rate and uniformity of coastline erosion in Arctic Alaska. Geophysical Research Letters **36**.

Jorgenson, M. T., Y. L. Shur, and E. R. Pullman. 2006. Abrupt increase in permafrost degradation in Arctic Alaska. Geophysical Research Letters **33**.

Kattsov, V. M., J. E. Walsh, W. L. Chapman, V. A. Govorkova, T. V. Pavlova, and X. Zhang. 2007. Simulation and projection of arctic freshwater budget components by the IPCC AR4 global climate models. Journal of Hydrometeorology **8**:571-589.

Kawahigashi, M., K. Kaiser, K. Kalbitz, A. Rodionov, and G. Guggenberger. 2004. Dissolved organic matter in small streams along a gradient from discontinuous to continuous permafrost. Global Change Biology **10**:1576-1586.

Koven, C. D., B. Ringeval, P. Friedlingstein, P. Ciais, P. Cadule, D. Khvorostyanov, G. Krinner, and C. Tarnocai. 2011. Permafrost carbon-climate feedbacks accelerate global warming. Proceedings of the National Academy of Sciences of the United States of America **108**:14769-14774.

Lammers, R. B., A. I. Shiklomanov, C. J. Vorosmarty, B. M. Fekete, and B. J. Peterson. 2001. Assessment of contemporary Arctic river runoff based on observational discharge records. Journal of Geophysical Research-Atmospheres **106**:3321-3334.

Lantuit, H., P. P. Overduin, N. Couture, S. Wetterich, F. Are, D. Atkinson, J. Brown, G. Cherkashov, D. Drozdov, D. L. Forbes, A. Graves-Gaylord, M. Grigoriev, H. W. Hubberten, J. Jordan, T. Jorgenson, R. S. Odegard, S. Ogorodov, W. H. Pollard, V. Rachold, S. Sedenko, S. Solomon, F. Steenhuisen, I. Streletskaya, and A. Vasiliev. 2012. The Arctic Coastal Dynamics Database: A New Classification Scheme and Statistics on Arctic Permafrost Coastlines. Estuaries and Coasts **35**:383-400.

Lawrence, D. M., A. G. Slater, and S. C. Swenson. 2012. Simulation of Present-Day and Future Permafrost and Seasonally Frozen Ground Conditions in CCSM4. Journal of Climate **25**:2207-2225.

Loveland, T. R., B. C. Reed, J. F. Brown, D. O. Ohlen, Z. Zhu, L. Yang, and J. W. Merchant. 2000. Development of a global land cover characteristics database and IGBP DISCover from 1 km AVHRR data. International Journal of Remote Sensing **21**:1303-1330.

Mann, P. J., A. Davydova, N. Zimov, R. G. M. Spencer, S. Davydov, E. Bulygina, S. Zimov, and R. M. Holmes. 2012. Controls on the composition and lability of dissolved organic matter in Siberia's Kolyma River basin. Journal of Geophysical Research-Biogeosciences **117**.

McClelland, J. W., S. J. Dery, B. J. Peterson, R. M. Holmes, and E. F. Wood. 2006. A pan-arctic evaluation of changes in river discharge during the latter half of the 20th century. Geophysical Research Letters **33**.

McClelland, J. W., R. M. Holmes, B. J. Peterson, R. Amon, T. Brabets, L. Cooper, J. Gibson, V. V. Gordeev, C. Guay, D. Milburn, R. Staples, P. A. Raymond, I. Shiklomanov, R. Striegl, A. Zhulidov, T. Gurtovaya, and S. Zimov. 2008. Development of a Pan-Arctic Database for River Chemistry. Eos, Transactions American Geophysical Union **89**:217-218.

McClelland, J. W., M. Stieglitz, F. Pan, R. M. Holmes, and B. J. Peterson. 2007. Recent changes in nitrate and dissolved organic carbon export from the upper Kuparuk River, North Slope, Alaska. Journal of Geophysical Research-Biogeosciences **112**.

McGuire, A. D., L. G. Anderson, T. R. Christensen, S. Dallimore, L. Guo, D. J. Hayes, M. Heimann, T. D. Lorenson, R. W. Macdonald, and N. Roulet. 2009. Sensitivity of the carbon cycle in the Arctic to climate change. Ecological Monographs **79**:523-555.

Michaelson, G. J., C. L. Ping, G. W. Kling, and J. E. Hobbie. 1998. The character and bioactivity of dissolved organic matter at thaw and in the spring runoff waters of the arctic tundra north slope, Alaska. Journal of Geophysical Research-Atmospheres **103**:28939-28946.

Neff, J. C., J. C. Finlay, S. A. Zimov, S. P. Davydov, J. J. Carrasco, E. A. G. Schuur, and A. I. Davydova. 2006. Seasonal changes in the age and structure of dissolved organic carbon in Siberian rivers and streams. Geophysical Research Letters **33**.

O'Donnell, J. A., G. R. Aiken, M. A. Walvoord, and K. D. Butler. 2012. Dissolved organic matter composition of winter flow in the Yukon River basin: Implications of permafrost thaw and increased groundwater discharge. Global Biogeochemical Cycles **26**.

Opsahl, S., R. Benner, and R. M. W. Amon. 1999. Major flux of terrigenous dissolved organic matter through the Arctic Ocean. Limnology and Oceanography **44**:2017-2023.

Osterkamp, T. E. 2007. Characteristics of the recent warming of permafrost in Alaska. Journal of Geophysical Research-Earth Surface **112**.

Osterkamp, T. E. and J. C. Jorgenson. 2006. Warming of permafrost in the Arctic National Wildlife Refuge, Alaska. Permafrost and Periglacial Processes **17**:65-69.

Osterkamp, T. E., M. T. Jorgenson, E. A. G. Schuur, Y. L. Shur, M. Z. Kanevskiy, J. G. Vogel, and V. E. Tumskoy. 2009. Physical and Ecological Changes Associated with Warming Permafrost and Thermokarst in Interior Alaska. Permafrost and Periglacial Processes **20**:235-256.

Osterkamp, T. E. and V. E. Romanovsky. 1999. Evidence for warming and thawing of discontinuous permafrost in Alaska. Permafrost and Periglacial Processes **10**:17-37.

Overeem, I. and J. P. M. Syvitski. 2010. Shifting Discharge Peaks in Arctic Rivers, 1977-2007. Geografiska Annaler Series a-Physical Geography **92A**:285-296.

Parmentier, F. J. W., T. R. Christensen, L. L. Sorensen, S. Rysgaard, A. D. McGuire, P. A. Miller, and D. A. Walker. 2013. The impact of lower sea-ice extent on Arctic greenhouse-gas exchange. Nature Climate Change **3**:195-202.

Peterson, B. J., R. M. Holmes, J. W. McClelland, C. J. Vorosmarty, R. B. Lammers, A. I. Shiklomanov, I. A. Shiklomanov, and S. Rahmstorf. 2002. Increasing river discharge to the Arctic Ocean. Science **298**:2171-2173.

Peterson, B. J., J. McClelland, R. Curry, R. M. Holmes, J. E. Walsh, and K. Aagaard. 2006. Trajectory shifts in the Arctic and subarctic freshwater cycle. Science **313**:1061-1066.

Rachold, V., M. N. Grigoriev, F. E. Are, S. Solomon, E. Reimnitz, H. Kassens, and M. Antonow. 2000. Coastal erosion vs riverine sediment discharge in the Arctic Shelf seas. International Journal of Earth Sciences **89**:450-460.

Rawlins, M. A., M. Steele, M. M. Holland, J. C. Adam, J. E. Cherry, J. A. Francis, P. Y. Groisman, L. D. Hinzman, T. G. Huntington, D. L. Kane, J. S. Kimball, R. Kwok, R. B. Lammers, C. M. Lee, D. P. Lettenmaier, K. C. McDonald, E. Podest, J. W. Pundsack, B. Rudels, M. C. Serreze, A. Shiklomanov, Ø. Skagseth, T. J. Troy, C. J. Vörösmarty, M. Wensnahan, E. F. Wood, R. Woodgate, D. Yang, K. Zhang, and T. Zhang. 2010. Analysis of the Arctic System for Freshwater Cycle Intensification: Observations and Expectations. Journal of Climate **23**:5715-5737.

Saito, K., M. Kimoto, T. Zhang, K. Takata, and S. Emori. 2007. Evaluating a high-resolution climate model: Simulated hydrothermal regimes in frozen ground regions and their change under the global warming scenario. Journal of Geophysical Research-Earth Surface **112**.

Schaefer, K., T. Zhang, L. Bruhwiler, and A. P. Barrett. 2011. Amount and timing of permafrost carbon release in response to climate warming. Tellus Series B-Chemical and Physical Meteorology:no-no.

Smith, L. C., T. M. Pavelsky, G. M. MacDonald, A. I. Shiklomanov, and R. B. Lammers. 2007. Rising minimum daily flows in northern Eurasian rivers: A growing influence of groundwater in the high-latitude hydrologic cycle. Journal of Geophysical Research-Biogeosciences **112**.

Spencer, R. G. M., G. R. Aiken, K. P. Wickland, R. G. Striegl, and P. J. Hernes. 2008. Seasonal and spatial variability in dissolved organic matter quantity and composition from the Yukon River basin, Alaska. Global Biogeochemical Cycles **22**.

Striegl, R. G., G. R. Aiken, M. M. Dornblaser, P. A. Raymond, and K. P. Wickland. 2005. A decrease in discharge-normalized DOC export by the Yukon River during summer through autumn. Geophysical Research Letters **32**.

Stroeve, J., M. M. Holland, W. Meier, T. Scambos, and M. Serreze. 2007. Arctic sea ice decline: Faster than forecast. Geophysical Research Letters **34**.

Tank, S. E., K. E. Frey, R. G. Striegl, P. A. Raymond, R. M. Holmes, J. W. McClelland, and B. J. Peterson. 2012. Landscape-level controls on dissolved carbon flux from diverse catchments of the circumboreal. Global Biogeochemical Cycles **26**.

Tarnocai, C. 2009. Arctic Permafrost Soils. Soil Biology:3-16.

Vonk, J. E. and O. Gustafsson. 2013. Permafrost-carbon complexities. Nature Geoscience **6**:675-676.

Vonk, J. E., P. J. Mann, S. Davydov, A. Davydova, R. G. M. Spencer, J. Schade, W. V. Sobczak, N. Zimov, S. Zimov, E. Bulygina, T. I. Eglinton, and R. M. Holmes. 2013. High biolability of ancient permafrost carbon upon thaw. Geophysical Research Letters:40.

Vonk, J. E., L. Sanchez-Garcia, B. E. van Dongen, V. Alling, D. Kosmach, A. Charkin, I. P. Semiletov, O. V. Dudarev, N. Shakhova, P. Roos, T. I. Eglinton, A. Andersson, and O. Gustafsson. 2012. Activation of old carbon by erosion of coastal and subsea permafrost in Arctic Siberia. Nature **489**:137-140.

Waldrop, M. P., K. P. Wickland, R. White, A. A. Berhe, J. W. Harden, and V. E. Romanovsky. 2010. Molecular investigations into a globally important carbon pool: permafrost-protected carbon in Alaskan soils. Global Change Biology **16**:2543-2554.

Walvoord, M. A. and R. G. Striegl. 2007. Increased groundwater to stream discharge from permafrost thawing in the Yukon River basin: Potential impacts on lateral export of carbon and nitrogen. Geophysical Research Letters **34**.

Wickland, K. P., G. R. Aiken, K. Butler, M. M. Dornblaser, R. G. M. Spencer, and R. G. Striegl. 2012. Biodegradability of dissolved organic carbon in the Yukon River and its tributaries: Seasonality and importance of inorganic nitrogen. Global Biogeochemical Cycles **26**.

Woods, G. C., M. J. Simpson, B. G. Pautler, S. F. Lamoureux, M. J. Lafreniere, and A. J. Simpson. 2011. Evidence for the enhanced lability of dissolved organic matter following permafrost slope disturbance in the Canadian High Arctic. Geochimica Et Cosmochimica Acta **75**:7226-7241.

Zhang, T., R.G. Barry, K. Knowles, J.A. Heginbottom, and J. Brown. 1999. Statistics and characteristics of permafrost and ground ice distribution in the Northern Hemisphere. Polar Geography **23**:147-169.

Zimov, S. A., S. P. Davydov, G. M. Zimova, A. I. Davydova, E. A. G. Schuur, K. Dutta, and F. S. Chapin. 2006. Permafrost carbon: Stock and decomposability of a globally significant carbon pool. Geophysical Research Letters **33**.

Chapter 3. Elevated dissolved organic carbon biodegradability from thawing and collapsing permafrost[1]

3.1 Key Points

- Dissolved organic carbon from thawing permafrost is highly biodegradable
- Elevated biodegradability only persists during permafrost collapse
- Controls on dissolved organic carbon processing are tested

3.2 Abstract

As high latitudes warm, a portion of the large organic carbon pool stored in permafrost will become available for transport to aquatic ecosystems as dissolved organic carbon (DOC). If permafrost DOC is biodegradable, much will be mineralized to the atmosphere in freshwater systems before reaching the ocean, accelerating carbon transfer from permafrost to the atmosphere, whereas if recalcitrant, it will reach marine ecosystems where it may persist over long time periods. We measured biodegradable DOC (BDOC) in water flowing from collapsing permafrost (thermokarst) on the North Slope of Alaska and tested the role of DOC chemical composition and nutrient concentration in determining biodegradability. DOC from collapsing permafrost was some of the most biodegradable reported in natural systems. However, elevated BDOC only persisted during active permafrost degradation, with a return to pre-disturbance levels once thermokarst features stabilized. Biodegradability was correlated with background nutrient concentration, but nutrient addition did not increase overall BDOC, suggesting that chemical composition may be a more important control on DOC processing. Despite its high biodegradability, permafrost DOC showed evidence of substantial previous microbial processing and we present four hypotheses explaining this incongruity. Because thermokarst features form preferentially on river banks and lake shores and can remain active for decades, thermokarst may be the dominant short-term mechanism delivering sediment, nutrients, and biodegradable organic matter to aquatic systems as the Arctic warms.

[1]Published as Abbott, B. W., Larouche, J. R., Jones, J. B., Bowden, W. B., and Balser, A. W.: Elevated dissolved organic carbon biodegradability from thawing and collapsing permafrost, Journal of Geophysical Research: Biogeosciences, doi: 10.1002/2014JG002678, 2014. 2014JG002678.

3.3 Key words

Thermokarst, permafrost carbon, DOC, dissolved organic carbon, DOM, lability, biolability, biodegradability, arctic tundra, thermo-erosion gully, thaw slump

3.4 Introduction

Arctic rivers deliver between 34-38 Tg yr^{-1} of dissolved organic carbon (DOC) to the Arctic Ocean and surrounding basins [*Holmes et al.*, 2012]. Another 37-84 Tg yr^{-1} of DOC is delivered to inland waters but respired to the atmosphere or buried in lakes and streams before reaching the ocean [*Aufdenkampe et al.*, 2011; *McGuire et al.*, 2009]. As permafrost volume shrinks due to climate change, more of the 1670 Pg of soil organic carbon (C) contained in the permafrost region [*Tarnocai et al.*, 2009] will thaw and some portion will become available for transport to aquatic ecosystems as DOC. The quantity and quality of DOC release will depend on changes in local and regional hydrology [*Frey and McClelland*, 2009; *O'Donnell et al.*, 2012; *Tank et al.*, 2012]. The importance of this permafrost DOC to regional and global C cycles depends largely on its biodegradability—the degree to which DOC is available for uptake and mineralization by microorganisms [*McDowell et al.*, 2006]. If permafrost DOC is largely biodegradable, a larger portion will be mineralized in soil and freshwater systems before reaching the ocean, accelerating C transfer from permafrost to the atmosphere, whereas if this DOC is recalcitrant, more will reach marine ecosystems where it may persist on long time scales [*Amon and Meon*, 2004; *Bianchi*, 2011]. In arctic and boreal systems, biodegradable DOC (BDOC) ranges from <10% in soil water from the seasonally thawed active layer to 90% for some vegetation-derived DOC [*Kalbitz et al.*, 2003; *Michaelson et al.*, 1998; *Wickland et al.*, 2007]. Riverine BDOC varies seasonally from <10–40% with highest biodegradability typically during snowmelt [*Holmes et al.*, 2008; *Mann et al.*, 2012; *Wickland et al.*, 2012]. However, very little is known about BDOC from thawing permafrost, with conflicting evidence showing higher and lower biodegradability compared to DOC from litter and active layer soil [*Balcarczyk et al.*, 2009; *Cory et al.*, 2013; *Vonk et al.*, 2013].

Before permafrost DOC can enter the modern C cycle, regardless of its biodegradability, it has to come into contact with surface or ground waters. Because hydraulic conductivity in arctic mineral soil is often very low [*Frampton et al.*, 2011; *Zhang et al.*, 2000], much permafrost C may be inaccessible to hydrologic export, even after thaw. However, in soil where

ice volume exceeds pore space, permafrost thaw is accompanied by ground subsidence, or thermokarst [*Jorgenson et al.*, 2008], which can rapidly mobilize sediment, nutrients, and C [*Bowden et al.*, 2008]. On hillslopes, riverbanks, and lakeshores, thermokarst can release permafrost DOC from meters below the active layer [*Vonk et al.*, 2013], and may impact watershed-level BDOC and nutrient concentrations [*Bowden et al.*, 2008; *Woods et al.*, 2011]. The term thermokarst includes a suite of thermo-erosional features with different morphologies determined primarily by ice content, substrate type, landscape position, and slope [*Osterkamp et al.*, 2009]. In upland landscapes, the three most common thermokarst morphologies are retrogressive thaw slumps, active layer detachment slides, and thermo-erosion gullies [*Jorgenson and Osterkamp*, 2005]. In addition to surface subsidence due to ground ice loss, mechanical erosion and mass wasting play a role in the formation of these features, however, we will refer to them collectively as thermokarst following literature convention [*Kokelj and Jorgenson*, 2013]. Thaw slumps have a retreating headwall and are fueled by a variety of ground ice types, active layer detachment slides form when the seasonally thawed surface layer of vegetation and soil slips downhill over an ice-rich transition zone, and thermo-erosion gullies form due to ice wedge melt, growing with a generally linear or dendritic pattern (Supplementary Fig. 3.1). These three morphologies currently impact approximately 1.5% of the landscape in the western foothills of the Brooks Range [*Krieger*, 2012] and could affect up to 30% of the North Slope of Alaska with moderate warming [*Jorgenson et al.*, 2006].

In this study we measured the biodegradability of DOC released by thermokarst across common tundra vegetation and permafrost types on the North Slope of Alaska. We hypothesized that permafrost DOC would be more biodegradable than DOC from the active layer due to two non-mutually exclusive mechanisms. First, permafrost DOC may contain more biodegradable chemical compounds due to limited prior microbial processing or differences in original vegetation sources. Second, high nutrient concentrations in permafrost meltwater may accelerate DOC breakdown by relieving nutrient limitation of heterotrophic microorganisms. If DOC chemical composition is the main driver of biodegradability, we predicted that DOC aromaticity and the C:N ratio of dissolved organic matter (DOM) would be negatively correlated with biodegradability. If nutrient concentration is the dominant driver of DOC biodegradability, we predicted that the addition of nutrients would stimulate DOC processing, particularly at sites with low ambient nutrient concentrations. Likewise, we predicted that BDOC would differ by modern

vegetation community and thermokarst type since these factors influence DOC chemical composition and nutrient concentration. We tested these hypotheses and predictions by 1) characterizing DOC composition released by thermokarst, 2) incubating DOC with and without added nutrients, 3) comparing BDOC between feature and vegetation types, and 4) developing relationships between DOC composition, nutrient content, and BDOC.

3.5 Methods

3.5.1 Study sites

We collected water from 19 thermokarst features and 8 reference water tracks in arctic We collected water from 19 thermokarst features and 8 reference water tracks in arctic tundra near the Toolik Field Station and Feniak Lake (Fig. 3.1, Table 3.1). Both areas are situated in the foothills of the Brooks Range on the North Slope of Alaska. Toolik Field Station is located 254 km north of the Arctic Circle and 180 km south of the Arctic Ocean. The average annual temperature is -10°C and average monthly temperatures range from -25°C in January to 11.5°C in July. The Toolik area receives 320 mm of precipitation annually with 200 mm falling between June and August [*Toolik Environmental Data Center Team*, 2011]. Feniak Lake is located 360 km west of Toolik in the central Brooks Range at the northeast boarder of the Noatak National Preserve. The Feniak Lake region receives more precipitation than the Toolik area with annual average precipitation at 450 mm [*WRCC*, 2011]. Both Toolik and Feniak Lake are underlain by continuous permafrost with glacial till, bedrock, and loess parent materials ranging in age from 10-400 ka [*Hamilton*, 2003].

3.5.2 Sample collection and analysis

We collected water from thermokarst feature outflows and reference water tracks near the Toolik Field Station (June to August in 2011 and August 2012) and near Feniak Lake (July 2011). In the Toolik area we sampled eight retrogressive thaw slumps (hereafter thaw slump), one active layer detachment slide, six thermo-erosion gullies (hereafter gully), and six reference water tracks. In the Feniak area we sampled two thaw slumps, one active layer detachment slide, one gully, and two reference water tracks. At each site, we collected four replicate samples from the main channel, which we filtered (0.7 μm effective pore size, Advanctec GF-75) into 250 ml amber LDPE bottles for transport to the lab where we performed photometric analysis and set up incubations within 24 hours of collection. For most sites a 60 ml HDPE bottle for background

nutrient concentrations was also filtered (0.7 μm) in the field and frozen upon return to the lab until analysis, typically within three months.

We measured DOC with a Shimadzu TOC-5000 connected to an Antek 7050 chemiluminescent detector to quantify total dissolved nitrogen (N) after combustion to NO_x. We characterized DOC composition by UV absorbance at 254 nm ($SUVA_{254}$), a photometric measure of DOC aromaticity [*Weishaar et al.*, 2003], and the C:N of DOM, an indicator of DOM source and degree of prior processing [*Amon et al.*, 2012]. UV absorbance was measured on a Shimadzu UV-1601 using a 1.0 cm quartz cell, and $SUVA_{254}$ was calculated by dividing UV absorbance by DOC concentration. NO_3^-, NH_4^+, PO_4^{3-}, and K were analyzed on a Dionex DX-320 ion chromatograph. Dissolved organic N (DON) was calculated by subtracting inorganic N (NO_3^-, NH_4^+, and NO_2^-) from total dissolved N. To distinguish rain from snowmelt and permafrost meltwater, δ D and $\delta^{18}O$ were analyzed on a Picarro L1102-i via cavity ringdown spectroscopy.

3.5.3 BDOC assays

DOC biodegradability is the degree to which DOC is available for uptake and mineralization by microorganisms. Operationally, biodegradable DOC (BDOC) is often defined as the percent DOC mineralized or taken up over a certain time period, usually 7-40 days [*McDowell et al.*, 2006], though DOC breakdown can also be characterized by single or multiple exponential models [*Wickland et al.*, 2007]. We assessed DOC biodegradability by DOC drawdown after 10 and 40 days. After initial collection and filtration in the field, 31 ml aliquots from each field bottle were filtered through 0.22 μm polyethersulfone membrane filters (Sterivex GP 0.22, Millipore) to remove bacteria, and were placed in 70 ml glass incubation vials. To control for variability in microbial community among sites, we made a common inoculum by shaking the 0.22 μm filters from all sites with 100 ml of de-ionized water and allowing them to soak for 30 minutes. Prior to initial sampling, 1 ml of this bacterial inoculum was added to each incubation vial. In 2011, all vials received a nutrient amendment, increasing ambient concentrations by 80 μM NH_4^+/NO_3^- and 10 μM PO_4^{3-} [*Holmes et al.*, 2008], to relieve potential nutrient limitation of DOC processing and facilitate comparison with other studies [*McDowell et al.*, 2006]. In 2012, we compared DOC drawdown between amended and ambient nutrient incubations performed in tandem, to test the effect of added nutrients on DOC processing.

Samples were stored in the dark at room temperature for the duration of the incubation. Incubation vials were tightly capped to limit evaporation but were opened and wafted weekly to ensure adequate oxygen supply.

To quantify DOC loss, we sampled each vial three times during the incubation, at day 0, day 10, and day 40 (t_0, t_{10}, and t_{40} respectively). At samplings, 5 ml was drawn from each vial, filtered (0.22 μm) into acid-washed, glass scintillation vials, and acidified with 100 μl of 2N HCl to remove inorganic C and kill any residual bacteria not removed during filtration. Because this method removes microbial biomass before measuring DOC, the change in DOC concentration represents DOC loss due to both mineralization and microbial uptake. Acidified samples were stored tightly capped in the dark at room temperature until analysis within three months. Average DOC concentration of the four analytical replicates for each site and sampling time step was used to calculate loss. Analytical replicates with evidence of contamination or analytical error were excluded from the means, though this occurred less than 5% of the time and never resulted in dropping a site or sampling time step.

Because no single metric of DOC biodegradability is agreed upon as the most ecologically relevant, we characterized DOC biodegradability in several ways. We hereafter refer to the DOC loss by t_{40} as biodegradable DOC (BDOC), and further separate fast BDOC as loss from t_0-t_{10} and slow BDOC as loss from t_{10}-t_{40}. We refer to DOC remaining at t_{40} as recalcitrant. To compare fast and slow BDOC in a single metric we calculated the proportion of fast BDOC (fast BDOC μM/total BDOC μM). The 10-day increment for fast BDOC corresponds to the average stream transport time of 10.9 days (range of 3-20 days) for rivers in the study area based on average stream velocity and channel length [*Dery et al.*, 2005; *McNamara et al.*, 1998]. Because this simplified estimate of residence time does not include transient storage within the channel or layovers in lakes and estuaries, the 40-day increment may better represent typical transit time from headwater to sea.

3.5.4 Nutrients and DOC chemical composition

We used Pearson product-moment correlation and multiple linear regression to compare the relative importance of nutrients and DOC composition to BDOC. All regression and correlation analyses were based on BDOC data from nutrient amended incubations and therefore test indirect correlations between nutrients and other factors such as vegetation type, flowpath,

DOM source, or micronutrients rather than direct effects of N or phosphorus (P) on BDOC. We compared the explanatory power of NH_4^+, NO_3^-, PO_4^{3-}, K, $\delta^{18}O$, $SUVA_{254}$, DOC:DON, DOC:DIN, and thermokarst activity level (defined below) in predicting fast, slow, and total BDOC. Activity was recoded low to high and treated as a continuous variable for correlations but was excluded from other analyses since it is non-parametric and was highly correlated with both potassium (K) and ammonium (NH_4^+). Akaike information criterion (AIC) was used to identify the most parsimonious models and rank predictors within each model. To determine differences between amended and ambient nutrient treatments for fast, slow, and total BDOC, we applied a single population two-way t-test.

3.5.5 Thermokarst activity, type, and vegetation

To understand the release of BDOC as thermokarst features develop through time, we classified features on a 0 – 3 activity index based on turbidity of outflow, rate of thermo-degradation, and state of revegetation. This qualitative index uses space for time substitution to follow the development of a hypothetical feature from before initiation (0) to after stabilization (3). Activity levels are defined as follows: 0. No apparent present or past thermo-degradation, 1. Active thermo-degradation (>25% of headwall is actively expanding) with completely turbid outflow, 2. Moderate thermo-degradation (<25% of headwall is expanding) with somewhat turbid outflow, 3. Stabilized or limited thermo-degradation with complete or partial revegetation and clear outflow. We performed a one-way analysis of variance (ANOVA), testing for differences in BDOC between thermokarst activity levels, and applied Tukey's HSD to determine significant differences.

Because vegetation community influences both active layer and permafrost DOC composition and nutrient concentration, we grouped sites into three broad vegetation classes (Table 3.1): moist acidic tundra, moist nonacidic tundra, and shrub tundra. We tested for differences in total BDOC, $SUVA_{254}$, C:N, and nutrient concentration between the three vegetation types. Because feature activity varied between classes, we tested for differences between vegetation classes with an analysis of covariance (ANCOVA) that compared adjusted means after controlling for activity. To test how ground ice type and thermokarst morphology influence BDOC we performed an ANCOVA comparing BDOC from gullies and thaw slumps independent of activity. Comparisons with active layer detachment slides or more involved

vegetation classifications such as ecotype [*Jorgenson et al.*, 2009] were not possible due to limited sample size.

3.5.6 Seasonal changes in BDOC

To quantify seasonal variability of BDOC, repeat measurements were taken at the four most accessible sites (two gullies and adjacent water tracks) four times from June 15-August 18 2011, and repeat measurements were taken opportunistically at seven other sites. A two-way t-test for unequal variance was performed on the range (max-min) of BDOC to compare variability at impacted and reference sites through the 2011 season.

3.5.7 Additional statistics

Repeat measurements from four features (two gullies, one thaw slump, and one water track) were included in the regression analysis as independent samples because of substantial variability in BDOC and chemistry between sample dates, which were more than two months apart in every case. Repeat measurements from 12 sites (four gullies, four thaw slumps, and four water tracks) were also included as independent samples in ANOVAs and ANCOVAs for the same reasons and to capture seasonal variability in biodegradability and water chemistry.

For all analyses, we evaluated normality with normal probability plots and equal variance by plotting observed values against residuals. For multiple linear regression models, highly correlated predictors were removed prior to running the full model or applying AIC, and in addition to visual assessment, variance inflation factor, RESET, Breusch-Pagan, and Durbin-Watson tests were used to check colinearity, linearity, equal variance, and autocorrelation respectively. Variables were natural log transformed, raised to the 0.25 exponent, and/or were centered on zero by subtracting the mean when necessary to meet these assumptions. For ANCOVA analysis, homogeneity of regression slopes was checked with interaction plots between site activity and the variable of interest. A polynomial term for $\delta^{18}O$ was included to capture the non-linear relationship with BDOC due to depleted $\delta^{18}O$ both in snowmelt early in the season and ground ice in the mid to late season. All statistical tests were evaluated with $\alpha = 0.05$ and analysis was performed in R (version 3.0.2). See acknowledgments for access to the complete dataset.

3.6 Results

3.6.1 Site activity

Sites occurred on a variety of tundra vegetation and permafrost types and exhibited a range of activity levels (Table 3.1). Thermokarst increased BDOC relative to reference waters, with greatest impact at the most active features with concentrations approaching reference in the more stable features (Fig. 3.2, Table 3.2). DOC loss exceeded 50% after 10 days at several sites and reached 67% loss after 40 days at thaw slump 7 located in Pleistocene-aged Yedoma. Total BDOC varied significantly by activity ($F_{3,46} = 9.09$, $p < 0.001$) with means of 12.8, 40.9, 31.8, and 20.6% for activity levels 0-3, respectively (Fig. 3.2, Table 3.2). BDOC of the two highest activity levels differed significantly from reference water tracks ($p < 0.001$ and $p = 0.02$), but there was no significant difference in BDOC between stabilized sites and reference water tracks (levels 3 and 0; $p = 0.31$).

DOC concentrations from active thermokarst features (levels 1 and 2) were highly variable with average concentration over three times higher than in reference water tracks (Table 3.2). Differences in DON were even more pronounced with concentrations in active features nearly eight times higher than reference concentrations. Consequently, C:N of DOM for active features was half that of reference sites. Similarly, $SUVA_{254}$ values at impacted sites were half as high as in reference waters, indicating less aromatic DOC compounds in thermokarst outflow. Nutrient concentrations were generally much higher in thermokarst water (70, 39, and 15 times higher for K, NH_4^+, and PO_4^{3-} respectively), though NO_3^- concentration in the most active features was only 1.3 times higher than reference waters. Rainwater was enriched in $\delta^{18}O$ (-16.56‰, SD = 3.46) relative to ground ice from feature headwalls (-24.11‰, SD = 3.98) and snow meltwater (-27.58‰, SD = 3.15).

The proportion fast BDOC (fast BDOC/total BDOC) did not vary significantly with thermokarst activity ($p = 0.24$, $n = 50$, $SE = 0.34$), with an overall average of 0.58 of the total DOC loss occurring by t10 (Fig. 3.1). However the proportion fast BDOC varied widely among individual sites, from less than 0.01 to 1.0.

3.6.2 Nutrients and DOC chemical composition

We used correlation and multiple linear regression to assess the strength of associations between nutrients and DOC composition with DOC biodegradability. Pearson product-moment

correlations revealed moderate to strong relationships between the four metrics of BDOC and both DOC chemical composition and nutrient concentration (Table 3.3). Individual parameters were correlated with fast, slow, and total BDOC (%) as well as total BDOC concentration (μM). PO_4^{3-} had the strongest positive correlation with both fast and total BDOC, and PO_4^{3-} and C:N were equally correlated with total BDOC concentration. Thermokarst activity had the strongest relationship with slow BDOC. Fast BDOC was not significantly correlated with slow BDOC (Pearson's r = 0.27, n = 50, p = 0.054). All parameters, except the $\delta^{18}O$ terms, were correlated with thermokarst activity, with K and NH_4^+ expressing the strongest relationships (Pearson's r = 0.85 and 0.82 respectively, n = 27, $p < 0.001$; Table 3.3).

Multiple linear regression models accounted for 67 – 83% of the variation in the four metrics of BDOC, with chemical composition, nutrient content, and water isotopes all included as significant predictors in the various models (Table 3.4). PO_4^{3-} and NH_4^+ were retained after stepwise AIC for all four of the BDOC metrics, with $SUVA_{254}$ and $\delta^{18}O$ making three of the four final models (Table 3.4). Most predictors were individually significant ($\alpha < 0.05$) in their specific model with the exception of $SUVA_{254}$ and C:N in the fast BDOC model; DOC, PO_4^{3-}, and $SUVA_{254}$ in the slow BDOC model; and C:N and $\delta^{18}O$ in the BDOC concentration model (p = 0.07, 0.06, 0.07, 0.16, 0.13, 0.06, and 0.25, respectively). However, these terms were retained in the final models since they improved the AIC score and were not overly correlated with other predictors in their models. The model estimating fast BDOC had the weakest relationship with measured BDOC ($R^2 = 0.67$) and the BDOC concentration model had the strongest relationship ($R^2 = 0.83$; Fig. 3.3). Variance inflation factor was low for all parameters (< 3) and the RESET, Breusch-Pagan, and Durbin-Watson tests were all non-significant, indicating acceptable colinearity, linearity, equal variance, and autocorrelation.

We tested the effect of nutrient concentration on DOC processing by comparing amended and ambient nutrient incubations. The addition of inorganic N and P nearly doubled the amount of fast BDOC (SE = 3.48, $t_6 = 3.1$, p = 0.02), which averaged 9.2% for vials without added nutrients and 17.5% in amended incubations, but did not significantly affect slow BDOC (non-significant decrease of 2.7%, SE = 1.63, $t_6 = -1.64$, p = 0.15) or total BDOC (non-significant increase of 5.5%, SE = 3.01, $t_6 = 1.84$, p = 0.12; Fig. 3.4). Furthermore, variation in the response to nutrient addition was positively correlated with DIN concentration ($R^2 = 0.79$, $F_{1, 5} = 19.4$, p =

0.007), with sites higher in DIN showing a stronger response to nutrient addition (Δ fast BDOC (%) = 0.13 [DIN (μM)] + 1.5, Fig. 3.5).

3.6.3 Feature and vegetation type

We compared BDOC by feature and vegetation type to test for differences due to how DOC is released from permafrost and original DOC source. Slumps were higher in BDOC than gullies ($F_{1,29}$, p = 0.026) with adjusted means of 37.9% versus 25.0% total BDOC after controlling for differences in activity (Fig. 3.6). BDOC differed with vegetation type independent of activity ($F_{2,46}$, p = 0.006), with greater BDOC at sites located on moist non-acidic tundra compared to moist acidic tundra, with adjusted means of 36.6 and 21.2% total BDOC (Fig. 3.7). $SUVA_{254}$ varied by vegetation ($F_{2,44}$, p = 0.0001), with non-acidic sites lower than acidic sites with adjusted means of 4.3 and 2.2 L mg C^{-1} m^{-1}, but C:N ratio, DIN, and PO_4^{3-} did not significantly vary across vegetation types ($F_{2, 28}$, p = 0.28, 0.43, and 0.44 respectively). For all parameters, shrubs were intermediate between acidic and non-acidic tundra and did not vary significantly from either type.

3.6.4 Seasonal patterns of BDOC

While individual sites had high variability in BDOC between samplings through the season, there was no clear trend in BDOC seasonality for reference or impacted waters (Fig. 3.8). The average of BDOC range (max – min values for an individual site over the season) varied by up to 50% with an overall average of 20.4% (n = 12, SE = 4.8). Impacted sites were more variable than reference water tracks with a mean BDOC range of 28.7% compared to the reference mean of 12.4% ($t_{8.83}$ = -2.4, p = 0.04). For the two gullies and water tracks where repeat measurements were taken at least monthly, BDOC was highest in the mid to late season (July and August). Lowest BDOC for all sites occurred early in the season on 6/15.

3.7 Discussion

3.7.1 Permafrost DOC pools and biodegradability

DOC from collapsing permafrost on the North Slope is some of the most biodegradable reported in natural systems. Across multiple vegetation types, landscape ages, and thermokarst morphologies, DOC from permafrost is consistently more biodegradable than surface-derived DOC. High BDOC is accompanied by elevated DOC concentrations, resulting in extremely high rates of DOC mineralization from waters impacted by permafrost collapse. However, elevated

BDOC only persists during active permafrost degradation, and BDOC returns to pre-disturbance levels once thermokarst features stabilize and start to revegetate. This finding informs the importance of thermokarst morphology in determining BDOC release from permafrost. Though gully and active layer detachment features are more common on the landscape and make up a larger portion of total thermokarst area [*Krieger*, 2012], they typically stabilize within a few years [*Godin and Fortier*, 2012; *Lewkowicz and Harris*, 2005]. Thaw slumps, however, can remain active for decades [*Lantuit et al.*, 2012; *Lantz and Kokelj*, 2008], mobilizing biodegradable permafrost DOC from meters below the surface.

3.7.2 DOC composition

DOC aromaticity and C:N of DOM were negatively related to biodegradability, supporting our hypothesis that chemical composition of permafrost DOC contributes to its high biodegradability. The fact that fast and slow BDOC were poorly correlated and responded differently to nutrient addition is evidence that multiple pools of DOC with differing degrees of biodegradability are at play.

Arctic river DOC is typically most biodegradable during snowmelt [*Holmes et al.*, 2008; *Mann et al.*, 2012], when recently fixed vascular plant inputs dominate DOM sources [*Neff et al.*, 2006; *Spencer et al.*, 2008]. This DOM released during snowmelt has high $SUVA_{254}$ (~ 4.0), high C:N (> 40), and has undergone little microbial processing due to rapid transport across frozen soil [*Holmes et al.*, 2012; *Mann et al.*, 2012; *Spencer et al.*, 2008]. In contrast, permafrost DOM has low $SUVA_{254}$ (1.9) and low C:N (21.7) in the range of soil or microbially-derived DOM (10 – 25), suggesting considerable prior processing [*Amon and Meon*, 2004; *Amon et al.*, 2012; *Kawahigashi et al.*, 2004; *Neff et al.*, 2006]. Yet permafrost DOM is more biodegradable than DOM released during snowmelt. This inconsistency highlights the complexity of predicting BDOC, particularly when comparing fresh and degraded DOM. While the chemical composition of permafrost DOM is distinct from arctic snowmelt DOM, it is similar to late-winter DOM in the Yukon basin, which has high BDOC (40%), low $SUVA_{254}$ (2.0), and low C:N (20.7) [*O'Donnell et al.*, 2012; *Wickland et al.*, 2012]. A possible explanation for this similarity is that some of the DOM in wintertime baseflow is coming from permafrost via soilwater, groundwater, or thermokarst inputs. The Yukon basin is underlain by discontinuous permafrost and has experienced substantial warming and changes in precipitation [*Chapin et al.*, 2010] with large

areas experiencing permafrost degradation [*Belshe et al.*, 2013; *Lu and Zhuang*, 2011; *Osterkamp*, 2005]. The only other published estimate of pre-snowmelt, riverine BDOC is from the Kolyma basin in Eastern Siberia, where BDOC was less than 5% [*Mann et al.*, 2012]. If permafrost DOM is the source of winter BDOC in the Yukon, this could explain the large difference between these catchments. The Kolyma is underlain by continuous permafrost and has experienced less severe summer and winter warming [*Chapin et al.*, 2005; *Serreze et al.*, 2000], therefore the contribution of permafrost DOM to winter BDOC should be relatively lower than in the Yukon.

3.7.3 Nutrients

Nutrient addition had mixed effects on BDOC, in line with previous findings [*Balcarczyk et al.*, 2009; *Holmes et al.*, 2008]. The fact that sites with high DIN showed a greater response to nutrient addition was contrary to our prediction that low-nutrient sites would respond most strongly and does not support the hypothesis that nutrient availability limits DOC processing. Because DIN is highly correlated with site activity, the relationship between DIN and response to nutrient addition may indicate that sites with more biodegradable, permafrost-derived DOC are more sensitive to nutrient addition. This interaction coincides, albeit on a much faster time scale, with observations of bulk soil C processing in tundra soil, where higher nutrient availability enhances labile C processing but suppresses recalcitrant C processing [*Lavoie et al.*, 2011].

Regression and correlation analysis revealed that inorganic nutrients, particularly PO_4^{3-} and NH_4^+, are associated with DOC biodegradability. These relationships were robust in predicting the biodegradability of both surface and permafrost-derived DOM (Fig. 3.4), suggesting common controls on biodegradability, regardless of source. However, the fact that NH_4^+ was highly correlated with site activity may mean that its relationship with BDOC is partially or primarily correlative. PO_4^{3-} was relatively less correlated with activity and was generally a better predictor of BDOC, suggesting an influence on BDOC separate from activity. It is important to note that correlation and regression analysis was based on data from incubations with added nutrients. As such, relationships between initial nutrient concentration and BDOC are likely due to indirect correlations between nutrients and other factors such as

vegetation type, flowpath, DOM source, or micronutrients rather than direct effects of N or P on BDOC.

Mineral soil in the arctic is enriched in inorganic N relative to organic soil [*Harms et al.*, 2013; *Keuper et al.*, 2012] and increased active layer depth could modify hydrologic flowpaths, causing the simultaneous export of biodegradable permafrost DOC and DIN on a local or landscape scale [*Harms et al.*, 2013; *Jones et al.*, 2005; *Striegl et al.*, 2005; *Wickland et al.*, 2012]. Similarly, in the case of thermokarst, nutrient concentration is highly associated with feature activity, resulting in the features releasing the most permafrost DOC also releasing highest concentrations of inorganic nutrients. Another possibility explaining the correlation between BDOC and inorganic nutrients is that the nutrients associated with water rich in BDOC are at least partially derived from the DOM itself during mineralization.

3.7.4 Acidic and nonacidic tundra DOM biodegradability

Sites draining moist non-acidic tundra sites had higher BDOC than those draining moist acidic tundra sites. This pattern may be due to more decomposable DOM inputs from non-acidic tundra or accelerated decomposition of DOM in acidic tundra soil before reaching the stream. While litter decay rates are similar between acidic and non-acidic tundra, decomposition can occur up to 84% more rapidly at acidic sites, potentially due to increased N availability and differences in microbial community [*Hobbie and Gough*, 2004; *Hobbie et al.*, 2005; *Nordin et al.*, 2004]. If DOM is processed faster in acidic tundra, a larger portion of BDOC would be consumed before reaching the stream or being incorporated into permafrost, leading to lower BDOC in moist acidic tundra ground ice and surface water. Alternatively, there is evidence that DOM biodegradability may be inversely correlated with biodegradability of the plant residue from which it leached. Litter from sedges decomposes fastest, followed by deciduous shrubs, and mosses [*Hobbie*, 1996]. Leachate biodegradability follows the opposite pattern, with very high BDOC in moss-derived DOM, followed by deciduous shrubs, and sedges [*Wickland et al.*, 2007]. If this pattern holds, DOM from non-acidic sites with lower litter and soil decay rates may have higher BDOC.

3.7.5 BDOC and thermokarst morphology

Differences in the biodegradability of DOC released from thaw slumps and gullies suggest that ground ice type influences BDOC (Fig. 3.2). However, lower BDOC in gully

outflow may be due to dilution of permafrost meltwater by surface water inputs, rather than differences in ground ice BDOC. Gullies often form in convergent topography with a larger upslope catchments than thaw slumps [*Krieger*, 2012]. Consequently, gully outflow has a lower proportion of permafrost versus surface-derived water and DOM. This explanation is supported by the fact that the gully with the highest BDOC (gully 7, Table 3.1) was the only one without surface water input.

3.7.6 Why is permafrost DOC so biodegradable?

Different mechanisms potentially account for elevated BDOC in wedge and relic glacial ice formations, which are the most common ground ice types in our study area and are widespread throughout the arctic [*French and Shur*, 2010; *T Zhang et al.*, 1999]. Ice wedges form when spring runoff flows into surface cracks formed from thermal contraction during extreme cold in the previous winter [*Fortier and Allard*, 2004]. Because ice wedges are filled during the later stages of snowmelt [*Lauriol et al.*, 1995] the water that fills them is rich in the same litter and winter microbial activity-derived DOC that fuels patterns of high BDOC in arctic surface waters during snowmelt. Over centuries and millennia this unprocessed spring leachate could build up in ice wedges, providing a labile BDOC source upon thaw. However, the low C:N and $SUVA_{254}$ of permafrost DOM suggests it is derived from microbial or soil sources as opposed to fresh plant matter. If snowmelt DOM is the major source of ice wedge DOM, considerable processing must take place during or after incorporation. As for the source of BDOC in buried glacial ice, modern glacial ice can contain highly biodegradable DOC derived from microbial production (Hood et al. 2009), which more closely matches the DOM characteristics we observed in thermokarst outflows. If such DOC was present when relic glacial ice was stranded and buried, microbially-derived C could explain high BDOC in thaw slumps fueled by buried glacial ice. However, DOC concentrations in modern glacial ice are typically low, and ice ablation or another concentrating process would be necessary to produce the high concentrations of BDOC observed in thermokarst outflow.

If nutrient availability does not enhance BDOC, how can DOM from ground ice types such as ice wedges and transition ice be more biodegradable than the surface sources from which they derive? We hypothesize four potential mechanisms that could increase DOC biodegradability relative to modern DOC sources. First, permafrost mineral soil strongly sorbs

hydrophobic C species, which tend to be recalcitrant [*Kawahigashi et al.*, 2006; *Kawahigashi et al.*, 2004]. Upon permafrost thaw, the DOC available for export could have a higher biodegradability since the less bioavailable compounds have effectively been filtered by the mineral soil. Second, repeated freeze thaw cycles can release highly biodegradable DOC from the microbial community [*Schimel and Clein*, 1996]. This release is typically taken up rapidly or respired by microorganisms that survived the cycle [*Schimel and Clein*, 1996]. However, if these pulses of bioavailable DOC were released near a freezing front at the permafrost table, or near an ice wedge crack they could be incorporated into ground ice. Third, microbial metabolism has been shown to continue well below the freezing point [*Wilhelm et al.*, 2012] and it is not known what portion of microbial biomass and metabolites is incorporated into permafrost as DOC rather than respired. Although microbial metabolism rates are low at temperatures typical of continuous permafrost—processing 1-2 μg g^{-1} C day^{-1} [*Mikan et al.*, 2002; *Osterkamp*, 2005]—sub-zero metabolism could process a substantial portion of available soil organic matter over several millennia. Incomplete breakdown of frozen soil organic matter, either during freeze-thaw cycles or sub-zero metabolism, could lead to the accumulation of simple carbon compounds such as acetate, which could explain the low C:N and $SUVA_{254}$ of permafrost-derived DOM. Finally, some vegetation paleo-communities may have produced relatively biodegradable DOM compared to modern communities. This seems a likely explanation for the extremely high BDOC in Pleistocene-aged loess deposits where C derives primarily from grasses [*Zimov et al.*, 2006]. However, for other permafrost types on the North Slope, pollen records reveal spatially heterogeneous community shifts, rather than a landscape-scale pattern of more biodegradable DOM sources [*Anderson et al.*, 1994; *Fritz et al.*, 2012; *Oswald et al.*, 2003].

An additional factor not considered here, which may further enhance DOC mineralization after release from permafrost, is high photodegradability of permafrost DOM when exposed to sunlight after reaching the surface [*Cory et al.*, 2013]. Several features included in our study (ALD 1, gullies 1 and 2, and thaw slumps 2-4, and 8) showed more than a 40% increase in microbial conversion of DOC to CO_2 when exposed to sunlight [*Cory et al.*, 2013]. Actual rates of permafrost DOC mineralization may be higher than measured in our dark incubations in field conditions when exposed to sunlight.

3.8 Conclusions

As the Arctic warms, DOC from thawing permafrost will play an increasingly important role governing freshwater and estuarine C and nutrient dynamics through the season. The overall ecological importance of thermokarst BDOC depends on the number of features, their location on the landscape, and the length of their active period. Approximately a third of permafrost has ice content in excess of 10% [*T Zhang et al.*, 1999] and is susceptible to thermokarst upon thaw [*Jorgenson et al.*, 2006]. With up to 80% of near surface permafrost projected to degrade by 2100 if human greenhouse gas emissions are not reduced [*Slater and Lawrence*, 2013], thermokarst could impact up to 5.5×10^6 km^2 by the end of the century.

Since thermal disturbance from flowing or standing water often triggers gully and thaw slump formation, thermokarst may be the dominant short-term mechanism delivering sediment, nutrients, and biodegradable organic matter to aquatic systems as the Arctic warms. This could have significant local, landscape, and global consequences [*Bowden et al.*, 2008; *Thienpont et al.*, 2013]. Thermokarst outflow is most active when temperature is high in the mid to late summer, precisely when arctic surface water BDOC is lowest [*Holmes et al.*, 2008; *Mann et al.*, 2012; *Wickland et al.*, 2012]. Chronic loading of BDOC from widespread thermokarst could cause a substantial shift in late-season DOC dynamics in arctic streams, lakes, and estuaries. Permafrost BDOC release could also be important for the global C cycle, enhancing the permafrost C feedback due to direct CO_2 release from the decomposition of permafrost DOC and enhanced heterotrophic processing of non-permafrost DOC due to the priming effect [*Bianchi*, 2011; *Guenet et al.*, 2010].

High lability of permafrost DOC should be considered when estimating changes in DOC delivery to aquatic ecosystems. Due to substantial DOC losses on timescales less than residence time of many arctic waters, monitoring of river mouth or estuarine DOC could miss a large portion of DOC released from degrading permafrost which was processed in transit.

3.9 Acknowledgments

The complete dataset for this paper is available through the Advanced Cooperative Arctic Data and Information Service at www.aoncadis.org/project/collaborative_research_spatial_and_temporal_influences_of_thermokarst_failures_on_surface_processes_in_arctic_landscapes.html. This work was supported by the

National Science Foundation ARCSS program (OPP-0806465 and OPP-0806394). We thank the many individuals and organizations that assisted with this study. S. Godsey, A. Olsson, L. Koenig, and P. Tobin gave dedicated service in the lab and field, R. Cory and G. Kling provided technical assistance and advice with DOM analysis, Toolik Field Station and CH2M Hill Polar Services provided outstanding logistic support, T. Chapin gave valuable input on the manuscript, and the National Park Service and Bureau of Land Management facilitated research permits. We also thank two anonymous reviewers whose observations improved the manuscript. In memory of the late Christian Cabanilla and Bill Zeman who flew us to many of these sites.

3.10 References

Amon, R. M. W., and B. Meon (2004), The biogeochemistry of dissolved organic matter and nutrients in two large Arctic estuaries and potential implications for our understanding of the Arctic Ocean system, *Marine Chemistry*, *92*(1-4), 311-330.

Amon, R. M. W., et al. (2012), Dissolved organic matter sources in large Arctic rivers, *Geochimica Et Cosmochimica Acta*, *94*, 217-237.

Anderson, P. M., P. J. Bartlein, and L. B. Brubaker (1994), Late Quaternary History of Tundra Vegetation in Northwestern Alaska, *Quaternary Res*, *41*(3), 306-315.

Aufdenkampe, A. K., E. Mayorga, P. A. Raymond, J. M. Melack, S. C. Doney, S. R. Alin, R. E. Aalto, and K. Yoo (2011), Riverine coupling of biogeochemical cycles between land, oceans, and atmosphere, *Frontiers in Ecology and the Environment*, *9*(1), 53-60.

Balcarczyk, K. L., J. B. Jones, R. Jaffe, and N. Maie (2009), Stream dissolved organic matter bioavailability and composition in watersheds underlain with discontinuous permafrost, *Biogeochemistry*, *94*(3), 255-270.

Belshe, E. F., E. A. G. Schuur, and G. Grosse (2013), Quantification of upland thermokarst features with high resolution remote sensing, *Environmental Research Letters*, *8*(3).

Bianchi, T. S. (2011), The role of terrestrially derived organic carbon in the coastal ocean: A changing paradigm and the priming effect, *Proceedings of the National Academy of Sciences*, *108*(49), 19473-19481.

Bowden, W. B., M. N. Gooseff, A. Balser, A. Green, B. J. Peterson, and J. Bradford (2008), Sediment and nutrient delivery from thermokarst features in the foothills of the North Slope, Alaska: Potential impacts on headwater stream ecosystems, *J Geophys Res-Biogeo*, *113*(G2).

Chapin, F. S., et al. (2010), Resilience of Alaska's boreal forest to climatic change, *Canadian Journal of Forest Research-Revue Canadienne De Recherche Forestiere*, *40*(7), 1360-1370.

Chapin, F. S., et al. (2005), Role of Land-Surface Changes in Arctic Summer Warming, *Science*, *310*(5748), 657-660.

Cory, R. M., B. C. Crump, J. A. Dobkowski, and G. W. Kling (2013), Surface exposure to sunlight stimulates CO2 release from permafrost soil carbon in the Arctic, *P Natl Acad Sci USA*, *110*(9), 3429-3434.

Dery, S. J., M. Stieglitz, A. K. Rennermalm, and E. F. Wood (2005), The water budget of the Kuparuk River basin, Alaska, *Journal of Hydrometeorology*, *6*(5), 633-655.

Fortier, D., and M. Allard (2004), Late Holocene syngenetic ice-wedge polygons development, Bylot Island, Canadian Arctic Archipelago, *Canadian Journal of Earth Sciences*, *41*(8), 997-1012.

Frampton, A., S. Painter, S. W. Lyon, and G. Destouni (2011), Non-isothermal, three-phase simulations of near-surface flows in a model permafrost system under seasonal variability and climate change, *J. Hydrol.*, *403*(3-4), 352-359.

French, H., and Y. Shur (2010), The principles of cryostratigraphy, *Earth-Science Reviews*, *101*(3,Äì4), 190-206.

Frey, K. E., and J. W. McClelland (2009), Impacts of permafrost degradation on arctic river biogeochemistry, *Hydrol Process*, *23*(1), 169-182.

Fritz, M., U. Herzschuh, S. Wetterich, H. Lantuit, G. P. De Pascale, W. H. Pollard, and L. Schirrmeister (2012), Late glacial and Holocene sedimentation, vegetation, and climate history from easternmost Beringia (northern Yukon Territory, Canada), *Quaternary Res*, *78*(3), 549-560.

Godin, E., and D. Fortier (2012), Geomorphology of a thermo-erosion gully, Bylot Island, Nunavut, Canada, *Canadian Journal of Earth Sciences*, *49*(8), 979-986.

Guenet, B., M. Danger, L. Abbadie, and G. Lacroix (2010), Priming effect: bridging the gap between terrestrial and aquatic ecology, *Ecology*, *91*(10), 2850-2861.

Hamilton, T. (2003), Surficial geology of the Dalton Highway (Itkillik-Sagavanirktok rivers) area, southern Arctic foothills, Alaska Division of Geological & Geophysical Surveys, Alaska.

Harms, T., B. Abbott, and J. Jones (2013), Thermo-erosion gullies increase nitrogen available for hydrologic export, *Biogeochemistry*, 1-13.

Hobbie, S. E. (1996), Temperature and plant species control over litter decomposition in Alaskan tundra, *Ecological Monographs*, *66*(4), 503-522.

Hobbie, S. E., and L. Gough (2004), Litter decomposition in moist acidic and non-acidic tundra with different glacial histories, *Oecologia*, *140*(1), 113-124.

Hobbie, S. E., L. Gough, and G. R. Shaver (2005), Species compositional differences on different-aged glacial landscapes drive contrasting responses of tundra to nutrient addition, *J Ecol*, *93*(4), 770-782.

Holmes, R. M., J. W. McClelland, P. A. Raymond, B. B. Frazer, B. J. Peterson, and M. Stieglitz (2008), Lability of DOC transported by Alaskan rivers to the arctic ocean, *Geophysical Research Letters*, *35*(3).

Holmes, R. M., et al. (2012), Seasonal and Annual Fluxes of Nutrients and Organic Matter from Large Rivers to the Arctic Ocean and Surrounding Seas, *Estuaries and Coasts*, *35*(2), 369-382.

Hood, E., J. Fellman, R. G. M. Spencer, P. J. Hernes, R. Edwards, D. D'Amore, and D. Scott (2009), Glaciers as a source of ancient and labile organic matter to the marine environment, *Nature*, *462*(7276), 1044-U1100.

Jones, J. B., K. C. Petrone, J. C. Finlay, L. D. Hinzman, and W. R. Bolton (2005), Nitrogen loss from watersheds of interior Alaska underlain with discontinuous permafrost, *Geophysical Research Letters*, *32*(2).

Jorgenson, M. T., and T. E. Osterkamp (2005), Response of boreal ecosystems to varying modes of permafrost degradation, *Canadian Journal of Forest Research-Revue Canadienne De Recherche Forestiere*, *35*(9), 2100-2111.

Jorgenson, M. T., Y. L. Shur, and E. R. Pullman (2006), Abrupt increase in permafrost degradation in Arctic Alaska, *Geophysical Research Letters*, *33*(2).

Jorgenson, M. T., Y. L. Shur, and T. E. Osterkamp (2008), Thermokarst in Alaska, in *Ninth International Conference On Permafrost*, University of Alaska Fairbanks, 117-124.

Jorgenson, M. T., J. E. Roth, P. F. Miller, M. J. Macander, M. S. Duffy, A. F. Wells, G. V. Frost, and E. R. Pullman (2009), An Ecological Land Survey and Landcover Map of the Arctic Network, *National Park Service, Ft Collins, CO. NPS/ARCN/NRTR—2009/270. 307.*

Kalbitz, K., J. Schmerwitz, D. Schwesig, and E. Matzner (2003), Biodegradation of soil-derived dissolved organic matter as related to its properties, *Geoderma*, *113*(3-4), 273-291.

Kawahigashi, M., K. Kaiser, A. Rodionov, and G. Guggenberger (2006), Sorption of dissolved organic matter by mineral soils of the Siberian forest tundra, *Glob. Change Biol.*, *12*(10), 1868-1877.

Kawahigashi, M., K. Kaiser, K. Kalbitz, A. Rodionov, and G. Guggenberger (2004), Dissolved organic matter in small streams along a gradient from discontinuous to continuous permafrost, *Glob. Change Biol.*, *10*(9), 1576-1586.

Keuper, F., P. M. van Bodegom, E. Dorrepaal, J. T. Weedon, J. van Hal, R. S. P. van Logtestijn, and R. Aerts (2012), A frozen feast: thawing permafrost increases plant-available nitrogen in subarctic peatlands, *Glob. Change Biol.*, *18*(6), 1998-2007.

Kokelj, S. V., and M. T. Jorgenson (2013), Advances in Thermokarst Research, *Permafrost and Periglacial Processes*, *24*(2), 108-119, doi:10.1002/ppp.1779.

Krieger, K. C. (2012), The Topographic Form and Evolution of Thermal Erosion Features: A First Analysis Using Airborne and Ground-Based LiDAR in Arctic Alaska, M.S. thesis, Dep. of Geosciences, Idaho State University.

Lantuit, H., W. H. Pollard, N. Couture, M. Fritz, L. Schirrmeister, H. Meyer, and H. W. Hubberten (2012), Modern and Late Holocene Retrogressive Thaw Slump Activity on the Yukon Coastal Plain and Herschel Island, Yukon Territory, Canada, *Permafrost and Periglacial Processes*, *23*(1), 39-51.

Lantz, T. C., and S. V. Kokelj (2008), Increasing rates of retrogressive thaw slump activity in the Mackenzie Delta region, NWT, Canada, *Geophysical Research Letters*, *35*(6).

Lauriol, B., C. Duchesne, and I. D. Clark (1995), Systématique du Remplissage en Eau des Fentes de Gel: Les Résultats d'une Étude Oxygène-18 et Deutérium, *Permafrost and Periglacial Processes*, *6*(1), 47-55.

Lavoie, M., M. C. Mack, and E. A. G. Schuur (2011), Effects of elevated nitrogen and temperature on carbon and nitrogen dynamics in Alaskan arctic and boreal soils, *J Geophys Res-Biogeo*, *116*.

Lewkowicz, A. G., and C. Harris (2005), Frequency and magnitude of active-layer detachment failures in discontinuous and continuous permafrost, northern Canada, *Permafrost and Periglacial Processes*, *16*(1), 115-130.

Lu, X. L., and Q. L. Zhuang (2011), Areal changes of land ecosystems in the Alaskan Yukon River Basin from 1984 to 2008, *Environmental Research Letters*, *6*(3).

Mann, P. J., A. Davydova, N. Zimov, R. G. M. Spencer, S. Davydov, E. Bulygina, S. Zimov, and R. M. Holmes (2012), Controls on the composition and lability of dissolved organic matter in Siberia's Kolyma River basin, *J Geophys Res-Biogeo*, *117*.

McDowell, W. H., A. Zsolnay, J. A. Aitkenhead-Peterson, E. G. Gregorich, D. L. Jones, D. Jodemann, K. Kalbitz, B. Marschner, and D. Schwesig (2006), A comparison of methods to determine the biodegradable dissolved organic carbon from different terrestrial sources, *Soil Biol Biochem*, *38*(7), 1933-1942.

McGuire, A. D., L. G. Anderson, T. R. Christensen, S. Dallimore, L. Guo, D. J. Hayes, M. Heimann, T. D. Lorenson, R. W. Macdonald, and N. Roulet (2009), Sensitivity of the carbon cycle in the Arctic to climate change, *Ecological Monographs*, *79*(4), 523-555.

McNamara, J. P., D. L. Kane, and L. D. Hinzman (1998), An analysis of streamflow hydrology in the Kuparuk River basin, Arctic Alaska: A nested watershed approach, *J. Hydrol.*, *206*(1-2), 39-57.

Michaelson, G. J., C. L. Ping, G. W. Kling, and J. E. Hobbie (1998), The character and bioactivity of dissolved organic matter at thaw and in the spring runoff waters of the arctic tundra north slope, Alaska, *J Geophys Res-Atmos*, *103*(D22), 28939-28946.

Mikan, C. J., J. P. Schimel, and A. P. Doyle (2002), Temperature controls of microbial respiration in arctic tundra soils above and below freezing, *Soil Biol Biochem*, *34*(11), 1785-1795.

Neff, J. C., J. C. Finlay, S. A. Zimov, S. P. Davydov, J. J. Carrasco, E. A. G. Schuur, and A. I. Davydova (2006), Seasonal changes in the age and structure of dissolved organic carbon in Siberian rivers and streams, *Geophysical Research Letters*, *33*(23).

Nordin, A., I. K. Schmidt, and G. R. Shaver (2004), Nitrogen uptake by arctic soil microbes and plants in relation to soil nitrogen supply, *Ecology*, *85*(4), 955-962.

O'Donnell, J. A., G. R. Aiken, M. A. Walvoord, and K. D. Butler (2012), Dissolved organic matter composition of winter flow in the Yukon River basin: Implications of permafrost thaw and increased groundwater discharge, *Global Biogeochemical Cycles*, *26*.

Osterkamp, T. E. (2005), The recent warming of permafrost in Alaska, *Global Planet Change*, *49*(3-4), 187-202.

Osterkamp, T. E., M. T. Jorgenson, E. A. G. Schuur, Y. L. Shur, M. Z. Kanevskiy, J. G. Vogel, and V. E. Tumskoy (2009), Physical and Ecological Changes Associated with Warming Permafrost and Thermokarst in Interior Alaska, *Permafrost and Periglacial Processes*, *20*(3), 235-256.

Oswald, W. W., L. B. Brubaker, F. S. Hu, and G. W. Kling (2003), Holocene pollen records from the central Arctic Foothills, northern Alaska: testing the role of substrate in the response of tundra to climate change, *J Ecol*, *91*(6), 1034-1048.

Schimel, J. P., and J. S. Clein (1996), Microbial response to freeze-thaw cycles in tundra and taiga soils, *Soil Biol Biochem*, *28*(8), 1061-1066.

Serreze, M. C., J. E. Walsh, F. S. Chapin, T. Osterkamp, M. Dyurgerov, V. Romanovsky, W. C. Oechel, J. Morison, T. Zhang, and R. G. Barry (2000), Observational evidence of recent change in the northern high-latitude environment, *Climatic Change*, *46*(1-2), 159-207.

Slater, A. G., and D. M. Lawrence (2013), Diagnosing Present and Future Permafrost from Climate Models, *Journal of Climate*, *26*(15), 5608-5623, doi:10.1175/jcli-d-12-00341.1.

Spencer, R. G. M., G. R. Aiken, K. P. Wickland, R. G. Striegl, and P. J. Hernes (2008), Seasonal and spatial variability in dissolved organic matter quantity and composition from the Yukon River basin, Alaska, *Global Biogeochemical Cycles*, *22*(4).

Striegl, R. G., G. R. Aiken, M. M. Dornblaser, P. A. Raymond, and K. P. Wickland (2005), A decrease in discharge-normalized DOC export by the Yukon River during summer through autumn, *Geophysical Research Letters*, *32*(21).

Tank, S. E., K. E. Frey, R. G. Striegl, P. A. Raymond, R. M. Holmes, J. W. McClelland, and B. J. Peterson (2012), Landscape-level controls on dissolved carbon flux from diverse catchments of the circumboreal, *Global Biogeochemical Cycles*, *26*.

Tarnocai, C., J. G. Canadell, E. A. G. Schuur, P. Kuhry, G. Mazhitova, and S. Zimov (2009), Soil organic carbon pools in the northern circumpolar permafrost region, *Global Biogeochemical Cycles*, *23*.

Thienpont, J. R., K. M. Ruehland, M. F. J. Pisaric, S. V. Kokelj, L. E. Kimpe, J. M. Blais, and J. P. Smol (2013), Biological responses to permafrost thaw slumping in Canadian Arctic lakes, *Freshwater Biology*, *58*(2), 337-353.

Toolik Environmental Data Center Team (2011), Meterological monitoring program at Toolik, Alaska, Toolik Field Station, Institute of Arctic Biology, University of Alaska Fairbanks.

Vonk, J. E., et al. (2013), High biolability of ancient permafrost carbon upon thaw, *Geophysical Research Letters*, 40.

Weishaar, J. L., G. R. Aiken, B. A. Bergamaschi, M. S. Fram, R. Fujii, and K. Mopper (2003), Evaluation of Specific Ultraviolet Absorbance as an Indicator of the Chemical Composition and Reactivity of Dissolved Organic Carbon, *Environmental Science & Technology*, *37*(20), 4702-4708.

Wickland, K. P., J. C. Neff, and G. R. Aiken (2007), Dissolved organic carbon in Alaskan boreal forest: Sources, chemical characteristics, and biodegradability, *Ecosystems*, *10*(8), 1323-1340.

Wickland, K. P., G. R. Aiken, K. Butler, M. M. Dornblaser, R. G. M. Spencer, and R. G. Striegl (2012), Biodegradability of dissolved organic carbon in the Yukon River and its tributaries: Seasonality and importance of inorganic nitrogen, *Global Biogeochemical Cycles*, *26*.

Wilhelm, R. C., K. J. Radtke, N. C. S. Mykytczuk, C. W. Greer, and L. G. Whyte (2012), Life at the Wedge: the Activity and Diversity of Arctic Ice Wedge Microbial Communities, *Astrobiology*, *12*(4), 347-360.

Woods, G. C., M. J. Simpson, B. G. Pautler, S. F. Lamoureux, M. J. Lafreniere, and A. J. Simpson (2011), Evidence for the enhanced lability of dissolved organic matter following permafrost slope disturbance in the Canadian High Arctic, *Geochimica Et Cosmochimica Acta*, *75*(22), 7226-7241.

WRCC (2011), Western Regional Climate Center, http://www.wrcc.dri.edu/.

Zhang, T., R.G. Barry, K. Knowles, J.A. Heginbottom, and J. Brown (1999), Statistics and characteristics of permafrost and ground ice distribution in the Northern Hemisphere, *Polar Geography*, *23*(2), 147-169.

Zhang, Z., D. L. Kane, and L. D. Hinzman (2000), Development and application of a spatially-distributed Arctic hydrological and thermal process model (ARHYTHM), *Hydrol Process*, *14*(6), 1017.

Zimov, S. A., S. P. Davydov, G. M. Zimova, A. I. Davydova, E. A. G. Schuur, K. Dutta, and F. S. Chapin (2006), Permafrost carbon: Stock and decomposability of a globally significant carbon pool, *Geophysical Research Letters*, *33*(20)

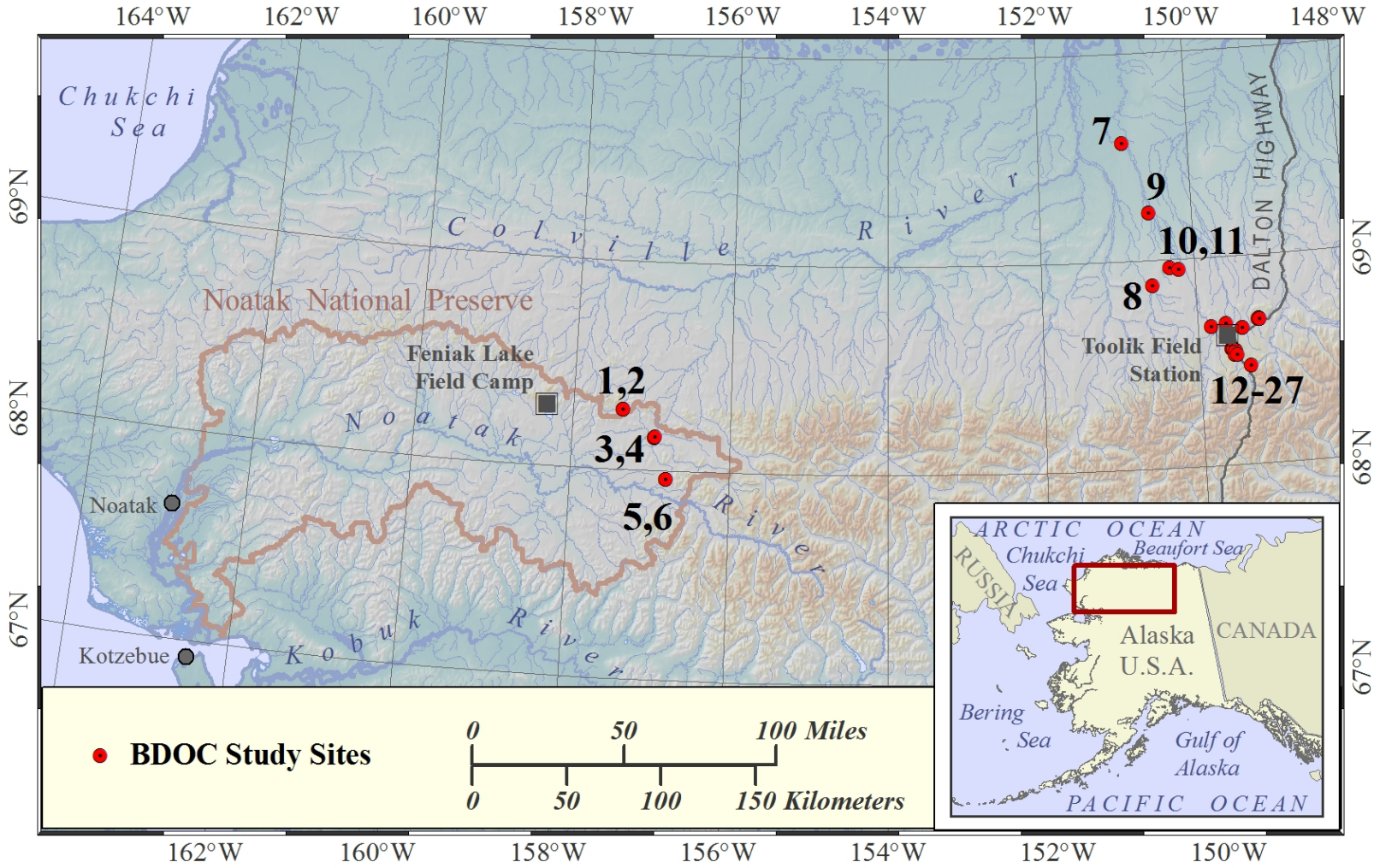

Figure 3.1 Map of study area.

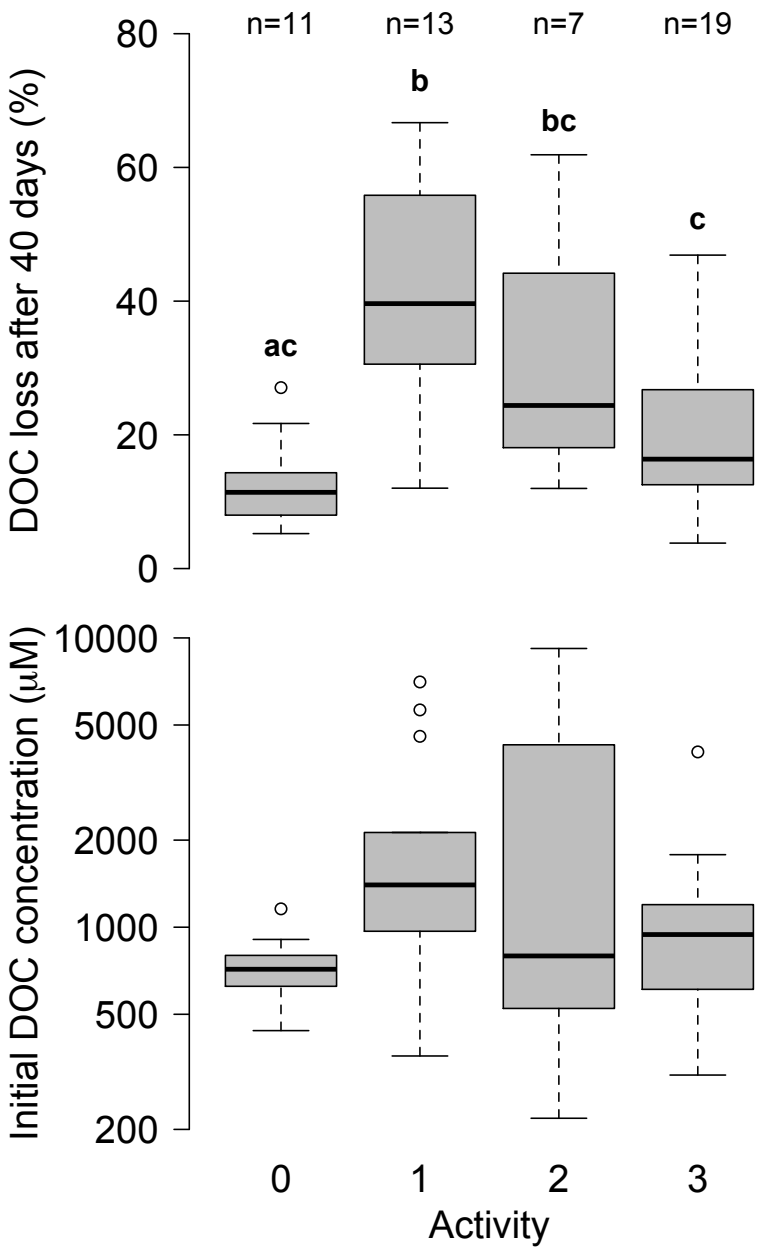

Figure 3.2 DOC loss in water from collapsing permafrost and reference water tracks after 40 days of lab incubation at room temperature and initial DOC concentration. See Table 3.1 or text for complete definition of activity index but 0=reference, 1=most active, and 3=stabilized. Box plots represent median, quartiles, minimum and maximum within 1.5 times the interquartile range, and outliers beyond 1.5 IQR. Different letters represent significant differences between activity levels, $\alpha = 0.05$.

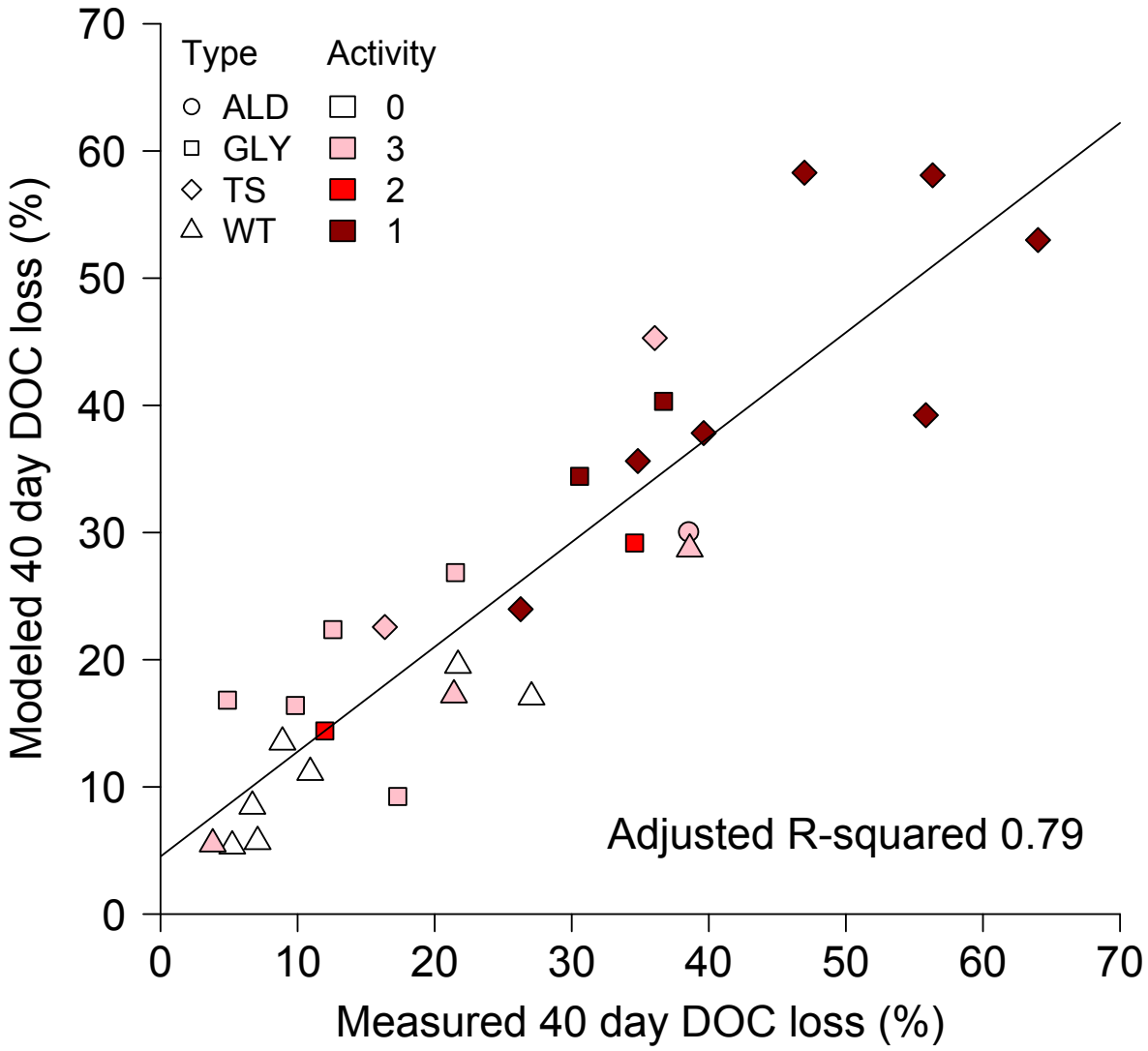

Figure 3.3 Fitted vs. actual DOC loss. The multiple linear regression model includes PO_4^{3-}, $\delta^{18}O$, SUVA254, and NH_4^+ as independent variables. Models estimating fast, slow, and total BDOC presented in Table 3.4. Shapes represent site type and shading represents activity level (defined in Fig. 3.1).

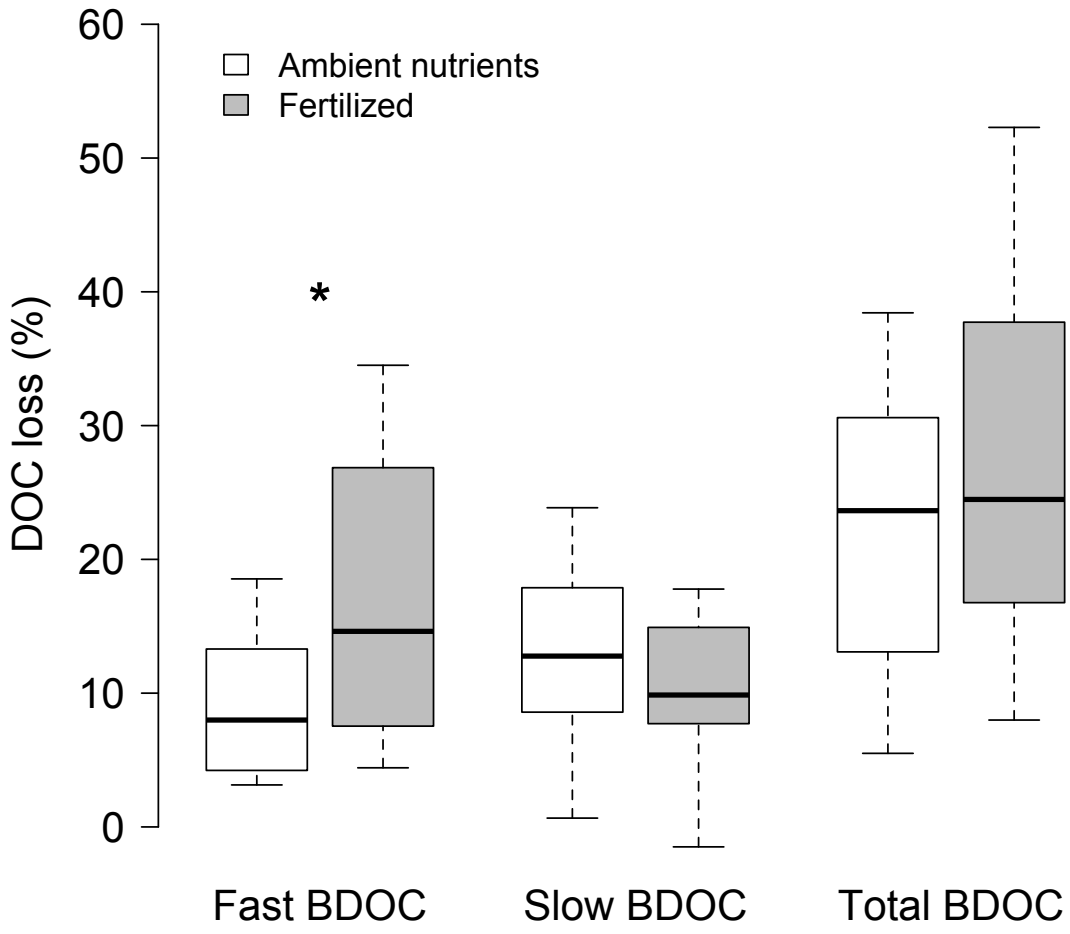

Figure 3.4 DOC loss after 40 day incubation at room temperature. Fertilized vials were amended with 80 μM NH_4^+/NO_3^- and 10 μM PO_4^{3-}. Fast BDOC was defined as loss from $t_0 - t_{10}$, slow as loss from $t_{10} - t_{40}$, and total as loss from $t_0 - t_{40}$. * represents significant difference at $\alpha = 0.05$. n = 7 for each column. Symbology defined in Fig. 3.2.

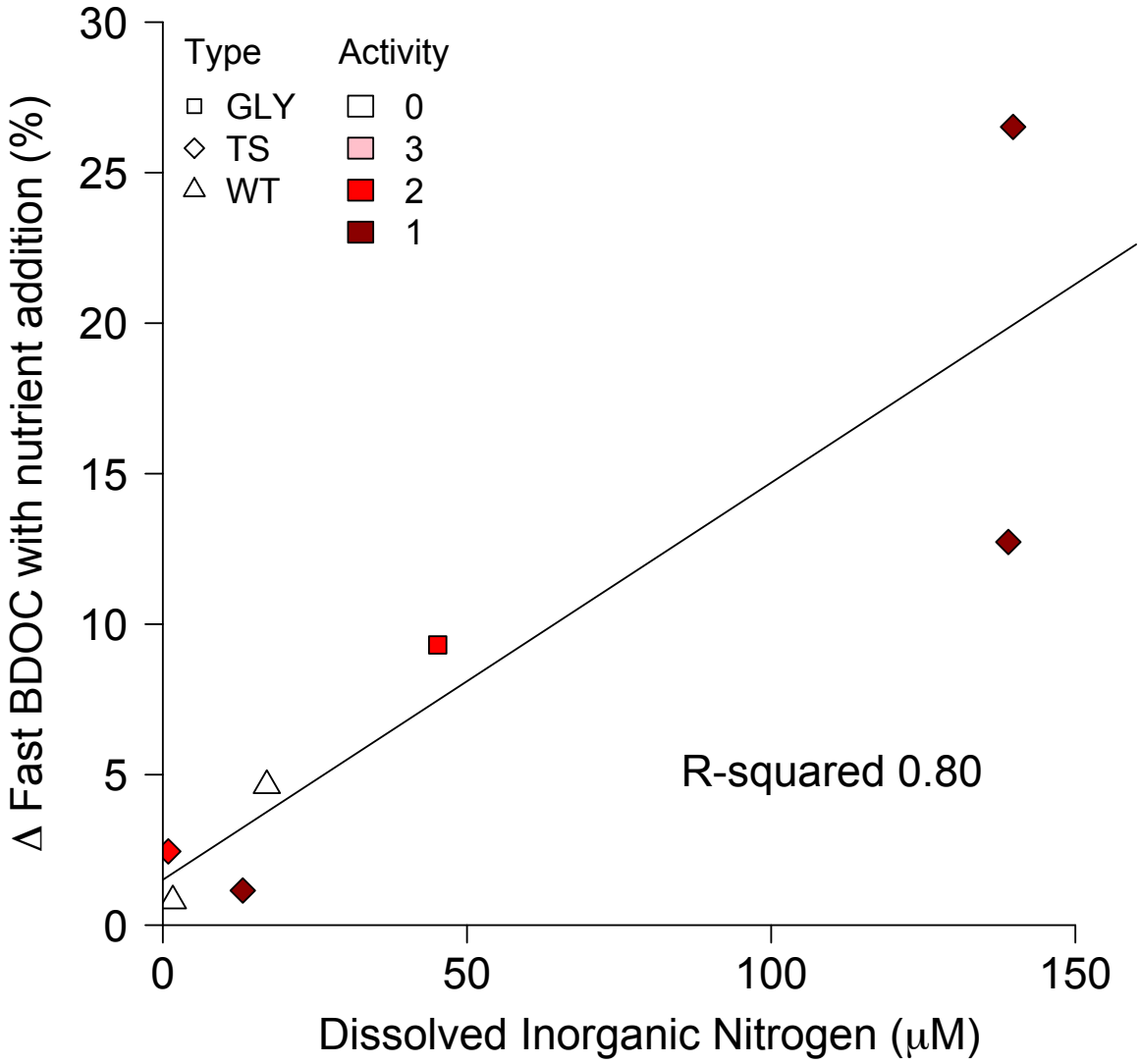

Figure 3.5 Response of fast BDOC (DOC loss from $t_0 - t_{10}$) to nutrient addition. Each point represents the fertilized DOC loss (%) minus the ambient nutrient DOC loss (%). Shapes represent site type and shading represents activity level (defined in Fig. 3.1).

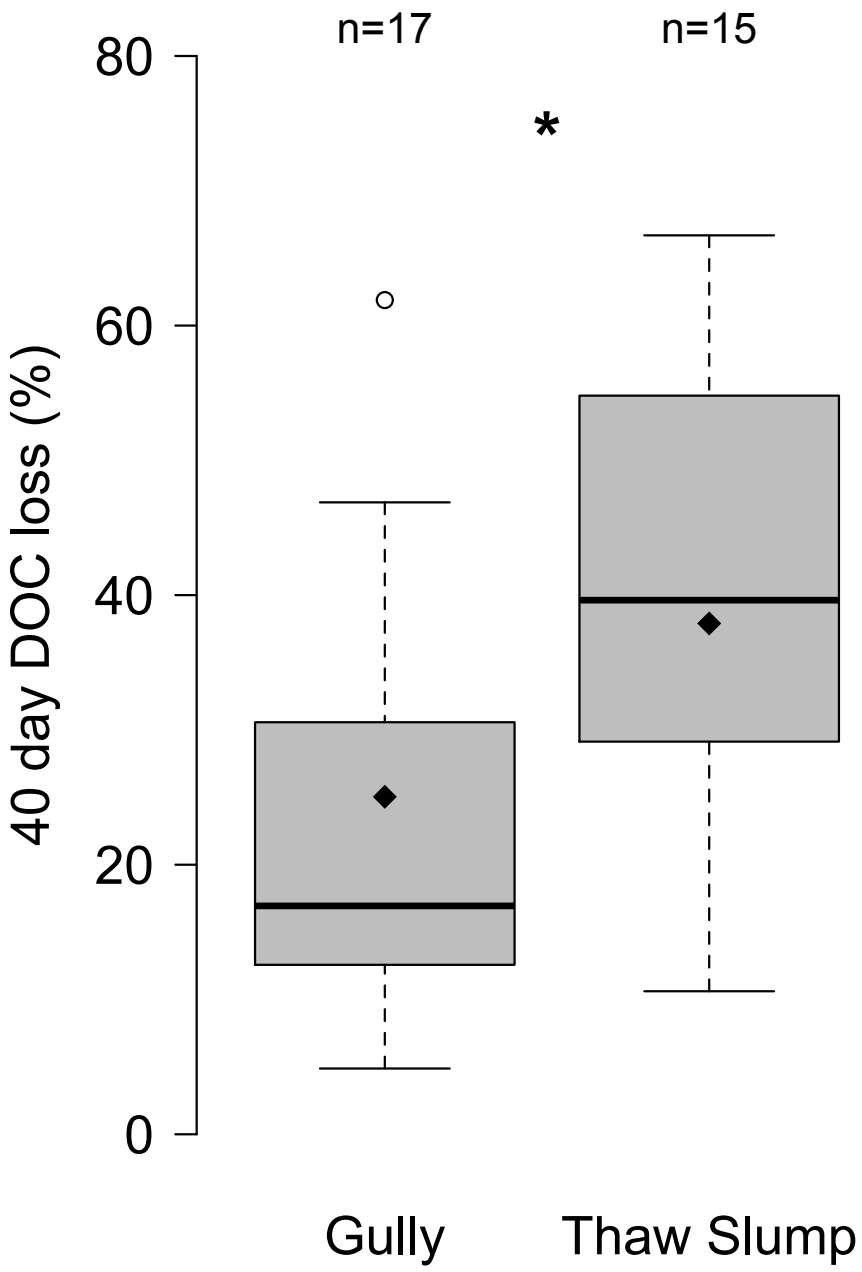

Figure 3.6 Comparison of BDOC between thaw slump and gully thermokarst features while controlling for activity level. Diamonds denote mean BDOC after adjusting for activity. * represents significant difference at $\alpha = 0.05$. Symbology defined in Fig. 3.2.

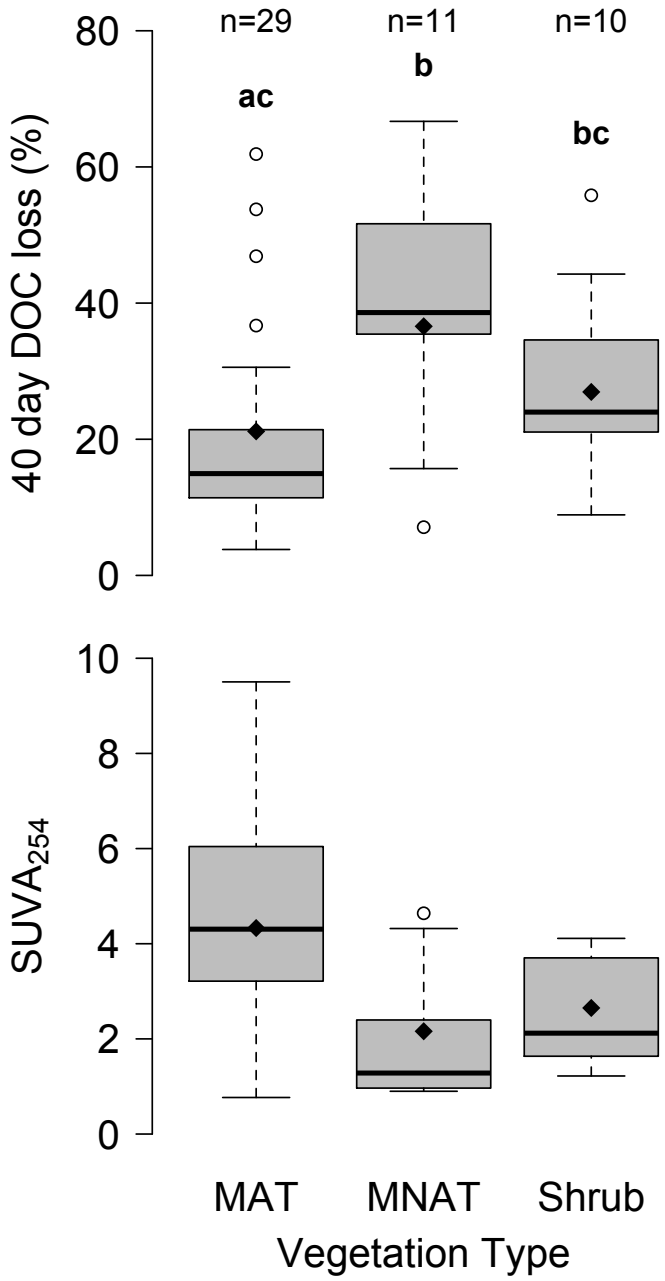

Figure 3.7 Comparison of BDOC and $SUVA_{254}$ between moist acidic tundra (MAT), moist non-acidic tundra (MNAT), and shrub tundra (Shrub), controlling for activity level. Diamonds denote mean BDOC after adjusting for activity. Different letters represent significant differences between activity levels, $\alpha = 0.05$.

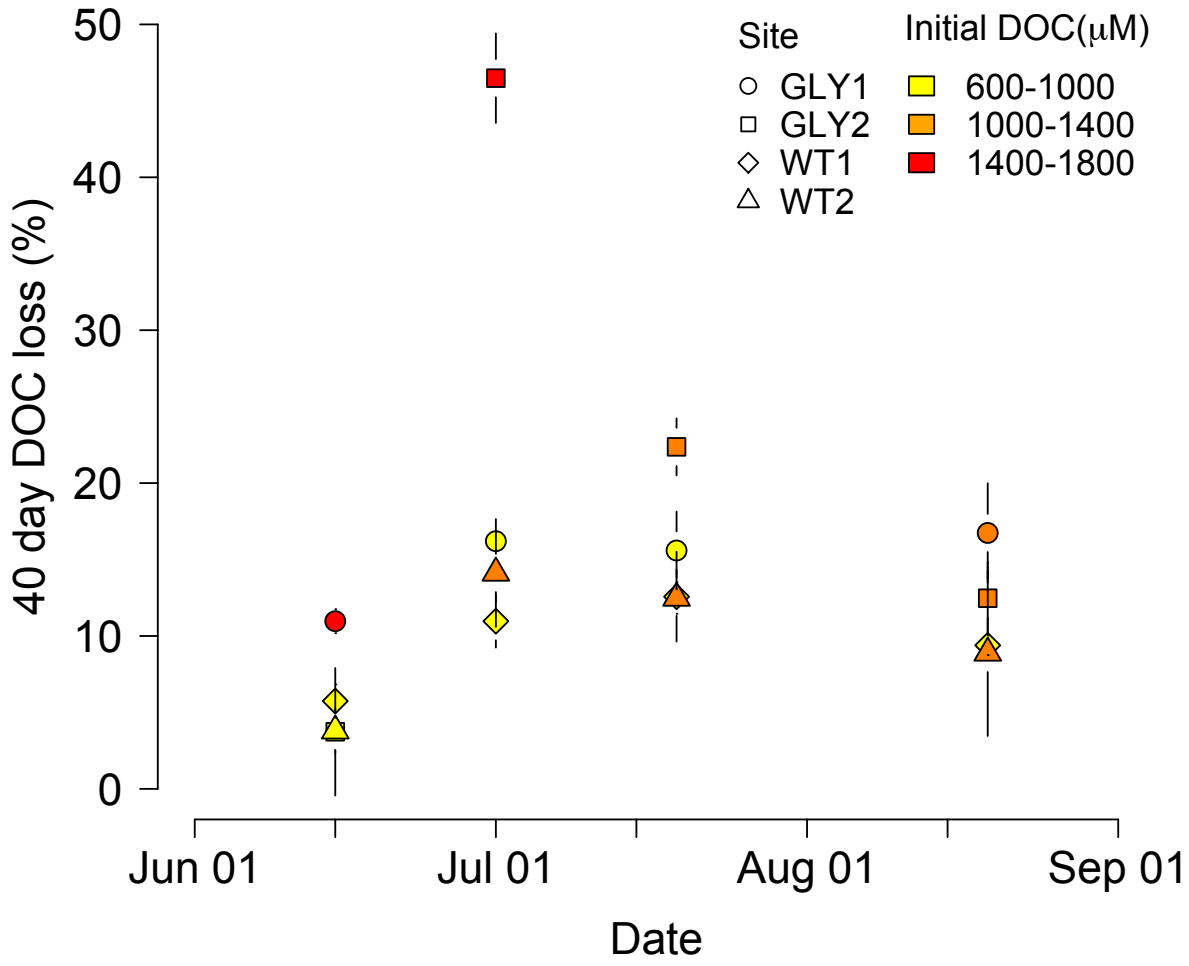

Figure 3.8 Seasonal patterns of DOC biodegradability for two gullies and two water tracks. Complete site information in Table 3.1. Shapes represent site type and shading represents the initial DOC concentration. Error bars are ± SE of replicate incubation vials.

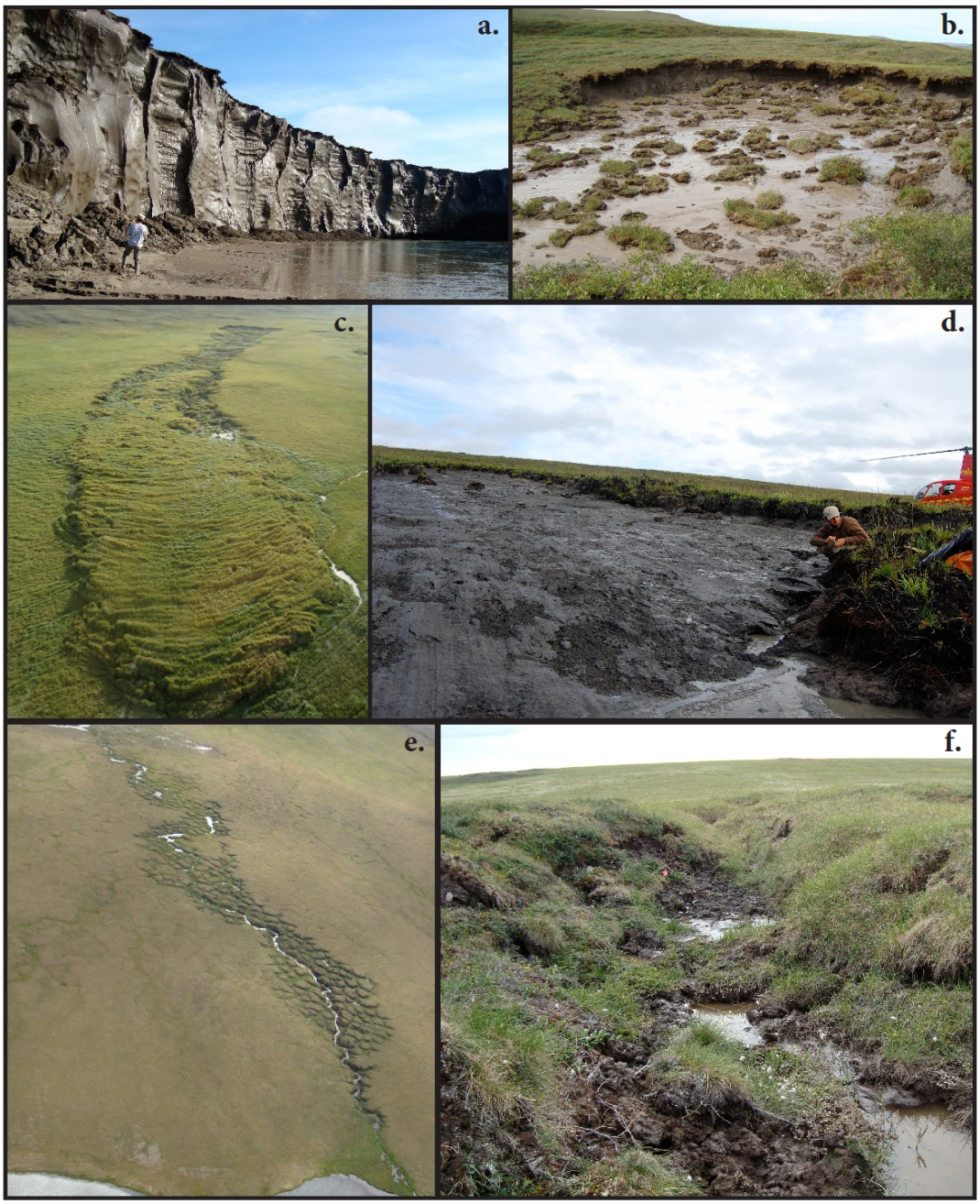

Supplementary Figure 3.1 Photos of the three most common upland thermokarst morphologies in the foothills of the Brooks Range on the North Slope of Alaska. Retrogressive thaw slumps (panels a,b), active layer detachment slides (c,d), and thermo-erosion gullies (e,f). Photo in panel c by A.W. Balser and panel d by J.R. Larouche.

Table 3.1. Summary of site characteristics including DOC concentration and biodegradability, feature type, vegetation, and ecotype

Site ID	Average BDOC (%)	Average DOC (µM)	$SUVA_{254}$	Activity index[a]	# times sampled	Primary ground ice type	Tundra vegetation[b]	Ecotype[c]	Map ID	Coordinates (UTM)
ALD 1	21.1	219	1.38	2	1	Transition/Glacial	Low to tall shrublands[d]	4	24	68.4704 -149.3435
ALD 2	38.5	344	2.40	3	1	Transition	Moist nonacidic tundra[d]	1	1	68.2866 -157.3640
GLY 1	14.8	1159	8.42	3	4	Ice wedge	Moist acidic tundra	3	19	68.5435 -149.5225
GLY 2	21.4	1180	3.71	3	4	Ice wedge (Pleistocene)	Moist acidic tundra	3	26	68.6923 -149.2067
GLY 3	12.0	1946	ND	1	1	Ice wedge	Moist acidic tundra[d]	3	9	69.2278 -150.5534
GLY 4	21.5	608	4.11	3	1	Ice wedge (Pleistocene)	Dwarf to low shrublands[d]	3	3	68.1589 -156.9533
GLY 5	28.1	1498	3.90	1	3	Ice wedge (Pleistocene)	Moist acidic tundra	2	15	68.5524 -149.5652
GLY 6	29.7	1075	3.33	2	3	Ice wedge	Moist acidic tundra	2	17	68.5541 -149.5577
GLY 7	34.6	469	3.70	2	1	Ice wedge	Dwarf to low shrublands	2	23	68.6523 -149.4202
TS 1	10.6	4036	2.41	3	1	Glacial/Lacustrine	Moist acidic tundra[d]	3	11	68.9514 -150.1943
TS 2	56.3	1707	0.97	1	1	Glacial	Moist nonacidic tundra	4	8	68.8793 -150.5563
TS 3	39.1	7943	0.77	2	2	Glacial/Lacustrine	Moist acidic tundra[d]	3	10	68.9614 -150.3154
TS 4	50.0	667	2.12	1	2	Glacial	Dwarf to low shrublands	3	14	68.5554 -149.5747
TS 5	36.1	612	1.96	3	1	Pore ice	Moist nonacidic tundra[d]	3	12	68.6666 -149.8188
TS 6	24.2	434	1.75	3	2	Glacial	Low to tall shrublands	4	13	68.6784 -149.6242
TS 7	59.2	5750	0.95	1	3	Ice wedge (Yedoma)	Moist non-acidic[d]	2	7	69.5683 -150.8701
TS 8	26.3	359	1.22	1	1	Glacial	Dwarf to low shrublands[d]	3	18	68.5254 -149.5438
TS 9	34.8	983	1.28	1	1	Glacial/Lacustrine	Moist nonacidic tundra[d]	3	6	67.9620 -156.7889
TS 10	39.6	1225	0.97	1	1	Glacial/Lacustrine	Moist nonacidic tundra[d]	4	5	67.9619 -156.7920
WT 1	9.5	740	4.40	0	4	na	Sedge, moss tundra (fen)	1	20	68.5442 -149.5214
WT 2	13.2	1043	7.27	3	4	na	Sedge, moss tundra (poor fen)	3	25	68.6911 -149.2084
WT 3	38.6	356	2.39	3	1	na	Moist nonacidic tundra[d]	1	2	68.2867 -157.3627
WT 4	21.7	509	3.75	0	1	na	Low to tall shrublands[d]	1	4	68.1594 -156.9451
WT 5	11.4	892	4.48	0	2	na	Moist nonacidic tundra	2	16	68.5537 -149.5588
WT 6	8.9	439	2.62	0	1	na	Low to tall shrublands	2	22	68.6515 -149.4223
WT 7	10.9	907	2.89	0	1	na	Moist acidic tundra	1	21	68.5270 -149.5110
WT 8	19.2	701	4.81	0	2	na	Low to tall shrublands	3	27	68.6906 -149.1922

BDOC (%) determined by DOC loss during a 40-day lab incubation in the dark at 20 C with added nutrients; $SUVA_{254}$ = specific UV absorbance at 254 nm (L mg C^{-1} m^{-1}); ND = no data

[a] Activity index is defined as: 0. No apparent present or past thermo-degradation, 1. Highly active thermo-degradation (active headwall collapse or lateral growth) with completely turbid outflow, 2. Moderate thermo-degradation (some headwall or lateral growth) with somewhat turbid outflow, 3. Stabilized or limited thermo-degradation with complete or partial revegetation and clear outflow

[b] Walker et al. 2010 unless otherwise noted

[c] Ecotype definitions follow Jorgenson et al. 2009 and coded as: 1. Alpine Wet Sedge Meadow, 2. Upland Birch-Willow Low Shrub, 3. Upland Dwarf Birch-Tussock Shrub, 4. Upland Sedge-Dryas Meadow

Table 3.2 Carbon, nitrogen and water chemistry parameters by thermokarst activity level.

Activity level	**0**			**1**			**2**			**3**		
	Median	Mean	SE	Median	Mean	SE	Median	Mean	SE	Median	Mean	SE
Parameter												
DOC	716	727	59	1400	2254	588	796	2828	1363	943	1071	189
BDOC (%)	11.4	12.8	2.0	39.6	40.9	4.7	24.4	31.8	7.3	16.4	20.6	2.8
Proportion fast	0.67	0.66	0.09	0.52	0.48	0.06	0.55	0.57	0.09	0.59	0.61	0.05
DON	17.0	16.6	2.21	71.8	109.5	36.2	22.9	145.0	124.9	22.3	26.3	5.64
DOC:DON	40.4	41.2	3.55	20.7	21.7	1.51	20.5	23.7	5.10	32.0	35.4	3.68
NO_3^-	0.10	2.32	2.19	2.73	3.61	0.81	2.74	4.87	3.48	0.21	4.87	3.48
NH_4^+	1.64	1.63	0.26	35.3	64.5	18.7	33.5	25.1	11.9	2.05	4.35	2.00
PO_4^{3-}	0.009	0.015	0.008	0.156	0.242	0.082	0.054	0.144	0.094	0.036	0.063	0.020
$SUVA_{254}$	4.26	4.13	0.29	1.25	1.94	0.38	3.09	2.64	0.52	4.52	4.97	0.70
$\delta^{18}O$	-20.495	-20.932	1.04	-21.569	-22.927	1.304	-22.880	-22.804	0.614	-19.550	-19.227	0.626

For activity levels 0-3, n = 11, 13, 7, and 19, respectively
BDOC (%) determined by DOC loss during a 40-day lab incubation in the dark at 20 C with added nutrients
Proportion fast is the proportion of total BDOC loss that occurred during the first ten days of the incubation
All concentrations in μM
$SUVA_{254}$ = specific UV absorbance at 254 nm (L mg C^{-1} m^{-1})
See Table 3.1 for definition of activity levels

Table 3.3 Correlations between water chemistry parameters, site activity, and DOC biodegradability.

	Activity	Fast BDOC (ln %)	Slow BDOC (%)	Total BDOC (%)	Total BDOC (ln µM)
Metrics of DOC Biodegradability					
Fast BDOC (ln %)	0.33 *				
Slow BDOC (%)	0.72 ***	0.27			
Total BDOC (%)	0.62 ***	0.82 ***	0.68 ***		
Total BDOC (ln µM)	0.59 **	0.58 ***	0.68 ***	0.81 ***	
Predictor variables					
Initial DOC (ln µM)	0.35 *	0.17	0.41 **	0.41 **	0.84 ***
$SUVA_{254}$ (ln (L mg C^{-1} m^{-1}))	-0.56 ***	-0.54 ***	-0.45 **	-0.62 ***	-0.52 ***
DOC:DON	-0.73 ***	-0.51 **	-0.66 ***	-0.62 ***	-0.68 ***
NH_4^+ (ln µM)	0.82 ***	0.37 *	0.68 ***	0.66 ***	0.66 ***
NO_3^- $(\mu M)^{0.25}$	0.55 **	0.28	0.2	0.28	-0.03
DIN (µM)	0.60 ***	0.47 ***	0.48 **	0.64 ***	0.64 ***
PO_4^{3-} $(\mu M)^{0.25}$	0.60 ***	0.64 ***	0.67 ***	0.78 ***	0.68 ***
K (ln µM)	0.85 ***	0.50 **	0.64 ***	0.64 ***	0.59 ***
^{18}O (ln (δ^2))	0.05	0.39 *	0.02	0.31	0.29
^{18}O (δ)	-0.31	-0.23	-0.11	-0.3	-0.36 *
DOC:DIN (ln)	-0.49 **	-0.31	-0.08	-0.27	0.00

Relationships were visually inspected and transformed when necessary to meet the assumption of linearity. Strength of relationship was determined by Pearson product-moment correlation. * $p < 0.05$, ** $p < 0.01$, and *** $p < 0.001$.

Table 3.4 Multiple linear regression models for four metrics of DOC biodegradability.

Variable	Equation	R^2	F
Fast BDOC (ln %)	$-0.36 \ln(SUVA+0.25) + -0.021 (DOC:DON) + 0.20 \ln((\delta^{18}O + 21.2)^2) - 0.60 \ln[DOC] + 2.52 [PO_4]^{0.25} + 6.1$	0.67	12.4
Slow BDOC (%)	$9.48 [PO_4]^{0.25} - 2.57 \ln(SUVA+0.25) + 4.87 \ln[DOC] + 3.30 \ln[NH_4] + 1.50 (\delta^{18}O+21.2) - 22.8$	0.70	13.9
Total BDOC (%)	$28.2 [PO_4]^{0.25} + 3.46 \ln((\delta^{18}O + 21.2)^2) - 8.84 \ln(SUVA+0.25) + 0.616 (\delta^{18}O + 21.2) + 6.35 \ln[NH_4] + 4.57$	0.79	21.5
Total BDOC (ln μM)	$0.054 (\delta^{18}O + 21.2) - 0.023 (DOC:DON) + 0.188 \ln((\delta^{18}O + 21.2)^2) + 0.385 \ln[NH_4] + 2.51 [PO_4]^{0.25} + 3.56$	0.83	27.8

Multiple linear regression models were selected for fast, slow, and total BDOC (%) from full models with the following predictors: initial DOC, $SUVA_{254}$, DOC:DON, NH_4^+, PO_4^{3-}, and $\delta^{18}O$. For total BDOC concentration, initial DOC was excluded as a predictor since it is a part of the response variable. Stepwise AIC was used to compare full models against models with subsets of predictors with lowest AIC score determining final models. Predictors are ordered within each model from lowest to highest individual AIC ranking. $\delta^{18}O$ was centered on zero before analysis by subtracting the mean (-21.1993) and a polynomial term was included to reflect the dual sources of depleted oxygen (snow and permafrost melt water). Models including the following terms were < 2 AIC units different than the final model (suggesting equal power and parsimony): Fast BDOC (%) including NH_4^+, Slow BDOC (%) including DOC:DON, Total BDOC (%) including initial DOC, and Total BDOC (ln uM) excluding polynomial $\delta^{18}O$ term. For all regressions n=29, and $p < 0.0001$.

Chapter 4. Patterns and persistence of hydrologic carbon and nutrient export from collapsing upland permafrost[1]

4.1 Abstract

As high latitudes warm, vast stocks of carbon and nitrogen stored in permafrost will become available for transport to aquatic ecosystems. While there is a growing understanding of the potential effects of permafrost collapse (thermokarst) on aquatic biogeochemical cycles, neither the spatial extent nor temporal duration of these effects are known, precluding the incorporation of thermokarst into coupled climate models. To test hypotheses concerning patterns and persistence of elemental export from upland thermokarst, we sampled hydrologic outflow from 83 thermokarst features in various stages of development across the North Slope of Alaska. We hypothesized that an initial pulse of carbon and nutrients would be followed by a period of elemental retention during feature recovery, and that the duration of these stages would depend on feature morphology. Thermokarst caused substantial increases of DOC and other solute concentrations with a particularly large impact on inorganic nitrogen. Magnitude and duration of thermokarst effects on water chemistry differed by feature type and secondarily by landscape age. Most solutes returned to undisturbed concentrations after feature stabilization, but elevated dissolved carbon, inorganic nitrogen, and sulfate concentrations persisted through stabilization for some feature types, suggesting that aquatic disturbance by thermokarst may be long-lived. Dissolved methane decreased by 90% in some features, potentially due to high concentrations of sulfate and inorganic nitrogen. Spatial patterns of carbon and nutrient export from thermokarst suggest that upland thermokarst may be a dominant linkage between terrestrial and aquatic ecosystems as the Arctic warms.

4.2 Introduction

Arctic tundra and boreal forest have accumulated a vast pool of organic carbon, twice as large as the atmospheric carbon pool and three times as large as the carbon contained by all living things (Tarnocai et al., 2009). Climate change is simultaneously causing widespread permafrost degradation (Slater and Lawrence, 2013) and altering high-latitude hydrology (Peterson et al., 2006; Rawlins et al., 2010), exposing carbon and other elements previously

[1]Prepared for submission to Biogeosciences. B.W. Abbott, J.B. Jones, S.E. Godsey, J.R. Larouche, W.B. Bowden.

protected in permafrost to transport and processing in Arctic rivers, lakes, and estuaries. Fluxes of dissolved organic carbon (DOC), nutrients, and other ions are already changing across the permafrost region and the rate of change is projected to accelerate in the future (Frey and McClelland, 2009; Jones et al., 2005; Laudon et al., 2012; McClelland et al., 2007; McClelland et al., 2014; O'Donnell et al., 2012; Petrone et al., 2006; Rawlins et al., 2010; Striegl et al., 2005; Tank et al., 2012). The interaction between changing hydrology and degrading permafrost is one of the key uncertainties in predicting the response of aquatic ecosystems to high-latitude climate change (Abbott et al., 2014a; Koch et al., 2013b; McClelland et al., 2008; Rawlins et al., 2010; Vonk and Gustafsson, 2013).

Permafrost degradation follows two basic trajectories. In permafrost with little ground ice, the soil profile can thaw from the top down without disturbing the surface, gradually exposing organic matter and solutes to hydrologic export (Koch et al., 2013a; Petrone et al., 2006; Striegl et al., 2005). Alternatively, in permafrost where ground ice volume exceeds soil pore space, thaw causes surface subsidence or collapse, termed thermokarst (Kokelj and Jorgenson, 2013). When thermokarst occurs on hillslopes it can abruptly mobilize sediment, organic matter, and solutes from meters below the surface, impacting kilometers of stream reach or entire lakes (Bowden et al., 2008; Kokelj et al., 2005; Kokelj et al., 2013; Schuur et al., 2008; Vonk et al., 2012).

The term thermokarst includes a suite of thermo-erosional features with different morphologies determined primarily by ice content, substrate type, landscape position, and slope (Jorgenson and Osterkamp, 2005; Jorgenson et al., 2008; Osterkamp et al., 2009). In upland landscapes, the three most common thermokarst morphologies are retrogressive thaw slumps, active-layer detachment slides, and thermo-erosion gullies (Jorgenson and Osterkamp, 2005; Kokelj and Jorgenson, 2013; Krieger, 2012). Thaw slumps often form on lakeshores, have a retreating headwall, and are fueled by a variety of ground ice types. Active-layer detachment slides form when the seasonally thawed surface layer of vegetation and soil slips downhill over an ice-rich transition zone. Thermo-erosion gullies form due to melting of ice wedges, growing with a generally linear or dendritic pattern, and are often associated with water tracks or headwater streams. These three morphologies currently impact ca. 1.5% of the landscape in the western foothills of the Brooks Range (Krieger, 2012) and could affect 20-50% of uplands in the

continuous permafrost region by the end of the century based on projected thaw and estimates of ground ice distribution (Slater and Lawrence, 2013; Zhang et al., 2000), though circumarctic prevalence and development of upland thermokarst are poorly constrained (Jorgenson et al., 2006; Lantz and Kokelj, 2008; Yoshikawa et al., 2002).

Upland thermokarst can alter the age and degradability of organic carbon, releasing older particulate organic carbon (Lafreniere and Lamoureux, 2013) and more labile dissolved organic carbon (DOC) during formation (Abbott et al., 2014b; Cory et al., 2013; Vonk et al., 2013). Mineral soil exposed by thermokarst can increase solutes available for hydrologic transport (Harms et al., 2013; Kokelj and Burn, 2003; Kokelj et al., 2013; Louiseize et al., 2014), but can also adsorb DOC, reducing concentration in feature outflows and receiving waters, resulting in greater water clarity after sediment loading and settling (Kokelj et al., 2005; Thompson et al., 2012). These changes in sediment delivery, light penetration, and nutrients can alter aquatic food webs in receiving ecosystems (Mesquita et al., 2010; Thienpont et al., 2013; Thompson et al., 2012).

Despite a growing understanding of the potential effects of upland thermokarst on aquatic biogeochemical cycles, there is conflicting evidence on the overall importance and temporal duration of these effects, precluding conceptualization of patterns of thermokarst impacts and their incorporation into coupled climate models. If thermokarst disturbance is hydrologically connected to aquatic ecosystems, it can cause substantial loading of sediment, carbon, and nutrients (Bowden et al., 2008; Kokelj et al., 2005; Kokelj et al., 2013; Shirokova et al., 2013; Thienpont et al., 2013; Vonk et al., 2013), though not all features connected to surface waters result in enhanced carbon and nutrient export (Thompson et al., 2012). Conversely, if thermokarst is hydrologically isolated from surface waters, such as when it occurs high on hillslopes, even dramatic disturbance can have little or no impact on aquatic chemistry and elemental budgets (Lafreniere and Lamoureux, 2013; Lewis et al., 2012). The duration of carbon and nutrient release, and the persistence of biogeochemical disturbance in affected ecosystems after feature stabilization is largely unknown, with altered surface water chemistry lasting for decades in some cases of nutrient loading or surface disturbance (Kokelj et al., 2005; Thienpont et al., 2013), or fading after less than a year in others (Lafreniere and Lamoureux, 2013).

To address these knowledge gaps, we sampled surface outflow from thermokarst features in various stages of development across a broad portion of the North Slope of Alaska. Our research focused on two questions. First, how does thermokarst formation alter hydrologic release of carbon and nutrients, and second, can the type and duration of hydrologic release be predicted based on feature morphology or landscape characteristics? We hypothesized that upland thermokarst would initially stimulate nutrient release due to disruption of soil aggregates, accelerated mineralization in impacted soils, decreased plant uptake, and direct release from melting ground-ice. However, following nutrient retention theory (Vitousek and Reiners, 1975) we hypothesized that this pulse of nutrients would be followed by a period of elemental retention due to enhanced nutrient uptake by recovering vegetation and diminished pools of organic matter and nutrients following disturbance. We hypothesized that DOC export would depend on the balance between DOC production from soil disruption and DOC removal by exposed mineral soil adsorbing DOC as well as enhanced processing of DOC within features due to abundant nutrients and biodegradable DOC from permafrost. In regards to feature morphology, we hypothesized that fundamental differences in formation and functioning of slides, gullies, and slumps, such as the amount of organic and mineral soil displaced, type of ground ice, location on the landscape, and duration of disturbance would result in systematic differences in carbon and nutrient release. We predicted that slumps would have the largest and longest impact, slides would have a large but short-lived impact, and gullies would have a muted impact of intermediate duration.

4.3 Methods

4.3.1 Study sites

We tested our hypotheses about thermokarst carbon and nutrient export with observations from 83 slides, gullies, and slumps on the North Slope of Alaska (Fig. 4.1). Features were identified by aerial surveys, satellite imagery, and previous studies (Abbott et al. 2014b; Bowden et al., 2008; Gooseff et al., 2009; Larouche, 2009) and were located in three areas of upland tundra underlain by continuous permafrost in the foothills of the Brooks Range. We collected samples during the growing season (June-August) of 2009-2012 and May of 2011 in the region surrounding the Toolik Field Station, with additional sampling in the Noatak National Preserve near the Kelly River Ranger Station in 2010 and Feniak Lake in 2011.

The Toolik Field Station is located 254 km north of the Arctic Circle and 180 km south of the Arctic Ocean. The mean annual temperature is -10°C with mean monthly temperatures ranging from -25°C in January to 11.5°C in July. The region receives 320 mm of precipitation annually with 200 mm falling between June and August (Toolik Environmental Data Center Team, 2014). Feniak Lake is located 360 km west of the Toolik Field Station in the central Brooks Range at the northeast boarder of the Noatak National Preserve. The average annual temperature is -7°C (Jorgenson et al., 2008) and average precipitation is 450 mm (WRCC, 2011). The Kelly River Ranger Station is located on the western boarder of the Noatak National Preserve, 170 km west of Feniak Lake. Average annual temperature is -5.4°C and the area receives an average of 300 mm of precipitation, a third of which falls during the growing season (Stottlemyer, 2001).

Vegetation is typical of Arctic tundra across the study region and includes moist acid tundra characterized by the tussock-forming sedge *Eriophorum vaginatum*, moist non-acidic tundra, and shrub tundra (Bhatt et al., 2010; Walker et al., 1998), with isolated stands of white spruce (*Picea glauca*) near the Kelly River Ranger Station (Sullivan and Sveinbjornsson, 2010). All three areas occur in bioclimate subzone E, the warmest region in the continuous permafrost zone (Walker et al., 2010). The foothills of the Brooks Range have been affected by multiple glaciations starting in the late Tertiary and continuing to 11 ka B.P. (Hamilton, 2003). Repeated rounds of glacial advance and retreat have resulted in a patchwork of glacial till, bedrock, and loess parent materials of various ages (Hamilton, 2010). Time since last glaciation can be associated with ecosystem properties including pH, organic layer depth, nutrient pools, vegetation community, and biogeochemical rates (Epstein et al., 2004; Hobbie et al., 2002; Lee et al., 2011; Walker et al., 1998).

4.3.2 Experimental design and sampling

To test our hypotheses concerning the intensity and duration of thermokarst impacts on aquatic chemistry, we sampled thermokarst features in all stages of development across landscape ages and vegetation types. We collected water from 83 thermokarst outflows and 61 adjacent undisturbed water bodies such as water tracks and first-order streams (22 locations did not have a suitable paired reference site). To quantify the evolution and duration of thermokarst effects through time, we classified features with a 0 – 3 activity index based on turbidity of

outflow, extent of thermo-degradation, and state of revegetation. This qualitative index uses space for time substitution to follow the development of a hypothetical feature from before initiation (0) to after stabilization (3). Activity levels were defined as follows: 0. No apparent present or past thermo-degradation, 1. Active thermo-degradation (>25% of headwall is actively expanding) with completely turbid outflow, 2. Moderate thermo-degradation (<25% of headwall is expanding) with somewhat turbid outflow, 3. Stabilized or limited thermo-degradation with complete or partial revegetation and clear outflow.

Vegetation class was determined in the field and cross-referenced with published vegetation maps when available (Walker et al., 2005). Glacial geology and surface age were based on recent maps of the study region (Hamilton, 2010, 2003; Kanevskiy et al., 2011). Most site ages ranged from 10-200 ka, though six sites occurred on surfaces unglaciated for more than 1000 ka. We classified sites on surfaces younger than 25 ka as young, and sites over 50 ka as old, corresponding to the split between the Itkillik I and II advances (Hamilton, 2003).

Samples for carbon and nutrient analysis were filtered in the field (0.7 μm effective pore size, Advanctec GF-75) into 60 ml HDPE bottles, except when excess sediment required settling overnight when they were filtered within 24 hours. After filtration, samples were frozen until analysis. We measured DOC and dissolved inorganic carbon (DIC) with a Shimadzu TOC-5000 connected to an Antek 7050 chemiluminescent detector to quantify total dissolved nitrogen after combustion to NO_x. We analyzed major ions (NO_3^-, NO_2^-, SO_4^{2-}, Cl^-, NH_4^+, Ca^{2+}, Na^+, Mg^{2+}, and K^+) on a Dionex DX-320 ion chromatograph. We calculated dissolved organic nitrogen (DON) by subtracting dissolved inorganic nitrogen ($DIN = NO_3^- + NH_4^+ + NO_2^-$) from total dissolved nitrogen, and we calculated the carbon to nitrogen ratio (C:N) of dissolved organic matter, an indicator of organic matter source and degree of prior processing (Amon et al., 2012). To determine the percentage of thermokarst outflow coming from ground ice, we analyzed δ D and $\delta^{18}O$ on a Picarro L1102-i via cavity ringdown spectroscopy.

Because lateral fluxes of dissolved gas can constitute a considerable portion of Arctic carbon budgets (Kling et al., 1992; Striegl et al., 2012), we measured dissolved CO_2, CH_4, and N_2O in feature outflows and reference water. At each site we collected a 30 ml sample of bubble-free water in a 60 ml gas-tight syringe accompanied by an ambient atmospheric sample in a 15 ml evacuated gas vial. Upon return to the lab or camp we added 30 ml of atmosphere to the

syringe and shook vigorously for two minutes to facilitate equilibration of dissolved gases with the introduced headspace, and then injected a sample of the headspace into an evacuated gas vial for storage until analysis. We determined CO_2, CH_4, and N_2O concentration of the headspace sample on a Varian 3300 gas chromatograph with a methanizer and flame ionization detector for carbon species and an electron capture detector for N_2O. We calculated the proportion of total gas dissolved in solution and in the headspace using Henry's constants adjusted for extraction temperature (Wilhelm et al., 1977), and subtracted ambient gas introduced during extraction to determine initial concentration. We calculated saturation as the percent of equilibrium water concentration based on atmospheric partial pressure and water temperatures at the time of sampling and extraction.

To determine the direct contribution of carbon and nutrients from ground ice, we sampled exposed headwall ice at 24 sites. We collected ice scrapings into Ziplock™ bags, which we filtered and analyzed after melt as previously described. We compared concentrations of carbon and nutrients in ground ice to feature outflows to determine what solutes were being taken up or diluted and what solutes were increasing as water flowed through the feature. At these sites we used the difference between the $\delta^{18}O$ of ground ice and adjacent reference water to determine the proportion of outflow contributed by ground ice. We calculated the proportion from ground ice with a simple two end-member model:

$$\text{Fraction from ground ice} = (\delta^{18}O_{out} - \delta^{18}O_{sw}) / (\delta^{18}O_{ice} - \delta^{18}O_{sw}) \qquad \text{(Equation 1)}$$

where sw is undisturbed surface water, out is feature outflow, and ice is headwall ice.

We measured discharge from 26 thermokarst features using salt-dilution gauging. We logged electrical conductivity with a YSI Professional Plus conductivity meter and added 10-100g of dissolved NaCl upstream of the probe by 10-20 m, depending on the size of the outflow. Discharge was determined by total dilution of the tracer as it passes by the probe (Wlostowski et al., 2013). We mapped feature perimeters with a commercial-grade, handheld GPS, except for four sites around Toolik, which were mapped by the Toolik Field Station GIS staff with a survey-grade GPS and base station.

4.3.3 Statistical analyses

We used a linear mixed-effects model to test for effects of thermokarst activity, feature type, vegetation, and landscape age on water chemistry while accounting for spatial and temporal non-independence in the data. For each water chemistry parameter we used a mixed-effects analysis of variance (ANOVA) with activity level crossed with feature type and including vegetation and landscape age as fixed effects. We included site as a random effect to pair thermokarst outflows with their adjacent reference water. We visually inspected residual plots for deviations from normality and homoscedasticity, and transformed response and predictor variables when necessary. We simplified the full model by automated backwards elimination, using restricted maximum likelihood to evaluate fixed effects and likelihood ratio tests for random effects. To test for differences between groups, we performed post-hoc Tukey honest significant difference tests on the least squares means using Satterthwaite approximation to estimate denominator degrees of freedom. We used Pearson product-moment correlation to test for associations between water chemistry parameters, including activity index, which we recoded low to high and treated as a continuous variable. A decision criterion of $\alpha = 0.05$ was used for all tests.

All analyses were performed in R 3.0.2 (R Core Team, 2013) with the lme4 and lmerTest packages (Bates et al., 2013; Kuznetsova et al., 2014). The complete dataset is available through the Advanced Cooperative Arctic Data and Information Service at www.aoncadis.org/project/collaborative_research_spatial_and_temporal_influences_of_thermokarst_failures_on_surface_processes_in_arctic_landscapes.html.

4.4 Results

4.4.1 Feature characteristics and distribution

Feature types were not distributed equally among vegetation classes with most active-layer detachment slides occurring on non-acidic tundra, most thermo-erosion gullies occurring on acidic tundra, and thaw slumps distributed among the tundra types (Table 4.1). Feature types were also unevenly distributed between activity levels with over half of slumps classified as activity-level-1 (very active) compared to approximately 30% of slides and gullies. Over 90% of all features were associated with, or intersected a water body (Table 4.1). Slides and gullies occurred primarily on or next to water tracks or headwater streams and the majority of thaw

slumps were on lakeshores. Slides tended to occur in the highest topographic positions, slumps were distributed across high and low gradient surfaces, and gullies were most common on foot slopes or valley bottoms.

Discharge from thermokarst features varied widely by feature type and individual features in the study, from no flow at some stabilized slumps and slides to 9.4 L sec^{-1} at one slide (Table 4.1). Mean discharge was highest for slides and lowest for slumps. For sites where we estimated the proportion of outflow derived from ground ice, the ice contribution varied from 0-97%. Slumps had the highest average ground ice contribution and slides had the lowest, though these values are not representative of all features, since they are only based on sites with exposed ground ice. Generally sites with high discharge (> 2 L sec^{-1}) were dominated by surface flow, except several large slumps with very active headwall retreat.

4.4.2 Effects of activity and morphology on concentrations

Thermokarst significantly altered concentrations of carbon, nitrogen, and other solutes but the magnitude and duration of these effects differed by feature type (Figs. 4.2, 4.3, and 4.4). For most parameters, effects were largest at the most active features, with differences tapering off as activity decreased. However, DOC in slide outflows as well as DIC, Mg^{2+}, Ca^{+}, and dissolved N_2O in gully outflows were highest in stabilized features. Slumps tended to have the largest effect on solute concentrations. For example, SO_4^{2-} concentration was 30-fold higher than reference in activity-level-1 outflows, compared to 3.3- and 1.5-fold higher for gullies and slides, respectively. Gully reference and outflow chemistry was generally distinct from slides and slumps, with higher dissolved gas concentrations and DOC:DON, but lower concentrations of ions and DIC.

Thaw slumps had the largest effect on dissolved organic matter concentration, increasing DOC and DON by 2.6- and 4.0-fold in activity-level-1 features, compared with 1.6- and 1.4-fold increases in slides, and 2.2- and 1.6-fold increases in gullies of DOC and DON, respectively (Fig. 4.2). Thermokarst had an even larger impact on inorganic nitrogen, increasing mean NH_4^{+} and NO_3^{-} concentrations by 9- to 27-fold in activity-level-1 features (Fig. 4.3). Consequently, thermokarst increased the relative proportion of DIN, which made up less than 10% of total nitrogen in reference waters but constituted 26 to 38% of total nitrogen in activity-level-1 features and 48% of total nitrogen in activity-level-2 gullies (Fig. 4.5). NH_4^{+} was the dominant

form of DIN for all feature types and activity levels except activity-level-3 slides where NO_3^- made up 70% of DIN. Elevated DIN persisted through activity-level-2 for slumps and through stabilization for gullies.

Dissolved CH_4 was 92% and 89% lower than reference for activity-level-1 gullies and slumps, respectively (Fig. 4.2). However, there were no significant differences for dissolved CO_2 and dissolved N_2O was only significantly elevated for stabilized gullies. Across all activity levels and feature types, 93% and 97% of all samples were supersaturated with CO_2 and CH_4, respectively, indicating flux to the atmosphere, whereas 51% of all samples were supersatured with N_2O, indicating net equilibrium.

4.4.3 Ground-ice, vegetation, and landscape age

Permafrost ice was high in dissolved carbon, nitrogen, and solutes and had a depleted $\delta^{18}O$ signature relative to reference waters (Table 4.3). Average concentrations of DIC, NH_4^+, and K^+ were higher in ground ice than feature outflow, indicating uptake or dilution during transport from the feature headwall to outflow. However, all other solutes, notably DOC, NO_3^-, and SO_4^{2-}, were higher in outflows than in ground ice, indicating net production or contribution from soils or more concentrated flowpaths during transit.

Landscape age modulated the effect of upland thermokarst on water chemistry, with much larger differences between impacted and undisturbed concentrations of DOC, NH_4^+, Cl^- and SO_4^{2-} at sites occurring on surfaces older than 50 ka (Fig. 4.5). Vegetation had a smaller effect on fewer parameters with only DOC, Ca^+, and Cl^- differing significantly by vegetation community independent of activity level, feature type, and landscape age, with different patterns between vegetation communities for each solute (Fig. 4.6).

4.5 Discussion

There is conflicting evidence of the impacts of upland thermokarst on concentrations and fluxes of DOC, nutrients, and other solutes (Bowden et al., 2008; Thompson et al., 2012), as well as the intensity and duration of these effects (Kokelj et al., 2005; Lafreniere and Lamoureux, 2013; Thienpont et al., 2013). Our spatially extensive sampling of active and stabilized thermokarst features revealed consistent increases of DOC and other solute concentrations with a particularly large impact on inorganic N. Magnitude and duration of thermokarst effects on water

chemistry differed by feature type and secondarily by landscape age. Most solutes returned to undisturbed concentrations after feature stabilization, but elevated inorganic N and several other parameters persisted in gully and slump outflows, suggesting these feature types could have long-lasting impacts on aquatic nutrient dynamics.

4.5.1 Patterns of carbon and nitrogen release from upland thermokarst

We hypothesized that thermokarst could increase or decrease DOC export depending on the balance of DOC production and removal processes active during feature formation. Despite large organic layer losses and abundant exposed mineral soil (Pizano et al., 2014), upland thermokarst significantly increased average DOC concentration and yield for all feature types. Additionally, DOC from active thermokarst features is three to four times more bio- and photo-degradable than active-layer-derived DOC (Abbott et al., 2014b; Cory et al., 2013) changing the implications of this release for different spatial scales. Thermokarst DOC is likely to be mineralized rapidly in receiving soils, streams, and lakes, accelerating transfer of permafrost carbon to the atmosphere (Vonk et al., 2013) but reducing the impact of this disturbance on estuaries of the Arctic Ocean (McClelland et al., 2012; Striegl et al., 2005).

Upland thermokarst had a relatively larger effect on aquatic nitrogen than carbon concentrations, reducing the C:N ratio of dissolved organic matter and causing substantial and long-lasting release of inorganic N. Phosphorus, not nitrogen, is typically the most limiting nutrient in Arctic freshwater systems (O'Brien et al., 2005; Slavik et al., 2004), however, nitrogen and silica limit productivity in Arctic estuaries and the Arctic Ocean (McClelland et al., 2012; Vancoppenolle et al., 2013). If thermokarst nitrogen release is accompanied by bioavailable phosphorus, more nitrogen will be retained in inland aquatic ecosystems, whereas if thermokarst outflows have relatively little phosphorus, a larger proportion of liberated nitrogen will reach the ocean. Thermokarst can increase phosphorus loading (Bowden et al., 2008; Hobbie et al., 1999), but the relative impact of upland thermokarst on nutrient stoichiometry remains an important unknown.

Along with changes in solute concentrations and characteristics, upland thermokarst may affect the seasonality of solute flux. For most aquatic ecosystems in the Arctic, the majority of annual carbon and nutrient load occurs during snowmelt or early spring (Holmes et al., 2012). However, carbon and nutrient release from upland thermokarst is determined by feature activity,

which depends primarily on air temperature and net radiation, peaking in mid to late summer (Kokelj and Jorgenson, 2013; Lantuit and Pollard, 2005; Lantz and Kokelj, 2008). Late-season delivery of carbon and nitrogen would have a larger relative impact on surface water concentrations, further modifying functioning of Arctic rivers and lakes. This shift could also affect Arctic estuaries, where nutrients and carbon are taken up quickly during open-water season but transported to the Arctic Ocean during ice cover (Townsend-Small et al., 2011).

Feature morphology strongly influenced magnitude and duration of thermokarst effects on water chemistry, with slides having a smaller and shorter impact than gullies or slumps. This could be due to differences in feature depth and duration of feature growth. In permafrost soil, leachable solutes are typically highest below the transition layer at the top of the permafrost table (Keller et al., 2007; Kokelj and Burn, 2003; Malone et al., 2013) and the age and characteristics of soil carbon differ strongly with depth (Guo et al., 2007; Neff et al., 2006; Nowinski et al., 2010; Schuur et al., 2009). Shallow slides are less likely to expose these solutes and carbon to hydrologic export compared to slumps and gullies, which cut meters into permafrost. However, slides had a similar effect as gullies and slumps on inorganic nitrogen concentration, suggesting that altered dynamics at the surface rather than depth of disturbance may determine nitrogen available for export. For all feature types, effects on carbon, nitrogen, and other solutes were largely limited to the period of active feature formation, meaning that the influence of upland thermokarst is directly related to period of active growth. In this regard slides, gullies, and slumps are dramatically different. Slides typically form suddenly, over a period of weeks, days, or even hours (Lewkowicz, 2007) and stabilize the same season they appear (Lafreniere and Lamoureux, 2013). In contrast, large thaw slumps commonly remain active for 12-50 years (Burn, 2000; Kokelj et al., 2013; Lewkowicz, 1987) though small slumps stabilize in less than ten years (Kokelj et al., 2009). Less is known about gully longevity, but based on average feature size and rates of headwall retreat, they remain active for five to ten years (Jorgenson and Osterkamp, 2005), with large features lasting over a decade (Godin and Fortier, 2012). Differences in outflow chemistry between feature types agree with findings from high Arctic systems suggesting that slide formation may have relatively limited impact on water chemistry (Lewis et al., 2012), and suggest that gullies and slumps, with their long active periods and influential position in hydrologic networks (Krieger, 2012), are likely to have a persistent and widespread effect on aquatic ecosystems.

4.5.2 Decrease in dissolved methane

There are several possible mechanisms behind the unexpected 90% decrease of dissolved CH_4 in gully and slump outflows. Greater thaw-depth within features could facilitate infiltration, creating a larger aerated zone where CH_4 oxidation can occur (Schuur et al., 2009). Slides may have had no effect on dissolved CH_4 because they do not affect thaw depth as profoundly as gullies and slumps. However soils affected by slides, gullies, and slumps have partial pressures of CH_4 higher or equal to reference tundra (Chapter 5), suggesting that low CH_4 in thermokarst outflows is due to changes in production or consumption in the water column, rather than in soils. For slumps this decrease may be due to high concentrations of SO_4^{2-} released during thermokarst formation. SO_4^{2-} is an energetically favorable electron acceptor compared to the low molecular weight organic compounds or CO_2 used by methanogens (Dar et al., 2008), and sulfate-reducing bacteria can halt methane production by competitive inhibition (Muyzer and Stams, 2008). SO_4^{2-} was negatively associated with dissolved CH_4 across site types and activity levels, further supporting this hypothesis. However, SO_4^{2-} release does not explain decreased dissolved CH_4 in gully outflows since we observed no change in gully SO_4^{2-}. One possibility is that high inorganic nitrogen concentration is stimulating CH_4 consumption in gully and slump outflows. While elevated DIN can suppress high-affinity methanotrophs responsible for CH_4 oxidation in low-CH_4 environments, DIN can stimulate consumption by low-affinity methanotrophs that dominate consumption in high CH_4 environments and are commonly nitrogen-limited (Bodelier and Laanbroek, 2004). This would explain the large CH_4 decrease in gully outflows where CH_4 concentration was high, and the lack of response in slide outflows where CH_4 is 10-fold lower despite similar DIN loading.

Similar concentration of SO_4^{2-} has been observed in outflows of thaw slumps in the Mackenzie delta (Kokelj et al. 2005, Malone et al., 2013) and there is evidence of enhanced sulfur availability in lakes throughout the Arctic (Drevnick et al., 2010). The widespread release of SO_4^{2-} from upland thermokarst may have important implications for carbon cycling as the permafrost region thaws. Increases in freshwater SO_4^{2-} could accelerate anaerobic decomposition of organic carbon liberated from permafrost (Einsele et al., 2001) and suppress CH_4 production after permafrost thaw, modulating one of the key feedbacks from the permafrost system on global climate (Walter et al., 2006).

4.5.3 Where is thermokarst nitrogen coming from?

Though primary production in high-latitude terrestrial ecosystems tends to be limited by nitrogen, suggesting that bioavailable forms of nitrogen should be retained (Vitousek and Reiners, 1975); there are numerous reports of inorganic nitrogen loss from landscapes affected by permafrost degradation (Jones et al., 2005; Mack et al., 2004; McClelland et al., 2007). Contrary to our hypothesis that high demand for nutrients by re-establishing plants would decrease nutrient concentrations in thermokarst outflows during recovery, NH_4^+ concentration was elevated in stabilized gullies and in no case was DIN significantly lower in recovering features than in undisturbed tundra. This suggests that either nitrogen is not limiting plant growth during revegetation or pathways of nitrogen loss bypass locations of high uptake (e.g. preferential flowpaths below plant rooting zones).

Microenvironments in thermokarst can favor deciduous shrub establishment including nitrogen-fixing species (Lantz et al., 2009). However, even in the absence of nitrogen-fixing species, surface soils in recovering features re-accumulate nitrogen more rapidly than expected (Pizano et al., 2014). Upland thermokarst can warm wintertime soil temperature by 6°C due to conductive heat flux to soils during summer and added insulation in winter from deeper snow (Burn, 2000). If nitrogen mineralization continues through the fall and winter in thawed soils underneath thermokarst scars, hydrologic activity in the spring or deep shrub roots could transport inorganic nitrogen to the surface, fueling productivity and hydrologic export. The isotopic signature of NO_3^- draining a high Arctic catchment impacted by upland thermokarst suggests DIN from thermokarst is derived from the heterotrophic decomposition of organic matter found in the mineral soil (Louiseize et al., 2014), supporting this hypothesis. Additionally or alternatively, a portion of inorganic nitrogen in upland thermokarst outflow may come from mineralization of labile dissolved organic matter in the water column. This would explain the strong correlation between DIN concentration and DOC biodegradability observed in several Arctic and boreal ecosystems (Abbott et al., 2014b; Balcarczyk et al., 2009; Wickland et al., 2012).

4.5.4 Shifts in landscape-scale water chemistry

As high latitudes warm, ecosystems are experiencing widespread shifts in aquatic chemistry including an increase in DOC flux in areas with peat and thick organic soil (Frey and

McClelland, 2009), a decrease in DOC where organic soil is shallow (McClelland et al., 2007; Petrone et al., 2006; Striegl et al., 2005), increases in major ion concentrations (Frey and McClelland, 2009; Giesler et al., 2014; Keller et al., 2010), and increased inorganic nutrient flux (Jones et al., 2005; McClelland et al., 2007; Petrone et al., 2006). These changes in catchment-scale solute fluxes have primarily been attributed to mechanisms associated with gradual thaw such as deepening of surface flowpaths and changes in residence time. However, thermokarst may also be contributing to these shifts in catchment-scale chemistry (Frey and McClelland, 2009). The chemical signature of dissolved organic matter from thermokarst closely matches biodegradable DOC recently detected in boreal rivers (Abbott et al., 2014b; Wickland et al., 2012) and increases of DIN and solutes from thermokarst match circumpolar changes attributed to a shift towards greater ground-water inputs.

Currently a scarcity of observations of the spatial extent and distribution of upland thermokarst features and the annual elemental yields for different feature and landscape types limits our ability to evaluate the relative importance of gradual thaw and thermokarst in determining the evolution of high-latitude biogeochemistry.

4.6 Conclusions

Upland thermokarst across the foothills of the Brooks Range caused substantial increases of inorganic nitrogen, DOC, and other solute concentrations. Thaw slumps and thermo-erosion gullies had larger impacts on solute concentrations and because they can remain active for multiple years, are likely more important than slides to surface water chemistry. The delivery of labile carbon and nutrients such as SO_4^{2-} and inorganic nitrogen to downstream or downslope ecosystems could have important consequences for offsite carbon cycling, accelerating decomposition of organic matter in anoxic environments and priming the decomposition of recalcitrant organic matter. The fact that individual features can impact entire lakes or river reaches over multiple years in combination with the large portion of the landscape underlain by ice-rich permafrost suggest that upland thermokarst may be a dominant linkage between terrestrial and aquatic ecosystems as the Arctic warms.

4.7 Citations

Abbott, B. W., Jones, J. B., Schuur, E. A. G., Chapin III, F. S., Bowden, W. B., Bret-Harte, M. S., Epstein, H. E., Flannigan, M. D., Harms, T. K., Hollingsworth, T. N., Mack, M. C.,

McGuire, A. D., Natali, S. M., Rocha, A. V., Tank, S. E., Turetsky, M. R., Vonk, J. E., Wickland, K. P., and Permafrost Carbon, N.: Can increased biomass offset carbon release from soils, streams, and wildfire across the permafrost region? An expert elicitation., Nature Climate Change, Submitted, 2014a.

Abbott, B. W., Larouche, J. R., Jones, J. B., Bowden, W. B., and Balser, A. W.: Elevated dissolved organic carbon biodegradability from thawing and collapsing permafrost, Journal of Geophysical Research: Biogeosciences, doi: 10.1002/2014JG002678, 2014b. 2014JG002678, 2014b.

Amon, R. M. W., Rinehart, A. J., Duan, S., Louchouarn, P., Prokushkin, A., Guggenberger, G., Bauch, D., Stedmon, C., Raymond, P. A., Holmes, R. M., McClelland, J. W., Peterson, B. J., Walker, S. A., and Zhulidov, A. V.: Dissolved organic matter sources in large Arctic rivers, Geochimica Et Cosmochimica Acta, 94, 217-237, 2012.

Balcarczyk, K. L., Jones, J. B., Jaffe, R., and Maie, N.: Stream dissolved organic matter bioavailability and composition in watersheds underlain with discontinuous permafrost, Biogeochemistry, 94, 255-270, 2009.

Bates, D., Maechler, M., Bolker, B., and Walker, S.: lme4: Linear mixed-effects models using Eigen and S4. R package version 1.0-5. http://CRAN.R-project.org/package=lme4, 2013. 2013.

Bhatt, U. S., Walker, D. A., Raynolds, M. K., Comiso, J. C., Epstein, H. E., Jia, G. S., Gens, R., Pinzon, J. E., Tucker, C. J., Tweedie, C. E., and Webber, P. J.: Circumpolar Arctic Tundra Vegetation Change Is Linked to Sea Ice Decline, Earth Interactions, 14, 2010.

Bodelier, P. L. E. and Laanbroek, H. J.: Nitrogen as a regulatory factor of methane oxidation in soils and sediments, Fems Microbiology Ecology, 47, 265-277, 2004.

Bowden, W. B., Gooseff, M. N., Balser, A., Green, A., Peterson, B. J., and Bradford, J.: Sediment and nutrient delivery from thermokarst features in the foothills of the North Slope, Alaska: Potential impacts on headwater stream ecosystems, J Geophys Res-Biogeo, 113, 2008.

Burn, C. R.: The thermal regime of a retrogressive thaw slump near Mayo, Yukon Territory, Canadian Journal of Earth Sciences, 37, 967-981, 2000.

Cory, R. M., Crump, B. C., Dobkowski, J. A., and Kling, G. W.: Surface exposure to sunlight stimulates CO2 release from permafrost soil carbon in the Arctic, P Natl Acad Sci USA, 110, 3429-3434, 2013.

Dar, S. A., Kleerebezem, R., Stams, A. J. M., Kuenen, J. G., and Muyzer, G.: Competition and coexistence of sulfate-reducing bacteria, acetogens and methanogens in a lab-scale anaerobic bioreactor as affected by changing substrate to sulfate ratio, Appl Microbiol Biot, 78, 1045-1055, 2008.

Drevnick, P. E., Muir, D. C. G., Lamborg, C. H., Horgan, M. J., Canfield, D. E., Boyle, J. F., and Rose, N. L.: Increased Accumulation of Sulfur in Lake Sediments of the High Arctic, Environmental Science & Technology, 44, 8415-8421, 2010.

Einsele, G., Yan, J. P., and Hinderer, M.: Atmospheric carbon burial in modern lake basins and its significance for the global carbon budget, Global Planet Change, 30, 167-195, 2001.

Epstein, H. E., Beringer, J., Gould, W. A., Lloyd, A. H., Thompson, C. D., Chapin, F. S., Michaelson, G. J., Ping, C. L., Rupp, T. S., and Walker, D. A.: The nature of spatial transitions in the Arctic, Journal of Biogeography, 31, 1917-1933, 2004.

Frey, K. E. and McClelland, J. W.: Impacts of permafrost degradation on arctic river biogeochemistry, Hydrol Process, 23, 169-182, 2009.

Giesler, R., Lyon, S. W., Morth, C. M., Karlsson, J., Karlsson, E. M., Jantze, E. J., Destouni, G., and Humborg, C.: Catchment-scale dissolved carbon concentrations and export estimates across six subarctic streams in northern Sweden, Biogeosciences, 11, 525-537, 2014.

Godin, E. and Fortier, D.: Geomorphology of a thermo-erosion gully, Bylot Island, Nunavut, Canada, Canadian Journal of Earth Sciences, 49, 979-986, 2012.

Gooseff, M. N., Balser, A., Bowden, W. B., and Jones, J. B.: Effects of Hillslope Thermokarst in Northern Alaska, Eos, Transactions American Geophysical Union, 90, 29-30, 2009.

Guo, L. D., Ping, C. L., and Macdonald, R. W.: Mobilization pathways of organic carbon from permafrost to arctic rivers in a changing climate, Geophysical Research Letters, 34, 2007.

Hamilton, T. D.: Surficial geologic map of the Noatak National Preserve, Alaska: U.S. Geological Survey Scientific Investigations Map 3036, 2010.

Hamilton, T. D.: Surficial geology of the Dalton Highway (Itkillik-Sagavanirktok rivers) area, souther Arctic foothills, Alaska Division of Geological & Geophysical Surveys, Alaska, 2003.

Harms, T., Abbott, B., and Jones, J.: Thermo-erosion gullies increase nitrogen available for hydrologic export, Biogeochemistry, doi: 10.1007/s10533-013-9862-0, 2013. 1-13, 2013.

Hobbie, J. E., Peterson, B. J., Bettez, N., Deegan, L., O'Brien, W. J., Kling, G. W., Kipphut, G. W., Bowden, W. B., and Hershey, A. E.: Impact of global change on the biogeochemistry and ecology of an Arctic freshwater system, Polar Research, 18, 207-214, 1999.

Hobbie, S. E., Miley, T. A., and Weiss, M. S.: Carbon and nitrogen cycling in soils from acidic and nonacidic tundra with different glacial histories in Northern Alaska, Ecosystems, 5, 761-774, 2002.

Holmes, R. M., McClelland, J. W., Peterson, B. J., Tank, S. E., Bulygina, E., Eglinton, T. I., Gordeev, V. V., Gurtovaya, T. Y., Raymond, P. A., Repeta, D. J., Staples, R., Striegl, R. G., Zhulidov, A. V., and Zimov, S. A.: Seasonal and Annual Fluxes of Nutrients and Organic Matter from Large Rivers to the Arctic Ocean and Surrounding Seas, Estuaries and Coasts, 35, 369-382, 2012.

Jones, J. B., Petrone, K. C., Finlay, J. C., Hinzman, L. D., and Bolton, W. R.: Nitrogen loss from watersheds of interior Alaska underlain with discontinuous permafrost, Geophysical Research Letters, 32, 2005.

Jorgenson, M. T. and Osterkamp, T. E.: Response of boreal ecosystems to varying modes of permafrost degradation, Canadian Journal of Forest Research-Revue Canadienne De Recherche Forestiere, 35, 2100-2111, 2005.

Jorgenson, M. T., Shur, Y. L., and Osterkamp, T. E.: Thermokarst in Alaska, Ninth International Conference On Permafrost, University of Alaska Fairbanks, 117-124, 2008.

Jorgenson, M. T., Shur, Y. L., and Pullman, E. R.: Abrupt increase in permafrost degradation in Arctic Alaska, Geophysical Research Letters, 33, 2006.

Kanevskiy, M., Shur, Y., Fortier, D., Jorgenson, M. T., and Stephani, E.: Cryostratigraphy of late Pleistocene syngenetic permafrost (yedoma) in northern Alaska, Itkillik River exposure, Quaternary Res, 75, 584-596, 2011.

Keller, K., Blum, J. D., and Kling, G. W.: Geochemistry of Soils and Streams on Surfaces of Varying Ages in Arctic Alaska, Arctic, Antarctic, and Alpine Research, 39, 84-98, 2007.

Keller, K., Blum, J. D., and Kling, G. W.: Stream geochemistry as an indicator of increasing permafrost thaw depth in an arctic watershed, Chemical Geology, 273, 76-81, 2010.

Kling, G. W., Kipphut, G. W., and Miller, M. C.: The flux of CO_2 and CH_4 from lakes and rivers in Arctic Alaska, Hydrobiologia, 240, 23-36, 1992.

Koch, J. C., Ewing, S. A., Striegl, R., and McKnight, D. M.: Rapid runoff via shallow throughflow and deeper preferential flow in a boreal catchment underlain by frozen silt (Alaska, USA), Hydrogeol J, 21, 93-106, 2013a.

Koch, J. C., Runkel, R. L., Striegl, R., and McKnight, D. M.: Hydrologic controls on the transport and cycling of carbon and nitrogen in a boreal catchment underlain by continuous permafrost, J Geophys Res-Biogeo, 118, 698-712, 2013b.

Kokelj, S. V. and Burn, C. R.: Ground ice and soluble cations in near−surface permafrost, Inuvik, Northwest Territories, Canada, Permafrost and Periglacial Processes, 14, 275-289, 2005.

Kokelj, S. V., Jenkins, R. E., Milburn, D., Burn, C. R., and Snow, N.: The influence of thermokarst disturbance on the water quality of small upland lakes, Mackenzie Delta Region, Northwest Territories, Canada, Permafrost and Periglacial Processes, 16, 343-353, 2005.

Kokelj, S. V. and Jorgenson, M. T.: Advances in Thermokarst Research, Permafrost and Periglacial Processes, 24, 108-119, 2013.

Kokelj, S. V., Lacelle, D., Lantz, T. C., Tunnicliffe, J., Malone, L., Clark, I. D., and Chin, K. S.: Thawing of massive ground ice in mega slumps drives increases in stream sediment and solute flux across a range of watershed scales, Journal of Geophysical Research: Earth Surface, 118, 681-692, 2013.

Kokelj, S. V., Lantz, T. C., Kanigan, J., Smith, S. L., and Coutts, R.: Origin and Polycyclic Behaviour of Tundra Thaw Slumps, Mackenzie Delta Region, Northwest Territories, Canada, Permafrost and Periglacial Processes, 20, 173-184, 2009.

Krieger, K. C.: The Topographic Form and Evolution of Thermal Erosion Features: A First Analysis Using Airborne and Ground-Based LiDAR in Arctic Alaska, Master of Science, Geosciences, Idaho State University, 98 pp., 2012.

Kuznetsova, A., Brockhoff, P. B., and Christensen, R. H. B.: lmerTest: Tests for random and fixed effects for linear mixed effect models (lmer objects of lme4 package). R package version 2.0-6. http://CRAN.R-project.org/package=lmerTest, 2014. 2014.

Lafreniere, M. J. and Lamoureux, S. F.: Thermal Perturbation and Rainfall Runoff have Greater Impact on Seasonal Solute Loads than Physical Disturbance of the Active Layer, Permafrost and Periglacial Processes, 24, 241-251, 2013.

Lantuit, H. and Pollard, W. H.: Temporal stereophotogrammetric analysis of retrogressive thaw slumps on Herschel Island, Yukon territory, Natural Hazards and Earth System Sciences, 5, 413-423, 2005.

Lantz, T. C. and Kokelj, S. V.: Increasing rates of retrogressive thaw slump activity in the Mackenzie Delta region, NWT, Canada, Geophysical Research Letters, 35, 2008.

Lantz, T. C., Kokelj, S. V., Gergel, S. E., and Henryz, G. H. R.: Relative impacts of disturbance and temperature: persistent changes in microenvironment and vegetation in retrogressive thaw slumps, Glob. Change Biol., 15, 1664-1675, 2009.

Larouche, J. R.: Environmental influences on the genetic diversity of bacterial communities in arctic streams, 2009. Natural resources, University of Vermont, 119 pp., 2009.

Laudon, H., Buttle, J., Carey, S. K., McDonnell, J., McGuire, K., Seibert, J., Shanley, J., Soulsby, C., and Tetzlaff, D.: Cross-regional prediction of long-term trajectory of stream water DOC response to climate change, Geophysical Research Letters, 39, L18404, 2012.

Lee, H., Schuur, E. G., Vogel, J. G., Lavoie, M., Bhadra, D., and Staudhammer, C. L.: A spatially explicit analysis to extrapolate carbon fluxes in upland tundra where permafrost is thawing, Glob. Change Biol., 17, 1379-1393, 2011.

Lewis, T., Lafreniere, M. J., and Lamoureux, S. F.: Hydrochemical and sedimentary responses of paired High Arctic watersheds to unusual climate and permafrost disturbance, Cape Bounty, Melville Island, Canada, Hydrol Process, 26, 2003-2018, 2012.

Lewkowicz, A. G.: Dynamics of active-layer detachment failures, Fosheim Peninsula, Ellesmere Island, Nunavut, Canada, Permafrost and Periglacial Processes, 18, 89-103, 2007.

Lewkowicz, A. G.: Nature and importance of thermokarst processes, Sand Hills Moraine, Banks Island, Canada Geogr Ann A, 69, 321-327, 1987.

Louiseize, N., Lafrenière, M., and Hastings, M.: Stable isotopic evidence of enhanced export of microbially derived NO_3^- following active layer slope disturbance in the Canadian High Arctic, Biogeochemistry, doi: 10.1007/s10533-014-0023-x, 2014. 1-16, 2014.

Mack, M. C., Schuur, E. A. G., Bret-Harte, M. S., Shaver, G. R., and Chapin, F. S.: Ecosystem carbon storage in arctic tundra reduced by long-term nutrient fertilization, Nature, 431, 440-443, 2004.

Malone, L., Lacelle, D., Kokelj, S., and Clark, I. D.: Impacts of hillslope thaw slumps on the geochemistry of permafrost catchments (Stony Creek watershed, NWT, Canada), Chemical Geology, 356, 38-49, 2013.

McClelland, J. W., Holmes, R. M., Dunton, K. H., and Macdonald, R. W.: The Arctic Ocean Estuary, Estuaries and Coasts, 35, 353-368, 2012.

McClelland, J. W., Holmes, R. M., Peterson, B. J., Amon, R., Brabets, T., Cooper, L., Gibson, J., Gordeev, V. V., Guay, C., Milburn, D., Staples, R., Raymond, P. A., Shiklomanov, I., Striegl, R., Zhulidov, A., Gurtovaya, T., and Zimov, S.: Development of a Pan-Arctic Database for River Chemistry, Eos, Transactions American Geophysical Union, 89, 217-218, 2008.

McClelland, J. W., Stieglitz, M., Pan, F., Holmes, R. M., and Peterson, B. J.: Recent changes in nitrate and dissolved organic carbon export from the upper Kuparuk River, North Slope, Alaska, J Geophys Res-Biogeo, 112, 2007.

McClelland, J. W., Townsend-Small, A., Holmes, R. M., Pan, F., Stieglitz, M., Khosh, M., and Peterson, B. J.: River export of nutrients and organic matter from the North Slope of Alaska to the Beaufort Sea, Water Resour Res, 50, 1823-1839, 2014.

Mesquita, P. S., Wrona, F. J., and Prowse, T. D.: Effects of retrogressive permafrost thaw slumping on sediment chemistry and submerged macrophytes in Arctic tundra lakes, Freshwater Biology, 55, 2347-2358, 2010.

Muyzer, G. and Stams, A. J. M.: The ecology and biotechnology of sulphate-reducing bacteria, Nature Reviews Microbiology, 6, 441-454, 2008.

Neff, J. C., Finlay, J. C., Zimov, S. A., Davydov, S. P., Carrasco, J. J., Schuur, E. A. G., and Davydova, A. I.: Seasonal changes in the age and structure of dissolved organic carbon in Siberian rivers and streams, Geophysical Research Letters, 33, 2006.

Nowinski, N. S., Taneva, L., Trumbore, S. E., and Welker, J. M.: Decomposition of old organic matter as a result of deeper active layers in a snow depth manipulation experiment, Oecologia, 163, 785-792, 2010.

O'Brien, W. J., Barfield, M., Bettez, N., Hershey, A. E., Hobbie, J. E., Kipphut, G., Kling, G., and Miller, M. C.: Long-term response and recovery to nutrient addition of a partitioned arctic lake, Freshwater Biology, 50, 731-741, 2005.

O'Donnell, J. A., Jorgenson, M. T., Harden, J. W., McGuire, A. D., Kanevskiy, M. Z., and Wickland, K. P.: The Effects of Permafrost Thaw on Soil Hydrologic, Thermal, and Carbon Dynamics in an Alaskan Peatland, Ecosystems, 15, 213-229, 2012.

Osterkamp, T. E., Jorgenson, M. T., Schuur, E. A. G., Shur, Y. L., Kanevskiy, M. Z., Vogel, J. G., and Tumskoy, V. E.: Physical and Ecological Changes Associated with Warming Permafrost and Thermokarst in Interior Alaska, Permafrost and Periglacial Processes, 20, 235-256, 2009.

Peterson, B. J., Deegan, L., Helfrich, J., Hobbie, J. E., Hullar, M., Moller, B., Ford, T. E., Hershey, A., Hiltner, A., Kipphut, G., Lock, M. A., Fiebig, D. M., McKinley, V., Miller, M. C., Vestal, J. R., Ventullo, R., and Volk, G.: Biological Responses of a Tundra River to Fertilization, Ecology, 74, 653-672, 1993.

Petrone, K. C., Jones, J. B., Hinzman, L. D., and Boone, R. D.: Seasonal export of carbon, nitrogen, and major solutes from Alaskan catchments with discontinuous permafrost, J Geophys Res-Biogeo, 111, 2006.

Pizano, C., Barón, A. F., Schuur, E. A. G., Crummer, K. G., and Mack, M. C.: Effects of thermo-erosional disturbance on surface soil carbon and nitrogen dynamics in upland arctic tundra, Environmental Research Letters, 9, 075006, 2014.

R Core Team: R: A language and environment for statistical computing. R Foundation for Statistical Computing, Vienna, Austria. URL http://www.R-project.org/. 2013.

Rawlins, M. A., Steele, M., Holland, M. M., Adam, J. C., Cherry, J. E., Francis, J. A., Groisman, P. Y., Hinzman, L. D., Huntington, T. G., Kane, D. L., Kimball, J. S., Kwok, R., Lammers, R. B., Lee, C. M., Lettenmaier, D. P., McDonald, K. C., Podest, E., Pundsack, J. W., Rudels, B., Serreze, M. C., Shiklomanov, A., Skagseth, Ø., Troy, T. J., Vörösmarty, C. J., Wensnahan, M., Wood, E. F., Woodgate, R., Yang, D., Zhang, K., and Zhang, T.: Analysis of the Arctic System for Freshwater Cycle Intensification: Observations and Expectations, Journal of Climate, 23, 5715-5737, 2010.

Schuur, E. A. G., Bockheim, J., Canadell, J. G., Euskirchen, E., Field, C. B., Goryachkin, S. V., Hagemann, S., Kuhry, P., Lafleur, P. M., Lee, H., Mazhitova, G., Nelson, F. E., Rinke,

A., Romanovsky, V. E., Shiklomanov, N., Tarnocai, C., Venevsky, S., Vogel, J. G., and Zimov, S. A.: Vulnerability of permafrost carbon to climate change: Implications for the global carbon cycle, Bioscience, 58, 701-714, 2008.

Schuur, E. A. G., Vogel, J. G., Crummer, K. G., Lee, H., Sickman, J. O., and Osterkamp, T. E.: The effect of permafrost thaw on old carbon release and net carbon exchange from tundra, Nature, 459, 556-559, 2009.

Shirokova, L. S., Pokrovsky, O. S., Kirpotin, S. N., Desmukh, C., Pokrovsky, B. G., Audry, S., and Viers, J.: Biogeochemistry of organic carbon, CO2, CH4, and trace elements in thermokarst water bodies in discontinuous permafrost zones of Western Siberia, Biogeochemistry, 113, 573-593, 2013.

Slater, A. G. and Lawrence, D. M.: Diagnosing Present and Future Permafrost from Climate Models, Journal of Climate, 26, 5608-5623, 2013.

Slavik, K., Peterson, B. J., Deegan, L. A., Bowden, W. B., Hershey, A. E., and Hobbie, J. E.: Long-term responses of the Kuparuk River ecosystem to phosphorus fertilization, Ecology, 85, 939-954, 2004.

Stottlemyer, R.: Biogeochemistry of a Treeline Watershed, Northwestern Alaska, J. Environ. Qual., 30, 1990-1998, 2001.

Striegl, R. G., Aiken, G. R., Dornblaser, M. M., Raymond, P. A., and Wickland, K. P.: A decrease in discharge-normalized DOC export by the Yukon River during summer through autumn, Geophysical Research Letters, 32, 2005.

Striegl, R. G., Dornblaser, M. M., McDonald, C. P., Rover, J. R., and Stets, E. G.: Carbon dioxide and methane emissions from the Yukon River system, Global Biogeochemical Cycles, 26, GB0E05, 2012.

Sullivan, P. F. and Sveinbjornsson, B.: Microtopographic Control of Treeline Advance in Noatak National Preserve, Northwest Alaska, Ecosystems, 13, 275-285, 2010.

Tank, S. E., Frey, K. E., Striegl, R. G., Raymond, P. A., Holmes, R. M., McClelland, J. W., and Peterson, B. J.: Landscape-level controls on dissolved carbon flux from diverse catchments of the circumboreal, Global Biogeochemical Cycles, 26, 2012.

Tarnocai, C., Canadell, J. G., Schuur, E. A. G., Kuhry, P., Mazhitova, G., and Zimov, S.: Soil organic carbon pools in the northern circumpolar permafrost region, Global Biogeochemical Cycles, 23, -, 2009.

Thienpont, J. R., Ruehland, K. M., Pisaric, M. F. J., Kokelj, S. V., Kimpe, L. E., Blais, J. M., and Smol, J. P.: Biological responses to permafrost thaw slumping in Canadian Arctic lakes, Freshwater Biology, 58, 337-353, 2013.

Thompson, M. S., Wrona, F. J., and Prowse, T. D.: Shifts in Plankton, Nutrient and Light Relationships in Small Tundra Lakes Caused by Localized Permafrost Thaw, Arctic, 65, 367-376, 2012.

Toolik Environmental Data Center Team: Meterological monitoring program at Toolik, Alaska. Toolik Field Station, Institute of Arctic Biology, University of Alaska Fairbanks, Fairbanks AK 99775, 2014.

Townsend-Small, A., McClelland, J. W., Holmes, R. M., and Peterson, B. J.: Seasonal and hydrologic drivers of dissolved organic matter and nutrients in the upper Kuparuk River, Alaskan Arctic, Biogeochemistry, 103, 109-124, 2011.

Vancoppenolle, M., Bopp, L., Madec, G., Dunne, J., Ilyina, T., Halloran, P. R., and Steiner, N.: Future Arctic Ocean primary productivity from CMIP5 simulations: Uncertain outcome, but consistent mechanisms, Global Biogeochemical Cycles, 27, 605-619, 2013.

Vitousek, P. M. and Reiners, W. A.: Ecosystem succession and nutrient retention: a hypothesis, Bioscience, 25, 376-381, 1975.

Vonk, J. E. and Gustafsson, O.: Permafrost-carbon complexities, Nature Geoscience, 6, 675-676, 2013.

Vonk, J. E., Mann, P. J., Davydov, S., Davydova, A., Spencer, R. G. M., Schade, J., Sobczak, W. V., Zimov, N., Zimov, S., Bulygina, E., Eglinton, T. I., and Holmes, R. M.: High biolability of ancient permafrost carbon upon thaw, Geophysical Research Letters, doi: 10.1002/grl.50348, 2013. 40, 2013.

Vonk, J. E., Sanchez-Garcia, L., van Dongen, B. E., Alling, V., Kosmach, D., Charkin, A., Semiletov, I. P., Dudarev, O. V., Shakhova, N., Roos, P., Eglinton, T. I., Andersson, A., and Gustafsson, O.: Activation of old carbon by erosion of coastal and subsea permafrost in Arctic Siberia, Nature, 489, 137-140, 2012.

Walker, D. A., Auerbach, N. A., Bockheim, J. G., Chapin, F. S., Eugster, W., King, J. Y., McFadden, J. P., Michaelson, G. J., Nelson, F. E., Oechel, W. C., Ping, C. L., Reeburg, W. S., Regli, S., Shiklomanov, N. I., and Vourlitis, G. L.: Energy and trace-gas fluxes across a soil pH boundary in the arctic, Nature, 394, 469-472, 1998.

Walker, D. A., Raynolds, M. K., Daniels, F. J. A., Einarsson, E., Elvebakk, A., Gould, W. A., Katenin, A. E., Kholod, S. S., Markon, C. J., Melnikov, E. S., Moskalenko, N. G., Talbot, S. S., Yurtsev, B. A., and Team, C.: The Circumpolar Arctic vegetation map, Journal of Vegetation Science, 16, 267-282, 2005.

Walker, D. A., Raynolds, M. K., Maier, H. A., Barbour, E. M., and Neufeld, G. P.: Circumpolar geobotanical mapping: a web-based plant-to-planet approach for vegetation-change analysis in the Arctic, Viten, 1, 125-128, 2010.

Walter, K. M., Zimov, S. A., Chanton, J. P., Verbyla, D., and Chapin, F. S.: Methane bubbling from Siberian thaw lakes as a positive feedback to climate warming, Nature, 443, 71-75, 2006.

Wickland, K. P., Aiken, G. R., Butler, K., Dornblaser, M. M., Spencer, R. G. M., and Striegl, R. G.: Biodegradability of dissolved organic carbon in the Yukon River and its tributaries: Seasonality and importance of inorganic nitrogen, Global Biogeochemical Cycles, 26, 2012.

Wilhelm, E., Battino, R., and Wilcock, R. J.: Low-pressure solubility of gases in liquid water, Chemical Reviews, 77, 219-262, 1977.

Wlostowski, A. N., Gooseff, M. N., and Wagener, T.: Influence of constant rate versus slug injection experiment type on parameter identifiability in a 1-D transient storage model for stream solute transport, Water Resour Res, 49, 1184-1188, 2013.

WRCC: http://www.wrcc.dri.edu/index.html, 2011.

Yoshikawa, K., Bolton, W. R., Romanovsky, V. E., Fukuda, M., and Hinzman, L. D.: Impacts of wildfire on the permafrost in the boreal forests of Interior Alaska, J Geophys Res-Atmos, 108, 2002.

Zhang, T., Heginbottom, J. A., Barry, R. G., and Brown, J.: Further statistics on the distribution of permafrost and ground ice in the Northern Hemisphere, Polar Geography, 24, 126-131, 2000.

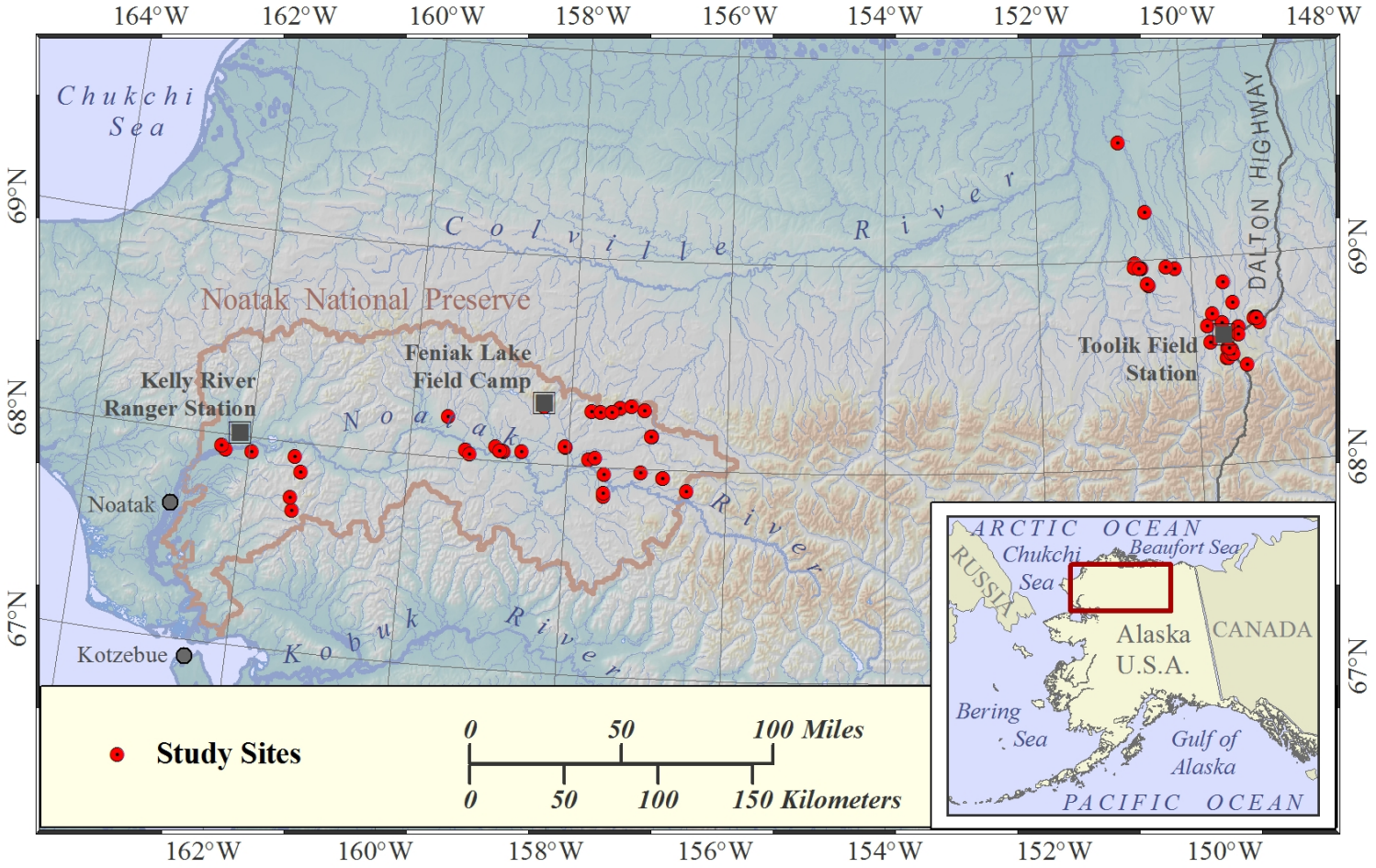

Figure 4.1 Map of study area. Features near the Kelly River Ranger Station were sampled in July of 2010, near Feniak Lake field camp in July of 2011, and near the Toolik Field Station in the summers of 2009-2012.

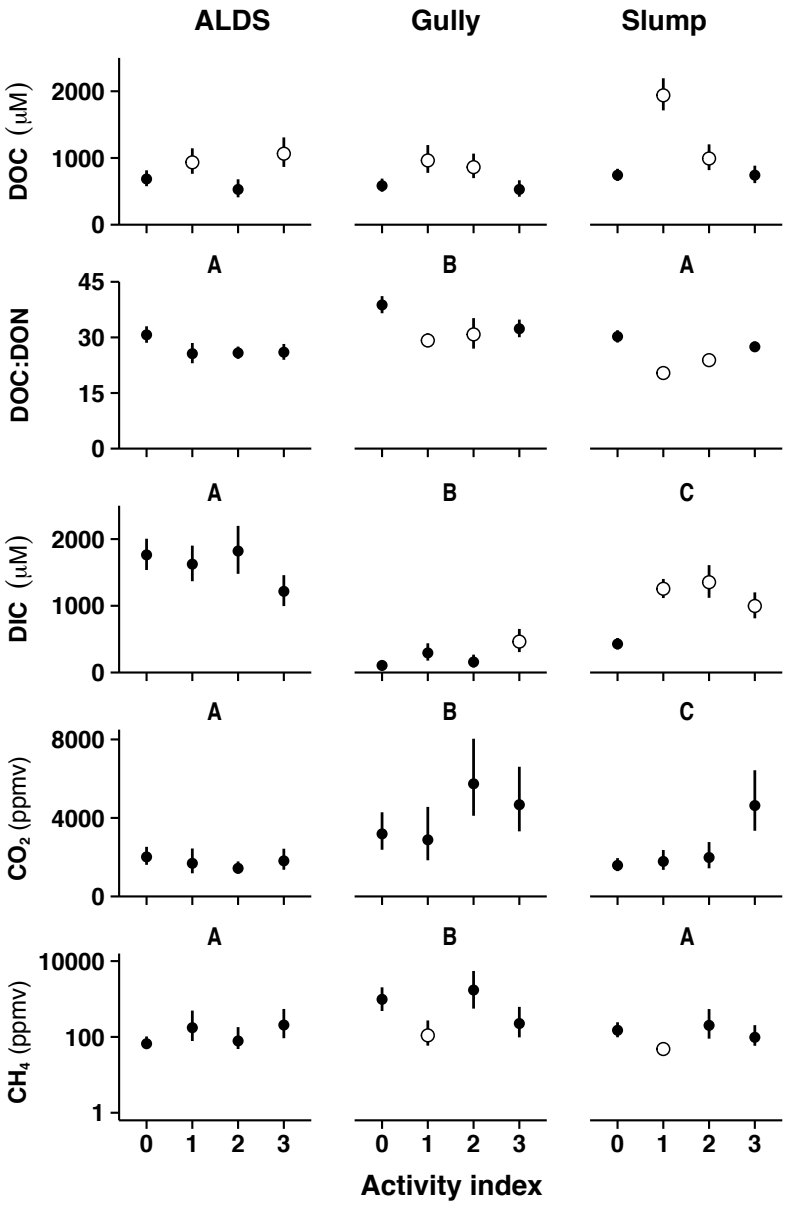

Figure 4.2 Dissolved carbon species and characteristics in outflow from 22 active-layer detachment slides, 19 thermo-erosion gullies, 42 thaw slumps, and 61 reference features in upland tundra on the North Slope of Alaska. Open circles signify statistical difference from activity-level-0 undisturbed sites, $\alpha = 0.05$. Different letters above panels represent significant differences between feature types. Error bars represent SE estimated by mixed-effects ANOVA after accounting for between-site variability. See Table 4.1 for complete definition of activity index but 0=reference, 1=most active, and 3=stabilized. Note the log scale for CH_4.

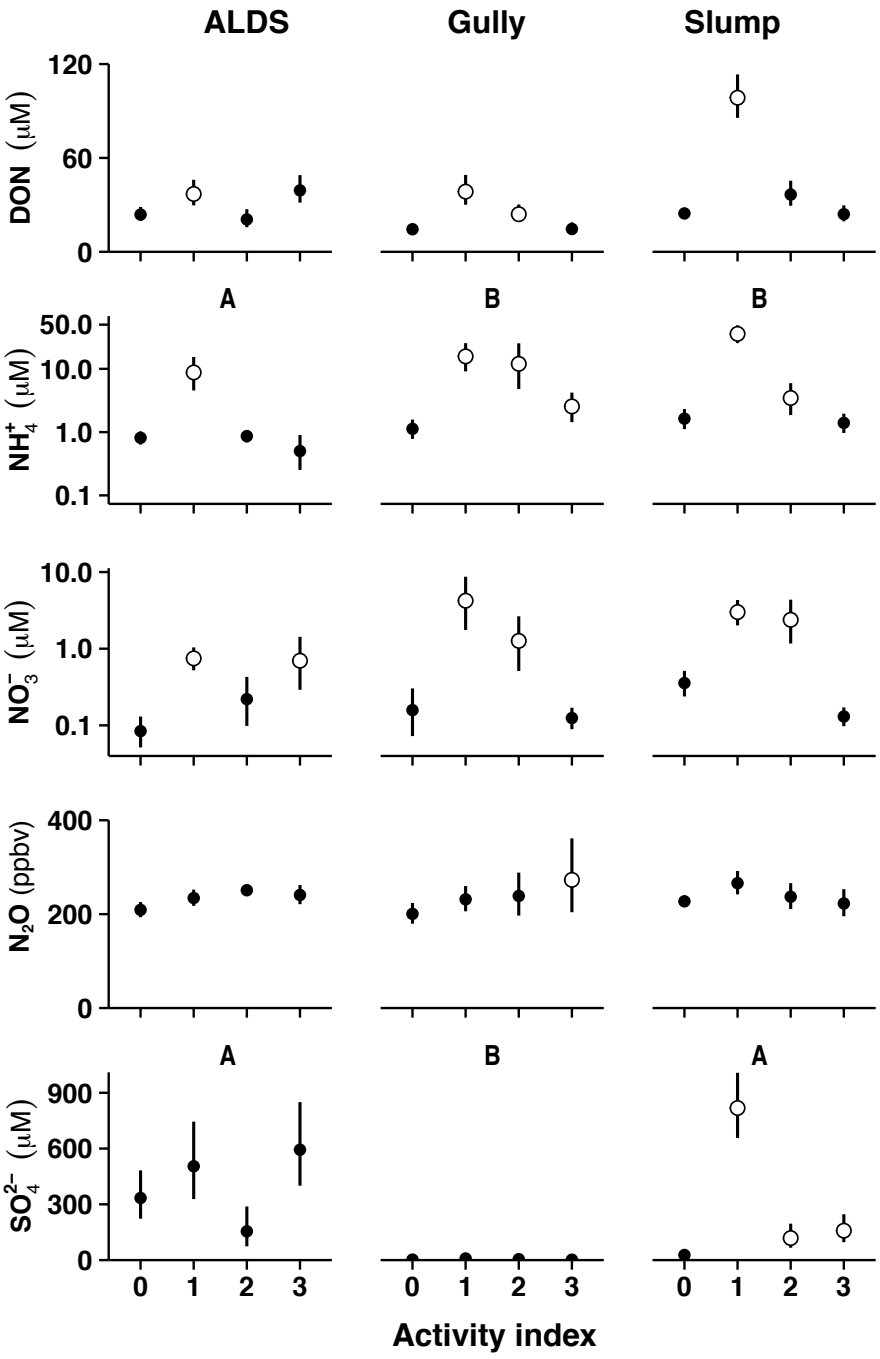

Figure 4.3 Dissolved nitrogen species and sulfate concentrations in outflow from 22 active-layer detachment slides, 19 thermo-erosion gullies, 42 thaw slumps, and 61 reference features. See Table 4.1 for complete definition of activity index but 0=reference, 1=most active, and 3=stabilized. Note log scales for NO_3^- and NH_4^+. Symbology the same as Fig. 4.2.

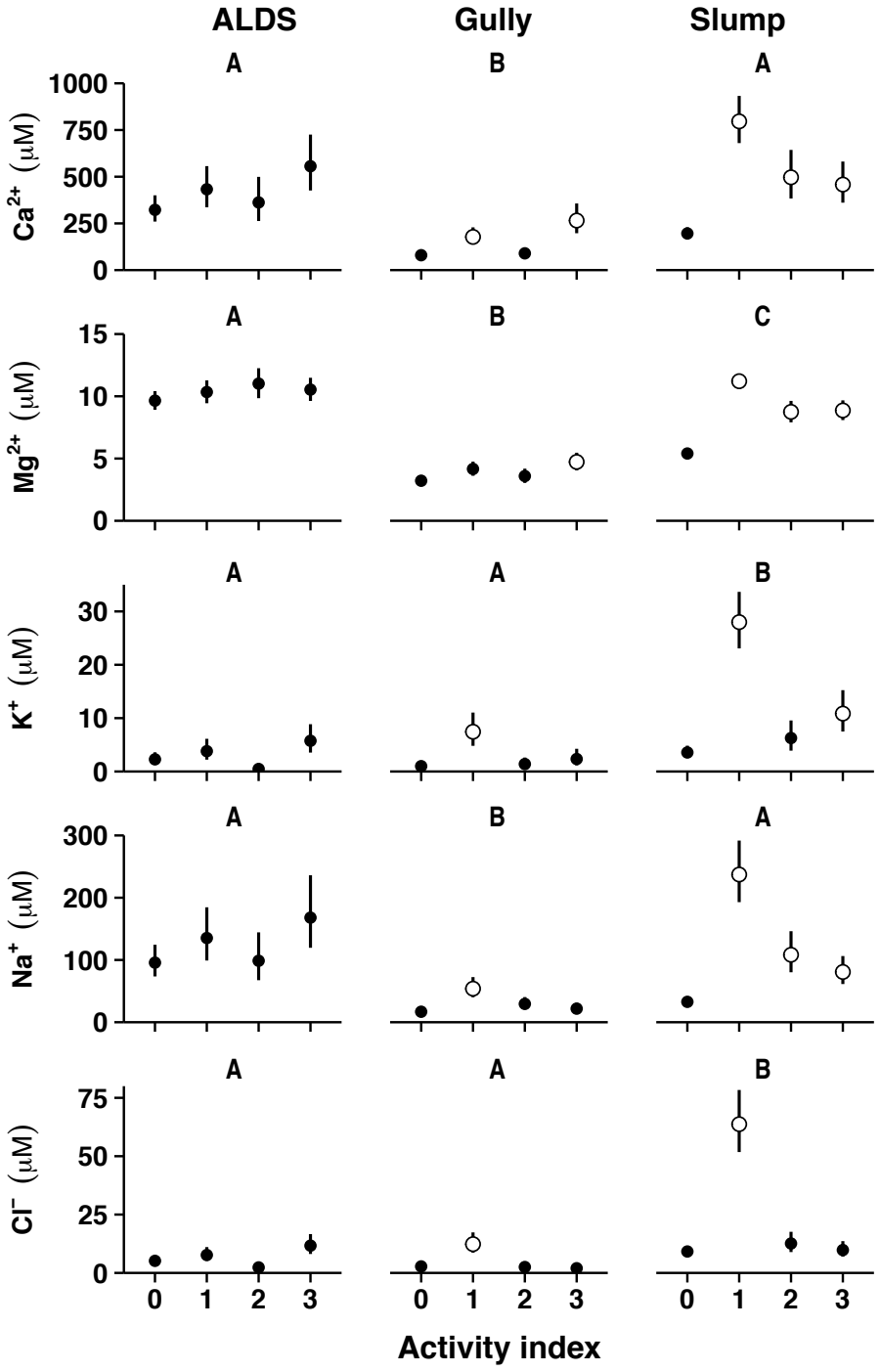

Figure 4.4 Major ion concentrations in outflow from 22 active-layer detachment slides, 19 thermo-erosion gullies, 42 thaw slumps, and 61 reference features. See Table 4.1 for complete definition of activity index but 0=reference, 1=most active, and 3=stabilized. Note log scales for NO_3^- and NH_4^+. Symbology the same as Fig. 4.2.

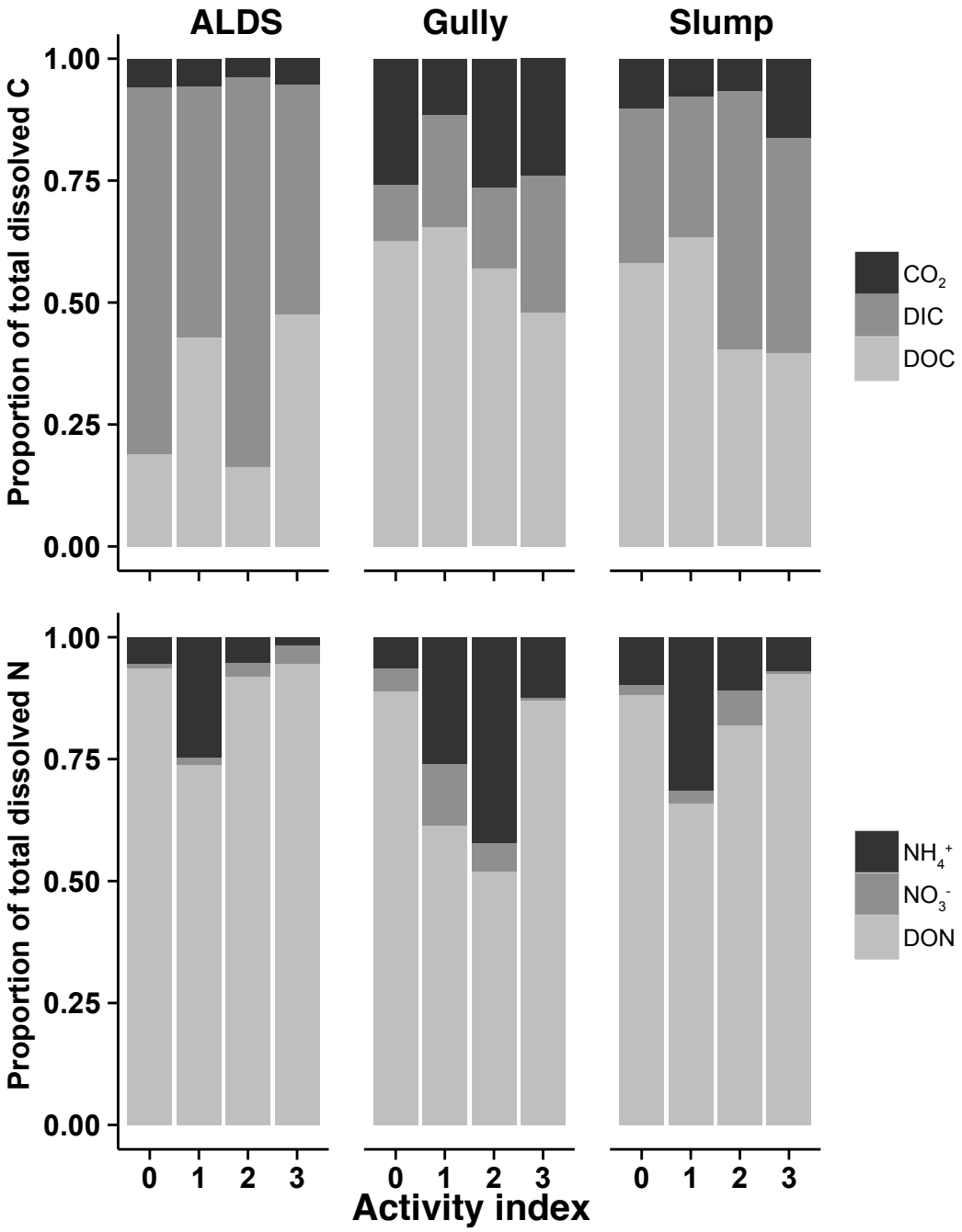

Figure 4.5 The relative proportion of carbon and nitrogen species in thermokarst outflow by feature type and activity index. See Figs. 4.2 and 4.3 for estimates of error and statistical tests for each parameter and Table 4.1 for complete definition of activity index but 0=reference, 1=most active, and 3=stabilized.

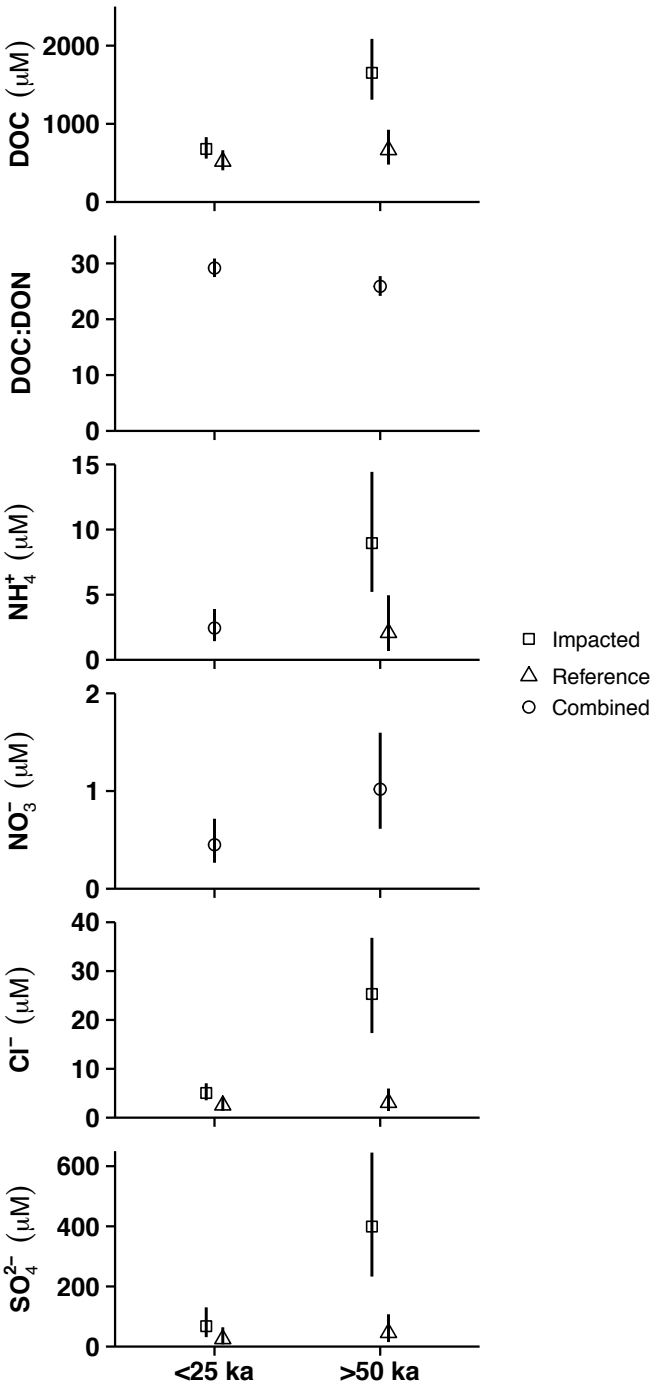

Figure 4.6 Mean (±95% CI) of parameters that varied significantly by surface age. Impacted and reference concentrations are shown independently when the interaction between thermokarst impact and surface age was significant, otherwise, results are combined.

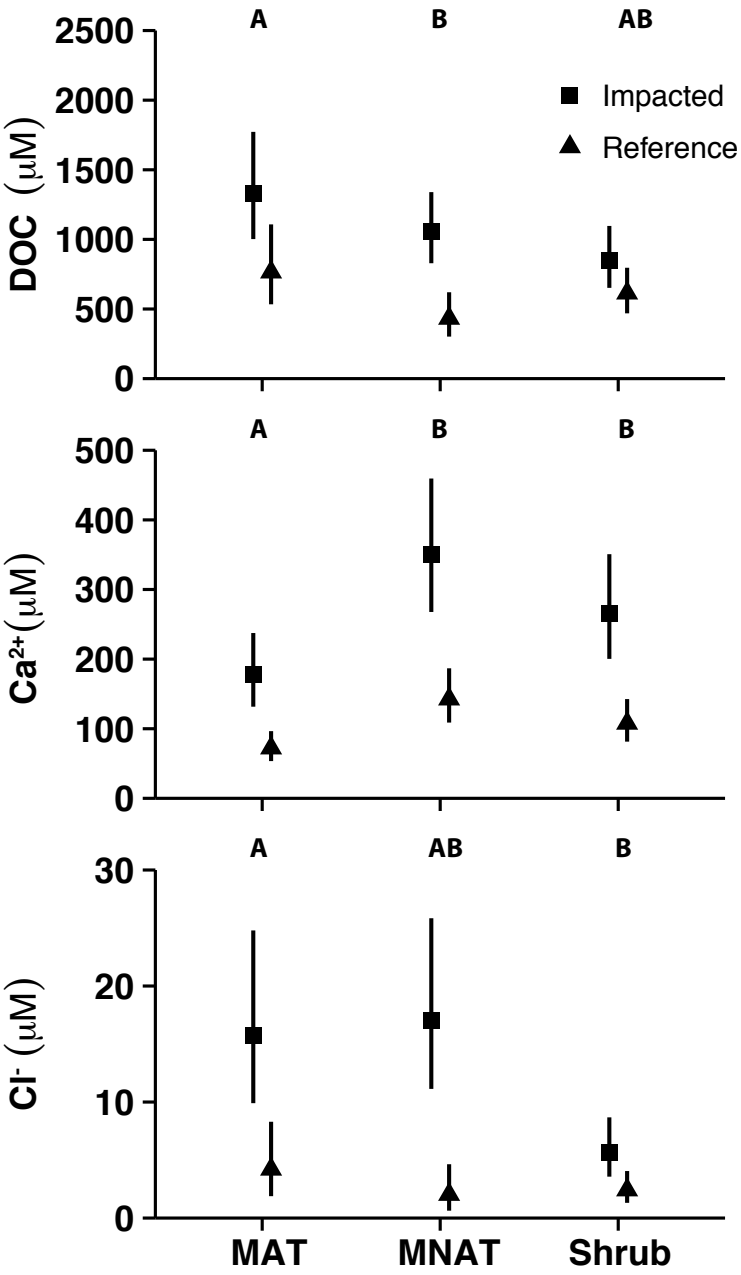

Figure 4.7 Mean (±95% CI) of solutes that varied by vegetation community in thermokarst outflow and reference water from sites occurring on moist acidic (MAT), non-acidic (MNAT), and shrub tundra. Different letters above panels represent significant differences between vegetation communities. DOC, Ca^{2+}, and Cl^{-} were the only parameters for which vegetation was a significant predictor in the mixed-effects ANOVA when accounting for activity level, feature type, and landscape age.

Table 4.1 Characteristics of upland thermokarst features in study.

	Active layer detachment slide	Thermo-erosion gully	Retrogressive thaw slump
Outflow discharge (L sec^{-1})	2.8 (1.1)	1.4 (0.4)	0.95 (0.3)
Percent of outflow from ground ice	8.6 (5.5)	37 (32)	49 (7.6)
n*	7	3	16
Percent of features			
intersecting river/stream/water track	92	56	40
flowing into lake	0	38	58
unassociated with water body	8	6	2
Percent of features occurring on			
moist acidic tundra	13	53	22
moist non-acidic tundra	64	5	45
shrub tundra	23	42	33
Percent of features in activity class			
1	28	32	57
2	36	42	17
3	36	26	26
n**	22	34	27

Mean (SE) characteristics of upland thermokarst on the North Slope of Alaska. *Sample size for discharge and ground ice contribution measurements, **Sample size for landscape position and activity. Activity index was defined as follows: 0. No apparent present or past thermo-degradation, 1. Active thermo-degradation (>25% of headwall is actively expanding) with completely turbid outflow, 2. Moderate thermo-degradation (<25% of headwall is expanding) with somewhat turbid outflow, 3. Stabilized or limited thermo-degradation with complete or partial revegetation and clear outflow.

Table 4.2 Correlations between water chemistry parameters for 83 thermokarst features and 61 reference water tracks and first order streams.

	Activity	DOC	DON	DOC:DON	CO_2	CH_4	DIC	NH_4^+	NO_3^-	N_2O	SO_4^{2-}	Ca^{2+}	Mg^{2+}	K^+	Na^+
ln(DOC)	**0.34**														
ln(DON)	**0.45**	**0.94**													
ln(DOC:DON)	**-0.43**	**-0.15**	**-0.46**												
$ln(CO_2)$	-0.08	**0.27**	**0.23**	0.13											
$ln(CH_4)$	-0.13	**0.18**	0.09	**0.25**	**0.59**										
$DIC^{0.5}$	**0.25**	-0.10	0.03	**-0.35**	**-0.22**	**-0.43**									
$NH_4^{+(0.25)}$	**0.52**	**0.57**	**0.59**	**-0.30**	**0.16**	0.05	0.08								
$NO_3^{-(0.25)}$	**0.42**	**0.16**	**0.24**	**-0.24**	-0.14	-0.07	0.00	**0.38**							
$N_2O^{(0.25)}$	0.12	**0.38**	**0.38**	-0.06	0.14	-0.02	0.03	**0.42**	**0.39**						
$SO_4^{2-(0.25)}$	**0.40**	0.12	**0.26**	**-0.44**	**-0.31**	**-0.41**	**0.52**	**0.23**	**0.34**	**0.24**					
$ln(Ca^{2+})$	**0.43**	0.07	**0.25**	**-0.52**	**-0.24**	**-0.39**	**0.67**	**0.18**	**0.34**	**0.20**	**0.79**				
$Mg^{2+(0.5)}$	**0.43**	0.13	**0.27**	**-0.45**	**-0.27**	**-0.45**	**0.70**	**0.27**	**0.24**	0.15	**0.83**	**0.84**			
$K^{+(0.25)}$	**0.42**	**0.30**	**0.39**	**-0.35**	**-0.22**	**-0.23**	**0.15**	**0.42**	**0.32**	**0.21**	**0.48**	**0.39**	**0.34**		
$ln(Na^+)$	**0.47**	0.02	**0.18**	**-0.45**	**-0.37**	**-0.50**	**0.57**	**0.15**	**0.29**	0.07	**0.72**	**0.69**	**0.73**	**0.48**	
$ln(Cl^-)$	**0.43**	**0.43**	**0.54**	**-0.41**	**-0.20**	**-0.25**	**0.21**	**0.47**	**0.43**	**0.27**	**0.48**	**0.37**	**0.35**	**0.63**	**0.42**

Strength of relationships was determined by Pearson product-moment correlation. Significant correlations ($p < 0.05$) are in bold. Relationships were visually inspected and transformed when necessary to meet the assumption of linearity (log and exponential transformations noted in the variable column on the left). All units are μM except dissolved gases (CO_2, CH_4, and N_2O), which are ppmv, DOC:DON, which is a unitless ratio, and activity, which was recoded 1-4 (low to high) and treated as a non-parametric continuous variable.

Table 4.3 Water chemistry for ground ice, thermokarst outflows and reference waters

Solute (μM)*	Ground ice	Feature outflow	Reference water
DOC	1213 (413)	2109 (349)	821 (120)
DOC:DON	18.7 (2.0)	27.1 (2.1)	33.8 (2.0)
DIC	953 (156)	893 (98)	587 (156)
NH_4^+	54.7 (11.2)	42.5 (8.9)	2.08 (0.65)
NO_3^-	2.68 (1.16)	3.95 (0.92)	1.96 (0.8)
SO_4^{2-}	329 (101)	1042 (295)	76.9 (30)
Mg^{2+}	416 (104)	854 (162)	219 (75)
Ca^{2+}	441 (64)	894 (234)	173 (37)
K^+	33.6 (5.4)	25.9 (4.5)	3.55 (1.1)
Na^+	238 (42.1)	890 (303)	71.7 (23)
Cl^-	137 (57.9)	1231 (561)	11.8 (3.9)
$\delta^{18}O$	-24.4 (0.92)	-21.6 (0.69)	-19.2 (0.49)

Mean (SE) water chemistry from ground ice, outflow, and reference water for the 5 slides, 3 gullies, and 16 slumps where we sampled ground ice exposed by thermokarst formation. *DOC:DON is a unitless ratio and $\delta^{18}O$ is ‰.

Chapter 5. Upland permafrost collapse stimulates N_2O production but effect on growing-season respiration depends on thermokarst morphology[1]

5.1 Abstract

Surface collapse due to permafrost degradation, termed thermokarst, may affect up to a third of the permafrost region by the end of the century, potentially accelerating greenhouse gas release to the atmosphere. When thermokarst forms in uplands it can mobilize organic matter from meters below the surface and dramatically alter soil moisture and temperature. While upland thermokarst has several fundamentally different morphologies, little is known about the comparative impacts of these forms on soil carbon and nitrogen release, limiting the incorporation of this process into quantitative coupled climate models. To address this knowledge gap, we measured soil organic matter displacement, respiration, and soil gas concentrations during the growing season at 26 upland thermokarst features on the North Slope of Alaska. Features included the three most common upland thermokarst morphologies: active-layer detachment slides, thermo-erosion gullies, and retrogressive thaw slumps. We found that thermokarst morphology interacted with landscape parameters to determine both the initial displacement of organic matter and strongly influenced subsequent carbon and nitrogen cycling. The large proportion of ecosystem carbon exported off-site by slumps and active-layer detachment slides resulted in decreased ecosystem respiration post-failure, while gullies removed a smaller portion of ecosystem carbon but strongly stimulated respiration and N_2O production. Elevated N_2O in gully soils persisted through most of the growing season indicating sustained nitrification and denitrification in disturbed soils, representing a potentially important non-C permafrost climate feedback. Across morphologies residual organic matter cover and pre-disturbance respiration explained 83% of the variation in respiration response. Consistent differences between upland thermokarst types may contribute to the incorporation of this non-linear process into projections of carbon and nitrogen release from degrading permafrost.

[1]Prepared for submission to Global Change Biology. B.W. Abbott and J.B. Jones.

5.2 Introduction

In high-latitude ecosystems, persistent cold and saturated soil conditions limit decomposition, leading to the buildup of soil organic matter (SOM) and nutrient limitation (Chapin et al. 1995, Ping et al. 1997, Weintraub and Schimel 2003, Jahn et al. 2010). Soil in the permafrost region contains more than half the world's SOM, storing 1400-1800 Pg carbon (Tarnocai et al. 2009), and 40-60 Pg nitrogen (Jonasson et al. 1999, Weintraub and Schimel 2003, Harden et al. 2012). As the Arctic warms and permafrost degrades, soil temperature and moisture conditions currently limiting SOM decomposition will also change. Because the permafrost SOM pool is so large, release of even a small portion could have substantial consequences for regional ecosystem function and global carbon and nutrient cycles (Schuur et al. 2013).

Widespread degradation of near-surface permafrost is projected by the end of the century (Jafarov et al. 2012, Slater and Lawrence 2013) but how quickly and how much permafrost SOM will be released to the atmosphere following thaw is unknown (Schneider von Deimling et al. 2011). While simulations of the extent of permafrost thaw by 2100 vary by a factor of two (from 40-80% permafrost loss), estimates of permafrost carbon release vary by a factor of thirty (from 17-500 Pg C) (Zhuang et al. 2006, MacDougall et al. 2012, Slater and Lawrence 2013, Schaefer et al. 2014). Even after permafrost thaws, soil at depth is likely to remain cold and wet, due to low hydrologic conductivity in mineral layers and short thaw seasons (Ping et al. 2008, Borden et al. 2010). Because the majority of tundra SOM is stored below the top meter of soil (Michaelson et al. 1996, Ping et al. 1997), permafrost thaw can only trigger rapid carbon and nutrient export to modern ecosystems and the atmosphere if SOM is brought to the surface, or conditions at depth become more favorable for in situ processing.

Thawing of ice-rich permafrost causes surface subsidence or collapse due to ground-ice melt, termed thermokarst (Kokelj and Jorgenson 2013). If thermokarst occurs on hillslopes, ground collapse can abruptly expose SOM from meters below the surface and alter soil conditions at depth, influencing SOM mineralization and export (Schuur et al. 2008, Vonk et al. 2012). The term thermokarst includes a suite of thermo-erosional features with various morphologies determined by ice content, substrate type, and slope (Jorgenson and Osterkamp 2005, Jorgenson et al. 2008, Osterkamp et al. 2009). In upland landscapes, the three most

common thermokarst morphologies are retrogressive thaw slumps, active-layer detachment slides, and thermo-erosion gullies (Jorgenson and Osterkamp 2005, Krieger 2012, Kokelj and Jorgenson 2013). Thaw slumps have a retreating headwall and are fueled by a variety of ground ice types, active-layer detachment slides form when the seasonally thawed surface layer of vegetation and soil slips downhill over an ice-rich transition zone, and thermo-erosion gullies form due to ice-wedge melt, growing with a generally linear or dendritic pattern. These three morphologies currently impact ca 1.5% of the landscape in the western foothills of the Brooks Range (Krieger 2012) and could affect 20-50% of uplands in the continuous permafrost region by the end of the century based on projections of permafrost thaw and the distribution of ground ice (Zhang et al. 2000, Grosse et al. 2011, Slater and Lawrence 2013). Upland thermokarst in the discontinuous permafrost zone already impacts 12% of the overall landscape in some areas (Belshe et al. 2013). Observations over the past half-century indicate accelerated upland thermokarst formation, but circumarctic prevalence and change of thermokarst extent are poorly constrained (Yoshikawa and Hinzman 2003, Jorgenson et al. 2006, Lantz and Kokelj 2008, Lacelle et al. 2010).

Thermokarst influences elemental cycles in two distinct ways: (1) by bringing material previously protected in permafrost soil and ice to the surface and (2) by altering physical conditions at the surface such as soil structure, temperature, moisture, and redox potential, which affects the processing of both permafrost and active-layer carbon and nutrients. Warm and fertile soil conditions following permafrost collapse can stimulate both photosynthesis and respiration, tipping the system toward carbon release or carbon uptake (Schuur et al. 2009, Lee et al. 2010). Thermokarst can displace all or a substantial portion of the organic layer (Lantuit et al. 2012, Pizano et al. 2014), increasing radiative and conductive heat transfer to soils (Burn 2000), and decreasing growing-season respiration from residual mineral soils (Beamish et al. 2014, Jensen et al. 2014). Coupled to changes in carbon cycling, thermokarst can modify nutrient uptake, export, and mineralization. The removal or disruption of surface vegetation during ground collapse can eliminate or reduce plant nutrient uptake (Osterkamp et al. 2009) and during recovery microenvironments in thermokarst can favor deciduous shrub establishment including nitrogen-fixing species (Tsuyuzaki et al. 1999, Lantz et al. 2009, Pizano et al. 2014) altering SOM and nitrogen inputs and turnover (Sturm et al. 2001, DeMarco et al. 2011). Increased nutrient availability and high quality carbon inputs can in turn accelerate decomposition of SOM

(Mack et al. 2004, Hartley et al. 2012). Therefore, overall surface carbon balance from an upland thermokarst feature depends on the amount of SOM exported offsite during formation and on physical conditions within the feature controlling photosynthesis and processing of residual SOM.

While thermokarst will likely play a key role in modulating carbon and nitrogen release from degrading permafrost, it is not adequately conceptualized or characterized to include in current coupled models (Schirrmeister et al. 2010, Belshe et al. 2013, Kokelj and Jorgenson 2013, Schuur et al. 2013). Furthermore, while gullies, slides, and slumps form by different processes, no studies have directly compared carbon and nitrogen release from these morphologies. To address these knowledge gaps, we tested hypotheses concerning carbon and nitrogen release from upland thermokarst features on the North Slope of Alaska. We hypothesized that the impact of thermokarst on respiration and trace gas flux would depend on changes in SOM, temperature, and moisture, which in turn would differ by feature morphology. We expected soil warming to stimulate mineralization in all features but we hypothesized multiple possible effects from changes in SOM and soil moisture. Thermokarst could stimulate respiration and trace gas flux by breaking apart soil aggregates, increasing nutrient availability, and bringing labile permafrost carbon to the surface. Alternatively, for morphologies that displace large volumes of organic and mineral soil, upland thermokarst could diminish carbon and nutrient pools, reducing respiration and gas production. We expected the effect of soil moisture to depend on microtopography, with O_2 limitation favoring CH_4 production in feature floors and enhanced draining and aerobic respiration in feature margins. We predicted that whole-feature respiration would be positively correlated with the amount of residual organic layer and that respiration fluxes would be higher in impacted soils on a per-gram basis.

5.3 Methods

5.3.1 Study sites

We tested our hypotheses with observations from 26 slides, gullies, and slumps on the North Slope of Alaska (Fig. 5.1). Features were identified by aerial surveys, satellite imagery, and previous studies (Bowden et al. 2008, Gooseff et al. 2009, Larouche 2009, Abbott et al. 2014) and were located in three areas of upland tundra underlain by continuous permafrost in the foothills of the Brooks Range. Active and stabilized features occurred across landscape ages and

vegetation types, representing a semi-random sample of thermokarst features in the study areas. We collected samples and observations during the growing season (June-August) of 2009-2011 in the region surrounding the Toolik Field Station, with additional sites sampled in the Noatak National Preserve near the Kelly River Ranger Station in 2010 and Feniak Lake in 2011. The Toolik Field Station is located 254 km north of the Arctic Circle and 180 km south of the Arctic Ocean. The mean annual temperature is -10°C with mean monthly temperature ranging from -25°C in January to 11.5°C in July. The region receives 320 mm of precipitation annually with 200 mm falling between June and August (Toolik Environmental Data Center Team 2014). The Kelly River Ranger Station is located on the western border of the Noatak National Preserve, 540 km west of the Toolik Field Station. Average annual temperature is -5.4°C and the area receives an average of 300 mm of precipitation, a third of which falls during the growing season (Stottlemyer 2001). Feniak Lake is located 360 km west of the Toolik Field Station in the central Brooks Range at the northeast border of the Noatak National Preserve. The average annual temperature is -7°C (Jorgenson et al. 2008) and average precipitation is 450 mm (WRCC 2011).

Vegetation is typical of Arctic tundra across the study region and includes moist acidic tundra characterized by the tussock-forming sedge *Eriophorum vaginatum*, moist non-acidic tundra, and shrub tundra (Walker et al. 1998, Bhatt et al. 2010), with isolated stands of white spruce (*Picea glauca*) near Kelly River (Sullivan and Sveinbjornsson 2010). All three areas occur in bioclimate subzone E, the warmest region in the continuous permafrost zone (Walker et al. 2010). The foothills of the Brooks Range have been affected by multiple glaciations starting in the late Tertiary and continuing to 11 ka B.P. (Hamilton 2003). Repeated rounds of glacial advance and retreat have resulted in a patchwork of glacial till, bedrock, and loess parent materials of various ages (Hamilton 2010). Time since last glaciation can be associated with ecosystem properties including pH, organic layer depth, nutrient pools, vegetation community, and carbon and nutrient turnover (Walker et al. 1998, Hobbie et al. 2002, Epstein et al. 2004, Lee et al. 2011).

5.3.2 Experimental design and analyses

To compare the effects of various thermokarst morphologies, we measured ecosystem respiration and collected soil cores and soil gas samples from four gullies, seven slides, and 16 slumps. Seven features were near the Kelly River Ranger Station, six near Feniak Lake, and 12

near the Toolik Field Station. To characterize seasonal and interannual variability, we took monthly respiration measurements at two gullies and three slumps accessible from the Toolik Field Station in June-August of 2009-2011.

Vegetation class was determined in the field and cross-referenced with published vegetation maps when available (Walker et al. 2005). Glacial geology and surface age were based on recent maps of the study region (Hamilton 2003, 2010, Kanevskiy et al. 2011). Site ages ranged from 10-200 ka, though one site occurred on a surface unglaciated for 2.5 Ma. Feature perimeters were mapped by commercial-grade, handheld GPS, except for four sites around Toolik, which were mapped by the Toolik Field Station GIS staff with a survey-grade GPS and base station. We compared perimeters measured in the field with satellite images from Google Earth from the previous 3-20 years to estimate rates of headwall retreat.

5.3.3 Respiration

Ecosystem respiration (R_{eco}) is the combined CO_2 release from plant metabolism (autotrophic respiration) and decomposition of plant material and SOM (heterotrophic respiration). We used a Li-COR Li-8100 respiration system with a 10 cm diameter chamber to measure R_{eco}. We chose a chamber approach to characterize R_{eco} because it allowed us to detect small-scale variation in carbon flux within features and because it was highly portable. We installed PVC rings (hereinafter collars) with a serrated knife into the top 5-15 cm of soil, onto which the automated chamber sealed. CO_2 production was measured over a 90 second time period with an infrared gas analyzer, and areal flux was calculated by fitting a linear or exponential curve to the data depending on goodness of fit. At each collar we measured volumetric soil moisture in the top 6 cm, soil temperature at 15 cm, and air temperature within the chamber with auxiliary probes attached to the Li-8100 (a ThetaProbe ML2x soil moisture sensor, stainless steel temperature probe, and onboard thermometer, respectively). To ensure R_{eco} measurements represented ambient conditions, we tested the duration of perturbation following collar installation for several mineral and organic soils. We measured R_{eco} immediately after collar installation and every 10 minutes afterward until R_{eco} stabilized. R_{eco} returned to ambient within an hour for exposed mineral soils and within 2.5 hours for organic soils. At sites where collars were installed the same day measurements were taken, we ensured that at least three hours passed between installation and measurement.

Because thermokarst formation creates a jumble of organic and mineral patches with potentially different physical conditions, we classified ground cover within and around features by severity and type of thermokarst impact (Fig. 5.3). Tundra more than 5m outside of visible impact was classified as control, margins were within 1m of collapse but had not experienced subsidence, drapes had subsided but were still attached to surrounding tundra, vegetated rafts had subsided and detached, and exposed patches were bare mineral soil. Drapes were the dominant patch within gullies while exposed and raft patches were most prevalent in slides and slumps (Table 5.1). At five locations, active slumps occurred adjacent to stabilized and revegetated features ranging in time since stabilization from 25-116 years (Pizano et al. 2014). Because established vegetation obscured what had previously been exposed or raft, we classified all surfaces within these features as revegetated. We installed 20-50 collars per site, depending on feature size, arranged in transects perpendicular to the downslope axis of the feature. When possible, each transect included all patch types, in order to control for upslope/downslope variation in R_{eco} and physical conditions.

In order to scale our point measurements to the feature level, we analyzed low-altitude aerial photos to determine the percentage cover of each patch type. We used open-source image-analysis software maintained by the National Institutes of Health (ImageJ 1.48v) to measure percent cover of rafts and exposed mineral soil. Because drapes had less contrast, they were manually delineated in each photo prior to analysis. We analyzed at least three photos per site and used the average value as the scaling factor. We weighted respiration and carbon pools by their proportional coverage to calculate feature-level fluxes and pools.

5.3.4 Soil characterization

To quantify surface soil SOM losses and redistribution between patches, we collected cores from the top 35 cm of the active layer with a stainless steel hand corer. This depth is similar to active-layer depth in the region (Hinzman et al. 1998, Bockheim 2007) and cores typically included the entire organic horizon and much of the mineral horizon within the active-layer, except for within features where thaw depth often exceeded 1 m. Cores were taken at roughly every other collar, resulting in 10-30 cores per site depending on feature size. We extruded intact cores into Ziplock™ bags that we rolled and packed for transport to the lab. We used the depth of the core hole, rather than the length of the core when calculating bulk density

to minimize effects of soil compression during sampling, and noted organic layer depth. Upon return to the field station or camp, cores were frozen until analysis.

In the lab, we separated organic and mineral horizons and homogenized each horizon by hand, removing rocks and organic debris >2 mm in diameter. Bulk density, moisture, and soil organic carbon (SOC) content were calculated for this <2 mm fraction. We measured gravimetric water content of each horizon by drying a subsample for 48 hours at 60°C. We tested for additional change in mass after drying at 110°C and found <1% difference for both organic and mineral soils. We determined bulk organic content by loss on ignition at 550°C for four hours, and estimated organic carbon by multiplying mass loss by 0.48 (Robertson et al. 1999). SOC m^{-2} was calculated by multiplying SOC (% by mass), bulk density, and horizon depth for organic and mineral horizons. We normalized SOC content to 35 cm by extending mineral layer length used in calculation to that depth for cores <35 cm in length. SOC in soil deeper than 35 cm was not sampled or estimated.

To quantify the amount of SOC displaced by thermokarst (SOC_{loss}), we considered changes in organic layer area and residual carbon pools remaining after collapse (drape, raft, and exposed patches). We calculated organic layer SOC loss as follows:

$$SOC_{loss} = C_{cont}o \times A_{exp}o - (C_{resid}o - C_{cont}o) \times A_{resid} - (C_{resid}m - C_{cont}m) \qquad \text{(Equation 1)}$$

Where C is SOC content in the top 35 cm (kg m^{-2}), A is the proportion of feature area, subscripts cont, expo, and resid denote control, exposed, and residual organic layer surfaces, respectively, and o and m indicate soil horizon. Note that this method only estimates changes in organic layer SOC, which may not necessarily represent the majority of total SOC export. However, in order to estimate SOC loss from mineral soils affected by thermokarst, pre-disturbance ice content and total volume displaced would be necessary. To determine carbon reallocation between soil horizons within features we compared SOC content (% by mass) of mineral and organic soil inside and outside features.

5.3.5 Soil gases

In 2010 and 2011 we sampled soil gas at collar sites to examine the spatial distribution of CO_2, CH_4, and N_2O production within and around features. We used a 0.3 cm (OD) stainless steel tube with intake ports drilled in the final 5 cm to collect an integrated soil gas sample from

10-15 cm depth. After inserting the tube to 15 cm, we drew up and flushed 5 ml of soil gas through the tube with an airtight syringe, and then collected a 30ml sample into an evacuated gas vial. Gas samples were analyzed for CH_4, CO_2, and N_2O on a Varian 3300 gas chromatograph with a methanizer and flame ionization detector for carbon species and an electron capture detector for N_2O. We regressed soil CO_2 concentration with R_{eco} to assess the possibility of estimating CH_4 and N_2O fluxes from soil gas concentration and to test the level of connectivity between the upper 15 cm of soil and the atmosphere.

5.3.6 Statistical analyses

We used linear mixed-effects models to test for differences and identify significant predictors. This approach allowed us to account for spatial and temporal non-independence in the data and simultaneously test for effects of feature morphology, vegetation, landscape age, and glacial geology. To test for differences in carbon content and bulk density of soils inside and outside of features, we used a two-way mixed-effects analysis of variance (ANOVA) with feature type and soil position (inside or outside) as fixed effects and individual feature as a random effect. For this and all models we visually inspected residual plots for deviations from normality and homoscedasticity, and transformed response and predictor variables when necessary. To test for differences in R_{eco}, soil temperature, soil moisture, and SOC content between patches, we used a mixed-effects ANOVA of patch crossed by feature type, vegetation, month, and landscape age as fixed effects. To account for spatial and temporal nesting of observations, we included collar, transect, feature, and glacial geology as random effects. We simplified the full model for each parameter by automated backwards elimination, using restricted maximum likelihood to evaluate fixed effects and likelihood ratio tests for random effects. We used the same model to test for differences in soil gas concentration, except we included an interaction term between patch and month instead of between patch and feature type due to strong seasonal patterns evident in preliminary analysis. To test for differences between groups, we performed post-hoc Tukey's honest significant difference tests on the least squares means using Satterthwaite approximation to estimate denominator degrees of freedom.

We evaluated controls on R_{eco} and soil gas concentration with a linear mixed-effects multiple regression model, including soil moisture, soil temperature, air temperature, total SOC (kg m^2), and SOC (%) at the surface as fixed effects. Because the relationship between soil

moisture and R_{eco} was non-linear, with low respiration in extremely wet and dry soils, we included a polynomial soil moisture term by centering the distribution on zero and squaring. We standardized all variables prior to analysis to allow the comparison of model coefficients and we examined regression plots between all predictors to test for collinearity before analysis. We used the same random effects structure and model simplification procedure as above to eliminate non-significant predictors. For R_{eco} we applied the model to all measurements as well as to each patch independently to test our hypotheses concerning changes in controls on R_{eco} inside and outside thermokarst impact. However, for N_2O and CH_4 soil concentrations we only applied the model to all measurements due to smaller sample size for some patches.

We used simple linear regression to assess the relationship between soil CO_2 concentration at 15 cm and R_{eco} for each patch to test the possibility of calculating areal fluxes from soil gas concentrations and assess differences in diffusion rates between patches. We used multiple linear regression to test the effects of undisturbed respiration rate and residual organic layer on the change in respiration after thermokarst. Because we could not measure percent residual organic layer cover for revegetated sites, we assumed they had the same cover characteristics as their adjacent active slumps at the time of formation to include them in the multiple linear regression.

All analyses were performed in R 3.0.2 (R Core Team 2013) with the lme4 and lmerTest packages (Bates et al. 2013, Kuznetsova et al. 2014). The complete dataset is available through the Advanced Cooperative Arctic Data and Information Service at www.aoncadis.org/project/collaborative_research_spatial_and_temporal_influences_of_thermokarst_failures_on_surface_processes_in_arctic_landscapes.html.

5.4 Results

5.4.1 Feature characteristics and distribution

Features had diverse physical characteristics both within and among morphologies (Table 5.1). Slumps and slides were nearly four times larger than gullies on average, though all feature types varied widely in shape and size with the smallest gully covering 1,498 m^2 and the largest slump covering 77,207 m^2. Due to their branched morphology, gullies had the lowest average area to perimeter ratio (8.1), followed by slides (15.4), which were oblong, and slumps (27.5), which were generally circular or horseshoe-shaped. Six of the seven slides in our study had

hybrid morphology where surface disturbance from the initial slide triggered a thaw slump. Slides had the highest rate of headwall retreat (12.1 m yr^{-1}) followed by slumps (10.2) and gullies (1.8). Feature types also differed in distribution on the landscape; with slides tending to be located in the highest topographic positions, slumps distributed across high and low gradient surfaces, and all gullies on footslopes or valley bottoms.

5.4.2 Soil carbon pools

Total SOC stocks in undisturbed soil adjacent to features differed substantially among feature morphologies, from a mean of 10.5 ± 0.4 kg m^{-2} for slides to 19.9 ± 0.8 kg m^{-2} for gullies (Table 5.1; Fig. 5.3a). Organic layer depths followed the same pattern: deepest for gullies, moderate for slumps, and shallowest for slides. For all feature types mineral-layer SOC made up the majority of total SOC in the top 35 cm, ranging from a mean of 68% for slides to 52% for slumps. Thermokarst formation did not increase the percent SOC in the top 35 cm of impacted mineral soil ($p = 0.96$; Fig. 5.3b). Rafts and drapes had lower percent SOC than reference organic layer for gullies and slumps by 8 and 5%, respectively ($p < 0.01$ and 0.05; Fig. 5.3b), indicating mixing of mineral soil into organic layers, though slides had no difference ($p = 0.19$). Mineral soil bulk density was 20% higher inside thaw slumps ($p < 0.001$), but did not differ across feature types and soil horizons ($p > 0.05$; Fig. 5.3c). Organic layer SOC per unit area was higher for vegetated rafts by 34% and lower for revegetated patches by 41% compared to undisturbed tundra ($p < 0.05$), and mineral horizon carbon per unit area was 28% higher for exposed patches in slides (Fig. 5.4e).

Slump floors had the highest mean proportion of exposed mineral soil at 57 ± 4.7%, followed by slides at 50 ± 5.6%, and gullies at 6.3 ± 1.2%. Because impacted mineral SOC content was not significantly different than reference soil (Fig. 5.3b), we eliminated the mineral soil terms from Equation 1 and calculated carbon displacement based only on changes in organic layer coverage and SOC pools. Organic-layer SOC loss averaged 870 g m^{-2} for slides (85-1800, propagated SE), 480 g m^{-2} (300-750) for gullies, and 2700 g m^{-2} (1600-4000) for slumps (Fig. 5.5). This constitutes the removal of 32, 6, and 51% of organic-layer SOC for slides, gullies, and slumps, respectively, or 8.3, 2.4, and 19% of total SOC in the top 35 cm. Accounting for increased SOC in raft patches reduced estimates of carbon loss by 16% on average, compared to

estimates based only on percent exposed mineral soil, though this reduction ranged from 0-80% for individual sites.

5.4.3 Respiration and soil gases

R_{eco} in undisturbed soil adjacent to features differed significantly among morphologies, with control patch means of 2.97 ± 0.4 g C m^{-2} day^{-1} for slides, 1.00 ± 0.25 g C m^{-2} day^{-1} for gullies, and 2.07 ± 0.2 g C m^{-2} day^{-1} for slumps (Fig. 5.4a). Within features, R_{eco} from exposed patches was 70 and 57% lower than reference for slides and slumps, respectively ($p < 0.001$), but was 26% higher for slump rafts and 71% higher for gully drapes ($p < 0.01$ and 0.0001; Fig. 5.4a). On a per-gram carbon basis R_{eco} followed generally the same pattern as areal R_{eco} among patches (Fig. 5.4b). Soil temperature was significantly elevated within features, including slump margins, with up to 4°C difference between control and impacted patches (Fig. 5.4c). Soil moisture in the top 6 cm only varied significantly for drape and exposed patches in gullies, where surface soils were 35% and 157% wetter than undisturbed tundra ($p < 0.0001$; Fig. 5.4d).

Soil gas concentration differed significantly by month, patch, and feature type (Fig. 5.6). CO_2 concentration was highest in July during peak growing season and in total, 96% of soil gas samples had CO_2 concentration above atmospheric (Fig. 5.6a). Soil CH_4 was elevated in both raft and exposed patches compared to reference through the season and was 2.8 fold higher in gully soil than slides and slumps ($p < 0.0001$; Fig. 5.6b). August mean CH_4 concentration dropped below atmospheric for control, margin, and drape patches. Concentration of N_2O was significantly elevated in drape patches, which were 29% higher than reference soil in June and 43% higher in August (Fig. 5.6c). Additionally, margin patches had elevated N_2O in June and exposed patches in July. N_2O concentration dropped 13% for all patches in July relative to June and August, and was 15% higher in old (>50 ka) compared to young landscapes (<25 ka). Soil CO_2 at 15 cm was significantly correlated with R_{eco} for control, margin, and drape patches, though the relationships were very weak for control and margin patches ($r^2 = 0.05$ and 0.15, $p < 0.01$) but strong for drapes ($r^2 = 0.62$, $p < 0.0000$).

The mixed-effects multiple regression model identified surface SOC, total SOC, and soil temperature as the most important predictors of R_{eco} (Table 5.2), with soil moisture exerting a negative effect and air temperature exerting a slight positive effect. However, the relationship between R_{eco} and soil conditions varied by patch type. Soil temperature most strongly predicted

R_{eco} for all patch types except exposed, where air temperature was the only significant predictor. Soil moisture was only significant for control and raft patches where it had opposite effects, suppressing R_{eco} in control but stimulating it in rafts. Total SOC and surface SOC were negatively associated with R_{eco} for the within patches analyses. For soil gases at 15 cm, soil moisture and temperature were positively associated with both CO_2 and CH_4 concentration and total SOC was negatively correlated with CO_2 (Table 5.2). N_2O was negatively correlated with soil moisture as well as percent SOC at the surface.

The repeat measurements at the five temporally intensive sites revealed stronger variability in R_{eco}, soil temperature, and soil moisture between months than between years (Fig. 5.7). Soil temperature was typically high in June and July and substantially cooler in August. Soil moisture followed different patterns each year, closely tracking trends in precipitation over the study period (Toolik Environmental Data Center Team 2014). R_{eco} followed soil temperature more strongly than soil moisture. July of 2009 stood out as the warmest in the time series and was also one of the driest, with elevated R_{eco} across sites.

When scaled to the feature-level, R_{eco} had fundamentally different responses to disturbance for different feature morphologies, with elevated R_{eco} in gullies compared to reference and depressed R_{eco} in slides and slumps (Fig. 5.8). Mean R_{eco} was 84% higher than reference soil for gullies, whereas it was 26 and 18% lower in slides and slumps. Though the percent decrease for slides was less than the increase for gullies, the absolute magnitude of difference in respiration was similar because undisturbed respiration at slides sites was three-times that of gullies (Fig. 5.8). Feature-level response of respiration to thermokarst disturbance was negatively correlated with undisturbed respiration rate ($R^2 = 0.63$, $p < 0.0001$), meaning features occurring on tundra with low ambient respiration were more likely to have larger increases in respiration after thermokarst disturbance (Fig. 5.9). Respiration response was positively correlated with percent cover of residual organic layer (rafts and drapes; $R^2 = 0.43$, $p < 0.0001$). These relationships held both between and within feature morphologies. The multiple linear regression including both reference respiration and residual organic layer as predictors explained 83% of the variation in the response of R_{eco} to thermokarst formation ($\Delta R_{eco} = -0.60 \times$ Reference $R_{eco} + 0.02 \times$ Percent residual organic layer $- 0.05$, $F(2, 21) = 55.7$, $p < 0.000$).

5.5 Discussion

5.5.1 Controls on respiration and soil gases

Upland thermokarst affected soil temperature, organic matter, and microtopography, three of the major controls on carbon and nitrogen cycling in tundra ecosystems (Weintraub and Schimel 2003, Oberbauer et al. 2007, Sommerkorn 2008). The effect of thermokarst formation on carbon and nitrogen cycling differed fundamentally by feature morphology. The large proportion of ecosystem carbon exported off-site or incorporated into deeper soil by slumps and slides resulted in decreased R_{eco} post-failure. Conversely, thermo-erosion gullies displaced a smaller portion of ecosystem carbon but nearly doubled post-failure R_{eco} and stimulated N_2O production through much of the growing season. Similar decreases in growing-season R_{eco} following slump and slide formation have been documented in boreal forest and high Arctic ecosystems, suggesting upland thermokarst may have minimal impact on surface gas flux (Beamish et al. 2014, Jensen et al. 2014). However, gullies, which strongly affect R_{eco} and N_2O production, are the most abundant form of upland thermokarst both in number and total area (Krieger 2012). Furthermore, while slumps and slides have a relatively small effect on growing-season R_{eco}, slumps and gullies, which create surface depressions, may have a profound impact on annual surface carbon balance by altering winter soil conditions. Experimental wintertime warming of 2-3°C in tundra soils can result in the net release of 20-30 g carbon m^{-2} yr^{-1} due to increased winter respiration (Natali et al. 2014). Upland thermokarst can warm annual soil temperature by 4°C and wintertime temperature by 6°C due to conductive heat flux to soils during summer and added insulation in winter from deeper snow, and these elevated temperatures can persist for decades (Burn 2000). If increases in wintertime respiration are proportional to those observed from experimental warming, gullies and slumps could substantially accelerate the flux of SOC stocks at depth to the atmosphere.

Based on experimental tundra warming, the temperature sensitivity of R_{eco} differs strongly by ecosystem type, complicating the integration of field measurements into process-based models at the landscape and biome level (Rustad et al. 2001, Oberbauer et al. 2007). We found the response of tundra soil to warming from thermokarst disturbance differed systematically across tundra types. We expected feature-level R_{eco} to be positively correlated with the percent of organic layer remaining after feature formation, however, we did not anticipate the strong relationship between reference respiration and the response of R_{eco} to

disturbance (Fig. 5.9). For sites with low pre-disturbance R_{eco} (< 2 g C m^{-2} day^{-1}) thermokarst tended to increase feature-level R_{eco}, while the opposite was true for sites with high pre-disturbance R_{eco}. One explanation for this relationship is that when R_{eco} is limited by physical conditions or substrate quality, physical disturbance from thermokarst formation increases R_{eco}, by reducing waterlogging and warming soil. However, in soils where conditions and substrate are already conducive to respiration, the negative impacts of thermokarst such as disruption of plant roots and removal of organic material decreases surface CO_2 flux. This hypothesis is supported by observations that R_{eco} tends to be more sensitive to warming in less productive tundra ecosystems (Oberbauer et al. 2007). Together, residual organic matter cover and pre-disturbance respiration explained 83% of the variation in respiration response for all feature and ecosystem types, potentially representing a useful scaling factor based on known or remotely sensed parameters.

As the permafrost region warms, the development of oxic and anoxic environments on the landscape will determine the ratio of CH_4 and CO_2 release(Schuur et al. 2008). Subsidence from lowland thermokarst impounds water, resulting in anoxic environments and CH_4 production (Walter et al. 2007). However, little is known about the overall effects of upland thermokarst on redox conditions (Kokelj and Jorgenson 2013). Surprisingly, slumps and slides did not have a significant effect on surface soil moisture. However, across feature types upland thermokarst fundamentally changed the relationship between soil moisture and R_{eco}, which was negative in reference tundra but positive or neutral within features. This suggests that in contrast to lowland thermokarst, upland thermokarst formation may favor aerobic processing of thawed organic matter.

5.5.2 Denitrification in a nitrogen-limited environment

Potential nitrification and denitrification rates are high in many Arctic soils (Siciliano et al. 2009, Buckeridge and Grogan 2010, Harms and Jones 2012), indicating the presence of microorganisms capable of producing N_2O, and pulses of N_2O have been observed from disturbed mineral surfaces such as frost boils (Repo et al. 2009) and experimentally manipulated soils (Elberling et al. 2010). However, sustained N_2O flux has not been demonstrated in upland tundra due to low rates of nitrogen mineralization, efficient nitrogen uptake by plants, and a lack of the heterogeneous soil moisture and O_2 conditions required for coupled nitrification and

denitrification (Stewart et al. 2014 and references therein). Thermo-erosion gullies appear to create conditions conducive to N_2O production over much of the growing season. Gullies modify microtopography and associated moisture gradients, creating adjacent oxic and anoxic soil conditions. Drapes are well aerated and strongly connected to the atmosphere, as evidenced by elevated respiration and the correlation between soil CO_2 concentration and surface flux. This connection also suggests that elevated soil N_2O concentration is not simply due to transport limitation but that rate of production is substantial. Organic layers in moist acidic tundra, where most gullies form, can contain large pools of NH_4^+ that are physically inaccessible until disruption of the organic soil structure (Darrouzet-Nardi and Weintraub 2014), and mineral soils in gully floors are high in inorganic N (Harms et al. 2013), two potential sources of inorganic nitrogen as substrate for nitrification. Disturbance during subsidence could liberate inaccessible NH_4^+ from the organic layer, and high flow events could deposit nitrogen-rich mineral soil from gully floors onto drape patches. Additionally, subsidence may inhibit plant uptake by shearing roots, and enhanced nitrogen mineralization in moist and warm gully soils could contribute to nitrogen availability after stabilization. Vertical and lateral hydrologic flow could then transport NO_3^- to low O_2 environments at the mineral soil interface and gully floor. Abundant organic carbon in gully mineral soils (Fig. 5.5) as well as labile dissolved organic carbon released from gully formation (Cory et al. 2013, Abbott et al. 2014) could serve as electron donor during denitrification. It is important to note that the presence of N_2O production observed here cannot be translated into N_2O flux and should be interpreted with caution. However, if gaseous loss of nitrogen from gullies is widespread it could influence coupled carbon and nutrient cycling (Mack et al. 2004) and represent a potential non-carbon permafrost climate feedback.

5.5.3 SOC displacement and redistribution within features

Upland thermokarst formation removed an average of 480-2700 g m^{-2} SOC from organic layers, constituting 6-51% of organic-layer SOC and 2.4-19% of SOC in the top 35 cm. These losses are comparable to SOC consumed during moderate-severity boreal and high-severity Arctic wildland fire (Mack et al. 2011). However, unlike wildland fire, which mineralizes SOC directly to the atmosphere, thermokarst delivers organic matter to downslope and downstream ecosystems where it may or may not be released to the atmosphere. Therefore, the overall effect of upland thermokarst on carbon release depends both on carbon flux from disturbed sites and the fate of organic matter transported offsite. Some receiving ecosystems stabilize and preserve

carbon over long time frames, such as anoxic lake sediments (Whalen and Cornwell 1985, Einsele et al. 2001, Cole et al. 2007), though these environments may also favor CH_4 release. Other environments favor aerobic decomposition, such as rivers and to a lesser extent hillslopes (Hinkel et al. 2003, Aufdenkampe et al. 2011), accelerating mineralization and decreasing CH_4 release. Consequently, the landscape position of thermokarst features will also influence the proportion of displaced organic matter eventually mineralized to the atmosphere.

While organic layer losses are visually conspicuous, they likely do not represent the majority of carbon displaced during thermokarst formation. Based on average carbon densities in thermokarst mineral soils (0.03-0.05 g C cm^{-3}; this study), the removal of 6, 1.5, and 12 cm across the feature floor for slides, gullies, and slumps, respectively, would equal organic layer losses. Given average feature depths and ground-ice contents (Jorgenson and Osterkamp 2005, Lantuit and Pollard 2005, Kokelj et al. 2013), it is likely that mineral layer SOC export exceeds losses from the organic layer by 5-100 fold. Quantifying mineral soil carbon displacement and reburial of surface carbon into deeper soil are critical to better constrain the full carbon-cycle consequences of upland thermokarst.

5.6 Conclusions

Thermokarst morphology interacted with landscape characteristics to determine both the initial displacement of organic matter and subsequent carbon and nitrogen cycling. Slides and slumps displaced one third to one half of organic-layer carbon, resulting in decreased R_{eco} post-failure, while gullies removed less than 10% of surface carbon but strongly stimulated R_{eco} and N_2O production. Consistent differences in gas flux between morphologies, as well as the strong relationship between pre- and post-failure respiration across morphologies may contribute to the incorporation of this non-linear process into model projections of greenhouse-gas flux from degrading permafrost. However, future investigation of winter respiration and the fate of organic matter exported offsite are necessary to quantify the overall impact of upland thermokarst on Arctic carbon and nitrogen dynamics. N_2O production in gully soil through the growing season represents one of the first observations of sustained denitrification in highly nitrogen-limited tundra systems. Given that gullies make up more than half of all upland thermokarst area, and that N_2O has a global warming potential 300 times that of CO_2, this may represent an important non-carbon permafrost climate feedback. Fundamental differences between thermokarst

morphologies underline the importance of considering not only the extent of permafrost collapse but also its form.

5.7 Acknowledgements

This work was supported by the National Science Foundation ARCSS program (OPP-0806465 and OPP-0806394). We thank the many individuals and organizations that assisted with this study. In particular, we thank S. Abbott, A. Olsson, L. Koenig, P. Tobin, for their work in the lab and field. A. Balser made figure 5.1, C. Jones assisted with spatial analyses, R. Fulweber and J. Stuckey provided feature perimeters, Toolik Field Station and CH2M Hill Polar Services gave logistic support, and the National Park Service and Bureau of Land Management facilitated research permits. Special thanks to E. Schuur, T. Chapin, S. Bret-Harte, and S. Godsey for their input on the experimental design and manuscript. In memory of A. Bali.

5.8 Citations

Abbott, B. W., J. R. Larouche, J. B. Jones, W. B. Bowden, and A. W. Balser. 2014. Elevated dissolved organic carbon biodegradability from thawing and collapsing permafrost. Journal of Geophysical Research: Biogeosciences:2014JG002678.

Aufdenkampe, A. K., E. Mayorga, P. A. Raymond, J. M. Melack, S. C. Doney, S. R. Alin, R. E. Aalto, and K. Yoo. 2011. Riverine coupling of biogeochemical cycles between land, oceans, and atmosphere. Frontiers in Ecology and the Environment **9**:53-60.

Bates, D., M. Maechler, B. Bolker, and S. Walker. 2013. lme4: Linear mixed-effects models using Eigen and S4. R package version 1.0-5. http://CRAN.R-project.org/package=lme4.

Beamish, A., A. Neil, I. Wagner, and N. A. Scott. 2014. Short-term impacts of active layer detachments on carbon exchange in a High Arctic ecosystem, Cape Bounty, Nunavut, Canada. Polar Biology **37**:1459-1468.

Belshe, E. F., E. A. G. Schuur, and G. Grosse. 2013. Quantification of upland thermokarst features with high resolution remote sensing. Environmental Research Letters **8**.

Bhatt, U. S., D. A. Walker, M. K. Raynolds, J. C. Comiso, H. E. Epstein, G. S. Jia, R. Gens, J. E. Pinzon, C. J. Tucker, C. E. Tweedie, and P. J. Webber. 2010. Circumpolar Arctic Tundra Vegetation Change Is Linked to Sea Ice Decline. Earth Interactions **14**.

Bockheim, J. G. 2007. Importance of cryoturbation in redistributing organic carbon in permafrost-affected soils. Soil Science Society of America Journal **71**:1335-1342.

Borden, P. W., C. L. Ping, P. J. McCarthy, and S. Naidu. 2010. Clay Mineralogy in Arctic Tundra Gelisols, Northern Alaska. Soil Science Society of America Journal **74**:580-592.

Bowden, W. B., M. N. Gooseff, A. Balser, A. Green, B. J. Peterson, and J. Bradford. 2008. Sediment and nutrient delivery from thermokarst features in the foothills of the North Slope, Alaska: Potential impacts on headwater stream ecosystems. Journal of Geophysical Research-Biogeosciences **113**.

Buckeridge, K. M. and P. Grogan. 2010. Deepened snow increases late thaw biogeochemical pulses in mesic low arctic tundra. Biogeochemistry **101**:105-121.

Burn, C. R. 2000. The thermal regime of a retrogressive thaw slump near Mayo, Yukon Territory. Canadian Journal of Earth Sciences **37**:967-981.

Chapin, F. S., G. R. Shaver, A. E. Giblin, K. J. Nadelhoffer, and J. A. Laundre. 1995. Responses of Arctic Tundra to Experimental and Observed Changes in Climate. Ecology **76**:694-711.

Cole, J. J., Y. T. Prairie, N. F. Caraco, W. H. McDowell, L. J. Tranvik, R. G. Striegl, C. M. Duarte, P. Kortelainen, J. A. Downing, J. J. Middelburg, and J. Melack. 2007. Plumbing the global carbon cycle: Integrating inland waters into the terrestrial carbon budget. Ecosystems **10**:171-184.

Cory, R. M., B. C. Crump, J. A. Dobkowski, and G. W. Kling. 2013. Surface exposure to sunlight stimulates CO2 release from permafrost soil carbon in the Arctic. Proceedings of the National Academy of Sciences of the United States of America **110**:3429-3434.

Darrouzet-Nardi, A. and M. N. Weintraub. 2014. Evidence for spatially inaccessible labile N from a comparison of soil core extractions and soil pore water lysimetry. Soil Biology & Biochemistry **73**:22-32.

DeMarco, J., M. C. Mack, and M. S. Bret-Harte. 2011. The Effects of Snow, Soil Microenvironment, and Soil Organic Matter Quality on N Availability in Three Alaskan Arctic Plant Communities. Ecosystems **14**:804-817.

Einsele, G., J. P. Yan, and M. Hinderer. 2001. Atmospheric carbon burial in modern lake basins and its significance for the global carbon budget. Global and Planetary Change **30**:167-195.

Elberling, B., H. H. Christiansen, and B. U. Hansen. 2010. High nitrous oxide production from thawing permafrost. Nature Geoscience **3**:332-335.

Epstein, H. E., J. Beringer, W. A. Gould, A. H. Lloyd, C. D. Thompson, F. S. Chapin, G. J. Michaelson, C. L. Ping, T. S. Rupp, and D. A. Walker. 2004. The nature of spatial transitions in the Arctic. Journal of Biogeography **31**:1917-1933.

Gooseff, M. N., A. Balser, W. B. Bowden, and J. B. Jones. 2009. Effects of Hillslope Thermokarst in Northern Alaska. Eos, Transactions American Geophysical Union **90**:29-30.

Grosse, G., J. Harden, M. Turetsky, A. D. McGuire, P. Camill, C. Tarnocai, S. Frolking, E. A. G. Schuur, T. Jorgenson, S. Marchenko, V. Romanovsky, K. P. Wickland, N. French, M. Waldrop, L. Bourgeau-Chavez, and R. G. Striegl. 2011. Vulnerability of high-latitude soil organic carbon in North America to disturbance. Journal of Geophysical Research-Biogeosciences **116**.

Hamilton, T. D. 2003. Surficial geology of the Dalton Highway (Itkillik-Sagavanirktok rivers) area, souther Arctic foothills. Alaska Division of Geological & Geophysical Surveys, Alaska.

Hamilton, T. D. 2010. Surficial geologic map of the Noatak National Preserve, Alaska: U.S. Geological Survey Scientific Investigations Map 3036.

Harden, J. W., C. D. Koven, C.-L. Ping, G. Hugelius, A. David McGuire, P. Camill, T. Jorgenson, P. Kuhry, G. J. Michaelson, J. A. O'Donnell, E. A. G. Schuur, C. Tarnocai, K. Johnson, and G. Grosse. 2012. Field information links permafrost carbon to physical vulnerabilities of thawing. Geophysical Research Letters **39**:L15704.

Harms, T., B. Abbott, and J. Jones. 2013. Thermo-erosion gullies increase nitrogen available for hydrologic export. Biogeochemistry:1-13.

Harms, T. K. and J. B. Jones. 2012. Thaw depth determines reaction and transport of inorganic nitrogen in valley bottom permafrost soils. Global Change Biology **18**:2958-2968.

Hartley, I. P., M. H. Garnett, M. Sommerkorn, D. W. Hopkins, B. J. Fletcher, V. L. Sloan, G. K. Phoenix, and P. A. Wookey. 2012. A potential loss of carbon associated with greater plant growth in the European Arctic. Nature Climate Change **2**:875-879.

Hinkel, K. M., W. R. Eisner, J. G. Bockheim, F. E. Nelson, K. M. Peterson, and X. Y. Dai. 2003. Spatial extent, age, and carbon stocks in drained thaw lake basins on the Barrow Peninsula, Alaska. Arctic Antarctic and Alpine Research **35**:291-300.

Hinzman, L. D., D. J. Goering, and D. L. Kane. 1998. A distributed thermal model for calculating soil temperature profiles and depth of thaw in permafrost regions. Journal of Geophysical Research-Atmospheres **103**:28975-28991.

Hobbie, S. E., T. A. Miley, and M. S. Weiss. 2002. Carbon and nitrogen cycling in soils from acidic and nonacidic tundra with different glacial histories in Northern Alaska. Ecosystems **5**:761-774.

Jafarov, E. E., S. S. Marchenko, and V. E. Romanovsky. 2012. Numerical modeling of permafrost dynamics in Alaska using a high spatial resolution dataset. Cryosphere **6**:613-624.

Jahn, M., T. Sachs, T. Mansfeldt, and M. Overesch. 2010. Global climate change and its impacts on the terrestrial Arctic carbon cycle with special regards to ecosystem components and the greenhouse-gas balance. Journal of Plant Nutrition and Soil Science **173**:627-643.

Jensen, A. E., K. A. Lohse, B. T. Crosby, and C. I. Mora. 2014. Variations in soil carbon dioxide efflux across a thaw slump chronosequence in northwestern Alaska. Environmental Research Letters **9**:025001.

Jonasson, S., A. Michelsen, and I. K. Schmidt. 1999. Coupling of nutrient cycling and carbon dynamics in the Arctic, integration of soil microbial and plant processes. Applied Soil Ecology **11**:135-146.

Jorgenson, M. T. and T. E. Osterkamp. 2005. Response of boreal ecosystems to varying modes of permafrost degradation. Canadian Journal of Forest Research-Revue Canadienne De Recherche Forestiere **35**:2100-2111.

Jorgenson, M. T., Y. L. Shur, and T. E. Osterkamp. 2008. Thermokarst in Alaska. Pages 117-124 Ninth International Conference On Permafrost, University of Alaska Fairbanks.

Jorgenson, M. T., Y. L. Shur, and E. R. Pullman. 2006. Abrupt increase in permafrost degradation in Arctic Alaska. Geophysical Research Letters **33**.

Kanevskiy, M., Y. Shur, D. Fortier, M. T. Jorgenson, and E. Stephani. 2011. Cryostratigraphy of late Pleistocene syngenetic permafrost (yedoma) in northern Alaska, Itkillik River exposure. Quaternary Research **75**:584-596.

Kokelj, S. V. and M. T. Jorgenson. 2013. Advances in Thermokarst Research. Permafrost and Periglacial Processes **24**:108-119.

Kokelj, S. V., D. Lacelle, T. C. Lantz, J. Tunnicliffe, L. Malone, I. D. Clark, and K. S. Chin. 2013. Thawing of massive ground ice in mega slumps drives increases in stream sediment and solute flux across a range of watershed scales. Journal of Geophysical Research: Earth Surface **118**:681-692.

Krieger, K. C. 2012. The Topographic Form and Evolution of Thermal Erosion Features: A First Analysis Using Airborne and Ground-Based LiDAR in Arctic Alaska. Idaho State University.

Kuznetsova, A., P. B. Brockhoff, and R. H. B. Christensen. 2014. lmerTest: Tests for random and fixed effects for linear mixed effect models (lmer objects of lme4 package). R package version 2.0-6. http://CRAN.R-project.org/package=lmerTest.

Lacelle, D., J. Bjornson, and B. Lauriol. 2010. Climatic and Geomorphic Factors Affecting Contemporary (1950-2004) Activity of Retrogressive Thaw Slumps on the Aklavik Plateau, Richardson Mountains, NWT, Canada. Permafrost and Periglacial Processes **21**:1-15.

Lantuit, H. and W. H. Pollard. 2005. Temporal stereophotogrammetric analysis of retrogressive thaw slumps on Herschel Island, Yukon territory. Natural Hazards and Earth System Sciences **5**:413-423.

Lantuit, H., W. H. Pollard, N. Couture, M. Fritz, L. Schirrmeister, H. Meyer, and H. W. Hubberten. 2012. Modern and Late Holocene Retrogressive Thaw Slump Activity on the Yukon Coastal Plain and Herschel Island, Yukon Territory, Canada. Permafrost and Periglacial Processes **23**:39-51.

Lantz, T. C. and S. V. Kokelj. 2008. Increasing rates of retrogressive thaw slump activity in the Mackenzie Delta region, NWT, Canada. Geophysical Research Letters **35**.

Lantz, T. C., S. V. Kokelj, S. E. Gergel, and G. H. R. Henryz. 2009. Relative impacts of disturbance and temperature: persistent changes in microenvironment and vegetation in retrogressive thaw slumps. Global Change Biology **15**:1664-1675.

Larouche, J. R. 2009. Environmental influences on the genetic diversity of bacterial communities in arctic streams. University of Vermont.

Lee, H., E. A. G. Schuur, and J. G. Vogel. 2010. Soil CO2 production in upland tundra where permafrost is thawing. Journal of Geophysical Research-Biogeosciences **115**:-.

Lee, H., E. G. Schuur, J. G. Vogel, M. Lavoie, D. Bhadra, and C. L. Staudhammer. 2011. A spatially explicit analysis to extrapolate carbon fluxes in upland tundra where permafrost is thawing. Global Change Biology **17**:1379-1393.

MacDougall, A. H., C. A. Avis, and A. J. Weaver. 2012. Significant contribution to climate warming from the permafrost carbon feedback. Nature Geosci **5**:719-721.

Mack, M. C., M. S. Bret-Harte, T. N. Hollingsworth, R. R. Jandt, E. A. G. Schuur, G. R. Shaver, and D. L. Verbyla. 2011. Carbon loss from an unprecedented Arctic tundra wildfire. Nature **475**:489-492.

Mack, M. C., E. A. G. Schuur, M. S. Bret-Harte, G. R. Shaver, and F. S. Chapin. 2004. Ecosystem carbon storage in arctic tundra reduced by long-term nutrient fertilization. Nature **431**:440-443.

Michaelson, G. J., C. L. Ping, and J. M. Kimble. 1996. Carbon storage and distribution in tundra soils of Arctic Alaska, USA. Arctic and Alpine Research **28**:414-424.

Natali, S. M., E. A. G. Schuur, E. E. Webb, C. E. H. Pries, and K. G. Crummer. 2014. Permafrost degradation stimulates carbon loss from experimentally warmed tundra. Ecology **95**:602-608.

Oberbauer, S. F., C. E. Tweedie, J. M. Welker, J. T. Fahnestock, G. H. R. Henry, P. J. Webber, R. D. Hollister, M. D. Walker, A. Kuchy, E. Elmore, and G. Starr. 2007. Tundra CO2 fluxes in response to experimental warming across latitudinal and moisture gradients. Ecological Monographs **77**:221-238.

Osterkamp, T. E., M. T. Jorgenson, E. A. G. Schuur, Y. L. Shur, M. Z. Kanevskiy, J. G. Vogel, and V. E. Tumskoy. 2009. Physical and Ecological Changes Associated with Warming Permafrost and Thermokarst in Interior Alaska. Permafrost and Periglacial Processes **20**:235-256.

Ping, C. L., G. J. Michaelson, and J. M. Kimble. 1997. Carbon storage along a latitudinal transect in Alaska. Nutrient Cycling in Agroecosystems **49**:235-242.

Ping, C. L., G. J. Michaelson, J. M. Kimble, V. E. Romanovsky, Y. L. Shur, D. K. Swanson, and D. A. Walker. 2008. Cryogenesis and soil formation along a bioclimate gradient in Arctic North America. Journal of Geophysical Research-Biogeosciences **113**.

Pizano, C., A. F. Barón, E. A. G. Schuur, K. G. Crummer, and M. C. Mack. 2014. Effects of thermo-erosional disturbance on surface soil carbon and nitrogen dynamics in upland arctic tundra. Environmental Research Letters **9**:075006.

R Core Team. 2013. R: A language and environment for statistical computing. R Foundation for Statistical Computing, Vienna, Austria. URL http://www.R-project.org/.

Repo, M. E., S. Susiluoto, S. E. Lind, S. Jokinen, V. Elsakov, C. Biasi, T. Virtanen, and P. J. Martikainen. 2009. Large N(2)O emissions from cryoturbated peat soil in tundra. Nature Geoscience **2**:189-192.

Robertson, G. P., D. C. Coleman, C. S. Bledsoe, and P. Sollins. 1999. Standard soil methods for long-term ecological research. Oxford University Press.

Rustad, L. E., J. L. Campbell, G. M. Marion, R. J. Norby, M. J. Mitchell, A. E. Hartley, J. H. C. Cornelissen, J. Gurevitch, and N. Gcte. 2001. A meta-analysis of the response of soil respiration, net nitrogen mineralization, and aboveground plant growth to experimental ecosystem warming. Oecologia **126**:543-562.

Schaefer, K., H. Lantuit, V. E. Romanovsky, E. A. G. Schuur, and R. Witt. 2014. The impact of the permafrost carbon feedback on global climate. Environmental Research Letters **9**:085003.

Schirrmeister, L., G. Grosse, V. V. Kunitsky, M. C. Fuchs, M. Krbetschek, A. A. Andreev, U. Herzschuh, O. Babyi, C. Siegert, H. Meyer, A. Y. Derevyagin, and S. Wetterich. 2010. The mystery of Bunge Land (New Siberian Archipelago): implications for its formation based on palaeoenvironmental records, geomorphology, and remote sensing. Quaternary Science Reviews **29**:3598-3614.

Schneider von Deimling, T., M. Meinshausen, A. Levermann, V. Huber, K. Frieler, D. M. Lawrence, and V. Brovkin. 2011. Estimating the permafrost-carbon feedback on global warming. Biogeosciences:4727-4767.

Schuur, E. A. G., B. W. Abbott, W. B. Bowden, V. Brovkin, P. Camill, J. G. Canadell, J. P. Chanton, F. S. Chapin, III, T. R. Christensen, P. Ciais, B. T. Crosby, C. I. Czimczik, G. Grosse, J. Harden, D. J. Hayes, G. Hugelius, J. D. Jastrow, J. B. Jones, T. Kleinen, C. D. Koven, G. Krinner, P. Kuhry, D. M. Lawrence, A. D. McGuire, S. M. Natali, J. A. O'Donnell, C. L. Ping, W. J. Riley, A. Rinke, V. E. Romanovsky, A. B. K. Sannel, C. Schädel, K. Schaefer, J. Sky, Z. M. Subin, C. Tarnocai, M. R. Turetsky, M. P. Waldrop,

K. M. Walter Anthony, K. P. Wickland, C. J. Wilson, and S. A. Zimov. 2013. Expert assessment of vulnerability of permafrost carbon to climate change. Climatic Change:1-16.

Schuur, E. A. G., J. Bockheim, J. G. Canadell, E. Euskirchen, C. B. Field, S. V. Goryachkin, S. Hagemann, P. Kuhry, P. M. Lafleur, H. Lee, G. Mazhitova, F. E. Nelson, A. Rinke, V. E. Romanovsky, N. Shiklomanov, C. Tarnocai, S. Venevsky, J. G. Vogel, and S. A. Zimov. 2008. Vulnerability of permafrost carbon to climate change: Implications for the global carbon cycle. Bioscience **58**:701-714.

Schuur, E. A. G., J. G. Vogel, K. G. Crummer, H. Lee, J. O. Sickman, and T. E. Osterkamp. 2009. The effect of permafrost thaw on old carbon release and net carbon exchange from tundra. Nature **459**:556-559.

Siciliano, S. D., W. K. Ma, S. Ferguson, and R. E. Farrell. 2009. Nitrifier dominance of Arctic soil nitrous oxide emissions arises due to fungal competition with denitrifiers for nitrate. Soil Biology & Biochemistry **41**:1104-1110.

Slater, A. G. and D. M. Lawrence. 2013. Diagnosing Present and Future Permafrost from Climate Models. Journal of Climate **26**:5608-5623.

Sommerkorn, M. 2008. Micro-topographic patterns unravel controls of soil water and temperature on soil respiration in three Siberian tundra systems. Soil Biology & Biochemistry **40**:1792-1802.

Stottlemyer, R. 2001. Biogeochemistry of a Treeline Watershed, Northwestern Alaska. J. Environ. Qual. **30**:1990-1998.

Sturm, M., J. P. McFadden, G. E. Liston, F. S. Chapin, C. H. Racine, and J. Holmgren. 2001. Snow-shrub interactions in Arctic tundra: A hypothesis with climatic implications. Journal of Climate **14**:336-344.

Sullivan, P. F. and B. Sveinbjornsson. 2010. Microtopographic Control of Treeline Advance in Noatak National Preserve, Northwest Alaska. Ecosystems **13**:275-285.

Tarnocai, C., J. G. Canadell, E. A. G. Schuur, P. Kuhry, G. Mazhitova, and S. Zimov. 2009. Soil organic carbon pools in the northern circumpolar permafrost region. Global Biogeochemical Cycles **23**:-.

Toolik Environmental Data Center Team. 2014. Meterological monitoring program at Toolik, Alaska. Toolik Field Station, Institute of Arctic Biology, University of Alaska Fairbanks, Fairbanks AK 99775.

Tsuyuzaki, S., T. Ishizaki, and T. Sato. 1999. Vegetation structure in gullies developed by the melting of ice wedges along Kolyma River, northern Siberia. Ecological Research **14**:385-391.

Vonk, J. E., L. Sanchez-Garcia, B. E. van Dongen, V. Alling, D. Kosmach, A. Charkin, I. P. Semiletov, O. V. Dudarev, N. Shakhova, P. Roos, T. I. Eglinton, A. Andersson, and O. Gustafsson. 2012. Activation of old carbon by erosion of coastal and subsea permafrost in Arctic Siberia. Nature **489**:137-140.

Walker, D. A., N. A. Auerbach, J. G. Bockheim, F. S. Chapin, W. Eugster, J. Y. King, J. P. McFadden, G. J. Michaelson, F. E. Nelson, W. C. Oechel, C. L. Ping, W. S. Reeburg, S. Regli, N. I. Shiklomanov, and G. L. Vourlitis. 1998. Energy and trace-gas fluxes across a soil pH boundary in the arctic. Nature **394**:469-472.

Walker, D. A., M. K. Raynolds, F. J. A. Daniels, E. Einarsson, A. Elvebakk, W. A. Gould, A. E. Katenin, S. S. Kholod, C. J. Markon, E. S. Melnikov, N. G. Moskalenko, S. S. Talbot, B. A. Yurtsev, and C. Team. 2005. The Circumpolar Arctic vegetation map. Journal of Vegetation Science **16**:267-282.

Walker, D. A., M. K. Raynolds, H. A. Maier, E. M. Barbour, and G. P. Neufeld. 2010. Circumpolar geobotanical mapping: a web-based plant-to-planet approach for vegetation-change analysis in the Arctic. Viten **1**:125-128.

Walter, K. M., M. E. Edwards, G. Grosse, S. A. Zimov, and F. S. Chapin. 2007. Thermokarst lakes as a source of atmospheric CH(4) during the last deglaciation. Science **318**:633-636.

Weintraub, M. N. and J. P. Schimel. 2003. Interactions between carbon and nitrogen mineralization and soil organic matter chemistry in arctic tundra soils. Ecosystems **6**:129-143.

Whalen, S. C. and J. C. Cornwell. 1985. Nitrogen, Phosphorus, and Organic Carbon Cycling in an Arctic Lake. Canadian Journal of Fisheries and Aquatic Sciences **42**:797-808.

WRCC. 2011. Western Regional Climate Center.

Yoshikawa, K. and L. D. Hinzman. 2003. Shrinking thermokarst ponds and groundwater dynamics in discontinuous permafrost near Council, Alaska. Permafrost and Periglacial Processes **14**:151-160.

Zhang, T., J. A. Heginbottom, R. G. Barry, and J. Brown. 2000. Further statistics on the distribution of permafrost and ground ice in the Northern Hemisphere. Polar Geography **24**:126-131.

Zhuang, Q., J. M. Melillo, M. C. Sarofim, D. W. Kicklighter, A. D. McGuire, B. S. Felzer, A. Sokolov, R. G. Prinn, P. A. Steudler, and S. Hu. 2006. CO2 and CH4 exchanges between land ecosystems and the atmosphere in northern high latitudes over the 21st century. Geophys. Res. Lett. **33**:L17403.

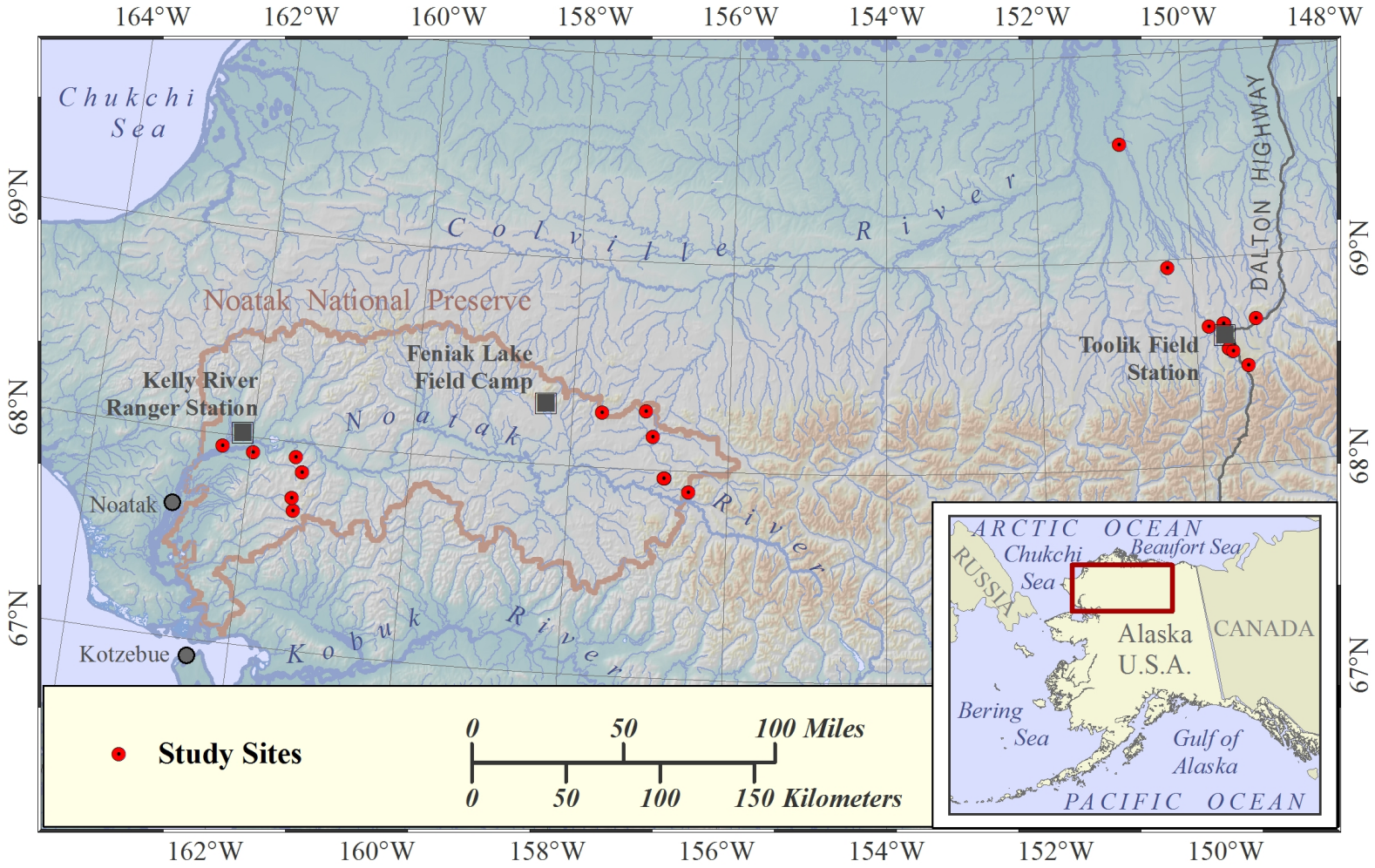

Figure 5.1 Map of study area. Features near the Kelly River Ranger Station were sampled in July of 2010, near Feniak Lake field camp in July of 2011, and near the Toolik Field Station in the summers of 2009-2012.

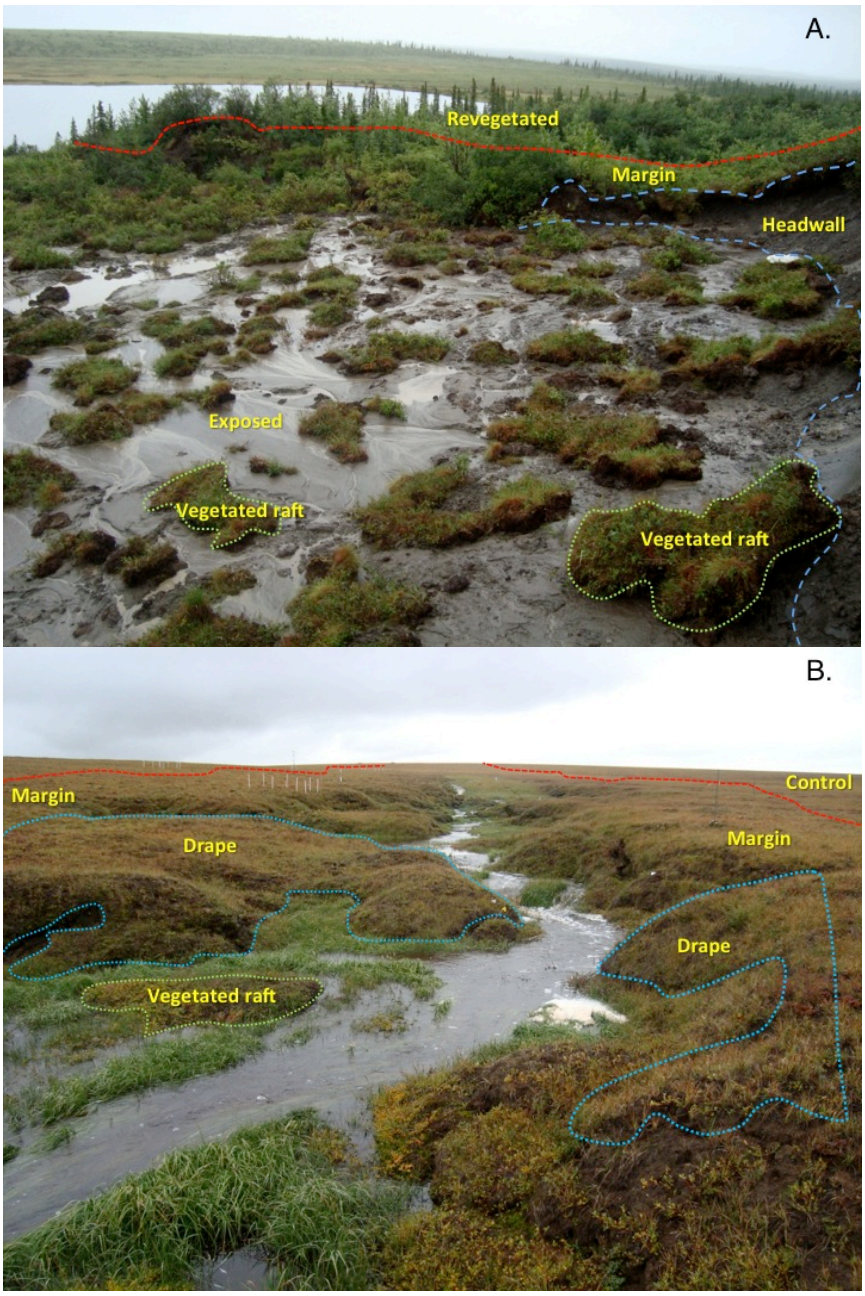

Figure 5.2 Ground cover classification based on type and severity of thermokarst impact for a thaw slump (A) and a thermo-erosion gully (B). Patches are defined as follows: C. Control tundra more than 5m outside any visible disturbance, M. Margin of feature within 1m of visible disturbance but not subsided, D. Drape of subsided vegetation still attached to surrounding tundra, V. Raft of detached vegetation on the feature floor, E. Exposed mineral soil.

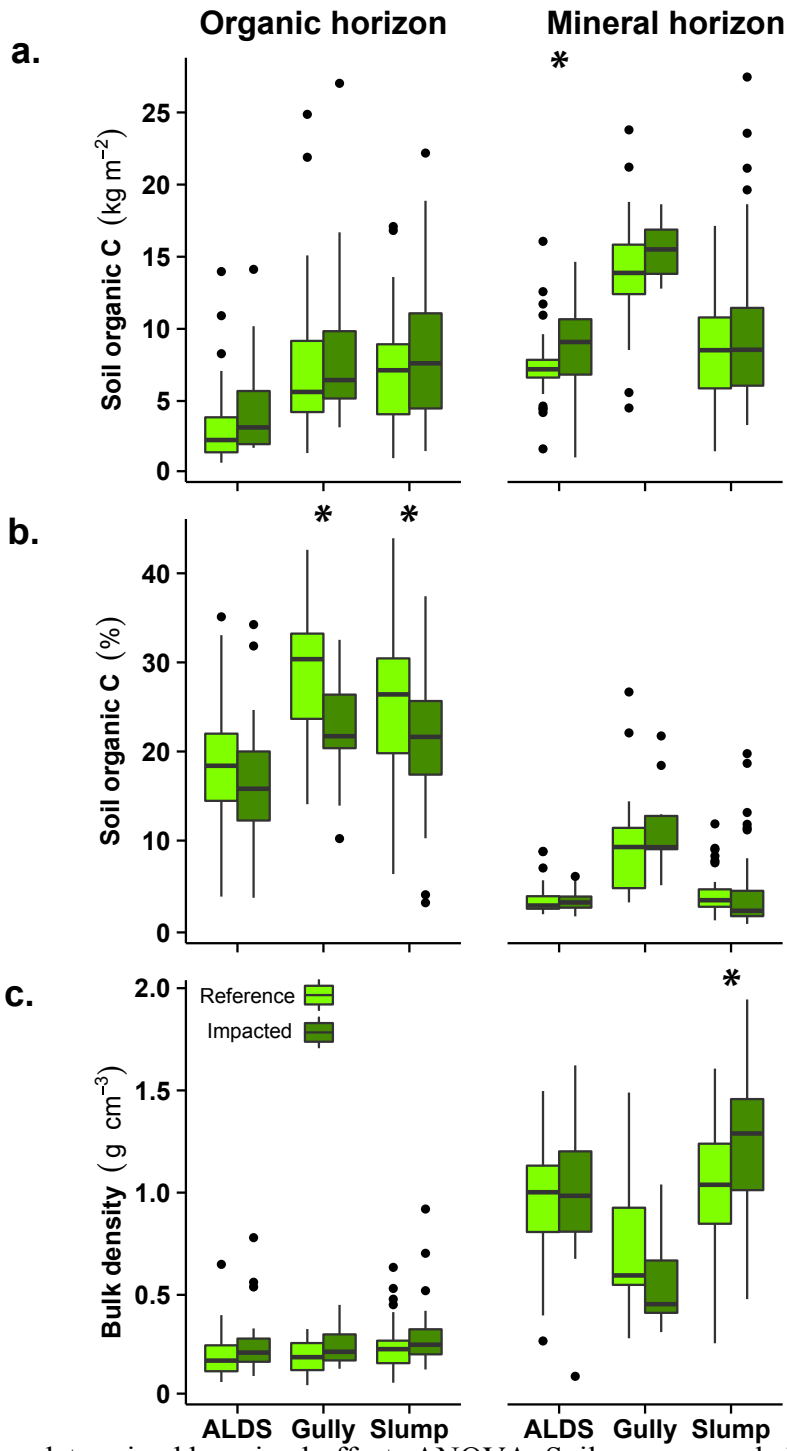

Figure 5.3 Organic carbon pools, percent, and bulk density in the top 35 cm of soil inside and outside seven active-layer detachment slides (ALDS), three thermo-erosion gullies, and sixteen retrogressive thaw slumps. Margin and control soils adjacent to features were compared to drape, exposed, raft, and revegetated soils within features (see Fig. 5.2 for complete patch definition). Total pools by horizon are the product of horizon depth, carbon content, and bulk density with mineral soils normalized to 35 cm. Significant differences denoted by * ($\alpha = 0.05$) as determined by mixed-effects ANOVA. Soils were sampled to 35cm with a hand corer. Data are from 425 individual cores collected at 354 individual locations distributed inside and around the 26 features. Box plots represent median, quartiles, minimum, and maximum within 1.5 times the interquartile range, and outliers beyond 1.5 interquartile range.

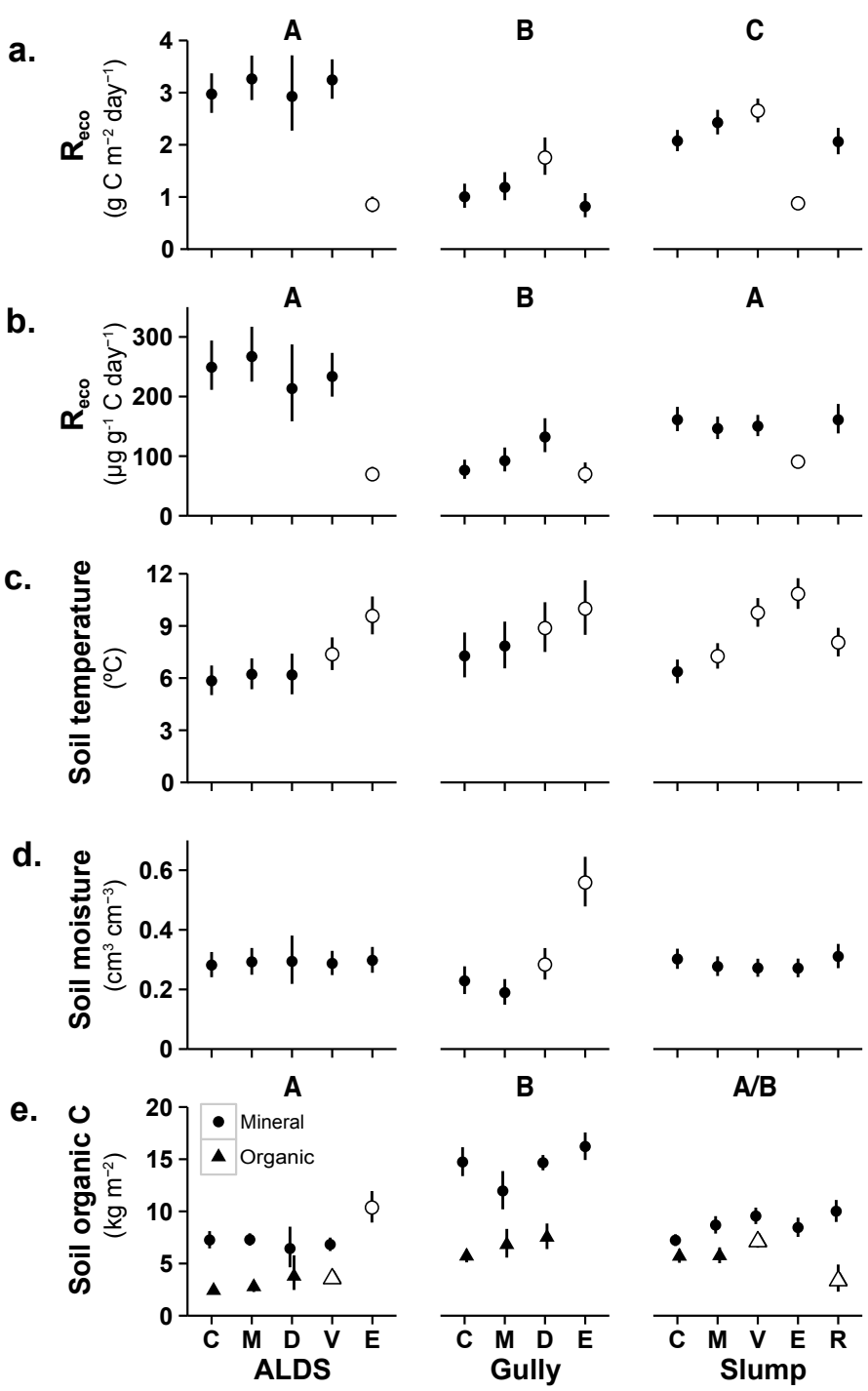

Figure 5.4 Mean (SE) ecosystem respiration (R_{eco}), heterotrophic respiration (R_h), and surface soil parameters by patch type for seven active-layer detachment slides (ALDS), three thermo-erosion gullies, and sixteen retrogressive thaw slumps. 1608 measurements were collected in the growing season from June-August (see Table 5.2 for sample size by patch). Open shapes signify statistical difference from control tundra (C) within each thermokarst morphology, $\alpha = 0.05$. Different letters above panels represent significant differences between morphologies. For complete patch definitions see Fig. 5.2 but M=margin, D=drape, V=vegetated raft, E=exposed mineral soil, and R=revegetated soil surface. Error bars represent SE estimated by mixed-effects ANOVA after accounting for between-site variability. Soil carbon pools are based on the data described in Fig. 5.3 and the dual lettering indicates that slumps differ from slides in organic but not mineral carbon content.

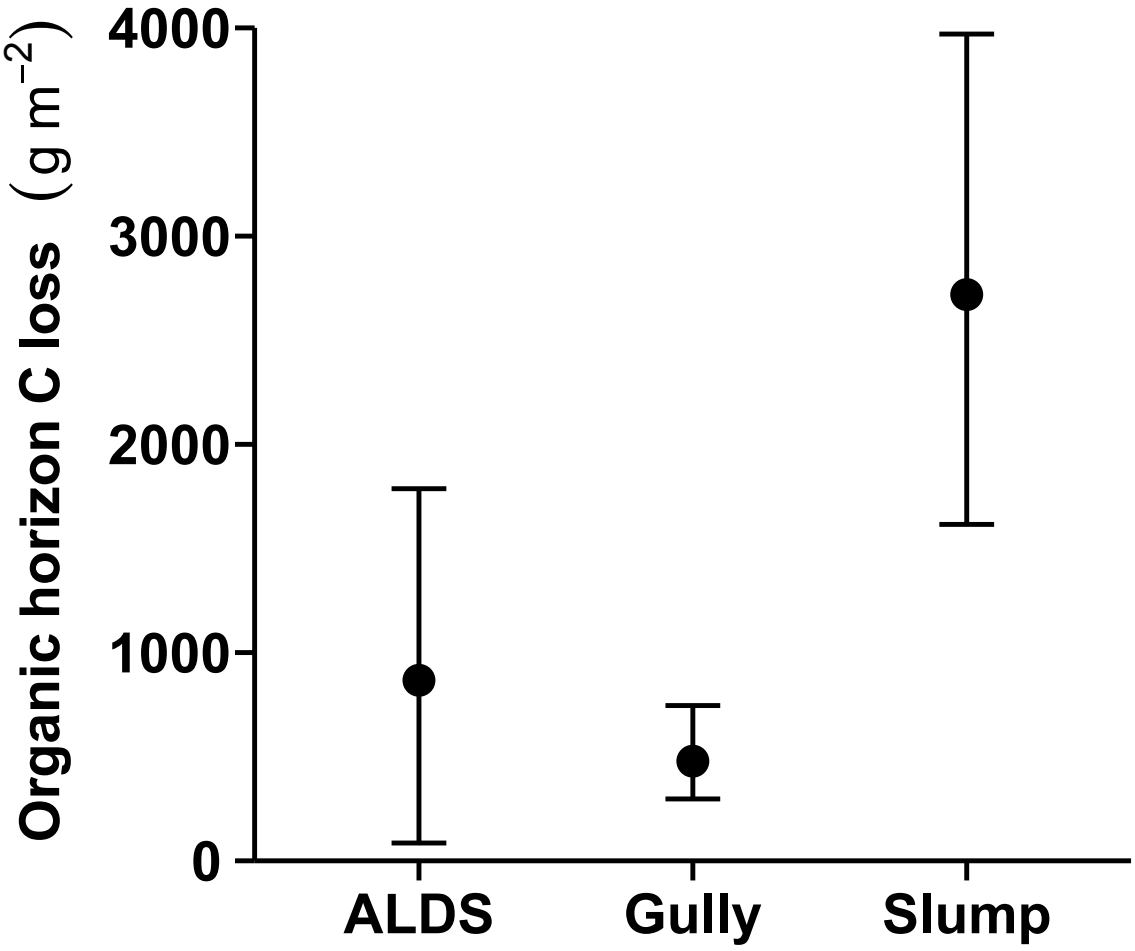

Figure 5.5 Carbon transported offsite from the organic horizon during formation of active-layer detachment slides (ALDS), thermo-erosion gullies, and thaw slumps. Loss was calculated from estimates of exposed soil area and changes in organic horizon carbon in residual soils (see Equation 1 and results for details). Error bars represent propagated SE.

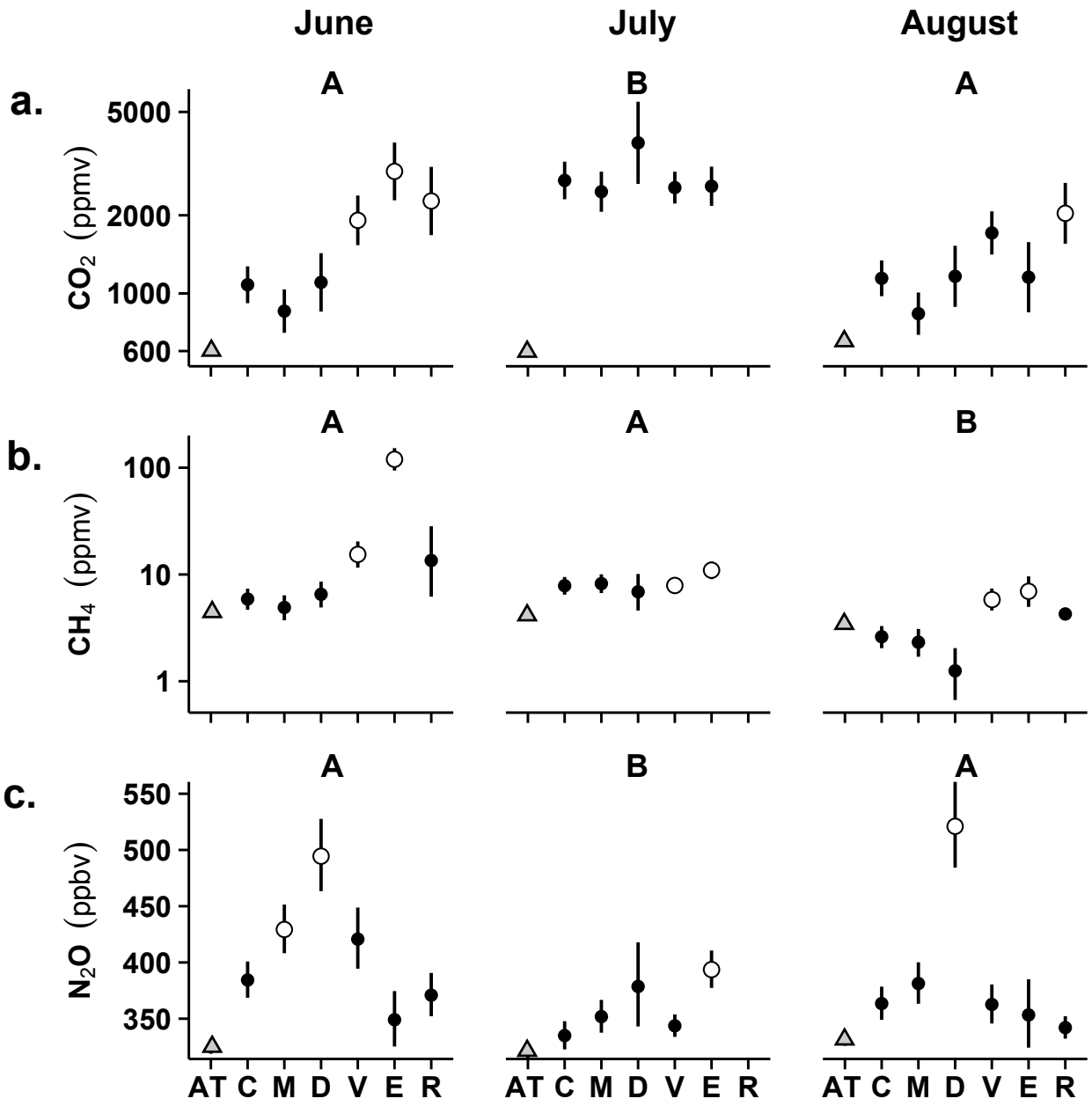

Figure 5.6 Seasonal patterns in soil gas concentration at 15 cm by patch type. Atmospheric gas concentration at time of sampling (AT) is represented by gray triangles. For complete patch definitions see Fig. 5.2 but M=margin, D=drape, V=vegetated raft, E=exposed mineral soil, and R=revegetated soil surface. Empty circles represent statistical difference from undisturbed tundra (C), $\alpha = 0.05$, as determined by mixed-effects ANOVA. 420 soil gas samples collected from 26 features were analyzed for all three gases. Note the log scale for CO_2 and CH_4, and the missing data for revegetated patches in July. Symbology is the same as Fig 5.4.

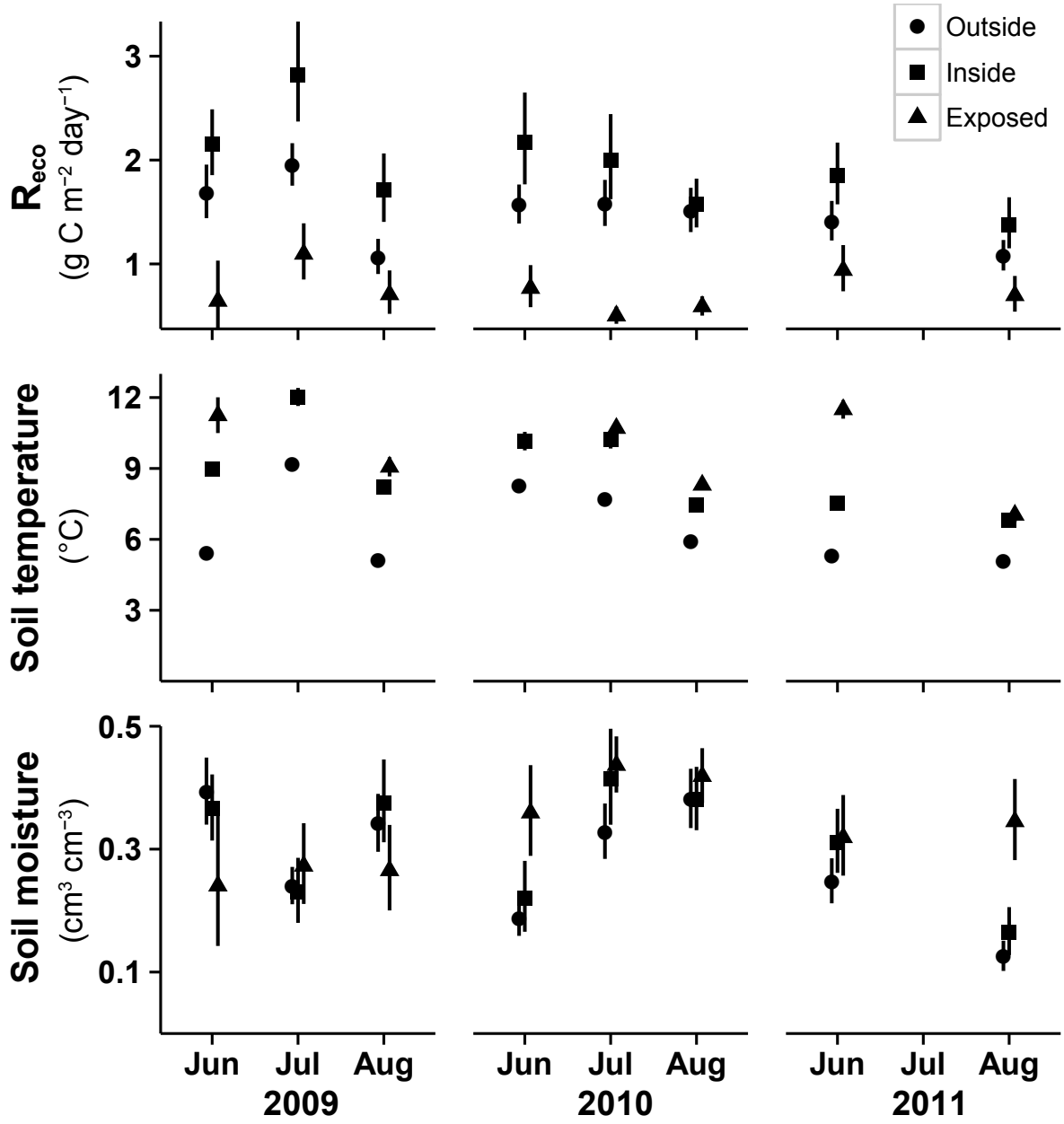

Figure 5.7 Mean (SE) seasonal and interannual variation in ecosystem respiration (R_{eco}), soil temperature, and soil moisture for two gullies and three slumps near the Toolik Field Station. The outside category comprises margin and control patches, inside includes drapes and rafts, and exposed is bare mineral soil. Data were not collected in July 2011 due to delayed arrival of equipment. Measurements were taken at ~250 locations between the five sites at each sampling.

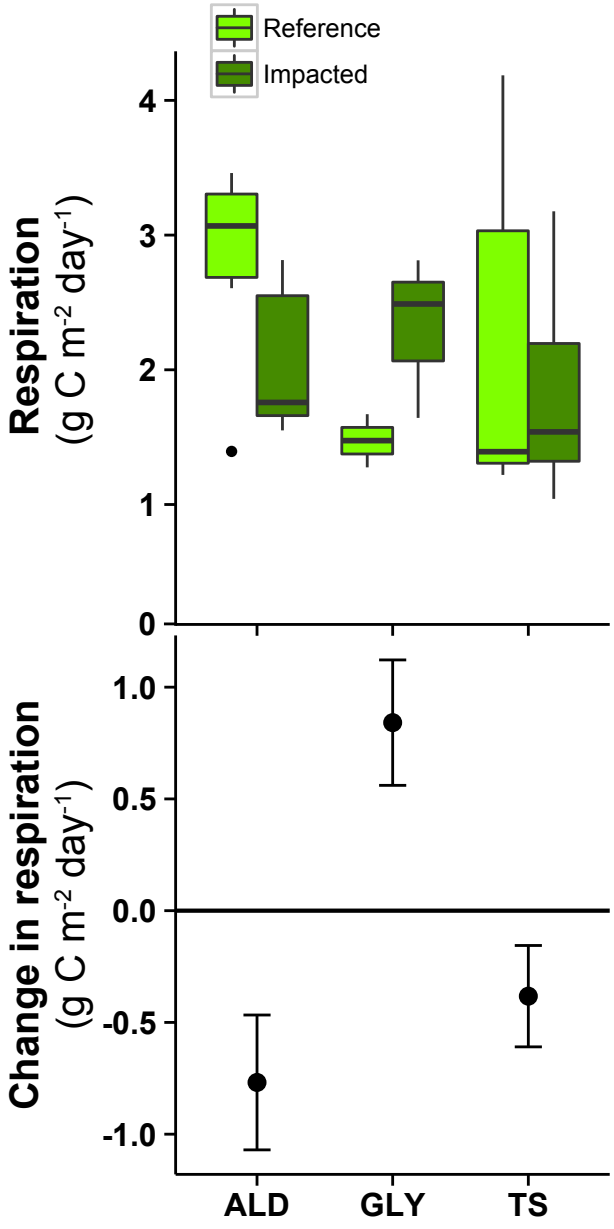

Figure 5.8 Distribution of ecosystem respiration at the feature level and mean (SE) of overall change in respiration due to thermokarst disturbance. Patch flux was weighted by percent coverage to estimate feature respiration (see methods for details). Symbology same as Fig 5.3.

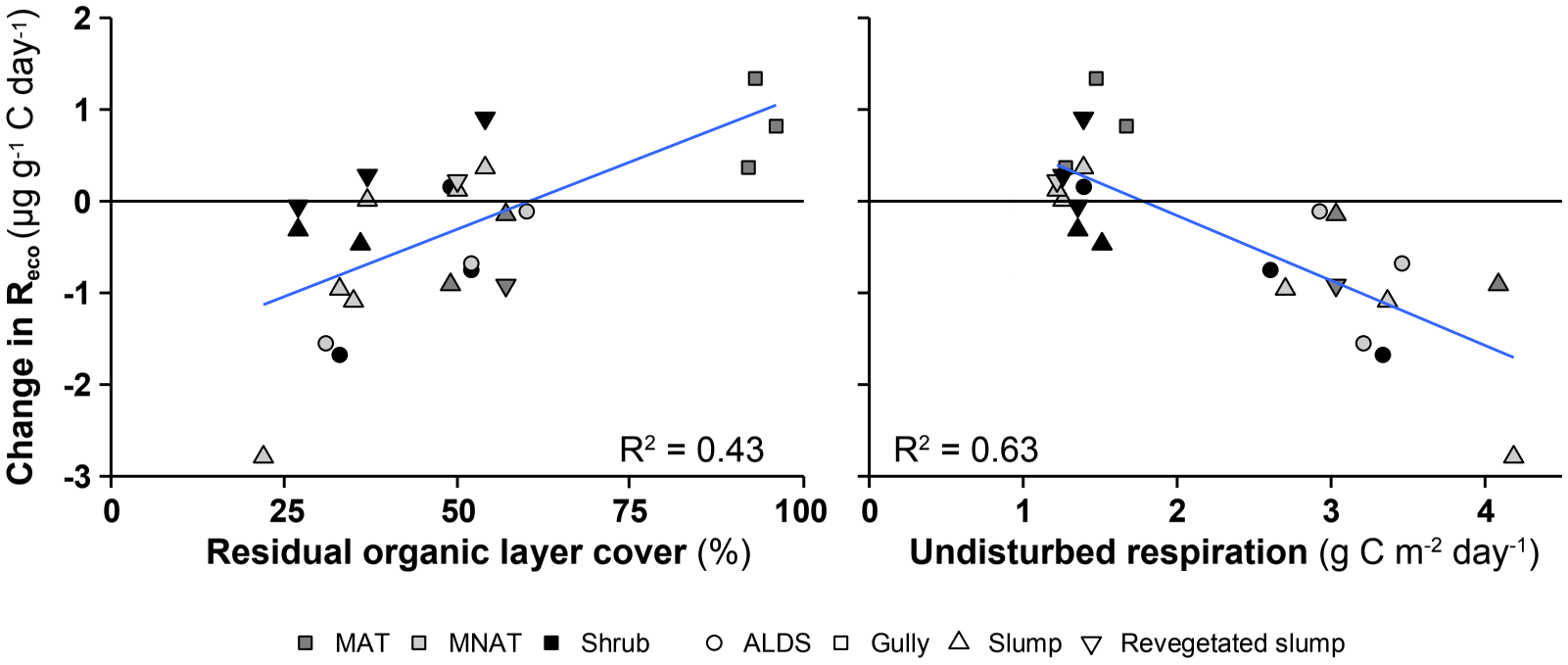

Figure 5.9 Linear regressions of change in feature-level respiration with percent cover of residual organic material (drapes + rafts) and undisturbed respiration rate from control patches. Shape represents feature type and shading represents vegetation: MAT= moist acidic tundra, MNAT = moist non-acidic tundra, and Shrub = shrub tundra. For multiple linear regression results consult text.

Table 5.1 Characteristics of 26 upland thermokarst features on the North Slope of Alaska

	Active-layer detachment slide	Thermo-erosion gully	Retrogressive thaw slump
Area (m^2)	16800 (3000)	4590 (1550)	17900 (4670)
Perimeter (m)	1091 (194)	567 (200)	652 (99)
Headwall retreat (m yr^{-1})	12.1 (5.1)	1.8 (0.33)	10.2 (2.8)
Active-layer SOC (kg m^{-2})	10.5 (0.4)	19.9 (0.8)	14.5 (0.5)
Organic horizon SOC (kg m^{-2})	3.3 (0.5)	7.5 (0.9)	6.9 (0.5)
Organic horizon depth (cm)	10.4 (1.0)	13.3 (1.0)	12.6 (0.8)
Groundcover within features (%)*			
Exposed	50 (5.6)	6.3 (1.2)	57 (4.7)
Vegetated raft	48 (5.3)	8.7 (6.4)	40 (3.7)
Drape	2 (1.1)	85 (8.7)	0.2 (0.2)
n	7	3	16
Mean period of activity (years)**	11 (8)	8 (5)	20 (10)

Values represent mean (SE). *see Fig. 5.2 for definition of groundcover classes. **period of activity was determined from published literature estimates and observations from this study and SE is a qualitative estimate of variation.

Table 5.2 Physical predictors of R_{eco} and soil concentrations of CO_2, N_2O, and CH_4

Variable	Patch	Fixed predictors*	Random predictors	n
R_{eco}	All	SC+TC+T-M^2-M+AT	Feature, Transect	1608
	C	T-TC-M^2-M+AT	Transect, Feature	431
	M	T-SC	Feature, Transect	315
	D	T-SC	Feature, Transect	132
	V	T-M^2+AT+M	Geology, Transect, Feature	342
	E	AT	Feature, Transect	287
	R	T-AT	Collar	121
CO_2		M+T-TC	Feature	399
N_2O		-M^2-SC-M	Geology, Feature	408
CH_4		M+T+M^2	Feature	400

*AT = air temperature, M = volumetric soil moisture, M^2= polynomial soil moisture term (centered and squared), SC = surface SOC (%), TC = total SOC (kg m^{-2}), T = soil temperature at 15 cm. Fixed predictors are ordered by the size of standardized coefficients. Random predictors are ordered by percent of residual variance explained. We used restricted maximum likelihood to compare models and performed an automated backwards elimination procedure to identify the most parsimonious model for each variable. The monomial moisture term was retained by default whenever the polynomial term was significant to determine the overall sign of the relationship.

Chapter 6. General conclusions

Climate is the strongest predictor of ecosystem type and function across latitudes (Chapin et al. 2011) and plays a particularly large role in the permafrost zone where not only ecosystem functioning but also the very stability of the ground depend on the persistence of cold. In this dissertation I investigated the potential and actual response of arctic and boreal net ecosystem carbon balance (NECB) to climate change. At a circumarctic scale I summarized current scientific understanding and identified uncertainties in the response of biomass, fire, and hydrologic carbon flux to warming over the next several centuries. This work revealed that little agreement exists on the magnitude and even sign of change in high-latitude biomass, and that most researchers expect fire emissions and hydrologic carbon release to exceed net ecosystem productivity by the end of the century, accelerating the release of permafrost carbon to the atmosphere. At a plot and regional scale I tested the effect of permafrost collapse (thermokarst) on carbon and nutrient release from upland tundra on the North Slope of Alaska. I demonstrated that thermokarst can stimulate or suppress ecosystem respiration depending on feature morphology; remove a large portion of ecosystem carbon; mobilize highly biodegradable dissolved organic carbon (DOC); disrupt the nitrogen cycle resulting in hydrologic and gaseous nitrogen export; and influence offsite organic matter decomposition by the release of labile DOC, nitrogen, and other nutrients. In this chapter I summarize five key findings from each component of my work and address a few overarching conclusions and implications.

6.1 Summary

6.1.1 Can increased biomass offset carbon release from soils, streams, and wildfire across the permafrost region? An expert elicitation.

- Expert estimates of the response of arctic and boreal biomass to warming differed fundamentally from current model projections and revealed little agreement on the magnitude or even sign of the response. Water-stress, disturbance, and nutrient limitation largely counteract the effects of CO_2 fertilization and extended growing season for higher warming scenarios. Boreal and arctic biomass may offset much or all of mid-century emissions from permafrost-region soil for lower warming scenarios. However, permafrost soil carbon release strongly outstrips projected carbon gains for all scenarios by 2100.

- Experts projected major changes in fire regime, with up to a seven-fold increase in fire emissions by 2100 for the business-as-usual human emissions scenario. While the boreal forest dominated total wildfire emissions, relative change was much greater for tundra fire, with 4- to 11-fold increases projected by 2100. Estimates of total emissions fell within the range of current model projections.
- Estimates of hydrologic carbon transport from the circumarctic watershed represent the first published projections of system response to warming, and are therefore difficult to put in context. Experts estimated up to a 3-fold increase in hydrologic carbon flux; however, 21% of experts predicted no change or a decrease in DOC, attributed to permafrost degradation, changes in hydrologic flowpath, and changes in carbon photo- and bio-lability.
- Experts identified water balance, vegetation shifts, and disturbance such as thermokarst and wildfire as the largest sources of uncertainty in predicting the response of permafrost carbon balance to climate change.
- Combining my results with previous findings suggests that net permafrost carbon emissions will be four times higher for the business-as-usual scenario than for a scenario of active reduction of human emissions. This suggests that 75% of permafrost-region emissions can still be prevented.

6.1.2 Elevated dissolved organic carbon biodegradability from thawing and collapsing permafrost

- DOC from upland thermokarst is some of the most biodegradable reported in natural systems. DOC in outflow from active features dropped 41% during a 40-day incubation, indicating a biodegradable pool approximately four-fold higher than in reference water. However, elevated biodegradable DOC (BDOC) only persisted during active permafrost degradation, with a return to pre-disturbance levels once thermokarst features stabilized.
- BDOC was correlated with both chemical composition and nutrients, with 83% of the variability in DOC biodegradability explained by these parameters. However, nutrient addition did not increase overall BDOC, indicating this is not a causal relationship.

- Differences in the biodegradability of DOC released from thaw slumps and thermo-erosion gullies suggest that ground ice type influences BDOC. Because thaw slumps, which had the highest concentrations of BDOC, can remain active for decades and a single feature can impact kilometers of stream reach, this form of permafrost degradation may have a particularly large impact on aquatic carbon cycling.
- Permafrost DOC is simultaneously more processed and more biodegradable than the surface sources from which it derives. This may be due to:
    - Preferential removal of hydrophobic carbon species, which tend to be recalcitrant, by adsorption to mineral soils
    - Incorporation of bioavailable compounds released from the microbial community during freeze-thaw cycles into permafrost
    - Biodegradable contributions from sub-zero microbial metabolism
    - Permafrost DOC derives from paleo-communities of vegetation with higher biodegradability than modern vegetation

6.1.3 Patterns and persistence of hydrologic carbon and nutrient export from collapsing permafrost

- Thermo-erosion gullies, retrogressive thaw slumps, and active-layer detachment slides resulted in substantial increases in elevated carbon and nutrient release during formation but the magnitude and persistence of these fluxes varied by feature type. Thaw slumps and gullies, which expose deeper permafrost soil had a larger impact on solute concentrations than slides.
- Contrary to our hypothesis, elevated carbon and nutrient release persisted during revegetation for some feature types, potentially due to physiological constraints of the plant community or spatial or temporal mismatch between nutrient supply and demand.
- The 90% decrease in dissolved CH_4 in gullies and slumps may be due to high concentrations of sulfate and inorganic nitrogen. Sulfate release from thaw slumps appears to be widespread across the arctic and could accelerate anaerobic decomposition of organic matter in lake sediments and decrease CH_4 production.

- The chemical signature of thermokarst outflow matches landscape-level shifts in inland water chemistry observed across the Arctic such as shifts in DOC composition and increasing inorganic nitrogen and solute loads. These changes have primarily been attributed to mechanisms associated with gradual thaw such as deepening of surface flowpaths and changes in residence time. However, thermokarst may also be contributing to these shifts in catchment-scale chemistry.
- Spatial patterns of carbon and nutrient export from thermokarst suggest that upland thermokarst may be a dominant linkage between terrestrial and aquatic ecosystems as the arctic warms and that the biogeochemical impacts of this disturbance will be modulated by feature morphology and position in the landscape.

6.1.4 Upland permafrost collapse stimulates N_2O production but effect on growing season respiration depends on thermokarst morphology

- Upland thermokarst removed 6-51% of organic-layer carbon, but mineral soil loss likely constitutes the bulk of carbon displacement.
- Thermokarst morphology determined both the initial displacement of organic matter and strongly subsequent elemental cycling. Gullies removed the least organic-layer carbon but most strongly impacted post-failure carbon and nitrogen dynamics.
- Feature respiration was positively correlated with amount of residual organic matter and negatively correlated with pre-disturbance respiration. Because these parameters are either known for typical tundra types or can be remotely sensed, these relationships may be useful in incorporating thermokarst effects on carbon cycling into numerical models.
- Elevated N_2O in gully soils persisted through most of the growing season indicating nitrification and denitrification in disturbed soils. This is one of the first observations of sustained N_2O production in upland tundra, which is typically strongly nitrogen-limited, and represents a potentially important non-carbon permafrost climate feedback.
- Because organic carbon displaced by thermokarst is not immediately released to the atmosphere, the impact of upland thermokarst on NECB depends on the rate

of offsite processing as well as the rate and degree of revegetation after disturbance.

6.2 General conclusions

One pattern emerging from these findings is that carbon balance in the permafrost zone will be directly coupled to nutrient dynamics, including nitrogen and sulfur. For example, not only can nitrogen feedback directly to climate via N_2O release from upland thermokarst, but the availability of nitrogen can modulate the response of arctic and boreal biomass to CO_2 fertilization, accelerate organic matter mineralization (Mack et al. 2004, Nowinski et al. 2008), and affect aquatic processing of carbon after permafrost thaw. Several lines of evidence suggest that these indirect effects of nitrogen may not stimulate increased carbon uptake. First, the widespread hydrologic and gaseous release of nitrogen suggests that while permafrost degradation causes an opening of the nitrogen cycle, much of this nitrogen is lost from terrestrial ecosystems before uptake by plants. Second, phosphorus, not nitrogen, is typically the most limiting nutrient in Arctic freshwater systems (Slavik et al. 2004, O'Brien et al. 2005), though nitrogen limits productivity in Arctic estuaries and the Arctic Ocean (McClelland et al. 2012, Vancoppenolle et al. 2013). If thermokarst nitrogen release is accompanied by bioavailable phosphorus, more nitrogen will be retained in inland aquatic ecosystems, whereas if thermokarst outflows have relatively little phosphorus, a larger proportion of liberated nitrogen will reach the ocean or be denitrified. The widespread release of SO_4^{2-} from upland thermokarst may have important implications for carbon cycling, simultaneously accelerating anaerobic decomposition of organic carbon liberated from permafrost and suppressing CH_4 production in receiving ecosystems, modulating key feedbacks from the permafrost system on global climate. The disregard of these and other multi-element interactions leads to inaccurate and sometimes unrealistic model projections of the response of permafrost NECB to climate change. I therefore suggest that we replace the mono-elemental term "permafrost carbon feedback" with "permafrost climate feedback" to emphasize the importance of considering direct and indirect non-carbon linkages between the permafrost zone and global climate.

Another theme from my work is the importance of ecosystem disturbance in determining NECB. Wildfire and thermokarst are the dominant forms of disturbance in boreal and arctic systems, respectively (Kasischke and Turetsky 2006, Kokelj and Jorgenson 2013). Some coupled

climate models do not include wildfire and virtually none include thermokarst. Every model is necessarily a simplification of the infinite complexity that exists in real earth systems. However, wildfire and thermokarst affect large portions of the landscape, causing profound alterations in elemental cycles, and therefore must be included in simulations of future carbon balance. For example the large difference between biomass projected by models and estimates from experts, which was due largely to the exclusion or inclusion of disturbance, demonstrates a disconnection between how we think the system works (or rather, will work) and what processes are adequately conceptualized (simplified) to include in quantitative simulations. The lack of conceptualization of upland thermokarst processes has been a major obstacle to incorporating this disruptive process in coupled carbon models (Schuur et al. 2008, Qian et al. 2010, Koven et al. 2011), though recent work, including this dissertation, is bridging this gap.

Because no process-based estimates of landscape-level carbon and nutrient fluxes from upland thermokarst exist, I present a first order regional and circumarctic extrapolation of my findings in Table 6.1 (assumptions described in Appendix 6.0). This scaling exercise suggests that upland thermokarst could displace 120-1200 Tg of organic-layer carbon by the end of the century, and 5-100 times this amount from mineral horizons based on qualitative estimates of mineral soil carbon loss in Chapter 5. Though upland thermokarst is only expected to directly impact 3% of the total circumarctic watershed, it may cause a 2.7-23% increase in annual circumarctic DOC flux and a 2.2-19% increase in dissolved inorganic nitrogen averaged over the 2050-2100. While these fluxes are highly speculative, they underline the potential of this spatially limited disturbance to influence landscape-level NECB.

The permafrost climate feedback has been portrayed in popular media (and to a lesser extent in peer-reviewed literature) as an all-or-nothing scenario. Permafrost greenhouse gas release has been described as a tipping point, a runaway climate feedback, and most dramatically a time bomb (Wieczorek et al. 2011, Treat and Frolking 2013, Whiteman et al. 2013). On the other extreme, some have dismissed the importance of this feedback, asserting that increases in biomass will offset any carbon losses from soil, or that changes will occur too slowly to concern current governments (Idso et al. 2014). Fortunately, or unfortunately depending on your perspective, the permafrost climate feedback does not depend on public opinion. As one reluctant survey participant protested, "You can't decide how much carbon is going to come out

of permafrost with a vote." While the size and momentum of the permafrost region mean that changes set in motion will likely be difficult to reverse, results from this work show that experts believe the strength of the permafrost climate feedback depends on human emissions. Estimates of carbon release (Schuur et al. 2013) minus increases in biomass indicate a four-fold difference in net permafrost emissions between warming scenarios based on sustained human emissions versus the cessation of emissions before 2100. This indicates that three-quarters of permafrost carbon release could be avoided, though the window of opportunity to keep that carbon in the ground is rapidly closing.

The permafrost region has responded differently to various climatic perturbations in the past, providing insight into possible future response (Zachos et al. 2008). While average global temperature increased 5°C during the Paleocene-Eocene Thermal Maximum (PETM), high-latitude warming was in excess of 10°C due to loss of sea ice, changes in stratospheric clouds, and changes in land surface albedo (Sloan and Pollard 1998, Zachos et al. 2001)—the same mechanisms responsible for current polar amplification of global warming (Holland and Bitz 2003). This warming caused almost complete loss of permafrost and the mineralization of most permafrost soil organic matter (Bowen and Zachos 2010, DeConto et al. 2012). More recently, the 2-4°C warming at high-latitudes during the early Holocene caused active-layer deepening throughout the permafrost region but did not trigger complete permafrost loss or widespread carbon release (French 1999, Schirrmeister et al. 2002). While there are many differences between the Paleozoic and Holocenic warming events, one clear distinction is the degree of warming. While the initial warming phase of both events lasted a few thousand years, there may have been a tipping point somewhere between 4 and 10°C of high-latitude warming. Temperature increase during the PETM reached a point of no return, potentially when the permafrost climate feedback overpowered short-term stabilizing feedbacks such as marine CO_2 dissolution, whereas the surficial thaw during the Holocene did not surpass the resilience of the permafrost system. If this tipping point exists it falls between representative concentration pathway (RCP) scenarios RCP4.5 and RCP8.5 from the IPCC Fifth Assessment Report, representing maximum atmospheric CO_2 of 650 and 850 ppm, respectively (Moss et al. 2010, Lawrence et al. 2012). RCP4.5 is still widely accepted as politically and technically attainable, though it assumes global CO_2 emissions peak before 2050 and decrease by half by 2080 (Moss et al. 2010).

The degradation of permafrost and widespread ecosystem shifts projected across the circumarctic watershed will influence many biogeochemical cycles and trigger multiple disturbance agents simultaneously. Climate-change-driven feedbacks in complex earth systems are not, and cannot be, precisely and definitively modeled. This fact is not reason to dismiss current findings and hypotheses, but increases the urgency and importance of early action. Uncertainty justifies heightened precaution, not disregard (Kriebel et al. 2001).

In some ways the vast and diverse boreal and arctic system can be resistant to disturbance and slow to react to perturbation. Deep permafrost has incredible thermal inertia that only responds to changes at the surface on centennial to millennial timescales. Other aspects of this system, such as near-surface permafrost, can be sensitive bellwethers that respond rapidly to direct human disturbance or changes in climate. Arctic and boreal ecosystems resemble human society in this regard. I look to the future with faith and hope that we can respond rather than ignore, and recognize our common interest in preserving these frozen places.

6.3 References

Abbott, B. W., J. R. Larouche, J. B. Jones, W. B. Bowden, and A. W. Balser. 2014. Elevated dissolved organic carbon biodegradability from thawing and collapsing permafrost. Journal of Geophysical Research: Biogeosciences:2014JG002678.

ACIA. 2005. Arctic Climate Impacts Assessment. Cambridge University Press, Cambridge, United Kingdom.

AMAP. 2011. Snow, Water, Ice and Permafrost in the Arctic (SWIPA): Climate Change and the Cryosphere. Arctic Monitoring and Assessment Programme (AMAP). Oslo, Norway.

Aufdenkampe, A. K., E. Mayorga, P. A. Raymond, J. M. Melack, S. C. Doney, S. R. Alin, R. E. Aalto, and K. Yoo. 2011. Riverine coupling of biogeochemical cycles between land, oceans, and atmosphere. Frontiers in Ecology and the Environment **9**:53-60.

Avis, C. A., A. J. Weaver, and K. J. Meissner. 2011. Reduction in areal extent of high-latitude wetlands in response to permafrost thaw. Nature Geosci **4**:444-448.

Balser, A. W., J. B. Jones, and R. Gens. 2014. Timing of retrogressive thaw slump initiation in the Noatak Basin, northwest Alaska, USA. Journal of Geophysical Research: Earth Surface **119**:2013JF002889.

Balshi, M. S., A. D. McGuire, P. Duffy, M. Flannigan, D. W. Kicklighter, and J. Melillo. 2009. Vulnerability of carbon storage in North American boreal forests to wildfires during the 21st century. Global Change Biology **15**:1491-1510.

Balshi, M. S., A. D. McGuire, Q. Zhuang, J. Melillo, D. W. Kicklighter, E. Kasischke, C. Wirth, M. Flannigan, J. Harden, J. S. Clein, T. J. Burnside, J. McAllister, W. A. Kurz, M. Apps, and A. Shvidenko. 2007. The role of historical fire disturbance in the carbon dynamics of the pan-boreal region: A process-based analysis. Journal of Geophysical Research-Biogeosciences **112**:-.

Battin, T. J., S. Luyssaert, L. A. Kaplan, A. K. Aufdenkampe, A. Richter, and L. J. Tranvik. 2009. The boundless carbon cycle. Nature Geosci **2**:598-600.

Belshe, E. F., E. A. G. Schuur, and B. M. Bolker. 2013a. Tundra ecosystems observed to be CO2 sources due to differential amplification of the carbon cycle. Ecology Letters **16**:1307-1315.

Belshe, E. F., E. A. G. Schuur, and G. Grosse. 2013b. Quantification of upland thermokarst features with high resolution remote sensing. Environmental Research Letters **8**.

Bockheim, J. G. 2007. Importance of cryoturbation in redistributing organic carbon in permafrost-affected soils. Soil Science Society of America Journal **71**:1335-1342.

Bowden, W. B., M. N. Gooseff, A. Balser, A. Green, B. J. Peterson, and J. Bradford. 2008. Sediment and nutrient delivery from thermokarst features in the foothills of the North Slope, Alaska: Potential impacts on headwater stream ecosystems. Journal of Geophysical Research-Biogeosciences **113**.

Bowen, G. J. and J. C. Zachos. 2010. Rapid carbon sequestration at the termination of the Palaeocene-Eocene Thermal Maximum. Nature Geoscience **3**:866-869.

Brown, J., J. O.J. Ferrians, J. A. Heginbottom, and E. S. Melnikov. 1998. Digital Circum-Arctic Map of Permafrost and Ground-Ice Conditions. International Permafrost Association, Data and Information Working Group, comp.

Burn, C. R. 2000. The thermal regime of a retrogressive thaw slump near Mayo, Yukon Territory. Canadian Journal of Earth Sciences **37**:967-981.

Chapin, F. S., P. A. Matson, and P. M. Vitousek. 2011. Principles of terrestrial ecosystem ecology. 2nd edition. Springer, New York.

Chapin, F. S., A. D. McGuire, R. W. Ruess, T. N. Hollingsworth, M. C. Mack, J. F. Johnstone, E. S. Kasischke, E. S. Euskirchen, J. B. Jones, M. T. Jorgenson, K. Kielland, G. P. Kofinas, M. R. Turetsky, J. Yarie, A. H. Lloyd, and D. L. Taylor. 2010. Resilience of Alaska's boreal forest to climatic change. Canadian Journal of Forest Research-Revue Canadienne De Recherche Forestiere **40**:1360-1370.

Chapin, F. S., G. M. Woodwell, J. T. Randerson, E. B. Rastetter, G. M. Lovett, D. D. Baldocchi, D. A. Clark, M. E. Harmon, D. S. Schimel, R. Valentini, C. Wirth, J. D. Aber, J. J. Cole, M. L. Goulden, J. W. Harden, M. Heimann, R. W. Howarth, P. A. Matson, A. D. McGuire, J. M. Melillo, H. A. Mooney, J. C. Neff, R. A. Houghton, M. L. Pace, M. G. Ryan, S. W. Running, O. E. Sala, W. H. Schlesinger, and E. D. Schulze. 2006. Reconciling carbon-cycle concepts, terminology, and methods. Ecosystems **9**:1041-1050.

Cole, J. J., Y. T. Prairie, N. F. Caraco, W. H. McDowell, L. J. Tranvik, R. G. Striegl, C. M. Duarte, P. Kortelainen, J. A. Downing, J. J. Middelburg, and J. Melack. 2007. Plumbing the global carbon cycle: Integrating inland waters into the terrestrial carbon budget. Ecosystems **10**:171-184.

Cory, R. M., B. C. Crump, J. A. Dobkowski, and G. W. Kling. 2013. Surface exposure to sunlight stimulates CO2 release from permafrost soil carbon in the Arctic. Proceedings of the National Academy of Sciences of the United States of America **110**:3429-3434.

Davidson, E. A. and I. A. Janssens. 2006. Temperature sensitivity of soil carbon decomposition and feedbacks to climate change. Nature **440**:165-173.

DeConto, R. M., S. Galeotti, M. Pagani, D. Tracy, K. Schaefer, T. J. Zhang, D. Pollard, and D. J. Beerling. 2012. Past extreme warming events linked to massive carbon release from thawing permafrost (vol 484, pg 87, 2012). Nature **490**:292-292.

DeMarco, J., M. C. Mack, and M. S. Bret-Harte. 2011. The Effects of Snow, Soil Microenvironment, and Soil Organic Matter Quality on N Availability in Three Alaskan Arctic Plant Communities. Ecosystems **14**:804-817.

Euskirchen, E. S., A. D. McGuire, D. W. Kicklighter, Q. Zhuang, J. S. Clein, R. J. Dargaville, D. G. Dye, J. S. Kimball, K. C. McDonald, J. M. Melillo, V. E. Romanovsky, and N. V. Smith. 2006. Importance of recent shifts in soil thermal dynamics on growing season length, productivity, and carbon sequestration in terrestrial high-latitude ecosystems. Global Change Biology **12**:731-750.

Field, C. B., D. B. Lobell, H. A. Peters, and N. R. Chiariello. 2007. Feedbacks of terrestrial ecosystems to climate change. Annual Review of Environment and Resources **32**:1-29.

Flannigan, M., B. Stocks, M. Turetsky, and M. Wotton. 2009a. Impacts of climate change on fire activity and fire management in the circumboreal forest. Global Change Biology **15**:549-560.

Flannigan, M. D., M. A. Krawchuk, W. J. de Groot, B. M. Wotton, and L. M. Gowman. 2009b. Implications of changing climate for global wildland fire. International Journal of Wildland Fire **18**:483-507.

Fortier, D., M. Allard, and Y. Shur. 2007. Observation of rapid drainage system development by thermal erosion of ice wedges on Bylot island, Canadian Arctic Archipelago. Permafrost and Periglacial Processes **18**:229-243.

French, H. M. 1999. Past and present permafrost as an indicator of climate change. Polar Research **18**:269-274.

Frey, K. E. and J. W. McClelland. 2009. Impacts of permafrost degradation on arctic river biogeochemistry. Hydrological Processes **23**:169-182.

Frey, K. E. and L. C. Smith. 2005. Amplified carbon release from vast West Siberian peatlands by 2100. Geophysical Research Letters **32**:-.

Giesler, R., S. W. Lyon, C. M. Morth, J. Karlsson, E. M. Karlsson, E. J. Jantze, G. Destouni, and C. Humborg. 2014. Catchment-scale dissolved carbon concentrations and export estimates across six subarctic streams in northern Sweden. Biogeosciences **11**:525-537.

Godin, E. and D. Fortier. 2012. Geomorphology of a thermo-erosion gully, Bylot Island, Nunavut, Canada. Canadian Journal of Earth Sciences **49**:979-986.

Grosse, G., J. Harden, M. Turetsky, A. D. McGuire, P. Camill, C. Tarnocai, S. Frolking, E. A. G. Schuur, T. Jorgenson, S. Marchenko, V. Romanovsky, K. P. Wickland, N. French, M. Waldrop, L. Bourgeau-Chavez, and R. G. Striegl. 2011. Vulnerability of high-latitude soil organic carbon in North America to disturbance. Journal of Geophysical Research-Biogeosciences **116**.

Harden, J. W., C. D. Koven, C.-L. Ping, G. Hugelius, A. David McGuire, P. Camill, T. Jorgenson, P. Kuhry, G. J. Michaelson, J. A. O'Donnell, E. A. G. Schuur, C. Tarnocai, K. Johnson, and G. Grosse. 2012. Field information links permafrost carbon to physical vulnerabilities of thawing. Geophysical Research Letters **39**:L15704.

Harms, T., B. Abbott, and J. Jones. 2013. Thermo-erosion gullies increase nitrogen available for hydrologic export. Biogeochemistry:1-13.

Hartley, I. P., M. H. Garnett, M. Sommerkorn, D. W. Hopkins, B. J. Fletcher, V. L. Sloan, G. K. Phoenix, and P. A. Wookey. 2012. A potential loss of carbon associated with greater plant growth in the European Arctic. Nature Climate Change **2**:875-879.

Hinkel, K. M. and F. E. Nelson. 2003. Spatial and temporal patterns of active layer thickness at Circumpolar Active Layer Monitoring (CALM) sites in northern Alaska, 1995-2000. Journal of Geophysical Research-Atmospheres **108**.

Hobbie, S. E. and L. Gough. 2002. Foliar and soil nutrients in tundra on glacial landscapes of contrasting ages in northern Alaska. Oecologia **131**:453-462.

Holland, M. M. and C. M. Bitz. 2003. Polar amplification of climate change in coupled models. Climate Dynamics **21**:221-232.

Holmes, R. M., J. W. McClelland, B. J. Peterson, S. E. Tank, E. Bulygina, T. I. Eglinton, V. V. Gordeev, T. Y. Gurtovaya, P. A. Raymond, D. J. Repeta, R. Staples, R. G. Striegl, A. V. Zhulidov, and S. A. Zimov. 2012. Seasonal and Annual Fluxes of Nutrients and Organic

Matter from Large Rivers to the Arctic Ocean and Surrounding Seas. Estuaries and Coasts **35**:369-382.

Idso, C. D., S. B. Idso, R. M. Carter, and S. F. Singer. 2014. Climate Change Reconsidered: Biological Impacts. Heartland Institute, Chicago, Illinois, U.S.A.

IPCC. 2007. Intergovernmental Panel on Climate Change Fourth Assessment Report (AR 4). Fourth Assessment Report (AR4):212.

Jahn, M., T. Sachs, T. Mansfeldt, and M. Overesch. 2010. Global climate change and its impacts on the terrestrial Arctic carbon cycle with special regards to ecosystem components and the greenhouse-gas balance. Journal of Plant Nutrition and Soil Science **173**:627-643.

Jensen, A. E., K. A. Lohse, B. T. Crosby, and C. I. Mora. 2014. Variations in soil carbon dioxide efflux across a thaw slump chronosequence in northwestern Alaska. Environmental Research Letters **9**:025001.

Jonasson, S., A. Michelsen, and I. K. Schmidt. 1999. Coupling of nutrient cycling and carbon dynamics in the Arctic, integration of soil microbial and plant processes. Applied Soil Ecology **11**:135-146.

Jones, B. M., C. D. Arp, M. T. Jorgenson, K. M. Hinkel, J. A. Schmutz, and P. L. Flint. 2009. Increase in the rate and uniformity of coastline erosion in Arctic Alaska. Geophysical Research Letters **36**.

Jones, J. B., K. C. Petrone, J. C. Finlay, L. D. Hinzman, and W. R. Bolton. 2005. Nitrogen loss from watersheds of interior Alaska underlain with discontinuous permafrost. Geophysical Research Letters **32**.

Jorgenson, M. T. and T. E. Osterkamp. 2005. Response of boreal ecosystems to varying modes of permafrost degradation. Canadian Journal of Forest Research-Revue Canadienne De Recherche Forestiere **35**:2100-2111.

Jorgenson, M. T., Y. L. Shur, and T. E. Osterkamp. 2008. Thermokarst in Alaska. Pages 117-124 Ninth International Conference On Permafrost, University of Alaska Fairbanks.

Jorgenson, M. T., Y. L. Shur, and E. R. Pullman. 2006. Abrupt increase in permafrost degradation in Arctic Alaska. Geophysical Research Letters **33**.

Kanevskiy, M., Y. Shur, D. Fortier, M. T. Jorgenson, and E. Stephani. 2011. Cryostratigraphy of late Pleistocene syngenetic permafrost (yedoma) in northern Alaska, Itkillik River exposure. Quaternary Research **75**:584-596.

Kasischke, E. S. and M. R. Turetsky. 2006. Recent changes in the fire regime across the North American boreal region-Spatial and temporal patterns of burning across Canada and Alaska (vol 33, art no L09703, 2006). Geophysical Research Letters **33**.

Kattsov, V. M., J. E. Walsh, W. L. Chapman, V. A. Govorkova, T. V. Pavlova, and X. Zhang. 2007. Simulation and projection of arctic freshwater budget components by the IPCC AR4 global climate models. Journal of Hydrometeorology **8**:571-589.

Kelly, R., M. L. Chipman, P. E. Higuera, I. Stefanova, L. B. Brubaker, and F. S. Hu. 2013. Recent burning of boreal forests exceeds fire regime limits of the past 10,000 years. Proceedings of the National Academy of Sciences of the United States of America **110**:13055-13060.

Keuper, F., P. M. van Bodegom, E. Dorrepaal, J. T. Weedon, J. van Hal, R. S. P. van Logtestijn, and R. Aerts. 2012. A frozen feast: thawing permafrost increases plant-available nitrogen in subarctic peatlands. Global Change Biology **18**:1998-2007.

Kicklighter, D. W., D. J. Hayes, J. W. McClelland, B. J. Peterson, A. D. McGuire, and J. M. Melillo. 2013. Insights and issues with simulating terrestrial DOC loading of Arctic river networks. Ecological Applications **23**:1817-1836.

Kling, G. W., G. W. Kipphut, and M. C. Miller. 1991. Arctic lakes and streams as gas conduits to the atmosphere - implications for tundra carbon budgets. Science **251**:298-301.

Kokelj, S. V. and C. R. Burn. 2003. Ground ice and soluble cations in near−surface permafrost, Inuvik, Northwest Territories, Canada. Permafrost and Periglacial Processes **14**:275-289.

Kokelj, S. V., R. E. Jenkins, D. Milburn, C. R. Burn, and N. Snow. 2005. The influence of thermokarst disturbance on the water quality of small upland lakes, Mackenzie Delta Region, Northwest Territories, Canada. Permafrost and Periglacial Processes **16**:343-353.

Kokelj, S. V. and M. T. Jorgenson. 2013. Advances in Thermokarst Research. Permafrost and Periglacial Processes **24**:108-119.

Kokelj, S. V., T. C. Lantz, J. Kanigan, S. L. Smith, and R. Coutts. 2009a. Origin and Polycyclic Behaviour of Tundra Thaw Slumps, Mackenzie Delta Region, Northwest Territories, Canada. Permafrost and Periglacial Processes **20**:173-184.

Kokelj, S. V., B. Zajdlik, and M. S. Thompson. 2009b. The Impacts of Thawing Permafrost on the Chemistry of Lakes across the Subarctic Boreal-Tundra Transition, Mackenzie Delta Region, Canada. Permafrost and Periglacial Processes **20**:185-199.

Koven, C. D., B. Ringeval, P. Friedlingstein, P. Ciais, P. Cadule, D. Khvorostyanov, G. Krinner, and C. Tarnocai. 2011. Permafrost carbon-climate feedbacks accelerate global warming. Proceedings of the National Academy of Sciences of the United States of America **108**:14769-14774.

Kriebel, D., J. Tickner, P. Epstein, J. Lemons, R. Levins, E. L. Loechler, M. Quinn, R. Rudel, T. Schettler, and M. Stoto. 2001. The precautionary principle in environmental science. Environmental Health Perspectives **109**:871-876.

Krieger, K. C. 2012. The Topographic Form and Evolution of Thermal Erosion Features: A First Analysis Using Airborne and Ground-Based LiDAR in Arctic Alaska. Idaho State University.

Lafreniere, M. J. and S. F. Lamoureux. 2013. Thermal Perturbation and Rainfall Runoff have Greater Impact on Seasonal Solute Loads than Physical Disturbance of the Active Layer. Permafrost and Periglacial Processes **24**:241-251.

Lammers, R. B., A. I. Shiklomanov, C. J. Vorosmarty, B. M. Fekete, and B. J. Peterson. 2001. Assessment of contemporary Arctic river runoff based on observational discharge records. Journal of Geophysical Research-Atmospheres **106**:3321-3334.

Lamoureux, S. F. and M. J. Lafrenière. 2014. Seasonal fluxes and age of particulate organic carbon exported from Arctic catchments impacted by localized permafrost slope disturbances. Environmental Research Letters **9**:045002.

Lantuit, H., P. P. Overduin, N. Couture, S. Wetterich, F. Are, D. Atkinson, J. Brown, G. Cherkashov, D. Drozdov, D. L. Forbes, A. Graves-Gaylord, M. Grigoriev, H. W. Hubberten, J. Jordan, T. Jorgenson, R. S. Odegard, S. Ogorodov, W. H. Pollard, V. Rachold, S. Sedenko, S. Solomon, F. Steenhuisen, I. Streletskaya, and A. Vasiliev. 2012a. The Arctic Coastal Dynamics Database: A New Classification Scheme and Statistics on Arctic Permafrost Coastlines. Estuaries and Coasts **35**:383-400.

Lantuit, H., W. H. Pollard, N. Couture, M. Fritz, L. Schirrmeister, H. Meyer, and H. W. Hubberten. 2012b. Modern and Late Holocene Retrogressive Thaw Slump Activity on the Yukon Coastal Plain and Herschel Island, Yukon Territory, Canada. Permafrost and Periglacial Processes **23**:39-51.

Lantz, T. C. and S. V. Kokelj. 2008. Increasing rates of retrogressive thaw slump activity in the Mackenzie Delta region, NWT, Canada. Geophysical Research Letters **35**.

Lantz, T. C., S. V. Kokelj, S. E. Gergel, and G. H. R. Henryz. 2009. Relative impacts of disturbance and temperature: persistent changes in microenvironment and vegetation in retrogressive thaw slumps. Global Change Biology **15**:1664-1675.

Lawrence, D. M., A. G. Slater, and S. C. Swenson. 2012. Simulation of Present-Day and Future Permafrost and Seasonally Frozen Ground Conditions in CCSM4. Journal of Climate **25**:2207-2225.

Lee, H., E. A. G. Schuur, and J. G. Vogel. 2010. Soil CO2 production in upland tundra where permafrost is thawing. Journal of Geophysical Research-Biogeosciences **115**:-.

Lewis, T., M. J. Lafreniere, and S. F. Lamoureux. 2012. Hydrochemical and sedimentary responses of paired High Arctic watersheds to unusual climate and permafrost disturbance, Cape Bounty, Melville Island, Canada. Hydrological Processes **26**:2003-2018.

Lewkowicz, A. G. 1987. Nature and importance of thermokarst processes, Sand Hills Moraine, Banks Island, Canada Geografiska Annaler Series a-Physical Geography **69**:321-327.

Lewkowicz, A. G. 1990. Morphology, frequency and magnitude of active-layer detachment slides, Fosheim Peninsula, Ellesmere Island, N.W.T. Pages 111-118 *in* Permafrost-Canada: Proceedings of the Fifth Canadian Permafrost Conference. Centre d'études nordiques, Université Laval, Quebec City.

Lewkowicz, A. G. 2007. Dynamics of active-layer detachment failures, Fosheim Peninsula, Ellesmere Island, Nunavut, Canada. Permafrost and Periglacial Processes **18**:89-103.

Lewkowicz, A. G. and C. Harris. 2005. Morphology and geotechnique of active-layer detachment failures in discontinuous and continuous permafrost, northern Canada. Geomorphology **69**:275-297.

Loveland, T. R., B. C. Reed, J. F. Brown, D. O. Ohlen, Z. Zhu, L. Yang, and J. W. Merchant. 2000. Development of a global land cover characteristics database and IGBP DISCover from 1 km AVHRR data. International Journal of Remote Sensing **21**:1303-1330.

MacDougall, A. H., C. A. Avis, and A. J. Weaver. 2012. Significant contribution to climate warming from the permafrost carbon feedback. Nature Geosci **5**:719-721.

Mack, M. C., E. A. G. Schuur, M. S. Bret-Harte, G. R. Shaver, and F. S. Chapin. 2004. Ecosystem carbon storage in arctic tundra reduced by long-term nutrient fertilization. Nature **431**:440-443.

McClelland, J. W., R. M. Holmes, K. H. Dunton, and R. W. Macdonald. 2012. The Arctic Ocean Estuary. Estuaries and Coasts **35**:353-368.

McClelland, J. W., R. M. Holmes, B. J. Peterson, R. Amon, T. Brabets, L. Cooper, J. Gibson, V. V. Gordeev, C. Guay, D. Milburn, R. Staples, P. A. Raymond, I. Shiklomanov, R. Striegl, A. Zhulidov, T. Gurtovaya, and S. Zimov. 2008. Development of a Pan-Arctic Database for River Chemistry. Eos, Transactions American Geophysical Union **89**:217-218.

McClelland, J. W., M. Stieglitz, F. Pan, R. M. Holmes, and B. J. Peterson. 2007. Recent changes in nitrate and dissolved organic carbon export from the upper Kuparuk River, North Slope, Alaska. Journal of Geophysical Research-Biogeosciences **112**.

McGuire, A. D., L. G. Anderson, T. R. Christensen, S. Dallimore, L. Guo, D. J. Hayes, M. Heimann, T. D. Lorenson, R. W. Macdonald, and N. Roulet. 2009. Sensitivity of the carbon cycle in the Arctic to climate change. Ecological Monographs **79**:523-555.

McGuire, A. D., J. M. Melillo, D. W. Kicklighter, and L. A. Joyce. 1995. Equilibrium Responses of Soil Carbon to Climate Change: Empirical and Process-Based Estimates. Journal of Biogeography **22**:785-796.

Mesquita, P. S., F. J. Wrona, and T. D. Prowse. 2010. Effects of retrogressive permafrost thaw slumping on sediment chemistry and submerged macrophytes in Arctic tundra lakes. Freshwater Biology **55**:2347-2358.

Moss, R. H., J. A. Edmonds, K. A. Hibbard, M. R. Manning, S. K. Rose, D. P. van Vuuren, T. R. Carter, S. Emori, M. Kainuma, T. Kram, G. A. Meehl, J. F. B. Mitchell, N. Nakicenovic, K. Riahi, S. J. Smith, R. J. Stouffer, A. M. Thomson, J. P. Weyant, and T. J. Wilbanks. 2010. The next generation of scenarios for climate change research and assessment. Nature **463**:747-756.

Nadelhoffer, K. J., A. E. Giblin, G. R. Shaver, and J. A. Laundre. 1991. Effects of temperature and substrate quality on element mineralization in 6 Arctic soils. Ecology **72**:242-253.

Nowinski, N. S., S. E. Trumbore, E. A. G. Schuur, M. C. Mack, and G. R. Shaver. 2008. Nutrient addition prompts rapid destabilization of organic matter in an arctic tundra ecosystem. Ecosystems **11**:16-25.

O'Brien, W. J., M. Barfield, N. Bettez, A. E. Hershey, J. E. Hobbie, G. Kipphut, G. Kling, and M. C. Miller. 2005. Long-term response and recovery to nutrient addition of a partitioned arctic lake. Freshwater Biology **50**:731-741.

O'Donnell, J. A., M. T. Jorgenson, J. W. Harden, A. D. McGuire, M. Z. Kanevskiy, and K. P. Wickland. 2012. The Effects of Permafrost Thaw on Soil Hydrologic, Thermal, and Carbon Dynamics in an Alaskan Peatland. Ecosystems **15**:213-229.

Oechel, W. C., S. J. Hastings, G. Vourlitis, M. Jenkins, G. Riechers, and N. Grulke. 1993. Recent Change of Arctic Tundra Ecosystems from a Net Carbon-Dioxide Sink to a Source. Nature **361**:520-523.

Osterkamp, T. E. 2007. Characteristics of the recent warming of permafrost in Alaska. Journal of Geophysical Research-Earth Surface **112**.

Osterkamp, T. E. and J. C. Jorgenson. 2006. Warming of permafrost in the Arctic National Wildlife Refuge, Alaska. Permafrost and Periglacial Processes **17**:65-69.

Osterkamp, T. E., M. T. Jorgenson, E. A. G. Schuur, Y. L. Shur, M. Z. Kanevskiy, J. G. Vogel, and V. E. Tumskoy. 2009. Physical and Ecological Changes Associated with Warming Permafrost and Thermokarst in Interior Alaska. Permafrost and Periglacial Processes **20**:235-256.

Osterkamp, T. E. and V. E. Romanovsky. 1999. Evidence for warming and thawing of discontinuous permafrost in Alaska. Permafrost and Periglacial Processes **10**:17-37.

Pan, Y., R. A. Birdsey, J. Fang, R. Houghton, P. E. Kauppi, W. A. Kurz, O. L. Phillips, A. Shvidenko, S. L. Lewis, J. G. Canadell, P. Ciais, R. B. Jackson, S. Pacala, A. D. McGuire, S. Piao, A. Rautiainen, S. Sitch, and D. Hayes. 2011. A Large and Persistent Carbon Sink in the World's Forests. Science.

Parmentier, F. J. W., T. R. Christensen, L. L. Sorensen, S. Rysgaard, A. D. McGuire, P. A. Miller, and D. A. Walker. 2013. The impact of lower sea-ice extent on Arctic greenhouse-gas exchange. Nature Climate Change **3**:195-202.

Peterson, B. J., J. McClelland, R. Curry, R. M. Holmes, J. E. Walsh, and K. Aagaard. 2006. Trajectory shifts in the Arctic and subarctic freshwater cycle. Science **313**:1061-1066.

Petrone, K. C., J. B. Jones, L. D. Hinzman, and R. D. Boone. 2006. Seasonal export of carbon, nitrogen, and major solutes from Alaskan catchments with discontinuous permafrost. Journal of Geophysical Research-Biogeosciences **111**.

Ping, C. L., G. J. Michaelson, and J. M. Kimble. 1997. Carbon storage along a latitudinal transect in Alaska. Nutrient Cycling in Agroecosystems **49**:235-242.

Pizano, C., A. F. Baron, E. A. G. Schuur, K. G. Crummer, and M. C. Mack. 2014. Effects of thermo-erosional disturbance on surfaces soil carbon and nitrogen dynamics in upland arctic tundra. Environmental Research Letters **8**.

Potter, C. S. and S. A. Klooster. 1997. Global model estimates of carbon and nitrogen storage in litter and soil pools: Response to changes in vegetation quality and biomass allocation. Tellus Series B-Chemical and Physical Meteorology **49**:1-17.

Qian, H., R. Joseph, and N. Zeng. 2010. Enhanced terrestrial carbon uptake in the Northern High Latitudes in the 21st century from the Coupled Carbon Cycle Climate Model Intercomparison Project model projections. Global Change Biology **16**:641-656.

Rachold, V., M. N. Grigoriev, F. E. Are, S. Solomon, E. Reimnitz, H. Kassens, and M. Antonow. 2000. Coastal erosion vs riverine sediment discharge in the Arctic Shelf seas. International Journal of Earth Sciences **89**:450-460.

Rawlins, M. A., M. Steele, M. M. Holland, J. C. Adam, J. E. Cherry, J. A. Francis, P. Y. Groisman, L. D. Hinzman, T. G. Huntington, D. L. Kane, J. S. Kimball, R. Kwok, R. B. Lammers, C. M. Lee, D. P. Lettenmaier, K. C. McDonald, E. Podest, J. W. Pundsack, B. Rudels, M. C. Serreze, A. Shiklomanov, Ø. Skagseth, T. J. Troy, C. J. Vörösmarty, M. Wensnahan, E. F. Wood, R. Woodgate, D. Yang, K. Zhang, and T. Zhang. 2010. Analysis of the Arctic System for Freshwater Cycle Intensification: Observations and Expectations. Journal of Climate **23**:5715-5737.

Raynolds, M. K., D. A. Walker, H. E. Epstein, J. E. Pinzon, and C. J. Tucker. 2012. A new estimate of tundra-biome phytomass from trans-Arctic field data and AVHRR NDVI. Remote Sensing Letters **3**:403-411.

Rocha, A. V., M. M. Loranty, P. E. Higuera, M. C. Mack, F. S. Hu, B. M. Jones, A. L. Breen, E. B. Rastetter, S. J. Goetz, and G. R. Shaver. 2012. The footprint of Alaskan tundra fires during the past half-century: implications for surface properties and radiative forcing. Environmental Research Letters **7**.

Saito, K., M. Kimoto, T. Zhang, K. Takata, and S. Emori. 2007. Evaluating a high-resolution climate model: Simulated hydrothermal regimes in frozen ground regions and their change under the global warming scenario. Journal of Geophysical Research-Earth Surface **112**:-.

Schaefer, K., H. Lantuit, V. E. Romanovsky, E. A. G. Schuur, and R. Witt. 2014. The impact of the permafrost carbon feedback on global climate. Environmental Research Letters **9**:085003.

Schaefer, K., T. Zhang, L. Bruhwiler, and A. P. Barrett. 2011. Amount and timing of permafrost carbon release in response to climate warming. Tellus Series B-Chemical and Physical Meteorology:no-no.

Schirrmeister, L., G. Grosse, S. Wetterich, P. P. Overduin, J. Strauss, E. A. G. Schuur, and H. W. Hubberten. 2011. Fossil organic matter characteristics in permafrost deposits of the northeast Siberian Arctic. Journal of Geophysical Research-Biogeosciences **116**.

Schirrmeister, L., C. Siegert, T. Kuznetsova, S. Kuzmina, A. Andreev, F. Kienast, H. Meyer, and A. Bobrov. 2002. Paleoenvironmental and paleoclimatic records from permafrost deposits in the Arctic region of Northern Siberia. Quaternary International **89**:97-118.

Schuur, E. A. G., B. W. Abbott, W. B. Bowden, V. Brovkin, P. Camill, J. G. Canadell, J. P. Chanton, F. S. Chapin, III, T. R. Christensen, P. Ciais, B. T. Crosby, C. I. Czimczik, G. Grosse, J. Harden, D. J. Hayes, G. Hugelius, J. D. Jastrow, J. B. Jones, T. Kleinen, C. D. Koven, G. Krinner, P. Kuhry, D. M. Lawrence, A. D. McGuire, S. M. Natali, J. A. O'Donnell, C. L. Ping, W. J. Riley, A. Rinke, V. E. Romanovsky, A. B. K. Sannel, C. Schädel, K. Schaefer, J. Sky, Z. M. Subin, C. Tarnocai, M. R. Turetsky, M. P. Waldrop, K. M. Walter Anthony, K. P. Wickland, C. J. Wilson, and S. A. Zimov. 2013. Expert assessment of vulnerability of permafrost carbon to climate change. Climatic Change:1-16.

Schuur, E. A. G., J. Bockheim, J. G. Canadell, E. Euskirchen, C. B. Field, S. V. Goryachkin, S. Hagemann, P. Kuhry, P. M. Lafleur, H. Lee, G. Mazhitova, F. E. Nelson, A. Rinke, V. E. Romanovsky, N. Shiklomanov, C. Tarnocai, S. Venevsky, J. G. Vogel, and S. A. Zimov. 2008. Vulnerability of permafrost carbon to climate change: Implications for the global carbon cycle. Bioscience **58**:701-714.

Schuur, E. A. G., K. G. Crummer, J. G. Vogel, and M. C. Mack. 2007. Plant species composition and productivity following permafrost thaw and thermokarst in alaskan tundra. Ecosystems **10**:280-292.

Schuur, E. A. G., J. G. Vogel, K. G. Crummer, H. Lee, J. O. Sickman, and T. E. Osterkamp. 2009. The effect of permafrost thaw on old carbon release and net carbon exchange from tundra. Nature **459**:556-559.

Shirokova, L. S., O. S. Pokrovsky, S. N. Kirpotin, C. Desmukh, B. G. Pokrovsky, S. Audry, and J. Viers. 2013. Biogeochemistry of organic carbon, CO2, CH4, and trace elements in thermokarst water bodies in discontinuous permafrost zones of Western Siberia. Biogeochemistry **113**:573-593.

Shur, Y., H. M. French, M. T. Bray, and D. A. Anderson. 2004. Syngenetic permafrost growth: Cryostratigraphic observations from the CRREL tunnel near fairbanks, Alaska. Permafrost and Periglacial Processes **15**:339-347.

Shur, Y. L. and M. T. Jorgenson. 2007. Patterns of permafrost formation and degradation in relation to climate and ecosystems. Permafrost and Periglacial Processes **18**:7-19.

Slater, A. G. and D. M. Lawrence. 2013. Diagnosing Present and Future Permafrost from Climate Models. Journal of Climate **26**:5608-5623.

Slavik, K., B. J. Peterson, L. A. Deegan, W. B. Bowden, A. E. Hershey, and J. E. Hobbie. 2004. Long-term responses of the Kuparuk River ecosystem to phosphorus fertilization. Ecology **85**:939-954.

Sloan, L. C. and D. Pollard. 1998. Polar stratospheric clouds: A high latitude warming mechanism in an ancient greenhouse world. Geophysical Research Letters **25**:3517-3520.

Smith, L. C., T. M. Pavelsky, G. M. MacDonald, A. I. Shiklomanov, and R. B. Lammers. 2007. Rising minimum daily flows in northern Eurasian rivers: A growing influence of groundwater in the high-latitude hydrologic cycle. Journal of Geophysical Research-Biogeosciences **112**.

Sterner, R. W. and J. J. Elser. 2002. Ecological Stoichiometry: The Biology of Elements from Molecules to the Biosphere. Princeton Press.

Striegl, R. G., G. R. Aiken, M. M. Dornblaser, P. A. Raymond, and K. P. Wickland. 2005. A decrease in discharge-normalized DOC export by the Yukon River during summer through autumn. Geophysical Research Letters **32**.

Stroeve, J., M. M. Holland, W. Meier, T. Scambos, and M. Serreze. 2007. Arctic sea ice decline: Faster than forecast. Geophysical Research Letters **34**.

Sturm, M., J. P. McFadden, G. E. Liston, F. S. Chapin, C. H. Racine, and J. Holmgren. 2001. Snow-shrub interactions in Arctic tundra: A hypothesis with climatic implications. Journal of Climate **14**:336-344.

Tank, S. E., K. E. Frey, R. G. Striegl, P. A. Raymond, R. M. Holmes, J. W. McClelland, and B. J. Peterson. 2012. Landscape-level controls on dissolved carbon flux from diverse catchments of the circumboreal. Global Biogeochemical Cycles **26**.

Tarnocai, C., J. G. Canadell, E. A. G. Schuur, P. Kuhry, G. Mazhitova, and S. Zimov. 2009. Soil organic carbon pools in the northern circumpolar permafrost region. Global Biogeochemical Cycles **23**:-.

Thienpont, J. R., K. M. Ruehland, M. F. J. Pisaric, S. V. Kokelj, L. E. Kimpe, J. M. Blais, and J. P. Smol. 2013. Biological responses to permafrost thaw slumping in Canadian Arctic lakes. Freshwater Biology **58**:337-353.

Thompson, M. S., F. J. Wrona, and T. D. Prowse. 2012. Shifts in Plankton, Nutrient and Light Relationships in Small Tundra Lakes Caused by Localized Permafrost Thaw. Arctic **65**:367-376.

Treat, C. C. and S. Frolking. 2013. Carbon Storage: A permafrost carbon bomb? Nature Clim. Change **3**:865-867.

Trumbore, S. 2009. Radiocarbon and Soil Carbon Dynamics. Annual Review of Earth and Planetary Sciences **37**:47-66.

Tsuyuzaki, S., T. Ishizaki, and T. Sato. 1999. Vegetation structure in gullies developed by the melting of ice wedges along Kolyma River, northern Siberia. Ecological Research **14**:385-391.

Vancoppenolle, M., L. Bopp, G. Madec, J. Dunne, T. Ilyina, P. R. Halloran, and N. Steiner. 2013. Future Arctic Ocean primary productivity from CMIP5 simulations: Uncertain outcome, but consistent mechanisms. Global Biogeochemical Cycles **27**:605-619.

Vonk, J. E., P. J. Mann, S. Davydov, A. Davydova, R. G. M. Spencer, J. Schade, W. V. Sobczak, N. Zimov, S. Zimov, E. Bulygina, T. I. Eglinton, and R. M. Holmes. 2013. High biolability of ancient permafrost carbon upon thaw. Geophysical Research Letters:40.

Vonk, J. E., L. Sanchez-Garcia, B. E. van Dongen, V. Alling, D. Kosmach, A. Charkin, I. P. Semiletov, O. V. Dudarev, N. Shakhova, P. Roos, T. I. Eglinton, A. Andersson, and O.

Gustafsson. 2012. Activation of old carbon by erosion of coastal and subsea permafrost in Arctic Siberia. Nature **489**:137-140.

Waelbroeck, C., P. Monfray, W. C. Oechel, S. Hastings, and G. Vourlitis. 1997. The impact of permafrost thawing on the carbon dynamics of tundra. Geophysical Research Letters **24**:229-232.

Walvoord, M. A. and R. G. Striegl. 2007. Increased groundwater to stream discharge from permafrost thawing in the Yukon River basin: Potential impacts on lateral export of carbon and nitrogen. Geophysical Research Letters **34**.

Weintraub, M. N. and J. P. Schimel. 2003. Interactions between carbon and nitrogen mineralization and soil organic matter chemistry in arctic tundra soils. Ecosystems **6**:129-143.

Whiteman, G., C. Hope, and P. Wadhams. 2013. Climate science: Vast costs of Arctic change. Nature **499**:401-403.

Wieczorek, S., P. Ashwin, C. M. Luke, and P. M. Cox. 2011. Excitability in ramped systems: the compost-bomb instability. Proceedings of the Royal Society a-Mathematical Physical and Engineering Sciences **467**:1243-1269.

Yoshikawa, K. and L. D. Hinzman. 2003. Shrinking thermokarst ponds and groundwater dynamics in discontinuous permafrost near Council, Alaska. Permafrost and Periglacial Processes **14**:151-160.

Zachos, J., M. Pagani, L. Sloan, E. Thomas, and K. Billups. 2001. Trends, rhythms, and aberrations in global climate 65 Ma to present. Science **292**:686-693.

Zachos, J. C., G. R. Dickens, and R. E. Zeebe. 2008. An early Cenozoic perspective on greenhouse warming and carbon-cycle dynamics. Nature **451**:279-283.

Zhang, T., J. A. Heginbottom, R. G. Barry, and J. Brown. 2000. Further statistics on the distribution of permafrost and ground ice in the Northern Hemisphere. Polar Geography **24**:126-131.

Zhang, T., R.G. Barry, K. Knowles, J.A. Heginbottom, and J. Brown. 1999. Statistics and characteristics of permafrost and ground ice distribution in the Northern Hemisphere. Polar Geography **23**:147-169.

Zhuang, Q., Melillo, J. M., Sarofim, M. C., Kicklighter, D. W., McGuire, A. D., Felzer, B. S., Sokolov, A., Prinn, R. G., Steudler, P. A., and Hu, S.: CO_2 and CH_4 exchanges between

land ecosystems and the atmosphere in northern high latitudes over the 21st century, Geophys. Res. Lett., 33, L17403, 2006.

Zimov, S. A., S. P. Davydov, G. M. Zimova, A. I. Davydova, E. A. G. Schuur, K. Dutta, and F. S. Chapin. 2006. Permafrost carbon: Stock and decomposability of a globally significant carbon pool. Geophysical Research Letters **33**:-.

Table 6.1 Estimates of upland thermokarst impact extrapolated to the North Slope and circumarctic

	North Slope		Circumarctic	
	Mean	Range	Mean	Range
Extent of uplands/hills (10^6 km^2)*	0.16		1.8	
Percent of uplands susceptible to thermokarst**	37	(28–45)	37	(28–45)
Permafrost degrading by 2100 (%)***	93	(70–100)	68	(52–86)
Current upland thermokarst coverage (%)#	1.5	(1.2–1.8)	1.5	(1.2–1.8)
Upland thermokarst coverage by 2100 (%)	34	(20–45)	25	(15–39)
Current fluxes from thermokarst				
Organic layer carbon displaced (Tg)	2.3	(1.3–7.2)	27	(10–54)
R_{eco} (Tg C yr^{-1})	0.02	(-0.03–0.10)	0.26	(-0.34–1.14)
DOC (Tg C yr^{-1})	0.02	(0.01–0.3)	0.73	(0.30–1.4)
DIN (10^9 g N yr^{-1})	0.19	(0.08–0.38)	6.7	(2.8–14)
Projected fluxes from thermokarst (2050-2100)				
Organic layer carbon displaced (Tg)	54	(14–115)	470	(120–1200)
R_{eco} (Tg C yr^{-1})	0.12	(-0.11–0.53)	1.1	(-1.1–6.2)
DOC (Tg C yr^{-1})	0.39	(0.11–0.78)	3.3	(0.93–7.9)
DIN (10^9 g N yr^{-1})	3.7	(1.1–8.30)	32	(9.3–84)

*Walker et al. 2005, **Zhang et al. 1999, ***Slater and Lawrence 2013, #Krieger 2012. See Appendix 2 for detailed treatment of assumptions.

Appendix 6.0 Methods and assumptions for extrapolated circumarctic fluxes in Chapter 6

I extrapolated thermokarst hydrologic flux, respiration, and displacement of soil SOC to the North Slope and circumarctic via linear scaling. While the uncertainties are large, this provides a first-order estimate of the potential significance of upland thermokarst to circumarctic carbon balance. I multiplied the area of the upland physiographic region for the North Slope and the circumarctic (Walker et al. 2005) by the current extent of upland thermokarst, ~1.5% (Krieger 2012). I weighted changes in respiration and carbon pools by each feature type's proportion of the current thermokarst coverage (33, 50, and 17% for active-layer detachment slides, thermo-erosion gullies, and retrogressive thaw slumps; Krieger 2012), and I weighted mean yield from each activity level by the proportion of features in that class (6%, 35%, and 59% for activity levels 1, 2, and 3; Krieger 2012).

I determined areal DOC and DIN daily yields from 26 upland thermokarst features by multiplying outflow concentration by discharge and dividing by the area of the feature. For sites with surface water flowing into the top of the feature (primarily gullies but also some slides and slumps) I subtracted the reference concentration of each solute before calculating yield, so the estimate represented only the contribution from the area disturbed by thermokarst assuming that all unmeasured water inputs have the same carbon and nitrogen concentrations.

To project possible impacts from upland thermokarst by the end of the century I used, 1. The proportion of uplands susceptible to thermokarst as determined by ground ice content and landscape characteristics (Zhang et al. 2000, Balser and Jones 2014), 2. Mean period of activity for each feature type, and 3. Regional and circumarctic projections of permafrost degradation. Estimates from the literature of period of activity (time spent in activity levels one and two) for slides, gullies, and slumps were 2, 8, and 20 years, respectively (Lewkowicz 1987, 1990, Burn 2000, Jorgenson and Osterkamp 2005, Lewkowicz 2007, Kokelj et al. 2009, Godin and Fortier 2012). However, because half of the slides in my study had triggered thaw slumps, substantially increasing their active lifespans, I estimated an 11-year period of activity for these features. I weighted period of activity for each feature morphology by the portion of current area as above, yielding a mean active period of 11 years. Concerning future extent of permafrost, models project that 52-86% of circumarctic, near-surface permafrost will be degrading or isothermal by 2100, with estimates for the North Slope of Alaska ranging from 70-100%, based on representative concentration pathways RCP4.5 and RCP 8.5 (Slater and Lawrence 2013).

However, nearly all of this change is expected to occur during the second half of the century for the continuous permafrost zone (Jafarov et al. 2013). Because I expected thermokarst activity to follow the same pattern, I calculated cumulative fluxes by 2100 divided by 50 to estimate annual thermokarst fluxes for 2050-2100. Given the compound assumptions associated with this extrapolation, I propagated error additively to obtain confidence intervals.

References

Balser, A. and J. B. Jones. 2014. Thermo-erosional Landslide Terrain Suitability in the Brooks Range Foothills, Northern Alaska, USA. . In prep.

Burn, C. R. 2000. The thermal regime of a retrogressive thaw slump near Mayo, Yukon Territory. Canadian Journal of Earth Sciences **37**:967-981.

Godin, E. and D. Fortier. 2012. Geomorphology of a thermo-erosion gully, Bylot Island, Nunavut, Canada. Canadian Journal of Earth Sciences **49**:979-986.

Jafarov, E. E., V. E. Romanovsky, H. Genet, A. D. McGuire, and S. S. Marchenko. 2013. The effects of fire on the thermal stability of permafrost in lowland and upland black spruce forests of interior Alaska in a changing climate. Environmental Research Letters **8**.

Jorgenson, M. T. and T. E. Osterkamp. 2005. Response of boreal ecosystems to varying modes of permafrost degradation. Canadian Journal of Forest Research-Revue Canadienne De Recherche Forestiere **35**:2100-2111.

Kokelj, S. V., T. C. Lantz, J. Kanigan, S. L. Smith, and R. Coutts. 2009. Origin and Polycyclic Behaviour of Tundra Thaw Slumps, Mackenzie Delta Region, Northwest Territories, Canada. Permafrost and Periglacial Processes **20**:173-184.

Krieger, K. C. 2012. The Topographic Form and Evolution of Thermal Erosion Features: A First Analysis Using Airborne and Ground-Based LiDAR in Arctic Alaska. Idaho State University.

Lewkowicz, A. G. 1987. Nature and importance of thermokarst processes, Sand Hills Moraine, Banks Island, Canada Geografiska Annaler Series a-Physical Geography **69**:321-327.

Lewkowicz, A. G. 1990. Morphology, frequency and magnitude of active-layer detachment slides, Fosheim Peninsula, Ellesmere Island, N.W.T. Pages 111-118 *in* Permafrost-

Canada: Proceedings of the Fifth Canadian Permafrost Conference. Centre d'études nordiques, Université Laval, Quebec City.

Lewkowicz, A. G. 2007. Dynamics of active-layer detachment failures, Fosheim Peninsula, Ellesmere Island, Nunavut, Canada. Permafrost and Periglacial Processes **18**:89-103.

Slater, A. G. and D. M. Lawrence. 2013. Diagnosing Present and Future Permafrost from Climate Models. Journal of Climate **26**:5608-5623.

Walker, D. A., M. K. Raynolds, F. J. A. Daniels, E. Einarsson, A. Elvebakk, W. A. Gould, A. E. Katenin, S. S. Kholod, C. J. Markon, E. S. Melnikov, N. G. Moskalenko, S. S. Talbot, B. A. Yurtsev, and C. Team. 2005. The Circumpolar Arctic vegetation map. Journal of Vegetation Science **16**:267-282.

Zhang, T., J. A. Heginbottom, R. G. Barry, and J. Brown. 2000. Further statistics on the distribution of permafrost and ground ice in the Northern Hemisphere. Polar Geography **24**:126.

Appendices

Appendix A. High risk of permafrost thaw[1]

Northern soils will release huge amounts of carbon in a warmer world, say Edward A. G. Schuur, Benjamin Abbott and the Permafrost Carbon Network.

Arctic temperatures are rising fast, and permafrost is thawing. Carbon released into the atmosphere from permafrost soils will accelerate climate change, but the magnitude of this effect remains highly uncertain. Our collective estimate is that carbon will be released more quickly than models suggest, and at levels that are cause for serious concern.

We calculate that permafrost thaw will release the same order of magnitude of carbon as deforestation if current rates of deforestation continue. But because these emissions include significant quantities of methane, the overall effect on climate could be 2.5 times larger.

Recent years have brought reports from the far north of tundra fires[1], the release of ancient carbon[2], CH_4 bubbling out of lakes[3] and gigantic stores of frozen soil carbon[4]. The latest estimate is that some 18.8 mil- lion square kilometres of northern soils hold about 1,700 billion tonnes of organic carbon[4] — the remains of plants and animals that have been accumulating in the soil over thousands of years. That is about four times more than all the carbon emitted by human activity in modern times and twice as much as is present in the atmosphere now.

This soil carbon amount is more than three times higher than previous estimates, largely because of the realization that organic carbon is stored much deeper in frozen soils than was thought. Inventories typically measure carbon in the top metre of soil. But the physical mixing during freeze–thaw cycles, in combination with sediment deposition over hundreds and thousands of years, has buried permafrost carbon many metres deep.

The answers to three key questions will determine the extent to which the emission of this carbon will affect climate change: How much is vulnerable to release into the atmosphere?

---

[1]Published as Schuur, E. A. G., B. W. Abbott, W. B. Bowden, V. Brovkin, P. Camill, J. P. Canadell, F. S. C. III, T. R. Christensen, J. P. Chanton, P. Ciais, P. M. Crill, B. T. Crosby, C. I. Czimczik, G. Grosse, D. J. Hayes, G. Hugelius, J. D. Jastrow, T. Kleinen, K. C.D, G. Krinner, P. Kuhry, D. M. Lawrence, S. M. Natali, C. L. Ping, A. Rinke, W. J. Riley, V. E. Romanovsky, A. B. K. Sannel, C. Schädel, K. Schaefer, Z. M. Subin, C. Tarnocai, M. Turetsky, K. M. Walter-Anthony, C. J. Wilson, and S. A. Zimov. 2011. Climate change: High risk of permafrost thaw. Nature **480**:32-33.

In what form it will be released? And how fast will it be released? These questions are easily framed, but challenging to answer.

AA.1 Known unknowns

As soils defrost, microbes decompose the ancient carbon and release CH_4 and carbon dioxide. Not all carbon is equally vulnerable to release: some soil carbon is easily metabolized and transformed to gas, but more complex molecules are harder to break down. The bulk of permafrost carbon will be released slowly over decades after thaw, but a smaller fraction could remain within the soil for centuries or longer. The type of gas released also affects the heat-trapping potential of the emissions. Waterlogged, low-oxygen environments are likely to contain microbes that produce CH_4 — a potent greenhouse gas with about 25 times more warming potential than CO_2 over a 100-year period. However, waterlogged environments also tend to retain more carbon within the soil. It is not yet understood how these factors will act together to affect future climate.

The ability to project how much carbon will be released is hampered both by the fact that models do not account for some important processes, and by a lack of data to inform the models. For example, most large-scale models project that permafrost warming depends on how much the air is warming above them. This warming then boosts microbial activity and carbon release. But this is a simplification. Abrupt thaw processes can cause ice wedges to melt and the ground surface to collapse, accelerating the thaw of frozen ground[5]. Evidence of rapid thaw is widespread: you can see it in the 'drunken' trees that tip dangerously as a result of ground subsidence, and in collapsed hill slopes marked by scars from landslides. These are just some of the complex processes that models don't include.

At the same time, few data are available to support these models because of the difficulties of gathering data in extreme environments. Only a handful of remote field stations around the world are collecting data to sup- port this research, even though the permafrost zone covers about almost one-quarter of the Northern Hemisphere's land area. The field studies that do exist confirm that permafrost thaw is tightly linked to ground subsidence and soil moisture as well as temperature. So modelling carbon emissions from permafrost thaw is much more complex than a simple response to temperature alone.

Models have flaws, but experts intimately familiar with these landscapes and processes have accumulated knowledge about what they expect to happen, based on quantitative data and qualitative understanding of these systems. We have attempted to quantify this expertise through a survey developed over several years.

AA.2 Survey Says

Our survey asks what percentage of the surface permafrost is likely to thaw, how much carbon will be released, and how much of that carbon will be CH_4, for three time periods and under four warming scenarios that will be part of the Intergovernmental Panel on Climate Change Fifth Assessment Report. The lowest warming scenario projects 1.5 °C Arctic warming over the 1985– 2004 average by the year 2040, ramping up to 2 °C by 2100; the highest warming scenario considers 2.5 °C by 2040, and 7.5 °C by 2100. In all cases, we posited that the temperature would remain steady from 2100 to 2300 so that we could assess opinions about the time lag in the response of permafrost carbon to temperature change.

The survey was filled out this year by 41 international scientists, listed as authors here, who publish on various aspects of permafrost. The results are striking. Collectively, we hypothesize that the high warming scenario will degrade 9–15% of the top 3 metres of permafrost by 2040, increasing to 47–61% by 2100 and 67–79% by 2300 (these ranges are the 95% confidence intervals around the group's mean estimate). The estimated car- bon release from this degradation is 30 billion to 63 billion tonnes of carbon by 2040, reaching 232 billion to 380 billion tonnes by 2100 and 549 billion to 865 billion tonnes by 2300. These values, expressed in CO_2 equivalents, combine the effect of carbon released as both CO_2 and as CH_4.

Our estimate for the amount of carbon released by 2100 is 1.7–5.2 times larger than those reported in several recent model- ling studies[6-8], all of which used a similar warming scenario. This reflects, in part, our perceived importance of the abrupt thaw processes, as well as our heightened aware- ness of deep carbon pools. Active research is aimed at incorporating these main issues, along with others, into models.

Are our projected rapid changes to the permafrost soil carbon pool plausible? The survey predicts a 7–11% drop in the size of the permafrost carbon pool by 2100 under the high-warming scenario. That scale of carbon loss has happened before: a 7–14% decrease has been measured in soil carbon inventories across thousands of sites in the temperate-zone United Kingdom as a

result of climate change[9]. Also, data scaled up from a single permafrost field site point to a potential 5% loss over a century as a result of widespread permafrost thaw[2]. These field results generally agree with the collective carbon-loss projection made by this survey, so it should indeed be plausible.

Across all the warming scenarios, we project that most of the released carbon will be in the form of CO_2, with only about 2.7% in the form of CH_4. However, because CH_4 has a higher global-warming potential, almost half the effect of future permafrost-zone car- bon emissions on climate forcing is likely to be from CH_4. That is roughly consistent with the tens of billions of tonnes of CH_4 thought to have come from oxygen-limited environments in northern ecosystems after the end of the last glacial period[10].

All this points towards significant carbon releases from permafrost-zone soils over policy-relevant timescales. It also highlights important lags whereby permafrost degradation and carbon emissions are expected to continue for decades or centuries after global temperatures stabilize at new, higher levels. Of course, temperatures might not reach such high levels. Our group's estimate for carbon release under the lowest warming scenario, although still quite sizeable, is about one-third of that predicted under the strongest warming scenario.

Knowing how much carbon will be released from the permafrost zone in this century and beyond is crucial for determining the appropriate response. But despite the massive amount of carbon in permafrost soils, emissions from these soils are unlikely to overshadow those from the burning of fossil fuels, which will continue to be the main source of climate forcing. Permafrost carbon release will still be an important amplifier of climate change, however, and is in some ways more problematic: it occurs in remote places, far from human influence, and is dispersed across the landscape. Trapping carbon emissions at the source — as one might do at power plants — is not an option. And once the soils thaw, emissions are likely to continue for decades, or even centuries.

The scientific community needs to collect more data and develop more-sophisticated models to test the hypotheses presented by this survey. Fortunately, awareness of the problem is increasing and these are starting to happen. The US Department of Energy, for example, has initiated a project called Next-Generation Ecosystem Experiments — Arctic, which aims to improve the representation of these processes in large-scale models. NASA is pursuing an Arctic–Boreal Vulnerability Experiment, which aims to improve satellite observations of this

region. The Vulnerability of Permafrost Carbon Research Coordination Network funded by the US National Science Foundation, of which we are part, is bringing together people and observations to synthesize results and validate models. These are just some of the many international initiatives aimed at filling these research gaps.

In the meantime, our survey outlines the additional risk to society caused by thawing of the frozen north, and underscores the urgent need to reduce atmospheric emissions from fossil-fuel use and deforestation. This will help to keep permafrost carbon frozen in the ground.

Edward Schuur *is in the Department of Biology at the University of Florida, Gainesville, Florida 32611, USA.* **Benjamin Abbott** *is in the Institute of Arctic Biology at the University of Alaska, Fairbanks, Alaska 99775, USA. The other experts in the* **Permafrost Carbon Research Network** *are listed at go.nature.com/kkidom. e-mail: tschuur@ufl.edu*

1. Mack, M. C. *et al. Nature* **475,** 489–492 (2011).
2. Schuur,E.A.G.*etal.Nature* **459,**556–559 (2009).
3. Walter, K. M., Zimov, S. A., Chanton, J. P., Verbyla, D. & Chapin, F. S. III *Nature* **443,** 71–75 (2006).
4. Tarnocai, C. *et al. Global Biogeochem. Cycles* **23,** GB2023 (2009).
5. Jorgenson,M.T.,Shur,Y.L.&Pullman,E.R. *Geophys. Res. Lett.* **33,** L02503 (2006).
6. Schaefer, K., Zhang, T., Bruhwiler, L. & Barrett, A. P. *Tellus B* **63,** 165–180 (2011).
7. Koven,C.D.*etal.Proc.NatlAcad.Sci.USA***108,** 14769–14774 (2011).
8. Schneider von Deimling, T. *et al. Biogeosciences Discuss.* **8,** 4727–4761 (2011).
9. Bellamy,P.H.Loveland,P.J.,Bradley,R.I.,Lark, R. M. & Kirk, G. J. *Nature* **437,** 245–248 (2005). 10.Fischer, H. *et al. Nature* **452,** 864–867 (2008)

Appendix B. Expert assessment of vulnerability of permafrost carbon to climate change[1]

E.A.G. Schuur[§1*], B.W. Abbott[2*], W.B. Bowden[3], V. Brovkin[4], P. Camill[5], J.G. Canadell[6], J.P. Chanton[7], F.S. Chapin III[2], T.R. Christensen[8], P. Ciais[9], B.T. Crosby[10], C.I. Czimczik[11], G. Grosse[2], J. Harden[12], D.J. Hayes[13], G. Hugelius[14], J.D. Jastrow[15], J.B. Jones[2], T. Kleinen[4], C.D, Koven[16], G. Krinner[17], P. Kuhry[10], D.M. Lawrence[18], A.D. McGuire[2,19], S.M. Natali[1], J.A. O'Donnell[20], C.L. Ping[2], W.J. Riley[16], A. Rinke[21], V.E. Romanovsky[2], A.B.K. Sannel[10], C. Schädel[1], K. Schaefer[22], J. Sky[23], Z.M. Subin[16], C. Tarnocai[24], M. Turetsky[25], M. Waldrop[13], K. M. Walter-Anthony[2], K. P. Wickland[20], C.J. Wilson[26], S.A. Zimov[27]

[§]corresponding author: [1]University of Florida, Gainesville, FL, tschuur@ufl.edu, 352-392-7913

[*]contributed equally to this publication

[2]University of Alaska Fairbanks, Fairbanks, AK; [3]University of Vermont, Burlington, VT; [4]Max Planck Institute for Meteorology, Hamburg, Germany; [5] Bowdoin College, Brunswick, ME; [6]Global Carbon Project CSIRO Marine and Atmospheric Research, Canberra, Australia; [7]Florida State University, Tallahassee, FL; [8]Lund University, Lund, Sweden; [9]LSCE, CEA-CNRS-UVSQ, Gif-sur-Yvette, France; [10]Idaho State University, Pocatello, ID; [11]University of California, Irvine, CA; [12]US Geological Survey, Menlo Park, CA; [13]Oak Ridge National Laboratory, Oak Ridge, TN; [14]Stockholm University, Stockholm, Sweden; [15]Argonne National Laboratory, Argonne, IL; [16]Lawrence Berkeley National Lab, Berkeley, CA; [17]CNRS/UJF-Grenoble 1, LGGE, Grenoble, France; [18]National Center for Atmospheric Research, Boulder, CO; [19]U.S. Geological Survey, Fairbanks, AK; [20]U.S. Geological Survey, Boulder, CO; [21]Alfred Wegener Institute, Potsdam, Germany; [22]National Snow and Ice Data Center, Boulder, CO; [23]University of Oxford, Oxford, UK; [24]AgriFoods, Ottawa, Canada; [25]University of Guelph, Guelph, Canada; [26]Los Alamos National Laboratory, Los Alamos, NM; [27]North-East Scientific Station, Cherskii, Siberia

AB.1 Abstract

Approximately 1700 Pg of soil carbon (C) are stored in the northern circumpolar permafrost zone, more than twice as much C than in the atmosphere. The overall amount, rate, and form of C released to the atmosphere in a warmer world will influence the strength of the permafrost C feedback to climate change. We used a survey to quantify variability in the perception of the vulnerability of permafrost C to climate change. Experts were asked to provide quantitative estimates of permafrost change in response to four scenarios of warming. For the highest warming scenario, experts hypothesized that C release from permafrost zone soils could

be 19-45 Pg C by 2040, 162-288 Pg C by 2100, and 381-616 Pg C by 2300 in CO_2 equivalent using 100-year CH_4 global warming potential (GWP). These values become 50% larger using 20-year CH_4 GWP, with a third to a half of expected climate forcing coming from CH_4. Experts projected that two-thirds of this release could be avoided under the lowest warming scenario. These results highlight the potential risk from permafrost thaw and serve to frame a hypothesis about the magnitude of this feedback to climate change.

Abbreviations: Petagrams:Pg; Carbon:C; Carbon dioxide:CO_2; Methane:CH_4; Representative concentration pathway:RCP; Global warming potential:GWP;

AB.2 Introduction

Recent scientific studies estimate that soils of the northern permafrost zone contain almost 1700 Petagrams (Pg) of organic carbon (C) (Tarnocai et al. 2009; Schuur et al. 2008), much more than previously recognized (Jobbagy and Jackson 2000; Gorham 1991). In part, this new insight was a result of C measurements much deeper in *permafrost*—perennially frozen—soils stored as a result of processes unique to frozen soils. Freeze-thaw mixing in combination with wind- and waterborne sediment deposition over hundreds and thousands of years has buried C many meters deep into permafrost soils, much deeper than had been traditionally accounted for by soil C inventories (Ping et al. 2010). The so-called *permafrost carbon* inventory considers the entire soil organic C stock including organic soils, mineral soils, peatlands, and soils above the surface of permafrost (*active layer*) that thaw seasonally. The top 3 m of all permafrost-zone soils contain 1024 Pg C, with 818 Pg of that contained in the actual Gelisol soil order (permafrost-affected soils). The remaining fraction is in other soil orders within the northern circumpolar permafrost zone, because only some ground is underlain by permafrost in the discontinuous and sporadic/isolated zone. In sum, permafrost-affected soils contain 88% of the total 1672 Pg C found in the northern circumpolar permafrost zone, when also accounting for the 648 Pg of deep permafrost C (>3 m) in Siberia, Alaska, and the Arctic river deltas (Zimov et al. 2006; Tarnocai et al. 2009). The uncertainty of this stock estimate is at present unknown but could be on the order of several hundred Pg (McGuire et al. 2010), and the estimate will continue to be revised as additional data from these remote places becomes available (Schirrmeister et al. 2010; Johnson et al. 2011; Kanevskiy et al. 2011). This C accumulated over thousands of years

under cold and sometimes waterlogged conditions, but these very factors that protect and retain organic C in northern soils are now changing as the climate warms.

In the Arctic, temperatures are rising ultimately as a result of greenhouse gas emissions primarily from fossil fuel burning, deforestation, and other human activities elsewhere on Earth. The magnitude of future temperature rise depends on the trajectory of human emissions in combination with the response of the Earth system to this forcing. Models agree that Arctic warming will be greater than average global warming, with some models projecting a 7-8°C warming over land in these regions by the end of the 21st century under the A2 emissions scenario (ACIA 2005; Meehl et al. 2007). For such high-warming scenarios, models project there will be large reductions in near-surface (top 2-3 m) permafrost by 2100, with some estimates ranging from 53% to 66% decrease from current areal extent (Euskirchen et al. 2006; Saito et al. 2007; Lawrence et al. 2011). Thawing of frozen ground has the potential to influence the future storage of permafrost C. Because the permafrost C pool is so large, release of even a fraction of this C into the atmosphere could accelerate the pace of climate warming.

How C emissions from the permafrost zone will influence the future pace of climate change can be framed by three key questions (Schuur et al. 2008). First, how much permafrost C is vulnerable to release into the atmosphere? As these soils thaw, ancient C is available for decomposition by soil organisms and is released to the atmosphere as greenhouse gases. Some of this C is easily metabolized and will be consumed quickly by microorganisms while other fractions are more difficult to break down and may remain within the soil for much longer. This mixture of C also dictates the second key question: how fast will this C release occur? Rapidly decomposing C can be released on timescales of less than one year after thaw, but this represents a small portion of the permafrost C pool (Zimov et al. 2006; Dutta et al. 2006). The bulk of permafrost C is likely to be released slowly over decades after thaw with a small proportion of C persisting within the soil for much longer. Finally, the third key question is: what will be the form of this C release? Whether soil microorganisms release carbon dioxide (CO_2) or methane (CH_4) will determine the ultimate radiative-forcing potential of these emissions. Methane is produced in waterlogged low-oxygen environments common in the Arctic and has around 33 times the global warming potential of CO_2 over a century time scale (Shindell et al. 2009). However, waterlogged environments that favor CH_4 release also slow overall emission rates and

retain higher amounts of C within soil. It is the balance between these two opposing factors as well as the overall distribution of upland (oxic) and lowland (anoxic) environments across the Arctic landscape that will determine the ratio of CO_2 to CH_4 emissions.

Aside from biological decomposition, fire could be an important abiotic mechanism for releasing permafrost C to the atmosphere. Fire frequency and severity are increasing in some parts of the boreal permafrost zone (Turetsky et al. 2011), and rare events such as the large Alaskan tundra wildfire in 2007 (Mack et al. 2011) may become more common in the future. Fires release C directly to the atmosphere via combustion and also indirectly by warming surface soils and permafrost, thus increasing microbial activity (Chambers and Chapin 2002; Yoshikawa et al. 2002; Grosse et al. 2011). Given the right set of dry conditions or changes in surface hydrology, thawing and fires could act together to expose and transfer permafrost C to the atmosphere very rapidly, especially in ecosystems with organic surface soils (McGuire et al. 2010). Together these biotic and abiotic factors will be some important determinants of the overall feedback from permafrost C to climate.

Questions concerning permafrost C release are easily framed but challenging to answer. Projections of change in permafrost and soil C remain limited by the range of mechanisms conceptualized within current models and by the scarcity of actual measurements from these remote landscapes. For example, future permafrost temperature is modeled over large scales as one-dimensional propagation of projected air temperature increase through soil and ground material (Romanovsky and Osterkamp 2000). This propagated warming then increases microbial activity and C release. But in ice-rich permafrost, abrupt thaw processes that cause ice wedges to melt and the ground surface to collapse irreversibly appear to be driven by three-dimensional heat and water redistribution across the landscape (Osterkamp et al. 2009; Shur and Jorgenson 2007). Internal feedback dynamics accelerate the degradation of frozen ground beyond what is driven by temperature alone, and evidence for this type of rapid thaw that can expose deep C is already widespread (Jorgenson et al. 2006; Sannel and Kuhry 2011) and likely to increase. Also, simple biogeochemistry modules that describe the biological exchange of C between ecosystems and the atmosphere do not necessarily describe soil development processes that have led to the accumulation of large permafrost C pools in the first place (Koven et al. 2009). Models that do not accurately set initial conditions are not likely to make credible projections of permafrost C

release under future conditions. Model development has been slowed by the difficulty in describing complex, non-linear threshold processes and also because the field and lab measurements needed for parameterization are difficult to obtain from these extreme environments. The few field studies that exist show that temperature interacts with permafrost thaw, ground subsidence, and changes in surface hydrology to control C emissions from ecosystems, and that these factors are likely to differ across moisture/waterlogging thresholds in upland and lowland environments (Vogel et al. 2009; Schuur et al. 2009; Turetsky et al. 2011; Wickland et al. 2006).

Most terrestrial models used to assess the exchange of carbon between the biosphere and the atmosphere have incomplete or no representation of permafrost C dynamics. However, expert knowledge on permafrost C dynamics is more advanced than the information that has been incorporated into models. This then presents an opportunity to draw on other approaches in order to frame the scientific understanding of this issue (e.g. Lenton 2008) . Here we used a survey to quantify and evaluate variability among experts concerning our hypotheses of future permafrost C emissions to the atmosphere. We asked a group of international experts to provide quantitative estimates of permafrost change in response to four scenarios of warming. This expert survey helps outlines the potential risk to society caused by permafrost thaw, and presents hypotheses that will be tested by new data collection and model development. Ultimately, the hypotheses about changes in permafrost C discussed here will need testing with improved quantitative models and comparison with other important land and ocean system changes such as increases in plant biomass (greening) and the influence of declining ice/snow cover on albedo, which either offset or contribute to the climate feedback from a warming Arctic.

AB.3 Methods

The survey used to collect expert assessment of the vulnerability of permafrost C was divided into three questions (A4.8). Experts were asked to provide quantitative estimates of surface permafrost degradation (Q1), permafrost carbon release (Q2), and methane emissions (Q3) for three time periods: 1) by the year 2040 where modeled Arctic temperature increases ranged from 1.5-2.5°C higher than the 1985-2004 average baseline, 2) by the year 2100 where temperature increases ranged from 2.0-7.5°C higher, and 3) by the year 2300 where it was assumed temperature increases reached by 2100 remained at that level. The warming scenarios

span possible atmospheric trajectories including one scenario of steadily increasing greenhouse gases, two scenarios of greenhouse gas stabilization after 2100, and one scenario of greenhouse gas stabilization then decline before 2100. Experts also provided self-reported expertise for each of the three questions and confidence ratings for each of the warming scenarios within each particular question. Survey results were obtained from a group of experts, selected from the larger scientific community because of their particular expertise and previous work on this topic, who attended a three-day workshop in June 2011 in Seattle, WA, USA, as part of the Vulnerability of Permafrost Carbon Research Coordination Network (RCN; A4.9).

For each response we also calculated C emissions in CO_2 equivalent (units of Pg C) by subtracting CH_4 emission (Q3) from total C emission (Q2), multiplying CH_4 by its 100-year or 20-year global warming potential (GWP) of 33 and 105 respectively while also accounting for the mass difference between CO_2 and CH_4 gas, and adding that value back to total C emission (Shindell et al. 2009). We recognize that calculations using GWP are an incomplete representation of the influence of permafrost C emissions on radiative forcing, but using this common unit allows for the influence of CH_4 and CO_2 emissions to be more directly compared because it accounts for the higher radiative forcing of CH_4. For the numbers reported in the text, responses with a self-rated expertise of 1 (little or no expertise) were excluded. This removed any answers provided by experts that judged themselves to be at the lowest end of the expertise scale for any particular question. We analyzed the effect of this data screening by comparing the statistical distribution of responses of the final dataset to unscreened data (all respondents), as well as to a dataset that used only answers from the upper half of the expertise scale (expertise $\geq$3 included). While this screening process did not end up having an overall directional effect on the mean or median response of the group for any particular question, it addressed imperfections in the expert selection process and considered the comfort level of individual experts in providing such an assessment.

Across much of the final dataset, the distribution of values was right-skewed such that mean responses across the dataset are larger in all cases than median values. To describe the distribution of the data most succinctly, we present back-transformed values of the mean and standard error of the mean derived from a natural log transformation of the raw data. All natural log distributions were normally distributed at $p>0.05$ unless otherwise noted. In four cases (of

36), the data were normally distributed and no transformation was necessary. Ranges reported in the text represent the 95% confidence interval.

AB.4 Results

AB.4.1 Surface permafrost degradation

Across the group with self-ranked expertise > 1, experts projected that surface permafrost would degrade 9-16% (n=33) from the current total areal extent over the next three decades, 48-63% by 2100, and 67-80% over the next several centuries under the highest warming scenario presented to the group (representative concentration pathway [RCP] 8.5) (Figure AB.1a). These values are approximately three times greater than permafrost degradation projected under the lowest warming scenario (RCP 2.6), which were 3-7%, 11-18%, and 20-30% for the three time frames, respectively. For the two lower warming scenarios, the rate of permafrost degradation was predicted to remain stable through 2040 and 2100 (assuming a constant rate over each respective time frame) (A4.10), corresponding to a relatively small change in warming between 2040 and 2100 in those scenarios (A4.8**)**. For the two higher warming scenarios, the change in warming was relatively greater between 2040 and 2100 and corresponded to higher projected rates of permafrost degradation in the later part of the century compared to the period before 2040. Rates after 2100 declined substantially but still resulted in significant additional permafrost degradation by 2300. This highlights expert agreement in the lag in the response of permafrost to changes in air temperature, given that the provided scenarios included no additional warming after 2100 but permafrost was still equilibrating to new, higher temperatures.

Of the twelve time-by-scenario combinations of permafrost degradation considered by the group, two-thirds had right-skewed distributions, while the remaining third had normal distributions. This differed somewhat from the opinions of C release, which were all right skewed. Normally distributed responses occurred only in the two higher warming scenarios and only for the 2100 and 2300 time frames. Log normal distributions might be expected in lower warming scenarios and shorter time frames because zero change acted as a lower limit cutoff point.

AB.4.2 Carbon release

Under the highest warming scenario the total projected magnitude of CO_2-equivalent emissions from permafrost zone soils was 19-45 Pg C (n=27) by 2040, 162-288 Pg C by 2100, and 381-616 Pg C by 2300. When Arctic temperature increase is limited to 2°C by 2100 (the lowest warming scenario considered by this group, RCP 2.6), CO_2-equivalent emissions of 6-17 Pg C (n=27) were projected by 2040, 41-80 Pg C by 2100, and 119-200 Pg C by 2300 (Figure AB.1b). These C emissions, although quite sizeable, are roughly one-third the high-warming scenario emissions. These values calculated with a 100-year CH_4 GWP underestimate warming that is expected to occur within this century. In comparison, the high warming scenario CO_2-equivalent emissions using a 20-year CH_4 GWP are 29-69 Pg C by 2040, 250-463 Pg C by 2100, and 572-1004 Pg C by 2300. The calculation of actual warming by 2100 is beyond the scope of the data collected this survey and may lie somewhere between these two, but serves to illustrate the influence of choice of time horizon on this metric.

Much of the actual C release by mass is expected to be in the form of CO_2. In terms of total C mass (of both CO_2 and CH_4), experts estimated that 15-33 Pg C (n=27) could be released by 2040, reaching 120-195 Pg C by 2100, and 276-414 Pg C by 2300 under the high warming scenario (Figure AB.1c). This net release by 2100 corresponds to a 7-11% decline in the 1700 Pg C pool currently contained in northern permafrost zone soils. Of that amount, only about 2.3% was expected to be in the form of CH_4, corresponding to 0.26-0.85 Pg CH_4-C by 2040, 2.03-6.21 Pg CH_4-C by 2100 and 4.61-14.24 Pg CH_4-C by 2300 (Figure AB.1d). The proportional release of CH_4 estimated by experts was relatively invariant across all warming scenarios and time horizons (Figure AB.1e). This two-order-of-magnitude difference in CO_2 release relative to CH_4 release incorporates the effects of both faster microbial decomposition in upland oxic environments compared to waterlogged anoxic environments, and the spatial distribution of these environments across the permafrost zone. However, the higher GWP of CH_4 means that roughly one-third (100-year GWP) to one-half (20-year GWP) of the effect of future permafrost-zone C emissions on climate forcing, when calculated in this metric of CO_2-equivalent, was expected to be a result of CH_4 emissions from wetlands, lakes, and other oxygen-limited environments where organic matter will be decomposing.

Similar to estimates for permafrost area in some scenarios, initial C emission rates in the present to 2040 period were then projected to increase in the latter part of the century (assuming a constant rate over a given time frame); this increase was consistent across warming scenarios (A4.10). Rates after 2100 were projected to decline but still were higher than present-2040 rates. As with permafrost degradation, the hypothesis of sustained 2100-2300 release resulted in substantial C emissions, even though there was no additional warming after 2100 in these scenarios. The source of these emissions from different geographical regions changed through time, even as cumulative emissions kept rising. By 2040, relatively more emissions were expected from the combined sporadic and discontinuous permafrost zones farther to the south as compared to the continuous permafrost zone even though the continuous zone is two times larger in land area (Figure AB.2). By 2100, relative emissions from the combined sporadic and discontinuous zones was expected to be roughly equal to those from the continuous zone, but by 2300 continuous-zone emissions were expected to be double that of the other zones. This predicted geographical shift in C emissions is consistent with the fact that permafrost in the sporadic and discontinuous zones is already closer to the thawing point, whereas continuous permafrost is colder. The more rapid response in the discontinuous and sporadic zones may then lead to lower emission rates after 2100 as a portion of the vulnerable soil C pool may have already been decomposed.

AB.4.3 Expertise and confidence

The distribution of responses for both total C and CH_4 emissions had right-skewed distributions for all scenarios and time frames. Again, because the group estimated C emissions at the lower end of the full possible range (0-1700 Pg C), zero change acted as a lower limit cutoff point. There were a small number of experts that thought C emissions could be significantly higher than the mean response of all experts; this pattern was consistent across scenarios and time frames.

As a group, the experts rated themselves as having a mean expertise of 2.4, 2.6, and 2.1 for permafrost degradation (Q1), total C emissions (Q2), and CH_4 emissions (Q3) respectively. For Q1 and Q2, self-ratings of 2 or 3 were most common. This pattern differed for Q3, which was dominated by ratings of 2 and had fewer 3s than 1s. Confidence values were reported by warming scenario individually within each given question so there were four times as many total

ratings. Mean confidence for Q1 was 2.1, Q2 was 1.9, and Q3 was 1.6. The most common confidence rating was 2, followed by 1, with the distribution of confidence also decreasing across the three questions. Confidence did not vary across the four warming scenarios for Q1, indicating that experts were equally confident of their low- and high-warming estimates of permafrost degradation. However, for Q2 and Q3, average confidence decreased slightly for each progressively warmer scenario (Pearson's, Q2 $r = -0.18$, Q3 $r = -0.19$ $p < 0.05$). Across all questions and scenarios, confidence was positively correlated with expertise (Pearson's, $r = 0.57$, $p < 0.0001$), showing the overall link between these two metrics.

To examine the influence of self-rated expertise values on the distribution and magnitude of responses we compared survey results from the full group of respondents with those from expertise values greater than 1, and those with expertise values 3 and greater. All of these groupings showed the same right-skewed distribution with a small number of experts projecting substantially higher C emissions, and zero acting as a lower limit cutoff. There was little change in mean values across expertise groups, with a small effect of increased sample size somewhat reducing the standard error of the estimate. This analysis is presented for total C emissions but the same pattern was observed for all questions.

AB.5 Discussion

Perception of the importance of the permafrost C feedback to climate change has been dominated by the improved quantification of the large size of the permafrost soil C pool. But the potential climate feedback of this C pool is determined by three factors: how much is vulnerable to release, how fast will it be released, and in what form (CO_2 and CH_4) will the release occur? At present there is a paucity of studies that provide comprehensive answers to these questions. The survey conducted here illustrates that experts in this field hypothesize significant C releases from permafrost zone soils over policy-relevant time horizons, and also hypothesize important lags whereby permafrost degradation and C emissions are expected to continue for decades and centuries even if average global temperature is stabilized. This exercise highlights both the potential risk from permafrost thaw, as well as the utility of expert elicitation in informing policy-relevant questions at the boundaries of our scientific understanding. Expert elicitation is a common methodology that has been used to define uncertainty in many scientific disciplines including the Earth sciences (Halpern et al. 2008; Lenton et al. 2008; Aspinall 2010), and is a

powerful tool allowing the integration of individual and community knowledge to help outline difficult questions. Our experience suggests that this process was a useful way to frame hypotheses about what the future might look like, as well as to gauge variability in hypotheses among scientists. We learned that significant time and energy was necessary to develop and revise the survey to ensure adequate specificity in question wording and format. And, the workshop proved critical for ensuring that experts understood seemingly straightforward questions in the same way.

Two general patterns about the scientific community opinion emerged from this process. First, the responses for many of the questions had right-skewed distributions. This was a consequence of the fact that, as a whole, the group viewed the vulnerable portion of the permafrost C pool to be only a fraction of the total pool (7-11%, 95% confidence interval) under the time frames and warming scenarios considered here, such that zero acted as a lower cutoff point. At the same time a small number of experts thought that considerably higher losses were possible, extending the upper tail of the distribution. The only deviation from this general pattern was observed in the responses for permafrost degradation in higher warming scenarios and longer time frames. Here, the larger magnitude of loss (~>50%) hypothesized by experts moved away from the lower limit cutoff such that the responses in those cases were more uniformly distributed. Interestingly, the distribution shape and magnitude of response did not differ when experts were screened by self-rated expertise. Even experts classified in the upper half of the expertise scale had a similar log normal distribution and confidence interval as the full group. For the full group, as well as within subsets of higher expertise respondents, most opinions were relatively clustered whereas some individuals thought the effects of warming could be substantially larger. This lack of difference between expertise levels emphasizes that scientific uncertainty on this issue is real and not just an artifact due to varying levels of experience with the subject matter. The initial workshop screening process, which selected leading scientists knowledgeable in some aspect of permafrost research, also likely contributed to removing some of the uncertainty that would have been present if surveying a more general group of scientists. The scientists that participated here are considered expert in this field as compared to scientists in general, or to earth system and climate scientists more specifically. It is important to recognize that the collective estimate set forth by the survey responses from this group is not the only possible set of hypotheses about the future feedback to climate from permafrost C. While this

activity lays important new groundwork in the form of a testable hypothesis, it cannot rule out alternative hypotheses.

While it is important to put this expert estimate in the context of published work using different methods, direct comparisons are difficult because the topic is relatively new. Modeling work has been underway recently, but these projections each are derived without some of the important mechanisms discussed in this paper. The expert prediction of total C release by 2100 under the high warming scenario presented here is still 1.7-5.2 times larger than several recent modeling predictions with comparable climate scenarios (Schaefer et al. 2011; Koven et al. 2011; Schneider von Deimling et al. 2011). By 2300, model estimates of C emissions (190±64 Pg C to 600-1000 Pg C) bracket the expert opinion (276-414 Pg C, 95% confidence interval), though noting that warming for model scenarios continued to increase between 2100 and 2300 but not in the question posed to the experts. Rapid C losses by 2100 projected by the experts likely reflect, in part, the perceived importance of abrupt thaw processes that are lacking within current models, as well as heightened awareness of the deep C pools. These areas, as well as others, are the subject of active model development for future permafrost C projections.

There are no comprehensive direct measurements of soil C loss from the permafrost zone at large scales. This is in part due to a scarcity of soil C measurement relative to other regions of the world, in combination with an overall difficulty of detecting changes in soil C pools due to large within-site soil heterogeneity. We do know the expected 7-11% decrease in the permafrost C pool size by 2100 is comparable to the 7-14% decrease measured over 1 to 2 decades in landscape soil C inventories in England and Wales possibly as a result of climate change (Bellamy et al. 2005). While this comparison is of two very different regions, it demonstrates that a similar magnitude of soil C loss is possible at a regional scale. However, the time frame for permafrost zone soil C loss was estimated by experts to be roughly 6 times slower than measured rates of loss in England and Wales, since this magnitude of loss was expected to occur by 2100. This difference in rate of loss is consistent with environmental differences between the two regions. Soil temperatures remain moderate for potential year round soil C loss in England and Wales, whereas the majority of permafrost soil C losses will be restricted to the short summer months, even with future warming. Because there is no broad set of historical measurements of

permafrost C pools, it will be difficult to detect even major permafrost C losses directly without an extensive network of repeated measurements.

The magnitude of loss projected by experts agrees with a flux-based estimate from a permafrost ecosystem in Alaska where it was estimated that 5% of the permafrost C pool could be lost over a century with widespread permafrost degradation (Schuur et al. 2009). Because flux measurements integrated the response of both increased plant C uptake and net soil C loss due to permafrost degradation, offsets by plant biomass might explain why the loss result is on the lower end of the range found in the survey that considered only net soil loss. While only based on a single site, this field-based estimate agrees generally that only a fraction of the permafrost C pool is likely to be vulnerable by 2100. Of course, even a fraction of this very large pool has important implications, especially considering the combined impact of CO_2 and CH_4 emissions. The expert projection of CH_4 emitted by 2300 is consistent in magnitude with the tens of Pg thought to have come from northern ecosystems after the end of the last glacial period (Fischer et al. 2008). That historic release is known to be biogenic in origin emitted from wetlands, lakes, and other oxygen-limited environments, with some proportion likely bubbling out of thaw lakes forming in permafrost as the climate warmed to present-day conditions (Walter et al. 2007).

Because permafrost zone C release accelerates the impact of anthropogenic emissions, knowing the amount of permafrost C that will be released this century and beyond is a critical consideration when identifying climate change mitigation goals. Even given the real uncertainty that exists, this study highlights that experts hypothesize that the release of C from permafrost zone soils is likely to influence the pace of climate change in this century and beyond. Hypothesized permafrost C release by 2100 under a high warming scenario may be of similar magnitude to other biogenic C sources such as tropical deforestation, if current rates of that activity estimated at 1.1 Pg C/yr (2000-2010 average) were to continue (Peters et al. 2011). While these biogenic C sources are very different, the fact that CH_4 makes up a substantial portion of permafrost C release means its overall radiative-forcing impact on climate could be more than two times larger than that from deforestation. Even so, these hypothesized emissions are unlikely to overshadow the impact of fossil fuel burning, which will continue to be the main source of C emissions and climate forcing under any scenario considered by this group. Permafrost C release in 100-year CO_2 equivalent under the high warming scenario are equivalent

to 8-18% (range based on expert confidence interval) of fossil fuel rates of 7.9 Pg C/yr (2000-2010 average) projected out to 2040, or 22-40% of current fossil fuel rates projected out to 2100. Of course, actual percentages will differ in the future as future fossil fuel emissions change through time. Under the lowest warming scenario, the percentages would only be one third of these values.

Because of the continued dominance of fossil fuel emissions, permafrost C release, if at a scale hypothesized here, is more likely to act as an important accelerator of climate change rather than a tipping point mechanism. In this way, permafrost C emissions on top of rapidly growing fossil fuel emissions would make temperature targets significantly harder to achieve than currently assessed by the IPCC. However, permafrost C release differs qualitatively from fossil fuel and deforestation emissions in that it occurs in remote places far from direct human influence. This not only makes these potential emissions difficult to observe and quantify, but also difficult to address through legislative or geoengineering solutions. One mitigation strategy might be to focus on limiting the overall magnitude of global temperature increase. The fact that the lowest warming scenario was hypothesized to avoid two thirds of the permafrost C release highlights the utility of a preventative approach. Many strategies for reducing fossil fuel and deforestation emissions to the atmosphere have been identified. The implementation of some of these strategies could have substantial benefits for permafrost C stability, keeping more of it frozen in the ground for longer thus reducing its impact on climate. It is important to reiterate that the high warming scenario is the trajectory of increasing greenhouse gas emissions that we are currently following, whereas the other scenarios require some restriction in atmospheric emissions over time.

This study focused on framing a hypothesis about permafrost soil C loss to the atmosphere, which has the potential to accelerate climate warming. But, as climate change occurs, other ecological and Earth system factors that affect C and energy exchange may act either to offset or augment some of the effects of C release from permafrost thaw. In the Arctic, increased plant biomass is likely to offset some of the C emissions from soil, driven both by warmer conditions and by nutrients released from decomposing organic matter (Walker et al. 2006). Based on steady-state vegetation and soil pools, it is likely that, over long time periods, emissions will still be significantly larger than uptake (Schuur et al. 2008), but uptake can have

important implications especially for short-term dynamics (Schuur et al. 2009). Also, because nutrient release is inextricably linked to changes in permafrost soil C, it will also be important to understand other fates of nutrients aside from plant uptake. Microbial activity can release N_2O (Elberling et al. 2010), which itself is a potent greenhouse gas with a GWP of 298 on a 100-year time scale (IPCC 2007). Small releases of N_2O could counterbalance the climate offset of C incorporated into plant biomass. A comprehensive review of these factors is beyond the scope of this survey, but testing the hypotheses presented here with improved models is important future work that will help place C emissions alongside estimates of plant uptake and the fate of other released elements to determine the overall potential climate feedback from permafrost C.

AB.6 Acknowledgements

Figure AB.2 was prepared by Reginald Muskett in the Permafrost Laboratory in the Geophysical Institute, UAF. Funding that supported the development of this paper was provided by National Science Foundation Vulnerability of Permafrost Carbon Research Coordination Network Grant #955713.

AB.7 Literature Cited

ACIA (2005) Arctic Climate Impacts Assessment. Cambridge University Press, Cambridge, United Kingdom

Aspinall W (2010) A route to more tractable expert advice. Nature 463 (7279):294-295. doi:10.1038/463294a

Bellamy PH, Loveland PJ, Bradley RI, Lark RM, Kirk GJD (2005) Carbon losses from all soils across England and Wales 1978-2003. Nature 437 (7056):245-248. doi:10.1038/nature04038

Chambers SD, Chapin FS (2002) Fire effects on surface-atmosphere energy exchange in Alaskan black spruce ecosystems: Implications for feedbacks to regional climate. J Geophys Res-Atmos 108 (D1). doi:10.1029/2001jd000530

Dutta K, Schuur EAG, Neff JC, Zimov SA (2006) Potential carbon release from permafrost soils of Northeastern Siberia. Glob Change Biol 12 (12):2336-2351. doi:10.1111/j.1365-2486.2006.01259.x

Elberling B, Christiansen HH, Hansen BU (2010) High nitrous oxide production from thawing permafrost. Nature Geoscience 3 (5):332-335. doi:10.1038/ngeo803

Euskirchen ES, McGuire AD, Kicklighter DW, Zhuang Q, Clein JS, Dargaville RJ, Dye DG, Kimball JS, McDonald KC, Melillo JM, Romanovsky VE, Smith NV (2006) Importance of recent shifts in soil thermal dynamics on growing season length, productivity, and carbon sequestration in terrestrial high-latitude ecosystems. Glob Change Biol 12 (4):731-750. doi:10.1111/J.1365-2486.2006.01113.X

Fischer H, Behrens M, Bock M, Richter U, Schmitt J, Loulergue L, Chappellaz J, Spahni R, Blunier T, Leuenberger M, Stocker TF (2008) Changing boreal methane sources and constant biomass burning during the last termination. Nature 452 (7189):864-867. doi:10.1038/Nature06825

Gorham E (1991) Northern Peatlands - Role in the carbon-cycle and probable responses to climatic warming. Ecological Applications 1 (2):182-195. doi:10.2307/1941811

Grosse G, Harden J, Turetsky M, McGuire AD, Camill P, Tarnocai C, Frolking S, Schuur EAG, Jorgenson T, Marchenko S, Romanovsky V, Wickland KP, French N, Waldrop M, Bourgeau-Chavez L, Striegl RG (2011) Vulnerability of high-latitude soil organic carbon in North America to disturbance. J Geophys Res-Biogeo 116. doi:10.1029/2010jg001507

Halpern BS, Walbridge S, Selkoe KA, Kappel CV, Micheli F, D'Agrosa C, Bruno JF, Casey KS, Ebert C, Fox HE, Fujita R, Heinemann D, Lenihan HS, Madin EMP, Perry MT, Selig ER, Spalding M, Steneck R, Watson R (2008) A global map of human impact on marine ecosystems. Science 319 (5865):948-952. doi:10.1126/science.1149345

Jobbagy EG, Jackson RB (2000) The vertical distribution of soil organic carbon and its relation to climate and vegetation. Ecological Applications 10 (2):423-436. doi:10.2307/2641104

Johnson KD, Harden J, McGuire AD, Bliss NB, Bockheim JG, Clark M, Nettleton-Hollingsworth T, Jorgenson MT, Kane ES, Mack M, O'Donnell J, Ping CL, Schuur EAG, Turetsky MR, Valentine DW (2011) Soil carbon distribution in Alaska in relation to soil-forming factors. Geoderma 167-68:71-84. doi:10.1016/j.geoderma.2011.10.006

Jorgenson MT, Shur YL, Pullman ER (2006) Abrupt increase in permafrost degradation in Arctic Alaska. Geophysical Research Letters 33 (2). doi:10.1029/2005gl024960

Kanevskiy M, Shur Y, Fortier D, Jorgenson MT, Stephani E (2011) Cryostratigraphy of late Pleistocene syngenetic permafrost (yedoma) in northern Alaska, Itkillik River exposure. Quaternary Res 75 (3):584-596. doi:10.1016/j.yqres.2010.12.003

Koven C, Friedlingstein P, Ciais P, Khvorostyanov D, Krinner G, Tarnocai C (2009) On the formation of high-latitude soil carbon stocks: Effects of cryoturbation and insulation by organic matter in a land surface model. Geophysical Research Letters 36:-. doi:10.1029/2009gl040150

Koven CD, Ringeval B, Friedlingstein P, Ciais P, Cadule P, Khvorostyanov D, Krinner G, Tarnocai C (2011) Permafrost carbon-climate feedbacks accelerate global warming. P Natl Acad Sci USA 108 (36):14769-14774. doi:10.1073/pnas.1103910108

Lawrence DM, Slater AG, Swenson SC (2011) Simulation of Present-day and Future Permafrost and Seasonally Frozen Ground Conditions in CCSM4. Journal of Climate. doi:10.1175/jcli-d-11-00334.1

Lenton TM, Held H, Kriegler E, Hall JW, Lucht W, Rahmstorf S, Schellnhuber HJ (2008) Tipping elements in the Earth's climate system. P Natl Acad Sci USA 105 (6):1786-1793. doi:10.1073/pnas.0705414105

Mack MC, Bret-Harte MS, Hollingsworth TN, Jandt RR, Schuur EAG, Shaver GR, Verbyla DL (2011) Carbon loss from an unprecedented Arctic tundra wildfire. Nature 475 (7357):489-492.

McGuire AD, Macdonald RW, Schuur EAG, Harden JW, Kuhry P, Hayes DJ, Christensen TR, Heimann M (2010) The carbon budget of the northern cryosphere region. Curr Opin Environ Sustain 2 (4):231-236. doi:10.1016/j.cosust.2010.05.003

Meehl GA, Stocker TF, Collins WD, Friedlingstein P, Gaye AT, Gregory JM, Kitoh A, Knutti R, Murphy JM, Noda A, Raper SCB, Watterson IG, Weaver AJ, Zhao Z-C (2007) Global Climate Projections. In: Climate Change 2007: The Physical Science Basis. Contribution of Working Group I to the Fourth Assessment Report of the Intergovernmental Panel on Climate Change [Solomon, S., D. Qin, M. Manning, Z. Chen, M. Marquis, K.B. Averyt, M. Tignor and H.L. Miller (eds.)]. Cambridge University Press, Cambridge, United Kingdom and New York, NY, USA

Osterkamp TE, Jorgenson MT, Schuur EAG, Shur YL, Kanevskiy MZ, Vogel JG, Tumskoy VE (2009) Physical and Ecological Changes Associated with Warming Permafrost and

Thermokarst in Interior Alaska. Permafrost and Periglacial Processes 20 (3):235-256. doi:10.1002/ppp.656

Ping CL, Michaelson GJ, Kane ES, Packee EC, Stiles CA, Swanson DK, Zaman ND (2010) Carbon Stores and Biogeochemical Properties of Soils under Black Spruce Forest, Alaska. Soil Sci Soc Am J 74 (3):969-978. doi:10.2136/sssaj2009.0152

Romanovsky VE, Osterkamp TE (2000) Effects of unfrozen water on heat and mass transport processes in the active layer and permafrost. Permafrost and Periglacial Processes 11 (3):219-239. doi:10.1002/1099-1530(200007/09)11:3<219::aid-ppp352>3.0.co;2-7

Saito K, Kimoto M, Zhang T, Takata K, Emori S (2007) Evaluating a high-resolution climate model: Simulated hydrothermal regimes in frozen ground regions and their change under the global warming scenario. J Geophys Res-Earth Surf 112 (F2):-. doi:10.1029/2006jf000577

Sannel ABK, Kuhry P (2011) Warming-induced destabilization of peat plateau/thermokarst lake complexes. J Geophys Res-Biogeo 116. doi:10.1029/2010jg001635

Schaefer K, Zhang T, Bruhwiler L, Barrett AP (2011) Amount and timing of permafrost carbon release in response to climate warming. Tellus B:no-no. doi:10.1111/j.1600-0889.2011.00527.x

Schirrmeister L, Grosse G, Kunitsky VV, Fuchs MC, Krbetschek M, Andreev AA, Herzschuh U, Babyi O, Siegert C, Meyer H, Derevyagin AY, Wetterich S (2010) The mystery of Bunge Land (New Siberian Archipelago): implications for its formation based on palaeoenvironmental records, geomorphology, and remote sensing. Quaternary Science Reviews 29 (25-26):3598-3614. doi:10.1016/j.quascirev.2009.11.017

Schneider von Deimling T, Meinshausen M, Levermann A, Huber V, Frieler K, Lawrence DM, Brovkin V (2011) Estimating the permafrost-carbon feedback on global warming. Biogeosciences (8):4727-4767

Schuur EAG, Bockheim J, Canadell JG, Euskirchen E, Field CB, Goryachkin SV, Hagemann S, Kuhry P, Lafleur PM, Lee H, Mazhitova G, Nelson FE, Rinke A, Romanovsky VE, Shiklomanov N, Tarnocai C, Venevsky S, Vogel JG, Zimov SA (2008) Vulnerability of permafrost carbon to climate change: Implications for the global carbon cycle. Bioscience 58 (8):701-714. doi:10.1641/B580807

Schuur EAG, Vogel JG, Crummer KG, Lee H, Sickman JO, Osterkamp TE (2009) The effect of permafrost thaw on old carbon release and net carbon exchange from tundra. Nature 459 (7246):556-559. doi:10.1038/Nature08031

Shindell DT, Faluvegi G, Koch DM, Schmidt GA, Unger N, Bauer SE (2009) Improved Attribution of Climate Forcing to Emissions. Science 326 (5953):716-718. doi:10.1126/science.1174760

Shur YL, Jorgenson MT (2007) Patterns of permafrost formation and degradation in relation to climate and ecosystems. Permafrost and Periglacial Processes 18 (1):7-19. doi:10.1002/ppp.582

Tarnocai C, Canadell JG, Schuur EAG, Kuhry P, Mazhitova G, Zimov S (2009) Soil organic carbon pools in the northern circumpolar permafrost region. Global Biogeochemical Cycles 23:-. doi:10.1029/2008gb003327

Turetsky MR, Donahue WF, Benscoter BW (2011) Experimental drying intensifies burning and carbon losses in a northern peatland. Nature Communications 2. doi:10.1038/ncomms1523

Vogel J, Schuur EAG, Trucco C, Lee H (2009) Response of CO(2) exchange in a tussock tundra ecosystem to permafrost thaw and thermokarst development. J Geophys Res-Biogeo 114. doi:10.1029/2008jg000901

Walter KM, Edwards ME, Grosse G, Zimov SA, Chapin FS (2007) Thermokarst lakes as a source of atmospheric CH(4) during the last deglaciation. Science 318 (5850):633-636. doi:10.1126/science.1142924

Wickland KP, Striegl RG, Neff JC, Sachs T (2006) Effects of permafrost melting on CO2 and CH4 exchange of a poorly drained black spruce lowland. J Geophys Res-Biogeo 111 (G2). doi:10.1029/2005jg000099

Yoshikawa K, Bolton WR, Romanovsky VE, Fukuda M, Hinzman LD (2002) Impacts of wildfire on the permafrost in the boreal forests of Interior Alaska. J Geophys Res-Atmos 108 (D1). doi:10.1029/2001jd000438

Zimov SA, Davydov SP, Zimova GM, Davydova AI, Schuur EAG, Dutta K, Chapin FS (2006) Permafrost carbon: Stock and decomposability of a globally significant carbon pool. Geophysical Research Letters 33 (20):-. doi:10.1029/2006gl027484

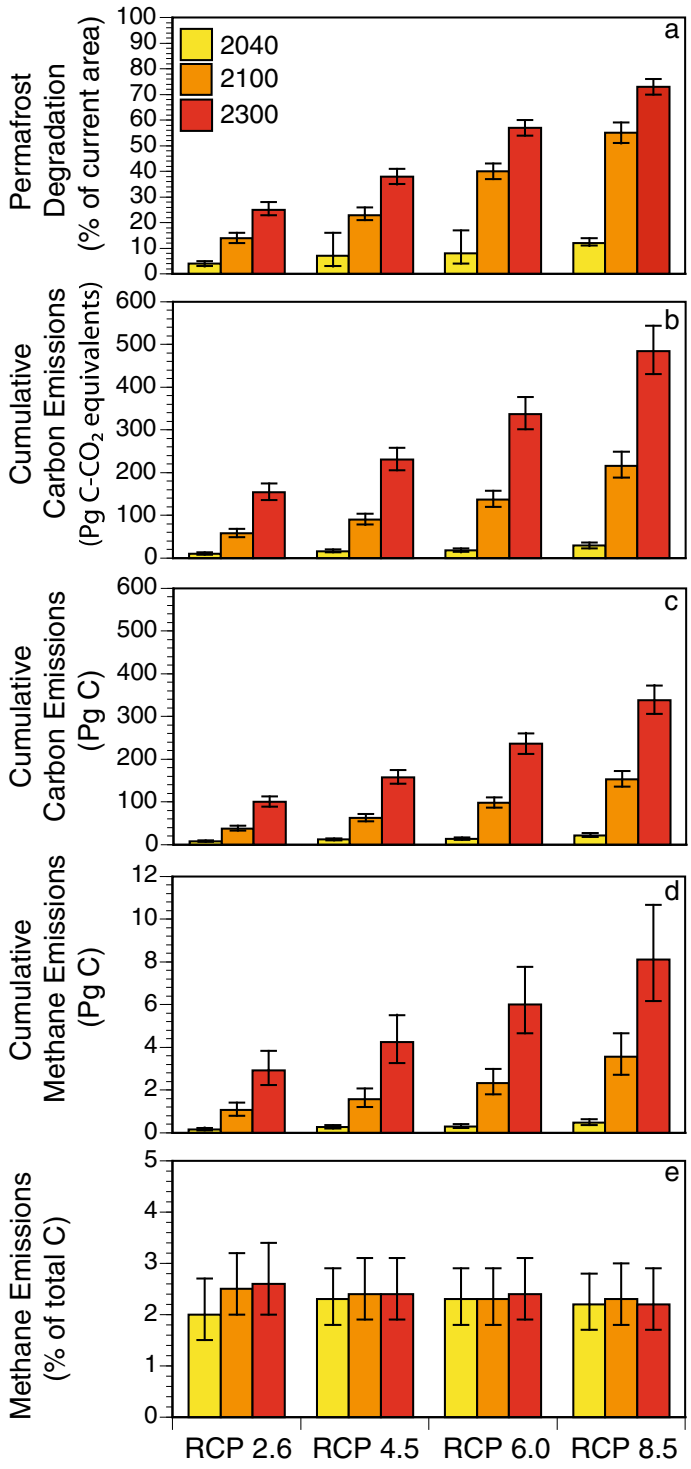

Figure AB.1 Expert survey responses for cumulative **a** surface permafrost degradation, **b** carbon emissions (CO_2-equivalents using 100-year GWP), **c** carbon emissions (by mass), **d** methane emissions (by mass), and **e** relative methane emissions (%), over three time frames (2040, 2100, 2300) in response to four IPCC warming scenarios. Values are means and standard error.

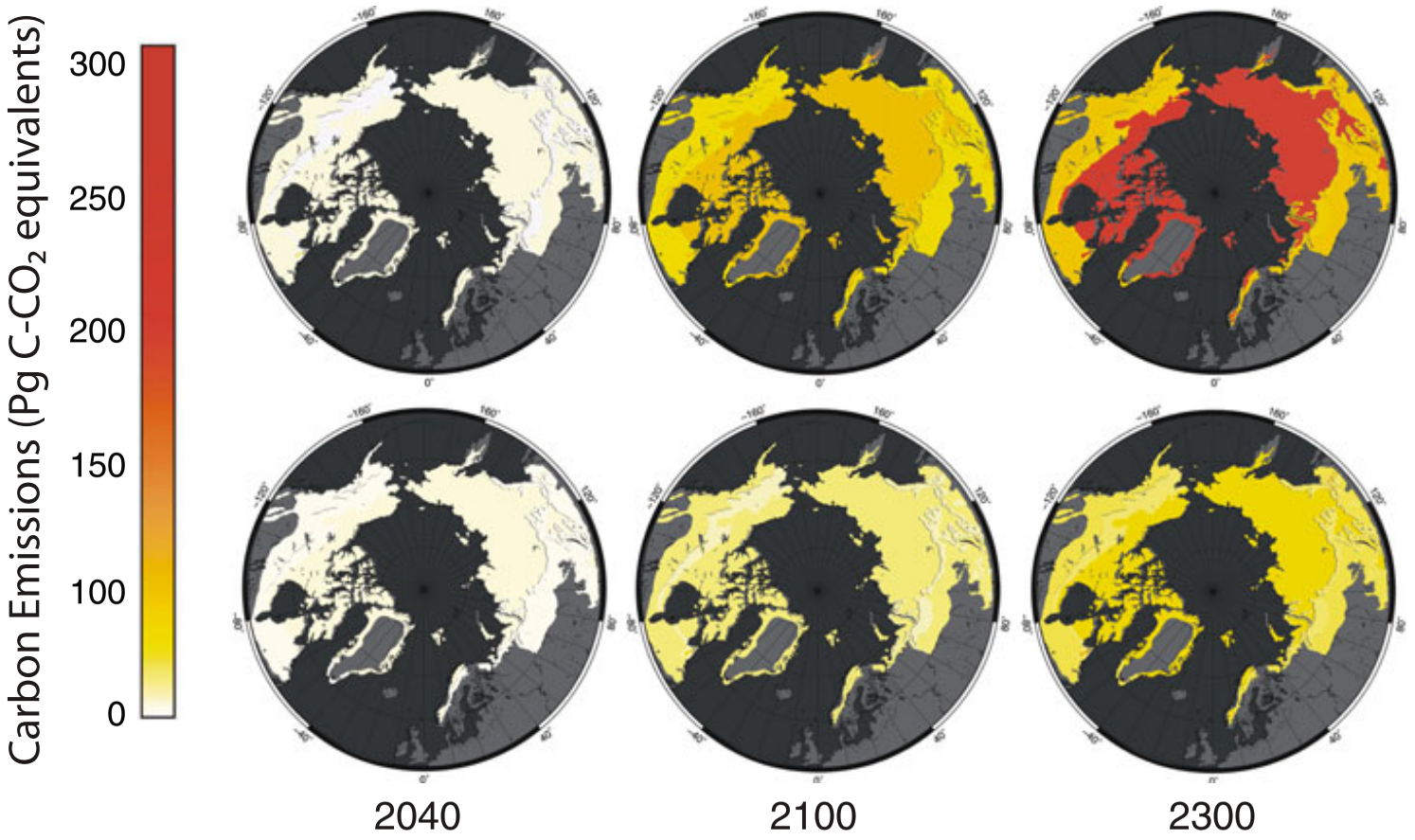

Figure AB.2 Cumulative carbon emissions projected by experts as a result of warming climate for three different time horizons. Top figures represent a lower warming trajectory (1.54 °C at 2040, 7.5 °C at 2100, 7.5 °C at 2300), and bottom figures represent a lower warming trajectory (1.54 °C at 2040, 2.0 °C at 2100, 2.0 °C at 2300). Values are Pg C (CO_2 plus CH_4) expressed on a common scale as CO_2-equivalents (using 100-year GWP) and are shown as median values (to account estimates of zero flux) for the continuous, the discontinuous, and the sporadic plus isolated permafrost zones.

AB.8 Supplementary methods and survey form

AB.8.1 Survey design

The survey used to collect expert assessment of the vulnerability of permafrost C was divided into three questions. Experts were asked to provide quantitative estimates of surface permafrost degradation (Q1), permafrost C release (Q2), and CH_4 emissions (Q3). Because permafrost temperature and extent vary within regions of the northern circumpolar permafrost zone, numerical estimates were reported separately for the continuous zone, discontinuous zone, and the sporadic/isolated zone (Brown et al. 1998). The assessment of permafrost change by zone was made for each of four warming scenarios over three time frames. Time frames were chosen to represent short-term change (cumulative change between present (~2010) and the year 2040), medium-term change (cumulative until 2100), and long-term change (cumulative to 2300). The short- and medium-term time frames are more directly policy-relevant, whereas the long-term time frame provides perspective on important Earth system changes.

The warming scenarios were based on four representative concentration pathways (RCP 2.6, 4.5, 6.0, 8.5) specified as part of the new Intergovernmental Panel on Climate Change Fifth Assessment Report (IPCC AR5) development process (Moss et al. 2010). These scenarios span possible atmospheric trajectories including one scenario of steadily increasing greenhouse gases (RCP 8.5, >1370 ppm CO_2 equivalent in 2100), two scenarios of atmospheric stabilization after 2100 (RCP 4.5, RCP 6.0, 650 ppm and 850 ppm CO_2 equivalent), and one scenario of atmospheric stabilization then decline before 2100 (RCP 2.6, 490 ppm CO_2 equivalent at peak). These RCPs were used to generate four scenarios of Arctic warming using the Community Climate System Model 4 (Gent et al. 2011). Future temperatures (Table 1, Figure 1 in A4.8) were plotted as a 7-yr running average anomaly from the 1985-2004 average baseline temperature for the terrestrial Arctic region (Greenland excluded). Modeled Arctic temperature increases over land are roughly 2.5 times that of the global average, thus the strongest warming scenario that predicted 7.5°C higher temperature by 2100 corresponds to ~3°C higher global mean temperature. By the year 2040, the modeled arctic surface air temperature increases ranged from 1.5-2.5°C higher than a 1985-2004 average baseline, and from 2.0-7.5°C higher by the year 2100. While modeled temperature under some RCPs continue to change beyond 2100, the scenarios presented in the survey assumed that the temperature increase reached by 2100

stabilized at that level and remained there through 2300. This evaluated the time lag in the response of permafrost C to climate change over longer time scales, rather than the influence of additional climate change that itself becomes less certain farther out in time. For every question, each expert provided 36 numerical responses that covered all warming scenario, time frame, and permafrost zone combinations.

For Q1, experts estimated change in surface permafrost extent reported in percent loss from the current extent of ~14.6×10^6 km^2 (Zhang et al. 1999). Surface permafrost was defined as permafrost occurring within the top 3 meters of the ground. For Q2, experts assessed the net change in soil C stocks in the permafrost region, reported in cumulative Pg (1×10^{15}g) C emitted to the atmosphere as CO_2 and CH_4. Current estimates of the permafrost region C pool size partitioned by zone and depth were provided as background. This question included the entire soil C stock in the northern circumpolar permafrost zone. It was noted that while the discontinuous and sporadic/isolated zones are only partially underlain by permafrost, there still may be changes in non-permafrost soils in a future warmer world. Experts were asked not to include changes in vegetation C stocks in their estimate, but to include losses and gains of C that may occur in the surface soil (*active layer*) that becomes unfrozen seasonally in permafrost soils. Question 3 asked for an assessment of the amount of C from Q2 that would be emitted as CH_4, reported in Tg (1×10^{12}g) C. For all three questions it is important to note that, while future climate scenarios were defined solely by temperature increase, experts were asked to include both direct and indirect changes in climate likely to be associated with each warming scenario. These changes included but were not limited to: climatic variables such as precipitation, seasonality, etc, and landscape changes such as fire regime, surface and subsurface hydrology, wetting/drying, etc.

For each of the three survey questions, respondents were asked to provide an overall score of their *expertise* in that particular area from 1 (low) to 4 (high) based on criteria outlined in the survey form. And finally, the respondents were asked to provide an overall *confidence* score for each different warming scenario within each question from 1 (low) to 4 (high) based on criteria outlined in the survey form. Thus, each question answered by an expert had 1 expertise rating and 4 confidence ratings corresponding to the 4 warming scenarios evaluated for each question.

AB.8.2 Survey Development and Implementation

Survey results were obtained from a group of experts that attended a three-day workshop in June 2011 in Seattle, WA, USA, as part of the Vulnerability of Permafrost Carbon Research Coordination Network (RCN) (www.biology.ufl.edu/permafrostcarbon; A4.9). Forty international participants attended the workshop, having been selected from the larger scientific community by the RCN steering committee (Schuur, McGuire, Canadell, Harden, Kuhry, Romanovsky, Turetsky) for their particular expertise and previous work on this topic. Thirty-eight of these participants returned completed survey forms, though some questions were intentionally left blank. In addition, three other experts (Chapin, Ciais, Zimov) who were unable to attend the workshop but were previously involved in the survey and/or workshop development process, returned surveys. In total, there were 38 responses for Question 1, 38 responses for Question 2, and 35 responses for Question 3.

The survey was revised on two occasions before final survey data were collected. The first iteration occurred in 2009 as part of larger assessment of Earth system change. This larger assessment was called the Dangerous Climate Change Assessment Project (DanCCAP), led by Oxford University and the Tyndall Centre for Climate Change Research (Sky et al. 2010). This project provided an outline for the survey methods used, and helped in the original development of the system definition and the format of the questions. The permafrost questions used in this study were a subset of a larger set of Arctic survey questions used for DanCCAP. Responses from a few individuals to the permafrost questions in that phase led to revisions in the questionnaire.

A near-final version of the survey was distributed to the RCN workshop participants with the format discussed by the group at the workshop. The survey was emailed a month prior to the meeting and the participants independently filled out the survey with the option of referring to relevant literature and data. These results were submitted before the start of the meeting. During the workshop, the participants were shown anonymous mean and median results of the compiled surveys. In the discussion that followed, it became clear that not all participants had considered the questions in the same way. Specific clarifications were identified over the course of the workshop and added to the survey instructions. Also as a result of that discussion, warming scenarios for the final survey were updated to correspond to the newly available IPCC

representative concentration pathways. For the dataset reported here, experts completed final surveys independently during a period 2-4 weeks after the Seattle workshop.

AB.8.3 Analyses

For each response we also calculated C emissions in CO_2 equivalent (units of Pg C) by subtracting CH_4 emission (Q3) from total C emission (Q2), multiplying CH_4 by its 100-year or 20-year global warming potential (GWP) of 33 and 105 respectively while also accounting for the weight difference between CO_2 and CH_4 gas, and adding that value back to total C emission (Shindell et al. 2009). While the use of a fixed GWP doesn't account for many important complexities in the climate system (Manning and Reisinger 2011; Shine et al. 2005; Forster et al. 2007), it still provides a quantitative method for the rough comparison of the impact of permafrost CH_4 and CO_2 emissions on climate. It is important to note that GWP for CH_4 increases when considering shorter time scales. Most values use the 100-year GWP for consistency with other literature, but the 20-year GWP is shown for comparison in some cases. The 100-year GWP CO_2-equivalent is viewed as the century-scale impact of C releases emitted within a particular time interval. We also calculated percentage CH_4 of the total C emission by dividing CH_4 emission (Q3) by the total C emission (Q2). Carbon emissions in CO_2 equivalent and percent CH_4 were calculated for each permafrost zone, time frame, and warming scenario individually.

For the numbers reported in the text, responses with a self-rated expertise of 1 (little or no expertise) were excluded. This removed individual answers provided by experts that judged themselves to be at the lowest end of the expertise scale for any particular question. For CO_2 equivalent and percent CH_4 (which are derived from Questions 2 and 3), any responses with an expertise of 1 for either Q2 or Q3 were excluded. While this screening process did not end up having an overall directional effect on the mean or median response of the group for any particular question, it addressed imperfections in the expert selection process and considered the comfort level of individual experts in providing such an assessment. The screened dataset had 33 responses for Q1, 34 for Q2, and 27 for Q3, and thus also 27 responses for CO_2 equivalent and percent methane. We analyzed the effect of this data screening by comparing the statistical distribution of responses of the final dataset to unscreened data (all respondents), as well as to a dataset that used only answers from the upper half of the expertise scale (expertise $\geq$3 included).

Results of screening are presented only for total C, but are representative of results from all questions.

Across much the final dataset, the distribution of values fit a lognormal distribution with a skew towards higher values such that mean responses across the dataset are larger in all cases than median values. To describe the distribution of the data most succinctly, we present untransformed values of the mean and standard error of the mean derived from a natural log transformation of the raw data. All natural log distributions were significant at $p<0.05$ unless otherwise noted. In four cases (of 36), the data were normally distributed and no transformation was necessary. Ranges reported in the text represent the 95% confidence interval.

AB.8.4 Literature Cited

Brown J, O.J. Ferrians J, Heginbottom JA, Melnikov ES (1998) Digital Circum-Arctic Map of Permafrost and Ground-Ice Conditions., vol Circumpolar Active-Layer Permafrost System (CAPS) version 1.0. International Permafrost Association, Data and Information Working Group, comp.,

Forster P, Ramaswamy V, Artaxo P, Berntsen T, Betts R, Fahey DW, Haywood J, Lean J, Lowe DC, Myhre G, Nganga J, Prinn R, Raga G, Schulz M, Van Dorland R (2007) Changes in Atmospheric Constituents and in Radiative Forcing. In: Climate Change 2007: The Physical Science Basis. Contribution of Working Group I to the Fourth Assessment Report of the Intergovernmental Panel on Climate Change [Solomon, S., D. Qin, M. Manning, Z. Chen, M. Marquis, K.B. Averyt, M.Tignor and H.L. Miller (eds.)]. Cambridge University Press, Cambridge, United Kingdom and New York, NY, USA.

Gent PR, Danabasoglu G, Donner LJ, Holland MM, Hunke EC, Jayne SR, Lawrence DM, Neale RB, Rasch PJ, Vertenstein M, Worley PH, Yang ZL, Zhang MH (2011) The Community Climate System Model Version 4. Journal of Climate 24 (19):4973-4991. doi:10.1175/2011jcli4083.1

Manning M, Reisinger A (2011) Broader perspectives for comparing different greenhouse gases. Philosophical Transactions of the Royal Society a-Mathematical Physical and Engineering Sciences 369 (1943):1891-1905. doi:10.1098/rsta.2010.0349

Moss RH, Edmonds JA, Hibbard KA, Manning MR, Rose SK, van Vuuren DP, Carter TR, Emori S, Kainuma M, Kram T, Meehl GA, Mitchell JFB, Nakicenovic N, Riahi K, Smith

SJ, Stouffer RJ, Thomson AM, Weyant JP, Wilbanks TJ (2010) The next generation of scenarios for climate change research and assessment. Nature 463 (7282):747-756. doi:10.1038/Nature08823

Shine KP, Fuglestvedt JS, Hailemariam K, Stuber N (2005) Alternatives to the global warming potential for comparing climate impacts of emissions of greenhouse gases. Climatic Change 68 (3):281-302. doi:10.1007/s10584-005-1146-9

Sky J, New M, Donner SD, Bamber JL, Chapin FS, Schuur EAG, Beniston M, Abbott BW (2010) Dangerous Climate Change Assessment Project Final Report. UK Met Office,

Zhang T, R.G. Barry, K. Knowles, J.A. Heginbottom, Brown J (1999) Statistics and characteristics of permafrost and ground ice distribution in the Northern Hemisphere. Polar Geography 23 (2):147-169

Survey form

Vulnerability of Permafrost Carbon: Survey Questions

Introduction

The goal of this survey is to determine the magnitude of permafrost degradation and subsequent carbon release in response to arctic and boreal warming scenarios. Possible thresholds and tipping points in the relationship between temperature increase and permafrost loss and carbon release are of particular interest, since such non-linearity is difficult to predict on the basis of models.

You will be asked to provide estimates of permafrost loss and carbon release for the three major permafrost zones (continuous, discontinuous, and sporadic/isolated) over short-term (2010-2040), medium-term (2010-2100), and long-term (2010-2300) time scales

We recognize that climate-change-driven feedbacks in complex Earth systems are not, and cannot be, precisely and definitively modeled. As such, we are only asking for your informed opinion, realizing that some of the included parameters may not be well understood. By administering this survey to scientists with the most applicable expertise, we want to identify and evaluate the possible and probable magnitude of permafrost response in the arctic and subarctic.

Instructions

In addition to answering each question, you will have a chance to indicate your level of confidence and expertise concerning your answer; and provide additional comments on how you selected your estimated magnitudes of climate/carbon feedback response. These follow-up questions allow us to compare responses from multiple experts. If the answer to a particular question is currently unknown, but there is a particular piece of research that you think could resolve some of that uncertainty, please indicate what that would be in the "comments" space provided, or at the end of the survey. If you have little or no expertise concerning a particular question, please skip it.

The four-point "**Confidence level**" scale is defined as follows:

1= My answer is my best guess but I am not confident in it; it could easily be far off the mark. Scientific uncertainty on this issue is very large.

2= I am moderately confident that my answer is as good as anyone can offer at this time but there is large scientific uncertainty on this issue and the true value may be quite different.

3= I am very confident that my answer is the best anyone can offer at this time; there is moderate scientific uncertainty, so the true value is likely to be somewhat different from my answer, but it is unlikely to be dramatically different.

4= I would be very surprised if my answer were far off from the true value.

The four-point "**Expertise level**" scale is defined as follows:

1= I have little familiarity with the literature and I do not actively work on these particular questions.

2= I have some familiarity with the literature and I've worked on related questions but haven't contributed to the literature on this issue; it is not an area of central expertise for me.

3= I have worked on related issues and have contributed to the relevant literature but do not consider myself one of the foremost experts on this particular issue.

4= I contribute actively to the literature directly concerned with this issue, and I consider myself one of the foremost experts on it.

We also ask that you provide key literature references in support of your view; however, in many cases there may be no clarity in the literature on the issue at hand. Nevertheless, if you have a view concerning the magnitude of the feedback, please provide it. If there is not yet clear supporting evidence in the literature, but you have some basis for an estimate based on expert professional judgment, please make a note of that.

Warming Scenarios

You will be asked to estimate the Arctic system response to four warming scenarios. These scenarios of regional Arctic warming were generated with NCAR's Community Climate System Model (CCSM4) with inputs from the most recent IPCC radiative forcing scenarios (**Figure 1**).

To minimize the possibility of misinterpretation, we have also provided a table showing the amount of warming predicted in Figure 1 by the end of each of the three time scales (**Table 1**).

	Warming at 2040 (°C)	Warming at 2100 (°C)	Warming at 2300 (°C)
WS 1	1.5	2.0	2.0
WS 2	2.0	3.0	3.0
WS 3	2.0	4.5	4.5
WS 4	2.5	7.5	7.5

Table 1. Temperature increases for the four warming scenarios (designated here as WS1-4). Values given represent the regional Arctic temperature increase achieved by the year indicated. Values for WS1-4 correspond to the IPCC representative concentration pathways (RCP): 2.6, 4.5, 6.0, and 8.5 respectively.

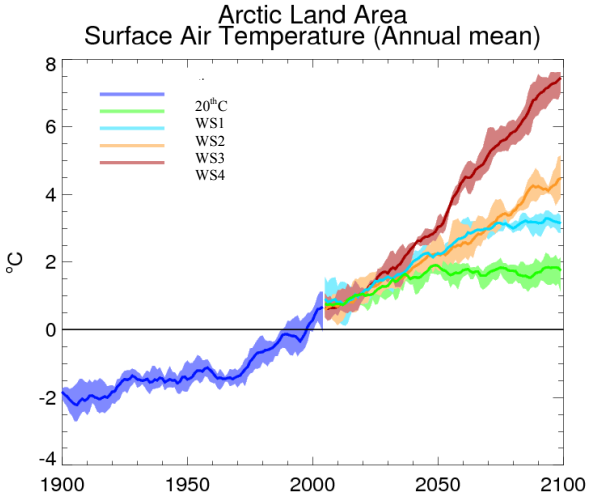

Figure 1. CCSM4: Anomaly from 1985-2004 (7-yr running average; Greenland excluded). Though not shown in this figure, temperature increase is assumed to stabilize and level off after 2100 for the purposes of this survey.

Updates from Workshop

The following decisions were discussed specifically at the workshop and are listed here for clarity:

1) Repeat survey as final statement of this group

2) Use actual IPCC Arctic warming scenarios (shown above)

3) Response should be **net change in the soil/permafrost C stock**, reported as cumulative Pg C, noting that it is also useful to check per year emission. Do not include changes in vegetation C, but do consider losses and gains of C that may occur in the surface soil as part of your response.

4) Remember to consider change in entire soil C stock in permafrost zone, noting that only some fraction is underlain by permafrost but there still may be changes in non-permafrost soils in a future warmer world.

5) Continuous, discontinuous, and sporadic+isolated permafrost zones should be considered in terms of their current geographic areas throughout all time horizons.

6) The warming scenarios are expressed as temperature increase, but your answer could reasonably include both direct and indirect changes in climate (i.e. precipitation, etc) and landscape changes (i.e. fire regime, etc) that are likely to be associated with warming at that magnitude.

7) Please revisit your expertise level (see page 1) based on the range of expertise found within our group

Questions

1. How much change in the extent of near-surface permafrost (loss of permafrost in at least the top three meters of soil from the current permafrost extent of ~14.6×10^6 km^2 [Zhang et al. 2000]) would result from the following pan-arctic warming scenarios? Note that a possible range of 0-100% should be used for each zone.

Warming Scenario (use Table 1 for temperature increase)	**Short-term** (2010-2040) **permafrost extent response** (% decrease)			**Medium-term** (2010-2100) **permafrost extent response** (% decrease)			**Long-term** (2010-2300) **permafrost extent response** (% decrease)			**Confidence level (1-4)**
	Continuous	**Discontinuous**	**Sporadic and Isolated**	**Continuous**	**Discontinuous**	**Sporadic and Isolated**	**Continuous**	**Discontinuous**	**Sporadic and Isolated**	
WS1										
WS2										
WS3										
WS4										
Comments:										**Expertise level (1-4)**
Additional key literature that you relied on, not yet cited in other materials with this survey:										

2. How much cumulative carbon release to the atmosphere (Pg carbon emitted as either CO_2 or CH_4 from soils in the circumpolar north permafrost region) would occur due to the following pan-arctic warming scenarios? **Note:** Your estimate of release should be a change current stock of **soil/permafrost carbon** in the entire permafrost zone. The table below provides estimates of the shallow and deep carbon pool sizes for the three permafrost zones, including carbon stored in both permafrost and non-permafrost soils. For a more detailed breakdown refer to the system definition text.

	% of total permafrost area*	**Shallow (0-3m) C Pg****	**Deep (>3 m) C Pg*****	**Total Pg C**
Continuous	60	614	570	1185
Discontinuous	13	133	130	263
Sporadic/Isolated	26	266		266

*Zhang et al. 1999, **Tarnocai et al. 2009, ***Tarnocai et al. 2009 but estimated by zone here

Warming Scenario (use Table 1 for temperature increase)	**Short-term** (2010-2040) **C release** (cumulative Pg C)			**Medium-term** (2010-2100) **C release** (cumulative Pg C)			**Long-term** (2010-2300) **C release** (cumulative Pg C)			**Confidence level (1-4)**
	Continuous	**Discontinuous**	**Sporadic and Isolated**	**Continuous**	**Discontinuous**	**Sporadic and Isolated**	**Continuous**	**Discontinuous**	**Sporadic and Isolated**	
WS1										
WS2										
WS3										
WS4										
Comments:									**Expertise level (1-4)**	
Additional key literature that you relied on, not yet cited in other materials with this survey:										

3. How much of the C release calculated for Question 2 will be emitted as methane (reported as **cumulative Tg** CH_4–C) from soils in the circumpolar north permafrost zone due to the following pan-arctic warming scenarios?

Warming Scenario (use Table 1 for temperature increase)	**Short-term** (2010-2040) **CH_4 release** (cumulative Tg as CH_4)			**Medium-term** (2010-2100) **CH_4 release** (cumulative Tg as CH_4)			**Long-term** (2010-2300) **CH_4 release** (cumulative Tg as CH_4)			**Confidence level (1-4)**
	Continuous	**Discontinuous**	**Sporadic and Isolated**	**Continuous**	**Discontinuous**	**Sporadic and Isolated**	**Continuous**	**Discontinuous**	**Sporadic and Isolated**	
WS1										
WS2										
WS3										
WS4										
Comments:									**Expertise level (1-4)**	
Additional key literature that you relied on, not yet cited in other materials with this survey:										

4. What additional comments or insights do you have concerning the content, format and implementation of this survey?

AB.9 Survey Participants: Name and Affiliation

Benjamin W. Abbott; University of Alaska Fairbanks, Fairbanks, AK

Dr. William (Breck) Bowden; University of Vermont, Burlington, VT

Dr. Victor Brovkin; Max Planck Institute for Meteorology, Hamburg, Germany

Dr. Philip Camill; Bowdoin College, Brunswick, ME

Dr. Josep G. Canadell; Global Carbon Project CSIRO, Canberra, Australia

Dr. Jeffrey P. Chanton; Florida State University, Tallahassee, FL

Dr. F. Stuart (Terry) Chapin, III; University of Alaska Fairbanks, Fairbanks, AK

Dr. Torben R. Christensen; Lund University, Lund, Sweden

Dr. Philippe Ciais; LSCE, CEA-CNRS-UVSQ, Gif-sur-Yvette, France

Dr. Patrick M. Crill; Stockholm University, Stockholm, Sweden

Dr. Benjamin T. Crosby; Idaho State University, Pocatello, ID

Dr. Claudia I. Czimczik; University of California, Irvine, CA

Dr. Guido Grosse; University of Alaska Fairbanks, Fairbanks, AK

Dr. Jennifer Harden; US Geological Survey, Menlo Park, CA

Dr. Daniel J. Hayes; Oak Ridge National Laboratory, Oak Ridge, TN

Dr. Gustaf Hugelius; Stockholm University, Stockholm, Sweden

Dr. Julie D. Jastrow; Argonne National Laboratory, Argonne, IL

Dr. Thomas Kleinen; Max Planck Institute for Meteorology, Hamburg, Germany

Dr. Charles D. Koven; Lawrence Berkeley National Lab, Berkeley, CA

Dr. Gerhard Krinner; CNRS/UJF-Grenoble 1, LGGE, Grenoble, France

Dr. Peter Kuhry; Stockholm University, Stockholm, Sweden

Dr. David M. Lawrence; National Center for Atmospheric Research, Boulder, CO

Dr. A. David McGuire; University of Alaska Fairbanks, Fairbanks, AK

Dr. Susan M. Natali; University of Florida, Gainesville, FL

Dr. Jonathan A. O'Donnell; US Geological Survey, Denver, CO

Dr. Chien-Lu Ping; University of Alaska Fairbanks, Fairbanks, AK

Dr. William J. Riley; Lawrence Berkeley National Lab, Berkeley, CA

Dr. Annette Rinke; Alfred Wegener Institute, Potsdam, Germany

Dr. Vladimir E. Romanovsky; University of Alaska Fairbanks, Fairbanks, AK

Dr. A. Britta K. Sannel; Stockholm University, Stockholm, Sweden

Dr. Christina Schädel; University of Florida, Gainesville, FL

Dr. Kevin Schaefer; National Snow and Ice Data Center, Boulder, CO

Dr. Edward (Ted) A. G. Schuur; University of Florida, Gainesville, FL

Zachary M. Subin; Lawrence Berkeley National Lab, Berkeley, CA

Dr. Charles Tarnocai; AgriFoods, Ottawa, Canada

Dr. Merritt Turetsky; University of Guelph, Guelph, Canada

Dr. Mark Waldrop; US Geological Survey, Menlo Park, CA

Dr. Katey M. Walter Anthony; University of Alaska Fairbanks, Fairbanks, AK

Dr. Kimberly P. Wickland; U.S. Geological Survey, Boulder, CO

Dr. Cathy J. Wilson; Department of Energy, Los Alamos National Laboratory, Santa Fe, NM

Sergey A. Zimov; North-East Scientific Station, Cherskii, Siberia

AB.10

Table AB.1 Annual rate of change confidence intervals estimated by time frame and warming scenario.

		2010-2040		2040-2100		2100-2300	
		Lower 95% CI	Upper 95% CI	Lower 95% CI	Upper 95% CI	Lower 95% CI	Upper 95% CI
Surface permafrost loss ($\% yr^{-1}$)	RCP2.6	0.10	0.22	0.13	0.18	0.05	0.06
	RCP4.5	0.18	0.32	0.22	0.31	0.07	0.08
	RCP6.0	0.21	0.35	0.46	0.59	0.08	0.09
	RCP8.5	0.31	0.52	0.64	0.79	0.09	0.09
Total C release ($Pg\ C\ yr^{-1}$)	RCP2.6	0.2	0.4	0.4	0.6	0.3	0.4
	RCP4.5	0.3	0.6	0.7	1.0	0.4	0.6
	RCP6.0	0.3	0.7	1.1	1.7	0.6	0.8
	RCP8.5	0.5	1.1	1.8	2.7	0.4	1.1
CH_4 release ($Tg\ C\ yr^{-1}$)	RCP2.6	3	12	9	25	6	16
	RCP4.5	5	17	13	38	8	23
	RCP6.0	5	19	20	56	11	31
	RCP8.5	9	28	30	89	13	40

Experts were asked for cumulative release; this calculation divided cumulative by numbers of years in a period and assumes a constant rate over each time interval. Rates are shown for emissions that occur within a given time period, rather than cumulative from present (2010). The estimates of release from the permafrost C pool do not strictly represent fluxes to the atmosphere because plant uptake (not estimated by this survey) may offset some portion of C release.

Appendix C. Thermo-erosion gullies increase nitrogen available for hydrologic export[1]

Tamara K. Harms[2], Benjamin W. Abbott, Jeremy B. Jones

Institute of Arctic Biology and Department of Biology & Wildlife, University of Alaska Fairbanks

[2]tamara.harms@alaska.edu, phone: 907-474-6117, fax: (907) 474-6967

Running head: Nitrogen in thermokarst soils

AC.1 Abstract

Formation of thermokarst features, ground subsidence caused by thaw of ice-rich permafrost, can result in increased export of inorganic nitrogen (N) from arctic tundra to downstream ecosystems. Subsidence exposes mineral soils, which tend to contain higher abundance of inorganic ions relative to surface soils, and may bring inorganic N into contact with flowing water. Alternatively, physical mixing may increase aeration and drainage of soils, which could promote N mineralization and nitrification while suppressing denitrification. Finally, some soil types are more prone to formation of thermokarst, and if these soils are relatively N-rich, thermokarst features may export more N than surrounding tundra. We compared physical characteristics, N pools, and rates of N transformations in soils collected at two depths from thermo-erosion gullies, intact water tracks (the typical precursor landform to thermo-erosion gullies), and undisturbed tundra to test these potential mechanisms. Integrated across depths, inorganic N pools in thermo-erosion gullies were similar to the mean for all tundra in this region, as well as to water tracks. Thus, soils prone to thermo-erosion are not intrinsically N-rich, and increased N availability in thermokarst features is apparent only at sub-regional spatial scales. However, vertical profiles of N pools and transformation rates were homogenized within thermo-erosion gullies compared to adjacent intact tundra, indicating that physical mixing brings inorganic N to the surface, where it may be subject to hydrologic export. Increased inorganic N availability caused by formation of thermo-erosion gullies may have acute, but

[1]Published as Harms, T., B. Abbott, and J. Jones. 2013. Thermo-erosion gullies increase nitrogen available for hydrologic export. Biogeochemistry:1-13.

spatially isolated consequences for downstream aquatic ecosystems, with strongest effects within drainage networks where gullies are likely to form.

Keywords: arctic tundra, denitrification, mineralization, nitrification, nitrogen, permafrost, thermo-erosion gully, thermokarst

AC.2 Introduction

Tundra landscapes are characterized by strong nitrogen (N) limitation that results in a closed N cycle, with little export of inorganic N to aquatic ecosystems and the atmosphere (Buckeridge and Grogan 2010; Yano et al. 2010). However, warming climate and loss of permafrost may disrupt the mechanisms regulating arctic N cycling and cause significant export of N. Experimental warming of arctic tundra results in elevated inorganic N availability (Buckeridge and Grogan 2010; Natali et al. 2011; Shaver et al. 1998), which may be subject to leaching, particularly from deep soils (Mack et al. 2004). Such patterns may result from introduction of previously frozen N into the cycling pool due to gradual thaw that deepens the zone of seasonally thawed soils, or from direct effects of temperature on microbial processes. In contrast, loss of ice-rich permafrost can cause rapid ground subsidence, termed thermokarst (Jorgenson and Osterkamp 2005), which can result in elevated concentrations of N in plant tissue (Schuur et al. 2007), and hydrologic export of ammonium (NH_4^+) (Bowden et al. 2008).

Seasonally thawed soils, termed the active layer, typically encompass organic soils in the arctic, and biological activity as well as flow of water is largely restricted to the active layer (Hinzman et al. 1991). In undisturbed tundra, plants and micro-organisms compete intensely for the nutrients available within the active layer (Jonasson and Shaver 1999; Schimel and Chapin 1996). For N, typically the limiting nutrient, such competition results in low net rates of N mineralization and nitrification, small inorganic N pools, and minimal gaseous and hydrologic losses of inorganic N (Buckeridge et al. 2010; Giblin et al. 1991; Yano et al. 2010).

Strong stratification of mineral and organic soil horizons in tundra soils is commonly disrupted by cryoturbation, vertical mixing of soil resulting from repeated freeze-thaw cycles (Ping et al. 1998). Cryoturbation incorporates surface-derived organic matter into mineral horizons below the permafrost table, preserving significant stocks of organic carbon (Bockheim 2007; Kaiser et al. 2007; Ping et al. 1998). Retention of nutrients in tundra soils is stimulated by high-quality organic matter due to heterotrophic uptake (DeMarco et al. 2011; Lavoie et al. 2011), and incorporation of surface-derived organic matter at depth may have similar effects on nutrient cycling. The consequences of moving mineral soils toward the surface, such as results from thermokarst formation, however, are less well studied. Mineral soils of arctic tundra contain larger pools of inorganic N than overlying organic soils as well as higher rates of N mineralization and nitrification (Hobbie and Gough 2002; Keuper et al. 2012; Nadelhoffer et al. 1991). In other ecosystems, physical mixing of soils can speed rates of N cycling, including increasing net rates of nitrification (Booth et al. 2006).

There are several modes of thermokarst formation; here we address thermo-erosion gullies, a common type of thermokarst on hillslopes (Jorgenson and Osterkamp 2005), which often occur on water tracks and therefore connect disturbed soils to stream networks. Thermo-erosion gullies form when heat transfer from water flowing across the soil or vegetation surface deepens the active layer in an area underlain by ice-rich permafrost (Jorgenson and Osterkamp 2005). A combination of ice-volume loss and mechanical erosion causes subsidence and channel incision through a process of thermo-erosional tunneling and surface collapse (Fortier et al. 2007; Godin and Fortier 2012; Fig. AC.1). This process can occur rapidly in a single season, but may continue over several years depending on the depth of ice-rich permafrost and the extent of the ice-wedge network (Fortier et al. 2007; Godin and Fortier 2012). Once a depression has

formed, thermo-erosion is accelerated by accumulation of windblown snow, which insulates underlying soil, reducing heat loss in winter (Osterkamp et al. 2009). During the thaw season, collection of surface water by the depression facilitates heat transfer, further promoting development of the feature (Jorgenson and Osterkamp 2005).

Herein we address the mechanisms that result in elevated N availability observed in receiving waters downstream of thermokarst features, and evaluate the relative effects of thermokarst on soil N availability across tundra landscapes. We hypothesize several mechanisms by which thermokarst formation influences N cycling in tundra soils. First, thermokarst-associated mixing brings mineral soils that are relatively rich in inorganic N to the surface where they may interact with surface water and contribute ions to hydrologic flowpaths. Second, mixing of organic soil horizons with mineral soils at depth brings a potentially labile source of carbon together with inorganic N from mineral soils, and may thereby stimulate heterotrophic retention of N in microbial biomass or removal via denitrification. Third, physical mixing may result in increased aeration and drainage of soils, which could promote N mineralization and nitrification, or restrict capacity for N loss via denitrification. Finally, some soil types are more prone to formation of thermokarst because of high ice content (Jorgenson and Osterkamp 2005; Walker and Everett 1991), and these soils can have elevated concentrations of exchangeable ions (Kokelj and Burn 2005). If thermokarst-prone soils are also N-rich relative to other soil types, thermokarst features may export more N than surrounding tundra.

We tested these hypotheses using a survey of soil N pools and rates of N transformations that included thermo-erosion gullies, water tracks, and undisturbed tundra soils in northern Alaska. We contrasted two soil depths to evaluate hypotheses associated with physical mixing, comparing inorganic N pools and rates of N mineralization, nitrification, and denitrification

assayed in the laboratory. Contrasts between undisturbed tundra and gully soils were used to evaluate the effects of thermokarst formation on N pools and processes. Comparison of gully soils with water tracks, which are often the precursor landform to thermo-erosion gullies, and data describing regional N content of soils was used to evaluate whether sites prone to thermokarst formation differ in N cycling relative to surrounding tundra. These comparisons provide an assessment of the potential for thermokarst features to contribute to increased N availability in warming arctic tundra.

AC.3 Methods

AC.3.1 Study sites

Soils were collected from seven thermo-erosion gullies in arctic tundra near the Toolik Field Station in the northern foothills of the Brooks Range, Alaska, USA (Table AC.1; Fig. AC.2). Thermokarst features were selected from those identified by Bowden et al. (2008) using aerial photography. One additional feature (site 8) was sampled that was not previously identified. Toolik Field Station is located 254 km north of the Arctic Circle and 180 km south of the Arctic Ocean. The average annual temperature is –10°C and average monthly temperature ranges from –25°C in January to 11.5°C in July. The region receives 320 mm of precipitation annually with 200 mm falling between June and August (Toolik Environmental Data Center Team 2011). Parent materials consist of glacial till and loess with thermo-erosion gullies occurring on landscapes of various glacial ages. Substrate age affects soil pH, which creates distinct vegetation groups including moist, acidic tussock tundra on older surfaces and non-acidic tundra on young substrates (Walker et al. 2010).

AC.3.2 Soil collection and analysis

Soils were collected in August 2010 from seven thermo-erosion gullies and three undisturbed water tracks using a manual auger (5 cm diameter). The living moss layer was discarded, cores were separated to 0-10 and 10-20 cm depths, and 3-6 cores were aggregated at each sampling location. Soils were collected from three replicate locations within each feature (hereafter referred to as gully), and three adjacent locations in undisturbed tundra, within 2m from the edge of the collapse (hereafter referred to as margin). Water tracks were sampled only within the track. Replicate sampling locations within each feature were at least 20 meters apart. Samples were transported to the laboratory where they were refrigerated for up to 24 h before processing for extractable pools of inorganic N and incubated for net mineralization and nitrification rates. Remaining soils were refrigerated for one week before potential nitrification and denitrification assays.

AC.3.3 Soil assays

The composited sample for each location was thoroughly homogenized, removing rocks by hand before soil analyses. Soil moisture was determined by mass after drying at 105ºC for 3 d, and organic matter as mass loss following combustion at 550ºC. Extractable pools of inorganic N were determined by extraction in 2 M KCl (Robertson et al. 1999). NH_4^+ concentration was determined using the phenol-hypochlorite method, and NO_3^- via cadmium reduction on a Bran+Luebbe Autoanalyzer 3. Soil pH was determined on slurries in deionized water that had equilibrated with the atmosphere for 30 minutes. Total C and N were measured following acidification of samples to remove inorganic C on a Costech 4010 elemental analyzer.

Net rates of N mineralization and nitrification were estimated as net change in inorganic N or NO_3^- pools, respectively following aerobic incubation for 7 d at 20ºC (Robertson et al. 1999). Potential rate of nitrification was measured in aerobic slurries supplemented with 0.5 mM NH_4^+

and 1 mM PO_4^{3-} (Robertson et al. 1999) that were sub-sampled four times in 24 hours. $CaCl_2$ was added to each sub-sample as a flocculant, and solids were separated using a centrifuge. NO_3^- concentration of the supernatant was analyzed as previously described. Potential rate of nitrification was calculated as the change in NO_3^- concentration over the incubation time. We assayed potential denitrification enzyme activity using the acetylene block method (Yoshinari et al. 1977). Media containing 722 mg NO_3^--N/L, 100 mg dextrose/L, and 10 mg chloramphenicol /L was purged of O_2 using N_2 and added to soils in gas-tight jars equipped with a stop-cock, followed by purging with N_2 for 2 minutes. Acetylene was added to the sample headspace (10% v/v) to prevent the reduction of N_2O to N_2, and samples were vented to bring pressure to ambient. Following vigorous shaking, headspace gas was sampled and stored in evacuated containers. Headspace was sampled again after four hours of incubation at 20ºC. Headspace N_2O concentration was analyzed on a Varian CP-3800 gas chromatograph via electron-capture detection. Bunsen coefficients were applied to determine the mass of N_2O dissolved in the slurry, and total N_2O produced by each sample was used to calculate production of N_2O over the incubation period.

AC.3.4 Statistical methods

To assess the contribution of thermokarst and water track soils to regional N pools, we calculated regional means of soil moisture, organic matter, and inorganic N pools using data collected by the Arctic Long-Term Ecological Research Program and the Department of Energy R4D Program. These datasets spanned a 15-120 ka gradient in land surface age and encompassed the major habitat types present within this tundra region: non-acidic tussock tundra, acidic tussock tundra, wet sedge tundra, riverside willow, heath/hillslopes, and footslopes. We calculated regional means of soil moisture and N pools based only on samples collected in

August, to compare with our dataset. The regional dataset reports values for whole soil cores, rather than depth-specific values, so we compared these to the mean of 0-10 and 10-20 cm values determined in this study. We determined the potential for formation of thermokarst to increase regional-scale heterogeneity in soil N pools by comparing the 95% confidence intervals of mean values across the sampled thermo-erosion gullies to the regional mean. We also assessed the potential for particular gully features to contribute to spatial heterogeneity at the regional scale by using Z-scores to compare each gully to the regional mean. These analyses were repeated for water tracks, typically the precursor landscape feature of thermo-erosion gullies, to determine whether pre-existing conditions may contribute to enhanced N availability in thermo-erosion gullies. We supplemented data collected in water tracks as part of this study with additional data available in the literature.

We used randomized block ANOVA to compare soil attributes and N processes in gullies and undisturbed margins. Position (gully and margin), soil depth, and their interaction were included as fixed effects, and site was applied as a random block, resulting in comparison of depths and positions within each site. Tukey's HSD was applied to determine significant differences among groups following significant ANOVAs. Assumptions of ANOVA were assessed for the residuals of the analysis. Normality was evaluated using normal probability plots and variance was visually assessed with plots of observed values compared to residuals. Response variables were ln-transformed when necessary to meet these assumptions. All statistical tests were evaluated with α=0.1.

AC.4 Results

AC.4.1 Comparison to regional patterns

Soils of thermo-erosion gullies differed from regional mean values of soil moisture and

organic matter, but not N pools, as determined by comparing overlap in confidence intervals about the means describing regional soils and gully features (Table AC.2). Gully soils were drier than the regional mean, and were also drier than water tracks. Both water track and gully soils contained less organic matter than the regional mean in the top 20 cm. Despite these differences, pools of extractable soil NH_4^+ and NO_3^- did not differ from the regional mean, and were similar when comparing water tracks and thermo-erosion gullies (Table AC.2). At the feature scale, only one gully had significantly elevated NH_4^+ and NO_3^- pools compared to the regional mean (site 2; Z-score>1.65).

Median N processing rates in the sampled water tracks were qualitatively similar to intact, margin soils. Net N mineralization rate spanned positive to negative values in soils 0-10 cm (median: -0.24 mg N kg dry soil*d^{-1}), with a range similar to margin soils (data not shown). Net immobilization occurred in all samples collected from 10-20 cm (median: -0.37 mg N kg dry soil*d^{-1}), a pattern that was unique to water tracks. Net nitrification occurred in only 2 samples from water tracks, both collected at 0-10 cm, with median values of 0, similar to margin soils. Median rate of denitrification in water track soils was lower than in margin or gully soils for both depths (0-10: 30.5, 10-20: 9.4 μg N kg dry soil*h^{-1})

AC.4.2 Feature-level patterns

Soil attributes differed significantly between intact margins and disturbed soils within the gully, as well as between soil depths. Soil moisture was significantly higher in gullies compared to margin soils (ln-transformed; $F_{1,74}$=4.3, P=0.04; Fig. AC.3), and in the surface layer compared with deeper soils ($F_{1,74}$=24.9, P<0.01; Fig. AC.3). Organic matter also differed between positions (ln-transformed; $F_{1,74}$=3.7, P=0.06) and depths ($F_{1,74}$=21.0, P<0.01). Whereas organic matter was significantly greater at 0-10 cm than 10-20 cm depths in margin soils, this difference was not

significant in gullies, where organic matter content of both depths was similar to surface soils of the margin (Fig. AC.3). Soil pH did not differ significantly between depths or positions (Table AC.1; P>0.1).

Total N tended to be greater in shallow soils ($F_{1,71}$=12.7, P<0.01), although this effect was driven by strong stratification of intact margin soils (Fig. AC.4). Extractable NH_4^+ contrasted between margin and gully positions (ln-transformed; $F_{1,73}$=6.8, P=0.01), but differences between depths were not significant ($F_{1,73}$=2.8, P=0.1). These patterns result from larger pools of extractable NH_4^+ in gully soils at both depths compared to the deep margin soils (Fig. AC.4). Non-normal distributions caused by numerous samples with NO_3^- concentration below detection limits constrained application of statistical tests. Nitrate was typically not detectable in the intact margin soils, but occurred in 43% (0-10 cm) to 50% (10-20 cm) of all samples from gullies (Fig. AC.4).

Some nitrogen transformations also contrasted between intact margins and disturbed gullies. Denitrification potential was significantly greater in surface compared with deeper soil ($F_{1,74}$ = 19.8, P<0.01), and there was a significant interaction between position and depth ($F_{1,74}$=3.1, P=0.09), which can be seen as a strong contrast between shallow and deeper soils of intact margins, but no contrast between depths in gullies (Fig. AC.5). Net nitrification and nitrification potential were not detectable in a large number of samples, constraining application of statistical tests. However, net nitrification occurred in 30% of gully soils, at each of the sampled depths, whereas only 1% of all margin soils supported nitrification (Fig. AC.5). Potential nitrification was distributed more evenly across gully and margin soils, but highest average rates were observed in gully soils at both depths, and potential rates were greater than net rates. No significant differences were observed in net N mineralization rates.

AC.4.3 Variation among thermo-erosion gullies

N pools and process rates varied up to 20-fold across gully sites. Randomized block ANOVA revealed a significant effect of site on moisture, organic matter, pH, NH_4^+, and denitrification ($P<0.01$), indicating significant heterogeneity among sites. Sites with highest inorganic N pools within the gully tended to occur on the oldest substrates, and mean depth-integrated N pools were significantly different between sites on surfaces <20 ka and those >100 ka (one factor ANOVA, ln-transformed; $F_{1,10}=2.7$, $P=0.04$; Fig. AC.6).

AC.5 Discussion

We investigated soil inorganic N pools and transformations in thermo-erosion gullies to determine how formation of thermokarst may result in increased inorganic N availability in arctic tundra. We hypothesized that thermokarst soils may contain elevated N pools either because soils prone to permafrost degradation have inherently high N content relative to stable tundra, or because physical processes leading to subsidence alter the distribution of N or abiotic conditions that influence biological processing of N. On average, thermo-erosion gullies contained similar soil inorganic N pools to other tundra landforms, indicating that gullies do not constitute hot spots for inorganic N storage at the regional scale. However, thermo-erosion appeared to alter the vertical distribution of inorganic N relative to adjacent undisturbed soils, which may promote export of dissolved N.

AC.5.1 Mechanisms of thermo-erosion influence on N cycling

Despite similarity in depth-integrated soil N between thermo-erosion gullies and intact tundra, we observed significant differences in the vertical distribution of N between gullies and adjacent undisturbed soils. This pattern could result from altered rates of N transformations

following subsidence or physical changes to the soil profile within gullies. Whereas intact profiles of margin soils had significant vertical structure, nearly all measured soil attributes were vertically homogenized in gullies, providing support for the hypothesis that physical processes associated with thermokarst formation contribute to elevated N export from thermo-erosion gullies. As gullies form, thermo-erosion causes the soil from the margins to collapse inward and move downslope within the feature, repeatedly overturning the soil profile (Godin and Fortier 2012; Jorgenson and Osterkamp 2005). This churning effect can be seen in soil organic matter content that is greater at depth within gullies compared to margins, indicating that burial of surface-derived organic matter has occurred during formation of the thermokarst features. Significantly larger inorganic N pools in mineral compared to organic horizons is characteristic of tundra soils (Hobbie and Gough 2002; Keuper et al. 2012), and indicates mineral soils as the source of inorganic N observed in shallow gully soils.

Vertical patterns in N transformation rates indicate that processing also differed between intact and disturbed soils, which may be a response to changes in abiotic conditions associated with mixing. Similar rates of net N mineralization between margins and gullies and between surface and subsurface soils suggest that differences in N processing do not account for homogenization of NH_4^+ within the soil profile of gully soils. In contrast, higher rates of nitrification in gully soils, coupled with a dampening of denitrification in surface soils likely contribute to the larger pools of NO_3^- observed in gullies compared to adjacent margins. Nitrate is infrequently observed in the active layer of tundra soils, and accordingly rates of nitrification are typically low or undetectable (Giblin et al. 1991; Hobbie et al. 2002; Lavoie et al. 2011). Increased available NH_4^+ in aerated, surface soils may support nitrification activity in thermo-erosion gullies. Indeed, higher rates of nitrification when NH_4^+ was added to laboratory assays of

nitrification potential compared to unamended net rate supports the notion that substrate availability limits nitrification in tundra soil. Thus the source of inorganic N for hydrologic export appears to be mineral soils, which are brought into contact with surface flowpaths during thermo-erosion, with the potential for changes in process rates to alter the forms of N available for export.

AC.5.2 Characteristics of thermo-erosion gullies contributing to N export

Although our observations provide evidence in support of a common physical mechanism explaining vertical distribution of inorganic N across sites, we observed significant variation in N pools and process rates among the sampled gullies, suggesting differences in the underlying drivers of N availability. At a regional scale, landscape age is correlated with the size of N pools, with larger pools in soils developed on older surfaces, particularly in mineral horizons (Hobbie and Gough 2002), and this pattern was detected across the sites investigated in the present study (Fig. AC.6). Older, acidic soils leach more dissolved organic N than younger soils (Whittinghill and Hobbie 2011) and support faster rates of decomposition and N mineralization (Hobbie et al. 2002). The relationship between substrate age and soil N may have significant consequences for N export from thermokarst terrain, because thermo-erosion gullies are more likely to form on older, acidic substrate where ice wedges are larger and more abundant (Bockheim and Hinkel 2012).

Strong contrasts in NO_3^- pools among the thermo-erosion gullies surveyed suggest that in addition to substrate age, characteristics of individual sites contribute to the capacity for thermokarst soils to serve as a source or sink for NO_3^-. Our survey of seven thermo-erosion gullies does not present sufficient statistical power to quantify relationships of N dynamics with potential site-level explanatory variables. However, we hypothesize that several factors are

important based on observations of intact tundra and other thermokarst features. Site characteristics related to the depth of the gully, including slope, aspect, and position within the drainage network, influence snow depth and depth of thaw within the feature. Deeper gullies accumulate more snow, providing insulation to soils, which promotes net N mineralization in intact tundra (DeMarco et al. 2011; Schimel et al. 2004). Similarly, deeper or larger water tracks may transport more heat, resulting in deeper permafrost thaw, and making available deeper mineral horizons to be turned over to the surface upon development of thermokarst. Both water track and gully soils were significantly drier than the regional mean for tundra soils, which is counterintuitive given that both contain advective flow. However, deeper thaw in water tracks (Chapin et al. 1988) and thermo-erosion gullies (SE Godsey, personal comm.) compared to other tundra types allows for deeper infiltration. Therefore, sampling surface soils late in the active season perhaps did not capture saturated depths (Cheng et al. 1998), and additional, deeper pools of inorganic N that may be an important source of N subject to hydrologic export late in the thaw season. Finally, ground subsidence increases heterogeneity of soil characteristics at scales smaller than whole features, due to redistribution of soil moisture caused by changes in topography (Lee et al. 2010), which may introduce small scale hot spots of N availability or transformation within features.

Previous studies have linked N pools in thermokarst features to shifts in vegetation communities. Older, revegetated retrogressive thaw slumps contained larger NO_3^- pools than younger thermokarst features, likely due to colonization by N-fixing plants (Lantz et al. 2009). However, thermo-erosion gullies rarely result in substantial shifts in plant communities (Jorgenson and Osterkamp 2005). Although the gullies observed in the present study contained revegetated islands, and spanned a range of thermo-erosion activity, N-fixing plant species were

not observed at high densities, suggesting that N inputs did not change following subsidence.

AC.5.3 Implications of thermo-erosion for N export

Despite a small spatial extent (~1% of continuous permafrost in Alaska; Jorgenson et al. 2009), thermo-erosion gullies occupy a focal point for transport of water and solutes, which may propagate the effects of permafrost thaw and soil disturbance to valley bottoms or stream networks. Enrichment of shallow soils with inorganic N due to physical mixing and subsequent changes to biological transformations of N could contribute to observed export of inorganic N and fertilization of oligotrophic ecosystems downstream of thermo-erosion gullies. This fertilization may be acute (Bowden et al. 2008), but it remains unclear whether elevated nutrient concentrations persist as thermokarst features stabilize and are revegetated, which occurs over a timescale of years (Godin and Fortier 2012). Thus, the direct consequences of thermo-erosion gullies for receiving waters may be significant, but relatively short-lived. However, about a third of all permafrost has medium or high ice-content (Zhang et al. 1999) and is therefore susceptible to formation of thermokarst, and the incidence of thermo-erosion is increasing (Jorgenson et al. 2009; Lantz and Kokelj 2008). The effects of multiple individual gullies may therefore cumulatively increase the effect of N fertilization on downstream ecosystems.

AC.6 Acknowledgements

We thank Andrew Balser for assistance with site selection and interpretation of map records, and Randy Fulweber and Jason Stuckey for providing the site map. We gratefully acknowledge Margit Jaeger and Ann Olsson for assistance in the laboratory. This work was supported by the National Science Foundation ARCSS program (OPP-0806465), and an NSF post-doctoral fellowship to TKH (OPP-0817056).

AC.7 Literature Cited

ARC-LTER Arctic Long-Term Ecological Research Program, Gus Shaver, Precipitation chemistry, ecosystems.mbl.edu/arc/datacatalog.html, accessed 2011.

Bockheim J, Hinkel K (2012) Accumulation of excess ground ice in an age sequence of drained thermokarst lake basins, arctic Alaska. Permafrost and Periglacial Processes 23:231-236

Bockheim JG (2007) Importance of cryoturbation in redistributing organic carbon in permafrost-affected soils. Soil Science Society of America Journal 71:1335-1342

Booth M, Stark J, Hart S (2006) Soil mixing effects on inorganic nitrogen production and consumption in forest and shrubland soils. Plant and Soil 289:5-15

Bowden WB, Gooseff MN, Balser A, Green A, Peterson BJ, Bradford J (2008) Sediment and nutrient delivery from thermokarst features in the foothills of the North Slope, Alaska: potential impacts on headwater stream ecosystems. Journal of Geophysical Research-Biogeosciences 113:G02026

Buckeridge KM, Cen YP, Layzell DB, Grogan P (2010) Soil biogeochemistry during the early spring in low arctic mesic tundra and the impacts of deepened snow and enhanced nitrogen availability. Biogeochemistry 99:127-141

Buckeridge KM, Grogan P (2010) Deepened snow increases late thaw biogeochemical pulses in mesic low arctic tundra. Biogeochemistry 101:105-121

Chapin FSI, Fetcher N, Kielland K, Everett KR, Linkins AE (1988) Productivity and nutrient cycling of Alaskan tundra: enhancement by flowing soil water. Ecology 69:693-702

Cheng W, Virginia RA, Oberbauer SF, Gillespie CT, Reynolds JF (1998) Soil nitrogen, microbial biomass, and respiration along an Arctic Toposequence. Soil Science Society of America Journal 62:654-662

DeMarco J, Mack MC, Bret-Harte MS (2011) The effects of snow, soil microenvironment, and soil organic matter quality on N availability in three Alaskan arctic plant communities. Ecosystems 14:804-817

Fortier D, Allard M, Shur Y (2007) Observation of rapid drainage system development by thermal erosion of ice wedges on Bylot Island, Canadian Arctic Archipelago. Permafrost and Periglacial Processes 18:229-243

Giblin AE, Nadelhoffer KJ, Shaver GR, Laundre JA, McKerrow AJ (1991) Biogeochemical diversity along a riverside toposequence in arctic Alaska. Ecological Monographs 61:415-435

Godin E, Fortier D (2012) Geomorphology of a thermo-erosion gully, Bylot Island, Nunavut, Canada. Canadian Journal of Earth Sciences 49:979-986

Hamilton TD (2003a) Glacial geology of Toolik Lake and the Upper Kuparuk River region. In: Walker DA (ed) Biological Papers of the University of Alaska, vol 26. University of Alaska, Fairbanks, AK

Hamilton TD (2003b) Surficial geology of the Dalton Highway (Itkillik-Sagavanirktok rivers) area, southern Arctic foothills, Alaska. In. Alaska Division of Geological & Geophysical Surveys, p 32

Hinzman LD, Kane DL, Gieck RE, Everett KR (1991) Hydrologic and thermal-properties of the active layer in the Alaskan Arctic. Cold Regions Science and Technology 19:95-110

Hobbie SE, Gough L (2002) Foliar and soil nutrients in tundra on glacial landscapes of contrasting ages in northern Alaska. Oecologia 131:453-462

Hobbie SE, Miley TA, Weiss MS (2002) Carbon and nitrogen cycling in soils from acidic and nonacidic tundra with different glacial histories in Northern Alaska. Ecosystems 5:761-774

Jonasson S, Shaver GR (1999) Within-stand nutrient cycling in arctic and boreal wetlands. Ecology 80:2139-2150

Jorgenson MT, Osterkamp TE (2005) Response of boreal ecosystems to varying modes of permafrost degradation. Canadian Journal of Forest Research 35:2100-2111

Jorgenson MT, Shur Y, Osterkamp T (2009) Thermokarst in Alaska. In: Ninth International Conference on Permafrost, University of Alaska Fairbanks, pp 117-124

Kaiser C, Meyer H, Biasi C, Rusalimova O, Barsukov P, Richter A (2007) Conservation of soil organic matter through cryoturbation in arctic soils in Siberia. Journal of Geophysical Research-Biogeosciences 112

Karlstrom TNV (1964) Surficial geology of Alaska. In, pp 2 sheets, scale 1:1,584,000

Keuper F et al. (2012) A frozen feast: thawing permafrost increases plant-available nitrogen in subarctic peatlands. Global Change Biology 18:1998-2007

Kokelj SV, Burn C (2005) Geochemistry of the active layer and near-surface permafrost, Mackenzie delta region, Northwest Territories, Canada. Canadian Journal of Earth Sciences 42:37-48

Lantz TC, Kokelj SV (2008) Increasing rates of retrogressive thaw slump activity in the Mackenzie Delta region, NWT, Canada. Geophysical Research Letters 35:L06502

Lantz TC, Kokelj SV, Gergel SE, Henryz GHR (2009) Relative impacts of disturbance and temperature: persistent changes in microenvironment and vegetation in retrogressive thaw slumps. Global Change Biology 15:1664-1675

Lavoie M, Mack MC, Schuur EAG (2011) Effects of elevated nitrogen and temperature on carbon and nitrogen dynamics in Alaskan arctic and boreal soils. Journal of Geophysical Research-Biogeosciences 116:G03013

Lee H, Schuur EAG, Vogel JG (2010) Soil CO_2 production in upland tundra where permafrost is thawing. Journal of Geophysical Research-Biogeosciences 115:G01009

Mack MC, Schuur EAG, Bret-Harte MS, Shaver GR, Chapin FS (2004) Ecosystem carbon storage in arctic tundra reduced by long-term nutrient fertilization. Nature 431:440-443

Nadelhoffer KJ, Giblin AE, Shaver GR, Laundre JA (1991) Effects of temperature and substrate quality on element mineralization in 6 arctic soils. Ecology 72:242-253

Natali SM, Schuur EAG, Trucco C, Hicks Pries CE, Crummer KG, Baron Lopez AF (2011) Effects of experimental warming of air, soil and permafrost on carbon balance in Alaskan tundra. Global Change Biology 17:1394-1407

Osterkamp TE et al. (2009) Physical and ecological changes associated with warming permafrost and thermokarst in interior Alaska. Permafrost and Periglacial Processes 20:235-256

Ping CL, Bockheim JG, Kimble JM, Michaelson GJ, Walker DA (1998) Characteristics of cryogenic soils along a latitudinal transect in Arctic Alaska. Journal of Geophysical Research-Atmospheres 103:28917-28928

Robertson GP, Coleman D, Bledsoe C, Sollins P (1999) Standard Soil Methods for Long-Term Ecological Research. Oxford University Press US

Schimel JP, Bilbrough C, Welker JA (2004) Increased snow depth affects microbial activity and nitrogen mineralization in two Arctic tundra communities. Soil Biology & Biochemistry 36:217-227

Schimel JP, Chapin FS (1996) Tundra plant uptake of amino acid and NH_4^+ nitrogen in situ: plants compete well for amino acid N. Ecology 77:2142-2147

Schuur EAG, Crummer KG, Vogel JG, Mack MC (2007) Plant species composition and productivity following permafrost thaw and thermokarst in alaskan tundra. Ecosystems 10:280-292

Shaver GR et al. (1998) Biomass and CO_2 flux in wet sedge tundras: responses to nutrients, temperature, and light. Ecological Monographs 68:75-97

Toolik_Environmental_Data_Center_Team (2011) Meteorological monitoring program at Toolik, Alaska. In. Toolik Field Station, Institute of Arctic Biology, University of Alaska Fairbanks, Fairbanks AK 99775

USGS/NPS (1999) State surficial geology map of Alaska. In. NPS AKSO, Anchorage, AK

Walker D, Raynolds M, Maier H, Barbour E, Neufeld G (2010) Circumpolar geobotanical mapping: a web-based plant-to-planet approach for vegetation-change analysis in the arctc. Viten 1:125-128

Walker DA (2008) Toolik-Arctic Geobotanical Atlas. In. Alaska Geobotany Center

Walker DA, Barry NC (1991) Toolik Lake permanent plots: site factors, soil physical and chemical properties, plant species cover, photographs, and soil descriptions. In. Department of Energy R4D Program data report, Joint Facility for REgional Ecosystem Analysis, Institute of Arctic and Alpine Research, National Snow and Ice Data Center, Boulder, CO

Walker DA, Everett KR (1991) Loess ecosystems of Northern Alaska: regional gradient and toposequence at Prudhoe Bay. Ecological Monographs 61:437-464

Whittinghill KA, Hobbie SE (2011) Effects of landscape age on soil organic matter processing in Northern Alaska. Soil Science Society of America Journal 75:907-917

Yano Y, Shaver GR, Giblin AE, Rastetter EB, Nadelhoffer KJ (2010) Nitrogen dynamics in a small arctic watershed: retention and downhill movement of ^{15}N. Ecological Monographs 80:331-351

Yoshinari T, Hynes R, Knowles R (1977) Acetylene inhibition of nitrous-oxide reduction and measurement of denitrification and nitrogen-fixation in soil. Soil Biology and Biochemistry 9:177-183

Zhang T, Barry R, Knowles J, Heginbottom J, Brown J (1999) Statistics and characteristics of permafrost and ground ice distribution in the Northern Hemisphere. Polar Geography 23:132-154

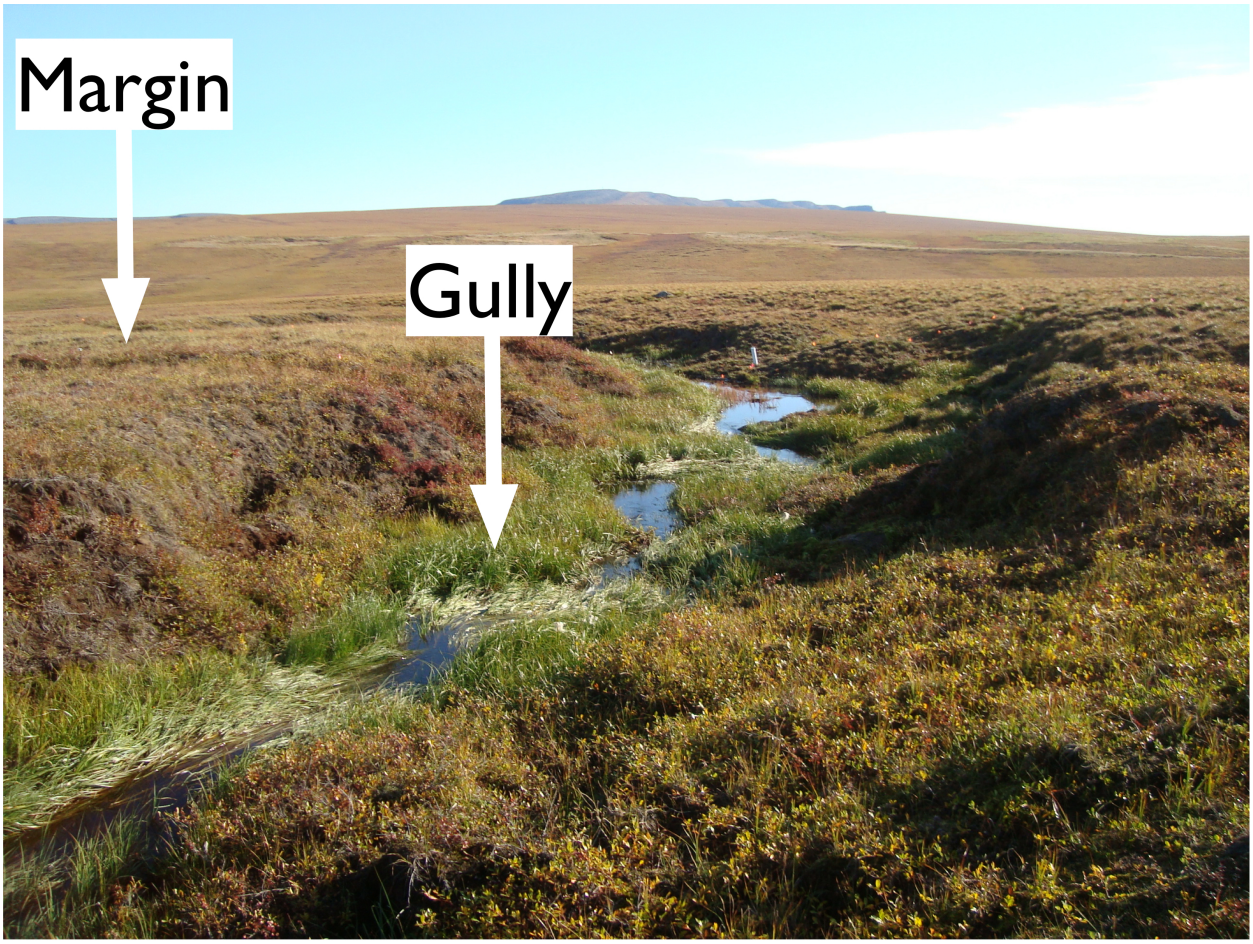

Figure AC.1 Ground view of a thermo-erosion gully (Site 3).

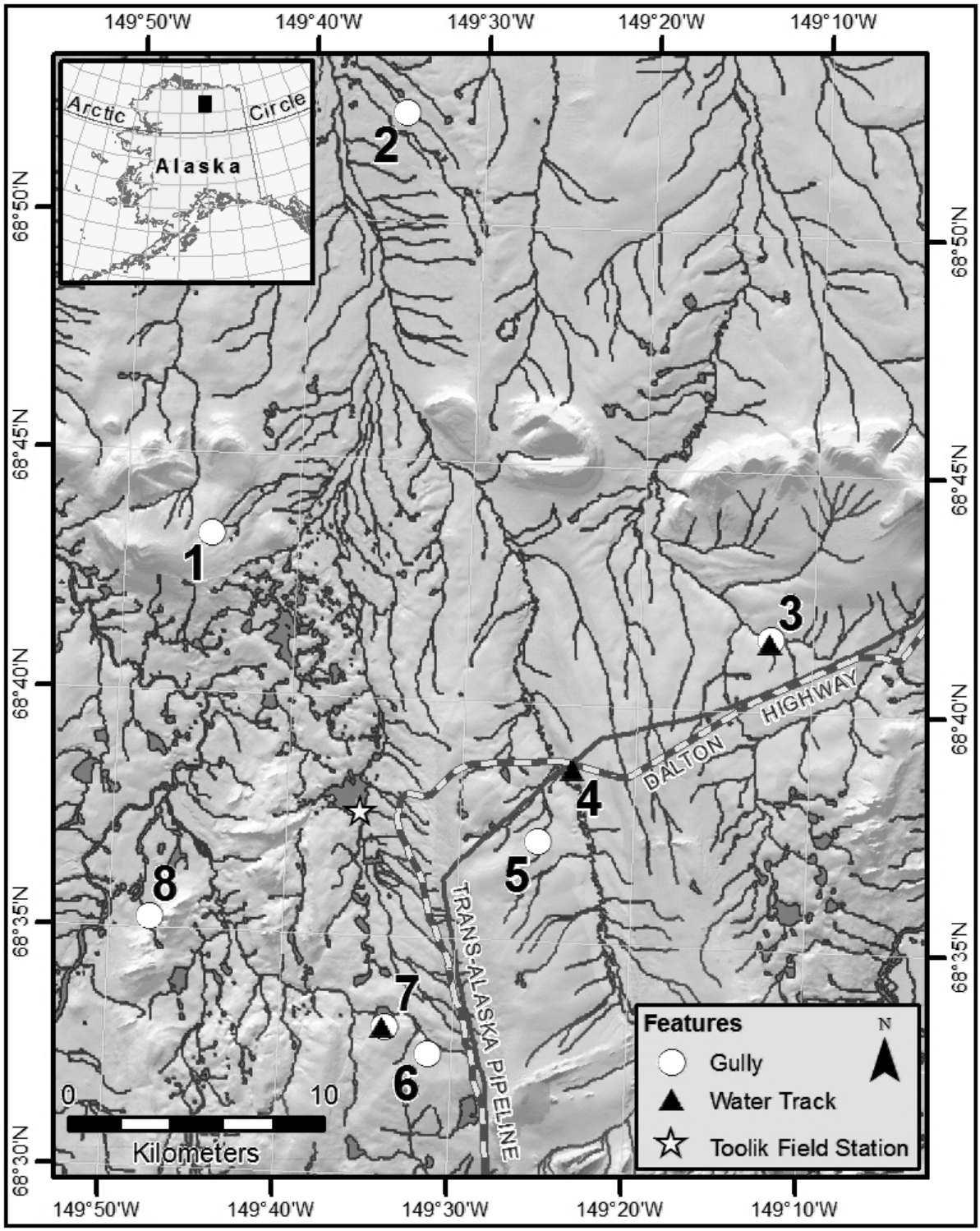

Figure AC.2 Thermo-erosion gullies and water tracks were sampled near the Toolik Field Station. Site-level attributes are summarized in Table AC.1.

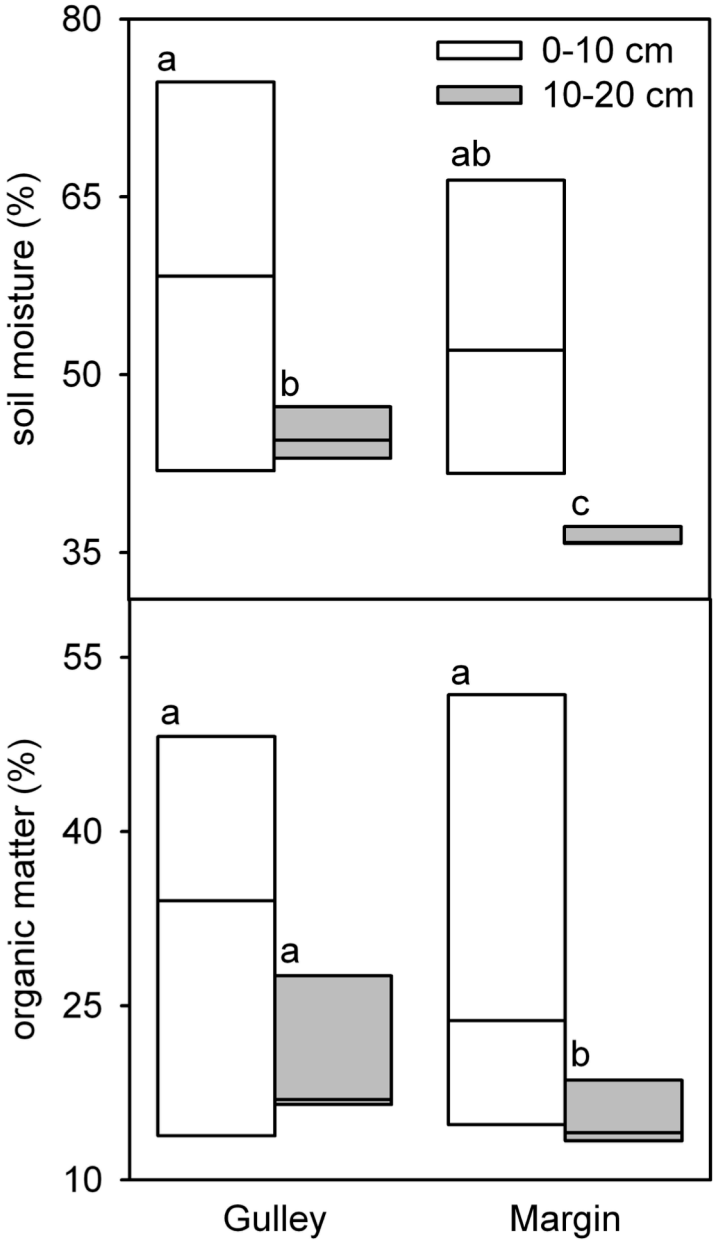

Figure AC.3 Soil moisture and organic matter content of soils within (gully) and adjacent to (margin) thermo-erosion gullies. Letters designate significant ($p<0.1$) differences determined by Tukey's HSD. Boxes designate 25 and 75 percentiles of data, center bar corresponds to the median value, n=7.

1

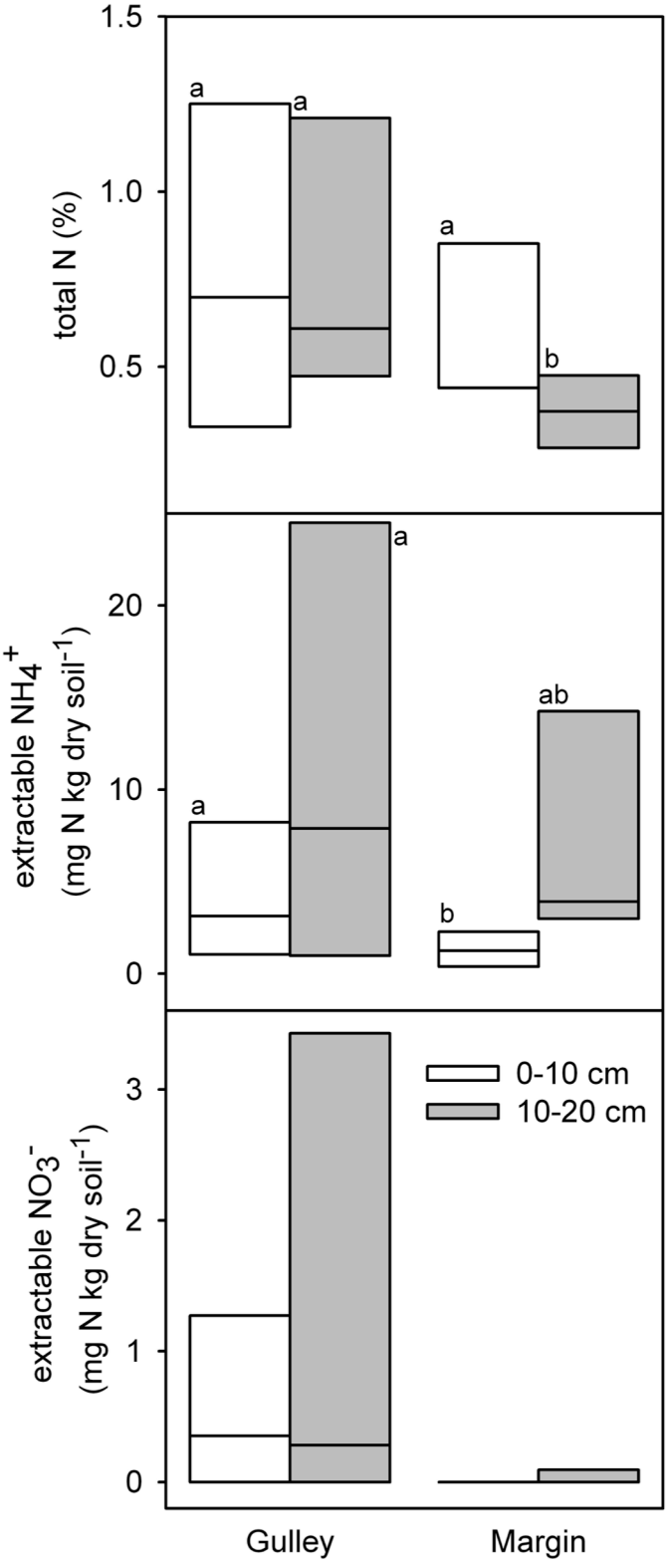

Figure AC.4 Inorganic N pools in soils of thermokarst gullies. Letters designate significant differences ($p<0.1$) determined by Tukey's HSD, n=7. Symbology as in Fig. AC.3.

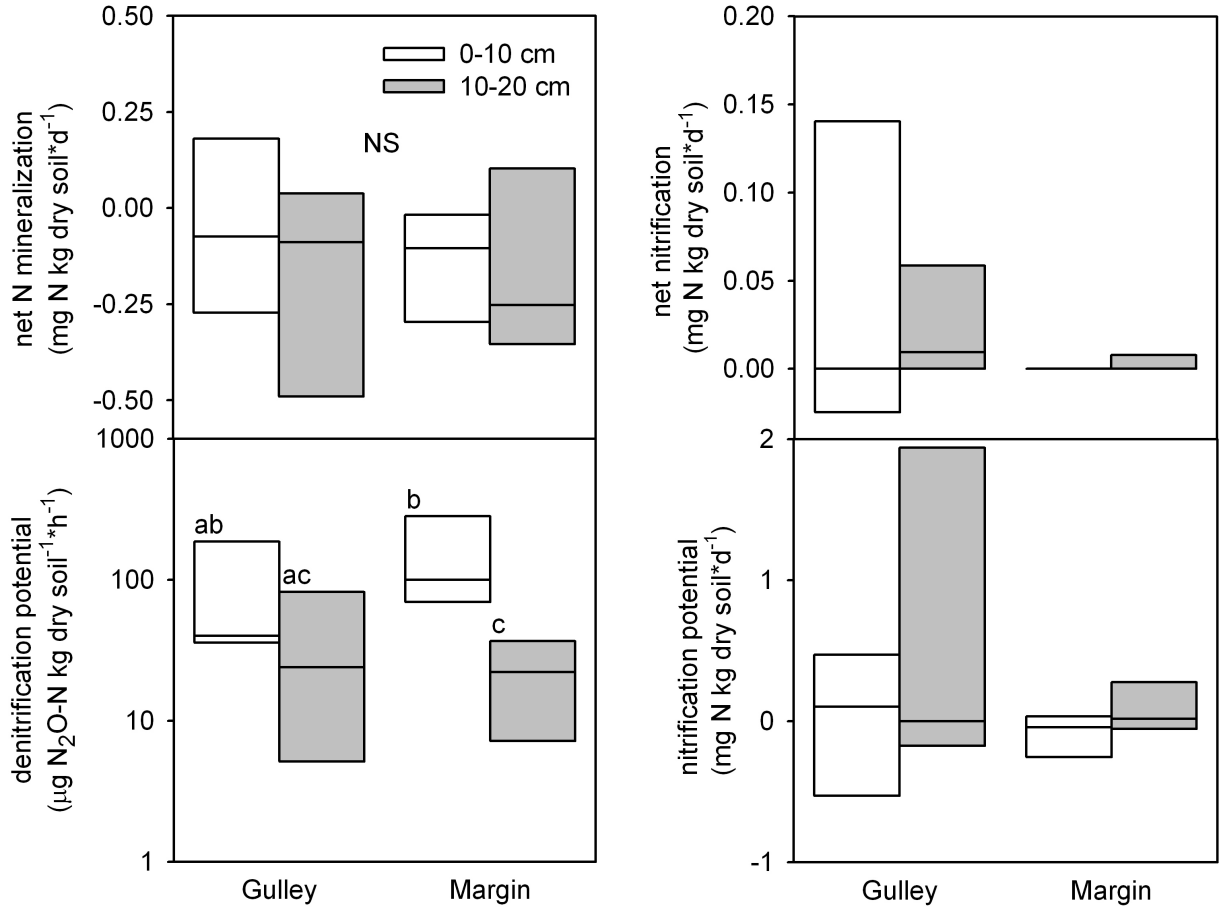

Figure AC.5 Transformation rates of inorganic N. Letters designate significant differences ($p<0.1$) determined by Tukey's HSD. Note log scale for denitrification, n=7. Symbology as in Fig. AC.3.

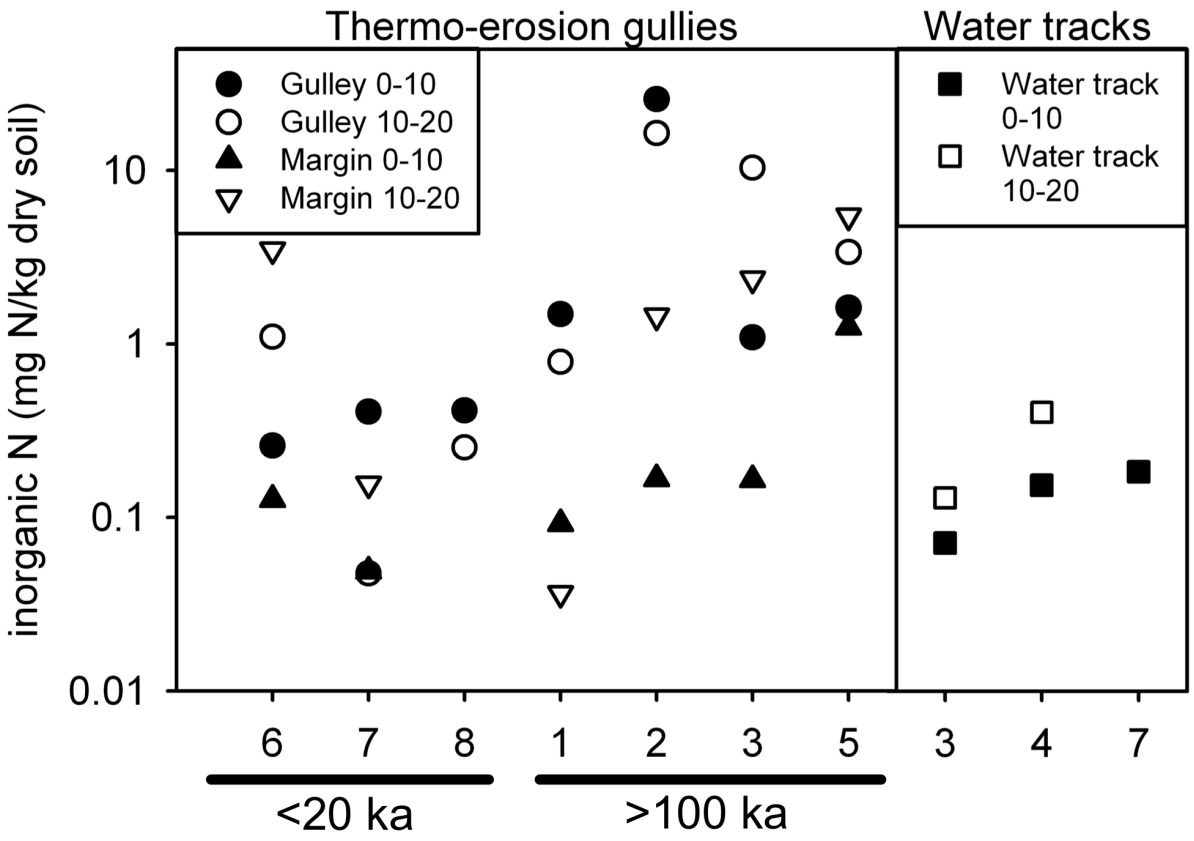

Figure AC.6 Inorganic N pools of soils within and adjacent to thermo-erosional gullies, and intact water tracks. Sites are categorized by geological substrate age. Note that inorganic N is displayed on a log scale. Pools of inorganic N were below the detection limit for margin soils of gully site 8.

Table AC.1 Feature-level attributes of thermo-erosion gullies and water tracks

Site ID	Type	Coordinates (UTM)	Glacial geology	Surface age (ka)*	Tundra vegetation	Activity index#	Elevation	Bearing (°)	Slope (°)	Max width (m)	Depth (m)	Length (m)	pH (10 cm)	pH (20 cm)
1	Gully	N68.7223 W149.7505	Drift of Sag river late advance (1)	150-60	Low shrub (6)	1	800	76	4	15	2	89	4.55	4.20
2	Gully	N68.8716 W149.5789	Sag age outwash (1,3,4)	400-250	Erect shrub (6)	3	560	316	3	15	4	190	4.03	3.96
3	Gully	N68.6923 W149.2067	Drift of older Sag age (2)	150	Tussock (5)	2	780	33	3	18	3	238	3.68	4.42
5	Gully	N68.6192 W149.4251	Sag River age drift overlain by thin solifluction sheet (2)	modern, overlying 150	Low shrub (5)	2	838	13	2	5	2	90	4.11	4.37
6	Gully	N68.5435 W149.5225	Drift of latest Itkillik readvance (2)	12.8-11.4	Low shrub (5)	2	885	9	4	20	1	206	4.09	4.17
7	Gully	N68.5524 W149.5652	Drift of Itkillik phase II (2)	25-11.5	Tussock (5)	5	841	2	4	3	4	20	4.42	4.23
8	Gully	N68.5875 W149.7942	Undifferentiated lacustrine deposits (1)	12-10	Low shrub (5)	3	654	307	4	11	2	30	5.21	4.70
3	Water track	N68.6911 W149.2084	Drift of older Sag age (2)	150	Sedge, moss, dwarf shrub (5)	0	792	10	3	8	<1	864	3.76	3.79
4	Water track	N68.6447 W149.3944	Drift of older Sag age (2)	150	Tussock (5)	0	758	247	3	10	<1	445	3.75	4.04
7	Water track	N68.5527 W149.5663	Drift of Itkillik phase II (2)	25-11.5	Tussock (5)	0	830	334	4	4	<1	110	4.93	ND

*Data sources same as for glacial geology

#Activity index: 0-no apparent current or past thermo-erosion activity, 1-stabilized with complete revegetation, 2=limited thermo-erosion activity but with coarse sediment in stream bottom (clear outflow), 3= moderate thermo-erosion activity with somewhat turbid outflow, 4=active thermo-erosion with turbid outflow and some lateral growth, 5=very active thermo-erosion (lateral growth and deepening) with turbid outflow.

ND=no data

(1) Hamilton 2003b, (2) Hamilton 2003a, (3) USGS/NPS 1999, (4) Karlstrom 1964, (5) Walker 2010, (6) this study

Table AC.2 Means and 95% confidence intervals for tundra soils from the Toolik Lake region, water tracks, and thermo-erosion gullies.

	N	moisture (%)	organic matter (%)	NH_4^+ (mg N/kg dry soil)	NO_3 (mg N/kg dry soil)
Regional	344-425	73.6 (72.0–75.1)	44.5 (38.6–50.4)	8.0 (7.1–9.0)	0.2 (0.2–0.3)
Water tracks	4-5	64.6 (44.6–84.6)	24.0 (10.1–37.8)	5.5 (-0.7–11.8)	0.3 (-0.2–0.9)
Thermo-erosion gullies	7	51.2 (45.4–57.0)	26.7 (16.1–37.2)	8.2 (-0.6–16.9)	1.0 (-0.6–2.6)

Notes: Regional mean calculated from samples collected from the Sagavanirktok and Toolik areas in Aug 1987-2002 (ARC-LTER) and organic matter from Walker & Barry (1991). The regional means represent non-acidic tussock tundra, acidic tussock tundra, wet sedge tundra, riverside willow, heath/hillslopes, and footslopes. Values are integrated over 0-20 cm. Water track data include samples collected in this study, supplemented with data from Chapin et al. (1988) and Cheng et al. (1998).